University of Southern Queensland

Measurements of evaporation during sprinkler irrigation

A dissertation submitted by

Md. Jasim Uddin

B. Sc. (Agril. Engg.)
M.S. (Irrigation and Water Management)

For the Award of

Doctor of Philosophy

2012

DEDICATED TO MY LATE PARENTS

MR. HAZIR ALI
MRS. ASTHORI ALI

MD. JASIM UDDIN
TOOWOOMBA, QLD 4350
AUSTRALIA

JANUARY 2012

ABSTRACT

The availability of water for irrigated agriculture is a concerning issue in the world especially in arid and semi-arid regions. Irrigators are facing a number of challenges, including reductions in the availability of water and increased competition with industrial and domestic uses. Irrigated agriculture is the largest water consumer all over the world as well as in Australia, and there is pressure to increase water use efficiency. Efficient utilization of water can improve the crop production per unit of water applied and can contribute to water conservation. Among the irrigation systems, sprinkler irrigation is one of the most popular methods for achieving high application efficiencies. However, the irrigators are still less interested to adopt this system due to the lack of accurate information regarding the losses in sprinkler irrigation often citing high evaporation losses along with high cost of operation.

Evaporation losses during sprinkler irrigation are still a vital issue to the irrigation community all over the world. Previous experimental results have shown that they may vary from 0 to 45% of the applied water and that a large proportion of the loss is droplet evaporation in the atmosphere. However, recent theoretical studies reported that the total losses should not be much more than a few percent. They also suggested a negligible (less than 1%) amount of droplet evaporation compared to the major canopy evaporation component. Due to the limitations of the existing methodology and technique these theoretical results could not be verified by field experiments in real crops. Accurate estimates of the losses are important to determine the strategies for the optimal design and management of sprinkler irrigation systems as well as irrigation scheduling considering the application efficiency of the system. It is also important to provide the accurate information regarding the evaporation losses which can significantly help farmers to choose a suitable irrigation system. The relatively recent development of the eddy covariance (ECV) technique has

provided the opportunity to overcome the limitations of the existing methods to measure the evaporation during sprinkler irrigation. Therefore, this work aimed to measure the additional evaporation that occurs during sprinkler irrigation adopting eddy covariance technique and to separate its components in conjunction with additional measurements. In this regard, three research objectives were identified including: (i) use the eddy covariance (ECV) technique to measure the total evapotranspiration (ET) during sprinkler irrigation; (iii) partition the total evaporation into its major components during irrigation and subsequent periods; and (iii) to demonstrate how the ECV-sap flow data can aid in management of sprinkler irrigation.

The ECV system is consists of a fast-response three dimensional sonic anemometer coupled with open path infrared gas analyser. Sap flow was measured using six dynagauge sap flow sensors each with a digital interface, a hub and a data logger. Additional measurements include net radiation using a four component net radiometer, soil heat flux (G) using heat flux plates temperature and relative humidity using two temperature and relative humidity probes and the crop canopy temperature using an infrared thermometer. A fixed sprinkler irrigation system was installed in a way to make a circle of 50 m with an area of 0.2 ha for all trials. Experimental measurements were conducted over a range of surfaces from bare soil to different stages of crop throughout the period 2010-11 at the agricultural experimental station at University of Southern Queensland, Toowoomba, Australia.

Preliminary measurements were conducted over the grass and bare soil to evaluate the capability of the ECV technique to measure the total ET during sprinkler irrigation. The preliminary measurements showed that the ECV technique successfully measured the increased ET during irrigation and the decreasing rate of ET during post irrigation drying period. Using the nondimensional (ET_{ecadj}/ET_{ref}) values of ET, the average additional evaporation over the grass was estimated as 32%. The decreasing trend of ET over the time post irrigation was an indication of

evaporation of the intercepted water from the grass surface. However, in case of bare soil the actual ET pre irrigation was well below the reference ET and increased to equal to the reference ET during the irrigation. In terms of nondimensional ET about 27% additional evaporation occurred over the bare soil during irrigation due to the increased soil moisture. Similar values of nondimensional ET post and pre irrigation illustrates that there was no intercepted water to evaporate on the surface in the case of bare soil.

Accordingly, a series of experimental trials were conducted over cotton at various growth stages, introducing the eddy covariance-sap flow method to measure the total evapotranspiration and sap flow. Nondimensionalisation of these measurements using ET_{ref} gave idealized curves of the total evapotranspiration and sap flow for each stage, i.e pre-, during and post-irrigation, which permits calculation of the additional evaporation caused by irrigation and suppression of transpiration. These calculations showed that the greatest effect of overhead sprinkler on water losses was the significant increase of ET as mostly canopy evaporation and reduction in sap flow due to the wetness of the canopy. The amount of additional evaporation varied significantly with crop canopy condition and climatic factors especially advection.

The significant increase of total ET from partial canopy to full canopy indicates that canopy evaporation was higher in full canopy due to the greater area of canopy surface in full crop canopy condition and hence greater interception capacity. This result supported the conclusion that canopy evaporation was the dominant component in sprinkler irrigation. Higher rate of ET measured during irrigation in advective conditions, indicates that advective conditions can increase the additional evaporation in sprinkler irrigation substantially on the basis of climatic conditions especially wind speed. The additional evaporation due to irrigation using impact sprinklers varied from 37% at partial canopy condition to 80% at full canopy condition. Adevctive conditions increased this additional amount by 12% to 20% depending on the climatic conditions.

It was shown how the total canopy evaporation can be subdivided into its different components including additional evaporation during irrigation and canopy interception capacity using idealized nondimensional ET and sap flow. However, the droplet evaporation could not be separated due to the limitations of the instruments used under this study.

It was also shown how the ECV-sap flow data can be used to predict the magnitude of additional evaporation for different regions in various operating and climatic conditions. This can aid the irrigators to predict the additional evaporation in sprinkler irrigation at any region for different time, climatic and operating conditions.

The results showed that canopy evaporation including droplet evaporation during irrigation is the dominant component (about 80%) in additional evaporation followed by the canopy interception (about 20%). The average amount of additional evaporation would be about 6% of applied water under normal conditions and about 8% in advective conditions in major cotton growing areas in Australia. It means that irrigators in those places may need to apply 6-8% of additional water.

CERTIFICATE OF DISSERTATION

I certify that the ideas, experimental work, results, analyses and conclusions reported in this dissertation are entirely my own effort, except where otherwise acknowledged. I also certify that the work is original and has not been previously submitted for any other award, except where otherwise acknowledged.

Endorsement:

_____ _____

Md Jasim Uddin, Candidate **Date**

_____ _____

Professor Rod Smith, Principal Supervisor **Date**

_____ _____

Associate Prof. Nigel Hancock, Associate Supervisor **Date**

_____ _____

Dr. Joseph Foley, Associate Supervisor **Date**

ACKNOWLEDGEMENTS

First and foremost, I wish to acknowledge the expert guidance I received from my principal supervisor, Professor Rod Smith. I am very grateful to Rod for the time and effort he has invested in helping me to achieve this goal and for being an inspiration at every step of the way. His invaluable technical advice is always highly cherished. I equally thank my associate supervisor, Associate Professor Nigel Hancock, for his support and encouragement of excellence in all phases of my research particularly his expertise on micrometeorology.

I would like to thank Dr. Joseph Foley, for his help, support and encouragement during the period of my research particularly his help and support regarding the establishment of crop and irrigation system at the university's experimental research station. I wish to extend my sincere appreciation to Dr. Jochen Eberheard for his valuable help time to time regarding the instrumentation.

I would like to thanks those provided valuable assistance and inspiration throughout the study. I am deeply thankful to the University of Southern Queensland (USQ) for providing the major scholarship and to the Faculty of Engineering and Surveying (FoES) for additional financial support. I am also grateful to the National Centre for Engineering in Agriculture (NCEA) for providing research funds and support to accomplish this research work. I would like to thank all lovely staff of FoES and NCEA for their support and encouragement.

Words are lacking to express my humble obligation to my affectionate parents in law for their moral and spiritual inspiration who always wish my great success and pray for me. Thanks also to my brothers and sisters for their unrivalled love, moral support and sincere prayers.

I have a deep appreciation and regard for the kindness, affection and support of wife Ishrat Jahan whose encouragement, continuous support and inspiration made it possible to accomplish this research work. I would thank my loving friend for her patience while enduring significant absence of my time over the period. I thank my beloved daughter, Juwairiayah Ibtisam for her great sacrifice and patience and allow me to spend more time in research especially during my busy writing time.

I would like to dedicate this thesis to my late parents who taught me more in life than anyone else and who would be thrilled beyond words to see their son submit this dissertation for PhD degree.

ABBREVIATION

ABS	Australian Bureau of Statistics
AE	Available energy
Agplot	Agricultural Experimental Station
AI	Advection index
BR	Bowen Ratio
CNF	Cumulative normalized contribution
DOY	Day of year
EBR	Energy balance ratio
EC	Electrical conductivity
ECV	Eddy covariance
EF	Model efficiency
ET	Evapotranspiration
ET_{ec}	Unadjusted actual evapotranspiration measured by eddy covariance
ET_{ecadj}	Adjusted actual evapotranspiration measured by eddy covariance
ET_{ref}	Reference evapotranspiration
FoES	Faculty of Engineering and Surveying
F	Sap flow
GM	Genetically modified
HB	Heat balance
HPV	Heat pulse velocity
IRGA	Infrared Gas Analyzer
Irri	During irrigation period
MBE	Mean bias error
NCEA	National Centre for Engineering in Agriculture
NSW	New South Wales
Post	After irrigation
Pre	Pre/Before irrigation
RH	Relative humidity
R_{et}	Nondimensional number of evapotranspiration
R_f	Nondimensional number of sap flow
RMSE	Root mean square error
T	Transpiration
T_a	Air temperature
T_c	Canopy temperature
λE	Latent heat flux
λE_{adj}	Adjusted latent heat flux
USQ	University of Southern Queensland
VPD	Vapour pressure deficit
WDEL	Wind drift and evaporation losses
WS	Wind speed

PUBLICATIONS ARISING FROM THIS RESEARCH

Uddin, J., Smith, R., Nigel, H., & Foley, J. (2010). Droplet evaporation losses during sprinkler irrigation: an overview. *One Water Many Future, Australian Irrigation Conference and Exhibition*, Sydney, 8-10 June.

Uddin, J., Smith, R., Nigel, H., & Foley, J. (2010). Evaporation losses during sprinkler irrigation measured by eddy covariance technique. *One Water Many Future, Australian Irrigation Conference and Exhibition*, Sydney, 8-10 June.

Uddin, J., Smith, R., Nigel, H., & Foley, J. (2011). Evaluation of sap flow sensors to measure the transpiration rate of the plants during sprinkler irrigation. *Paper presented at the conference Society for Engineering in Agriculture (SEAg),* Gold Coast, Australia, 29-30 September.

Uddin, J., Smith, R., Nigel, H., & Foley, J. (2011). Eddy covariance measurements of the total evaporation during sprinkler irrigation-Preliminary results. *Paper presented at the conference Society for Engineering in Agriculture (SEAg),* Gold Coast, Australia, 29-30 September.\

TABLE OF CONTENTS

LIST OF FIGURES

LIST OF TABLES

Chapter 1: Introduction

1.1 Background

Water has been a main issue on the international agenda for the last 30 years, starting with the 1st International Conference on Water (Mar de la Plata, 1977), and followed by the International Conference on Water Resources and Arid Environment **(**Saudi Arabia, 2010). The use of renewable water resources has grown six-fold, while the world's population tripled in the 20th century. This population growth coupled with industrialization and urbanization has increased the competition among water users. Consequently, the importance of water conservation is increasing as a result of ever increasing demands on scarce water resources. As a result, the irrigation industry is facing restrictions, and in some cases reductions, in water availability and entitlements all over the world especially in arid and semi-arid regions. Irrigated agriculture, the largest water consumer all around the world as well as in the Australia, is now under pressure to increase water use efficiency. This can improve the crop production per unit of water applied and will contribute to water conservation. Among the irrigation systems, sprinkler irrigation is considered one of the best methods for achieving high application efficiencies (McLean et al. 2000).

Irrigated agriculture is a significant contributor to the Australian economy and is significant in world trade for several commodities. The irrigation industry is the major water user in Australia consuming up to 75% of all water diverted for use (Goyne & McIntyre 2002, Fairweather et al. 2003) of which cotton accounted for 12%, cereals for grain 11%, pasture for dairy cattle 10% and sugar 10% (ABS 2010). During 2009-10, 41000 irrigating agricultural business used 6596 GL of water at an

average of 3.6 ML ha^{-1} (ABS 2010). The gross value from irrigated agriculture was $7.25 billion in 1996-97 (Fairweather et al. 2003) and increased to $9.1 billion in 2004-05 (ABS 2006). This represents about 23% of the total gross value of agricultural production in Australia.

Farmers use a variety of irrigation techniques to apply water to their crops and pastures. Common systems include surface (i.e. furrow, basin, or border check), drip or trickle, and sprinkler (i.e. micro sprinklers, travelling guns, booms, centre pivots, lateral moves and solid set systems) (ABS 2006). Although surface irrigation is the major form of application, irrigating 1.5 Mha of land in Australia, sprinkler irrigation is becoming a preferred method as the water availability for irrigation is becoming limited. A significant amount of land (about 0.7 Mha) is being irrigated by sprinkler irrigation which is about 30% by area of Australian irrigation (ABS 2006). Sprinkler irrigation systems (mainly centre pivot and lateral moves) are currently installed in each of the major cotton producing areas from Emerald in Queensland through Hillston in New South Wales as well as in other areas in other states of Australia (Foley & Raine 2002). Increasing pressures on water availability, the potential yield benefits of improved control of soil-water in the root zone, potential for reduced labour, fertiliser and pesticide costs (Foley & Raine 2001) and very recently the increase of water price nearly doubling from $0.40/kL to $0.78/kL (ABS 2010) has raised grower interest in alternative irrigation application (sprinkler) techniques including large mobile irrigation machines. However, little is known about the performance of sprinkler irrigation under field conditions (Smith et al. 2002) in terms of losses during irrigation. Due to the lack of accurate information regarding the losses, a remarkable number of irrigators are still less interested to use this system in Australia.

Performance of the irrigation system is a major determinant of water use efficiency in irrigated agriculture (Raine et al. 2008). The efficiency of sprinkler irrigation

depends on the various losses that take place from the sprinkler nozzle until the point that water reaches the root zone (Steiner et al. 1983). Since, a negligible amount of water is lost in the conveyance of sprinkler irrigation system, major losses are the evaporation losses (Clark & Finley 1975, Steiner et al. 1983, Kincaid et al. 1986). The total evaporation losses in sprinkler irrigation include droplet evaporation, soil evaporation and canopy evaporation. Among these, droplet evaporation is typically considered as a major source of water loss ranging from zero to 45%. Accordingly, most of the previous research regarding the evaporation losses (e.g. Kohl et al. 1987, Tarjuelo et al. 2000, Lorenzini, 2004) conducted internationally has used different approaches to quantify the droplet evaporation losses, resulting in conflicting outcomes. Irrigation engineers and manufacturers also consider that the droplet evaporation component is the larger part of the losses when designing the irrigation system. Farmers often mentioned this reason not to adopt sprinkler irrigation system along with the other reason high cost of operation.

However, recent theoretical studies conducted by Thompson et al. (1993b, 1997) in USA reported that the droplet evaporation losses is less than 1% and is almost negligible in comparison with the subsequent losses from the wet soil and vegetation. This work also suggested that the canopy evaporation is the main contributor to the evaporation losses during sprinkler irrigation followed by soil evaporation and droplet evaporation. Thompson et al. (1993b) also reported that about 8% of the applied water is evaporated during irrigation, but only 3% would be a true loss in overhead sprinkler considering the suppression of transpiration which would have occurred without irrigation. Nevertheless, these predicted results were not verified due to the lack of appropriate instruments and technique. Most recently, Yonts et al (2007) has also indicted in a report that the evaporation losses in sprinkler irrigation varied from 0.5 to 4% depending on sprinkler type. Therefore it is assumed that, the evaporation losses in sprinkler irrigation would not be much more than a few percent.

There is also no doubt that the use of advanced technology (e.g., eddy covariance technique) real time measurement techniques to measure the evapotranspiration in continuous mode has enhanced our research capabilities. It has been used successfully over the last decade to measure evaporation from watersheds, grasslands, lakes, surface and drip irrigated fields and has some significant advantages over the other methods. However, a review of the literature provided no instances of it being used to measure evaporation losses occurring during sprinkler irrigation. Instead, research has focused on using traditional methods acknowledged to have many limitations. It is hypothesized that these limitations can be overcome by adopting this advanced novel technique. It is also assumed that the continuous measurements of total evapotranspiration during irrigation and subsequent periods will allow separation of the components of evaporation losses in conjunction with some additional measurements.

De Wrachien & Lorenzini (2006) reported that notwithstanding all the efforts, the phenomenon of evaporation losses and its relationship to other soil-plant-atmospheric processes has not yet been completely understood. Something new has to be added to the description of the process to reach a better assessment of the events. Bhavi et al. (2009) indicated that to obtain an insight into the exact magnitude of losses in sprinkler irrigation, it is also of paramount importance to accurately define the relationship between the losses and the factors affecting them. Similarly, McLean et al. (2000) stated that the components of the losses in sprinkler irrigation system need to be quantified accurately before any the design of irrigation systems can be improved.

The more efficient use of irrigation depends on better design and management of the system. Irrigation principles and practises for sprinkler irrigation have been advanced to the point that water application efficiency is significantly influenced by the amount of evaporation losses. Therefore, reliable and accurate information regarding

the evaporation losses associated with sprinkler irrigation is needed for designers as well as the equipment manufacturers to design and manufacture more efficient systems. Moreover, accurate information regarding evaporation losses during sprinkler irrigation is also needed to help farmers to choose a suitable irrigation system. Hence, there is a need to answer the following questions including:

- What does actually happen in case of evaporation and transpiration during sprinkler irrigation?
- Is the additional water requirement due to evaporation losses in sprinkler irrigation significant compared with the quantity applied?
- Is eddy covariance system capable of measuring the evapotranspiration during sprinkler irrigation?
- Is it possible to separate the components of evaporation losses during irrigation and subsequent periods with measurements eddy covariance and additional measurements?
- What is the major component of the evaporation losses during sprinkler irrigation?
- What would be the implication of eddy covariance measured data for irrigation management?

1.2 Research aim and hypothesis

The aim of this work is to use advanced (eddy covariance-sap flow) techniques in conjunction with additional measurements to estimate the total additional evaporation and its components during sprinkler irrigation and subsequent periods. The overall hypothesis of this research is that the additional water requirements in

sprinkler irrigation due to evaporation losses is small compared to the applied water. This research is based on the following component of hypotheses:

i. Total evaporation occurring during sprinkler irrigation can be measured directly using the eddy covariance technique.

ii. Additional water requirements due to the evaporation losses is a much smaller component in sprinkler irrigation water balance than is commonly perceived by the irrigation community.

iii. Total evaporation during sprinkler irrigation can be partitioned into the different components using eddy covariance-sap flow data including the beneficial evapo-transpiration and various evaporation losses.

iv. Magnitude of additional evaporation during irrigation can be predicted from climatic data for other regions and different irrigation management.\

The specific objectives of the project are set out in the section 2.11 of chapter 2.

1.3 Structure of dissertation

This dissertation contains seven chapters. The relationship between the chapters is shown in Figure 1.1.

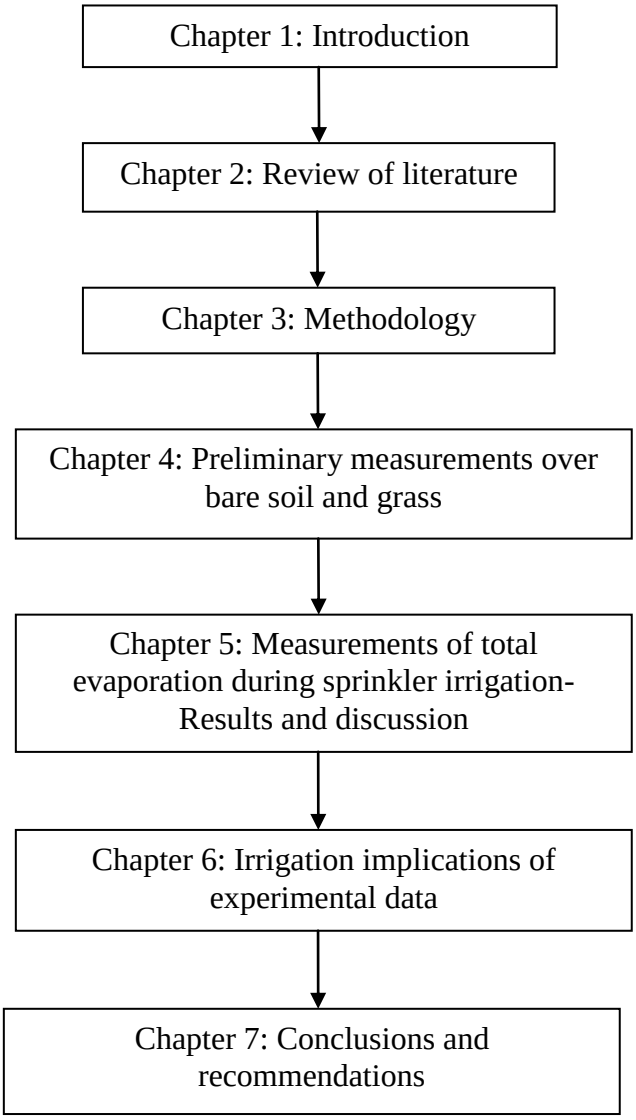

Figure 1.1: Structure of dissertation

Chapter 2 provides an overview of evaporation losses in sprinkler irrigation, comparison of existing methods to measure the evaporation losses including limitations of these methods and potential of alternative methods to overcome the limitations of the existing methods. This chapter also provides available literature regarding the additional measurement related to this method including appropriate methodology to measure the transpiration, canopy evaporation, canopy interception and soil evaporation.

Chapter 3 describes the detailed methodology to conduct the experiments. It includes the experimental description, measurements technique and the procedures followed for data quality assessment, processing and analysis. Chapter 4 provides the preliminary measurements of total evapotranspiration over the grass and bare soil to evaluate the capability of the ECV technique in measuring the total ET including the estimation of the additional evaporation during sprinkler irrigation.

Chapter 5 reports the results and discussion of the measurements of total evaporation and sap flow during irrigation and subsequent periods in different stages of a cotton crop. It illustrates the effect of irrigation on evaporation and transpiration including magnitude of increment and reduction. This chapter indicates the effect of advection on ET rates during sprinkler irrigation. It also provides the idealized curves with regression equations for ET and sap flow for different period of irrigation to establish predictive models.

Chapter 6 provides the irrigation implications of the experimental results including estimation of canopy interception capacity, components of additional evaporation and estimation of total volume of additional water requirements in sprinkler irrigation. This chapter also demonstrates the prediction of additional ET on the basis of climatic data for other selected parts of Australia. The major conclusions and recommendations for further research are presented in Chapter 7.

Chapter 2: Literature Review

2.1 Introduction

The magnitude of evaporation losses during sprinkler irrigation is still uncertain and there is disagreement in the published literature worldwide. Over the last fifty years, most of the theoretical and experimental research has been focused on quantifying the droplet evaporation losses and has concentrated on climate and equipment related factors. Although estimates are presented, limited studies have been reported so far to directly measure the total evaporation losses including canopy evaporation and droplet evaporation in a real crop in the field. This is possibly due to the lack of appropriate measurement technique.

The major objective of the present research is to measure the total additional evaporation and its components in sprinkler irrigation using a direct measurement technique. Therefore, a comprehensive review of the literature has been undertaken, firstly to understand the details of total evaporation losses and its components; and secondly to find an appropriate alternative measurement technique that can overcome the limitation of the current available methods.

This chapter reviews the published literature with respect to four main topics:

(i) an overview of evaporation losses and its components in sprinkler irrigation;
(ii) the strengths and weaknesses of the current measurement methods;
(iii) direct evaporation measurement by eddy covariance, as a potential alternative appropriate method, including its advantages and disadvantages; and

(iv) the requirements for additional measurements related to this method, including appropriate experimental methodology, to measure the transpiration, canopy evaporation, canopy interception and soil evaporation.

2.2 Overview of evaporation losses during sprinkler irrigation

2.2.1 Evaporation losses and its components

Sprinkler irrigation is a method of applying water to the soil by sprinkling (discharge of water from a nozzle) of water into air. In the most common sprinkler arrangement water emitted from the nozzle forms a jet, which impacts on a deflector plate and disperses as a thin sheet or as thin streams called ligaments. The ligaments then break up into droplets due to surface tension and aerodynamic drag forces as they travel from the nozzle to the soil surface. The difference between the amount of water leaving the sprinkler nozzle and the amount of water reaching at the soil surface is the evaporation loss.

During the travel through the air some portion of the water evaporates from the droplets to the atmosphere before it reaches the crop canopy or soil surface, called *droplet evaporation* and some drifts outside the irrigation area, called *drift loss* (McLean et al. 2000). The remainder of the water enters the canopy as precipitation. This portion of the water is partitioned between canopy interception and direct throughfall to the soil.

Canopy interception can be further divided into the portion remaining on the leaves and the remainder either dripping onto the lower leaves or the soil or running down the stem to the soil (Figure 2.1). The water remaining on the leaves, *intercepted*

water, interception, is then evaporated to meet the atmospheric demand and is called *canopy evaporation* (Wang et al. 2006).

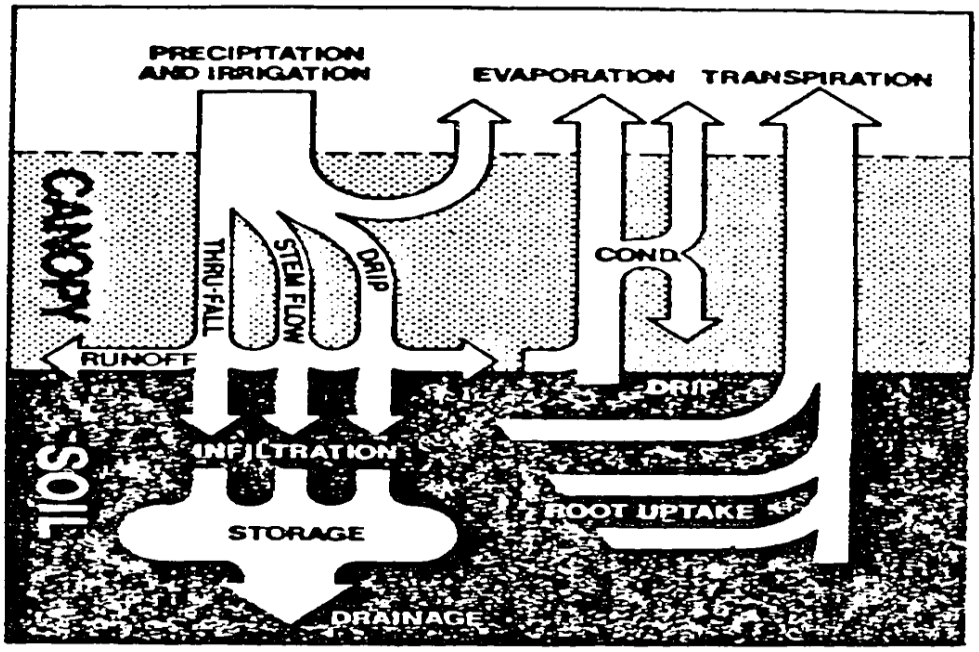

Figure 2.1: Diagram of the components of water flow through soil-plant-atmosphere system (source : Norman & Campbell 1983)

The soil water from direct throughfall is then similarly partitioned into four component viz.: (i) the portion of water evaporated from the surface through evaporation, *soil evaporation*, (ii) the portion that is lost by direct runoff, (iii) the portion which is available in the root zone of plant intake, and (iv) the portion lost by deep percolation. However, runoff and deep percolation can usually be considered negligible in sprinkler irrigation (Thompson 1986). McLean et al. (2000) pointed out that any drift losses that occur as a result of the wind are not considered a loss as long as the spray drift falls within the boundaries of the cultivated area. The drift component only affects the uniformity of water application. However, if the drift component leads to local over-application of water which results in deep percolation

below the root zone, then it should be taken into account in calculating the overall farm irrigation efficiency (McLean et al. 2000).

2.2.2 Magnitude of the losses

There is a substantial difference of opinion among researchers regarding evaporation losses in sprinkler irrigation. Field studies reported in the literature show estimates of evaporation losses ranging from near zero up to 45% (Frost & Schwalen 1955, Yazar 1984, Kohl et al. 1987) and it is commonly assumed that the droplet evaporation is a significant loss in sprinkler irrigation. On the other hand, theoretical studies reported that total evaporation losses should not be much more than 3% of applied water and where droplet evaporation should never be more than 1% (Thompson et al., 1993b, 1997).

Since droplet evaporation was considered the significant loss in sprinkler evaporation most of the studies (e.g. field tests, laboratory, analytic and physical-mathematical) have been conducted to quantify the magnitude of droplet evaporation loss during water application by means of sprinkler irrigation. However, these studies were not performed under the same terms and conditions, had different level of accuracy, and attained results that varied greatly (Table 2.1). Frost & Schwalen (1955) found that the droplet evaporation losses at the time of sprinkler irrigation were as high as 35-45% under extreme conditions. Analytic and laboratory investigations reported losses that ranged from 0.5 to 2% (Kohl et al. 1987). Yazar (1984), Kohl et al. (1987), Kincaid (1996) and Kincaid et al. (1996), reported losses that varied from 2 to 40% (mostly 10-20%) from field tests. From laboratory tests Kincaid & Longley (1989) found that droplet evaporation losses in sprinkler irrigation are usually smaller than 2-3%, even under high air temperature and low relative humidity. Under

normal conditions they were almost negligible. In comparison, under moderate evaporative condition the losses should not be more than be 5-10% (Keller & Bliesner 1990). Using the theory of heat transfer Inoue & Jayasinghe (1962) calculated that the droplet loss during sprinkler irrigation should not be more than 6% considering the rate of heat flow into the droplet. Similarly, Thompson (1986) observed that the transfer of energy to droplets during flight of sprinkled water is not sufficient for evaporating more than 1 to 2% of their volume. Using a modelling approach, Edling (1985) computed droplet evaporation losses during sprinkler irrigation ranging from 0.5-20% at different operating and climatic conditions. Most recently, Lorenzini (2004) estimated using an analytical model that the upper limit values of droplet evaporation varied from 3.7 to 8.6% for the droplet diameters ranging from 0.3 to 3 mm.

Table 2.1: Review of published evaporation studies regarding droplet evaporation losses

Investigator	year	Method	Evaporation range (%)
Christiansen	1942	Catch-can	1-42
Christiansen	1942	Thermodynamic	0.2-2
Frost & Schwalen	1955	Catch-can	3-45
George	1955	Catch-funnel	2-15
Inoue & Jayasinghe	1962	Thermodynamic	<6
Kraus	1966	Catch-can	3-9
Yazar	1984	Catch-funnel	2-31
Edling	1985	Modelling	0.5-20
Kohl et al.	1987	Chemical tracer in irrigation water	0.5-1.4
Kincaid & Longley	1989	Laboratory	2-3
Thompson et al.	1993b	Modelling	<1
Lorenzini	2004	Analytical and experimental	3.7-8.6

Thompson et al. (1993b, 1997) predicted that the droplet evaporation loss throughout the irrigation was less than 1% of applied water and is almost negligible in comparison with the subsequent losses from the wet soil and vegetation. This work over corn crop in USA also suggested that the canopy interception loss (more than 60%) is the main contributor to the evaporation during sprinkler irrigation followed by soil evaporation and droplet evaporation over the corn crop in USA. They also reported that the about 8% of the applied water was evaporated during irrigation, but only 3% would be the true loss in overhead sprinkler considering the suppression of transpiration which would have occurred without irrigation. Moreover, by calculating the energy available for evaporation, it was observed that the droplet evaporation should not be more than 2%. In this regard, Kume et al. (2006) pointed out that most of the water losses during wetting (rainfall) is due to evaporation of water intercepted and held on the canopy. The water vapour-exchange processes, which consist mainly of wet canopy evaporation and dry canopy transpiration, are quite different depending on whether the canopy is wet or dry. In dry condition, transpiration is the major part of ET over the crop surface while during irrigation canopy evaporation dominates the evapotranspiration due to the free water available to evaporate on the canopy (Kume et al. 2006).

Yonts et al. (2007) has also very recently reported that the canopy evaporation is the major contributing component in sprinkler evaporation losses. These researchers in Nebraska, USA compared different sprinkler devices with respect to the crop canopy and estimated the amount of water lost between the sprinkler nozzle and the top of the crop canopy, air evaporation and drift is 3% for low-angle impact sprinklers and 1% for spray heads. They have also provided a comparison of the different components of losses (Table 2.2).

Playan et al. (2005) reported that wind drift and evaporation losses (WDEL) represent a considerable amount in sprinkler irrigation, particularly in areas where the wind speed and atmospheric demand is high. They estimated the wind drift and evaporation losses (WDEL) for a solid-set sprinkler irrigation system was 15.4% and 8.5% during day and night, respectively in semi-arid weather conditions of Zaragoza (Spain). The loss was estimated as 9.8% during the day and 5.0% during the night for a lateral move sprinkler in the same condition.

Table 2.2: Components of evaporation losses for different types sprinkler devices (Yonts et al. 2007). The values within the bracket are (% of total losses)

Water Loss Component	Low-Angle Impact Sprinkler Water Loss (mm)	Spray Head Water loss (mm)	Low energy precision application (LEPA) Water loss (mm)
Air Evaporation and Drift	0.76 (20)	0.25 (3)	0.00 (0.00)
Net Canopy Evaporation	2.03 (53)	0.76 (38)	0.00 (0.00)
Plant Interception	1.02 (27)	1.02 (50)	0.00 (0.00)
Evaporation From Soil	Negligible	Negligible	0.51 (100)
Total Water Loss	3.81	2.03	0.51 (100)

2.2.3 Physical processes of the evaporation losses in sprinkler irrigation

Evaporation losses in sprinkler irrigation take place through the exchange of energy driven by the difference in temperature between droplets and their environment in three parts:

(i) energy exchange between the water droplets and atmosphere above the canopy,

(ii) exchange between water droplets and canopy, and finally

(iii) exchange of energy between water droplets and soil (Thompson 1986).

The evaporation of a liquid drop is essentially a combined process of mass and heat transfer. In this operation the heat for evaporation is transferred by conduction and convection from the environment to the surface of the droplet from which vapour is transferred by diffusion and convection back into the atmosphere (Ranz & Marshall 1952). In the process of evaporation the molecules absorb energy as latent heat. Whenever that individual molecule of water goes out, it takes that latent heat with it. Ranz & Marshall (1952) also stated that the rate of mass transfer per unit area of interface is a function of temperature, vapour pressure deficit, and the diameter and temperature of the droplets. Hardy (1947) described that when liquid is sprayed (discharged from the sprinkler nozzle) into air which has a different temperature, the temperature of the droplets will change depending upon the rate at which the heat is transferred to, or from, the air both by convection and evaporation.

2.2.4 Factors affecting evaporation losses

The amount of water that evaporates from droplets depends on many equipment-related factors (such as nozzle size, angle, operating pressure and height of the sprinkler) and climatic factors (like air temperature, air friction, relative humidity, and solar radiation and wind velocity). Besides this, travel time to reach the crop or soil surface is also an important factor which influences the losses.

2.2.4.1 Equipment-related factors

Playan et al. (2005) reported that, among the system variables, the nozzle size and droplet diameter have a significant effect on wind drift and evaporation losses

(WDEL). Equipment variables that affect the droplet diameter are the nozzle size, geometry, and operating pressure. Larger nozzle size produces larger diameter (Keller & Bliesner 1990).

Droplet size resulting from the nozzle is most important factor in evaporation losses. Kohl et al. (1987) reported that small droplets are more susceptible to evaporation. The size of droplets was found proportional to the nozzle diameter (Kohl & Wright 1974, Dadiao & Wallender 1985, Solomon et al. 1985) and inversely proportional to the operating pressure (Dadiao & Wallender 1985). Montero et al. (2003) indicted that an increase in operating pressure results in smaller droplet diameter with an increase in WDEL. Frost & Schwalen (1955) found that a 25% increase in nozzle operating pressure increased the evaporation losses by 25%. In addition, many researchers have found that the spray droplet size at any distance from the sprinkler is related to the nozzle size (Dadiao & Wallender 1985, Edling 1985, Hills & Gu 1989). Chaya & Hill (1991) reported that for a given nozzle size, the droplet size was found to be inversely proportional to the operating pressure. Kohl & DeBoer (1985) reported that for low-pressure agricultural sprinklers the geometry of the spray plate surface, rather than the nozzle size and operating pressure, was the dominant parameter that influenced drop size distribution. They also identified that smooth spray plates produce smaller droplets than coarse, grooved plates.

Smajstrla & Zazueta (2003) reported that since the evaporation occurs from the surface of the water droplets, the total surface area of the water droplets greatly affects the amount of evaporation loss. For a unit volume of water, the surface area doubles as the droplet diameter decreases by half. For this reason, evaporation rate increases as droplet size decreases if other factors remain constant, and the factors that cause droplet size to decrease will cause evaporation loss to increase. Frost and

Schwalen (1955) noted that smaller nozzle diameters tended to break up the fine droplets leading to greater evaporation losses. Edling (1985) & Thompson et al. (1993b) found that**,** the drift and evaporation losses are inversely proportional to the droplet diameter, whereas Lorenzini (2004) and De Wrachien & Lorenzini (2006) proposed a different analytical model and suggested, against all the available evidence (e.g. results of Edling 1985, Thompson et al. 1993b), that the evaporation losses are directly proportional to the droplet diameter.

2.2.4.2 Climatic factors

The amount of water that evaporates from the droplets as well from the wet canopy is closely related to the evaporative demand of the atmosphere, mainly influenced by the climatic factors. The most cited WDEL affecting climatic variables are wind speed, air temperature, and relative humidity and vapour pressure deficit mentioned by Tarjuelo et al. (2000). Among these, wind speed has often been recognized as the most vital factor affecting WDEL (Playan et al. 2005).

The evaporative demand is determined by the energy available for evaporation and the capacity of the air to store and transmit water vapour. The evaporation process requires 2.42 kilojoules of energy to convert 1 gram of water from the liquid to the vapour form. Therefore, the energy must be available from the environment surrounding the sprinkler.

A close relationship between losses and vapour pressure deficit of the air was obtained by Christiansen (1942) and Frost & Schwalen (1955). Ortega et al. (2000) estimated that the evaporation losses are a function of vapour pressure deficit to the power of 0.5 and wind speed. Frost & Schwalen (1955) found that losses vary approximately proportional to wind speed and inversely proportional to the relative humidity. Bavi et al. (2009) found that wind speed and vapour pressure deficit were

the most significant factors affecting evaporation losses which followed the exponential relationship.

Smajstrla & Zazueta (2003) pointed out that wind increases evaporation rates by transporting water vapour away from the evaporating surface. Wind also increases evaporation by transporting warmer or drier air from surrounding areas to displace the moist, cool air above an irrigated surface. Lorenzini (2002) found that the evaporation losses were greatly affected by air temperature with a logarithmic relation. Abu-Ghobar (1993) reported that the evaporation losses increased with decreasing relative humidity and increased with air temperature and wind velocity. Yazar (1984) observed that wind speed and vapour pressure deficit are the predominant factors that affect evaporation losses significantly during sprinkler irrigation. He concluded that the losses are exponentially correlated with wind speed and vapour pressure deficit. Hermsmeier (1973) suggested that air temperature and rate of application were more important factors responsible for evaporation losses than wind velocity or relative humidity.

McNaughton & Jarvis (1983) investigated the impact of dry or moist air advection on the local equilibrium saturation deficit and observed that this would result in either the enhancement or depression of the evapotranspiration (ET) rate. For extensive areas of short grass or crops with wet or dry surface, they found that the advection component was typically about one-fourth of the radiation component. Tolk et al. (2006) also reported that advective enhancement of ET occurs when drier, hot air is transported into the crop by wind and can be an important factor in the water balance of irrigated crops in a semi arid climate.

The time available for evaporation to occur is the relatively short time beginning when a water droplet leaves the nozzle and ending when it falls on the ground or

vegetated surface. When water is sprayed at greater heights and over greater distances, this opportunity time for evaporation is increased (Yazar 1984). Thus, more evaporation would be expected to occur from a sprinkler installed on a tall riser than from the same sprinkler (operated at the same pressure so that the drop size distribution is the same) installed on a short riser (De Wrachien & Lorenzini 2006, Thompson et al. 1993b). Wind speeds are higher at greater heights above the ground surface, where there are few obstacles to air movement. Thus, evaporation loss from sprinklers mounted on tall risers is also increased because of these higher wind speeds.

2.2.5 Impacts of sprinkler irrigation

2.2.5.1 Rate of evapotranspiration (ET)

Studies have estimated the differences in ET rates between wet and dry surfaces just after irrigation events, but not during the irrigation itself due to the lack of means of measurements. McMillan & Burgy (1960), Frost (1963) and Seginer (1967) observed similar ET rates for both wet and dry crops with non-limiting soil moisture condition. However, in the case of taller crops, like orchard the wetted foliage ET rate has been reported to be greater than dry foliage (McNaughton & Black 1973, Stewart 1977, Singh & Szeicz 1979). Waggoner et al. (1969), during typical summertime conditions in Connecticut (USA), found short-term ET rates of wet corn canopies to be more than double that of dry corn canopies. This difference only lasted for about 15 minutes, after which the ET rates became similar for both canopies. According to the literature, the only previous works where ET or transpiration has been measured during a sprinkler irrigation event are those of Frost & Schwalen (1960), Sternberg (1967) and Tolk et al. (1995), Frost & Schwalen (1960) reported that rate of evapotranspiration in dry-leaf condition equalled or exceeded wet-leaf evapotranspiration under similar atmospheric conditions using weighing lysimeters,

Sternberg (1967) used weighing lysimeters to study rye grass ET during and after sprinkler irrigation and reported that ET was almost suppressed during irrigation and was decreased by about 33% after irrigation, as compared with that of a non irrigated lysimeter. Thompson et al. (1993b) used their model to predict some additional evaporation during sprinkler irrigation. Most recently, Martinez-Cob et al. (2008) reported that during the day time irrigation there was a significant decrease in ET (32-40%). Playan et al. (2005) found that reference ET estimated by Penman-Monteith method decreased by 0.023 mm hr^{-1} (2.1% of WDEL) did not significantly contribute to the crop water requirements.

2.2.5.2 Rate of transpiration

Norman & Campbell (1983) stated that during sprinkler irrigation, transpiration may be zero due to evaporation from intercepted water on leaves and soil. Reduction of crop transpiration and soil evaporation results in the conservation of soil water that would otherwise be depleted by the crop (McNaughton 1981, Steiner et al. 1983). Tolk et al. 1995 reported that this can reduce the gross interception loss by 6.6% via suppression of transpiration by 50% or more during irrigation. Thompson et al. (1997) stated that a significant impact of sprinkler irrigation is the reduction of net evaporation losses (7.2% and 2.6% for impact and spray type sprinkler nozzles respectively) by depressing transpiration. More recently, Martinez-Cob et al. (2008) found a significant decrease in evapotranspiration (32-55%) and transpiration (58%) during irrigation period compared to the dry (without irrigation) period.

2.2.5.3 Modification of microclimate

Evaporation loses during sprinkler irrigation is not only a direct loss of water, but it also has a significant effect on microclimate. It improves the microclimate of the

irrigated area by reducing temperature (Thompson et al. 1993b, Tolk et al. 1995) and vapour pressure deficit (Tolk et al. 1995, Chen 1996, Saadia et al. 1996) which leads to a decrease in the transpiration (Tolk et al. 1995) and soil evaporation.

Liu & Kang (2006) reported that field microclimate can be affected significantly by sprinkler irrigation not only during the period of irrigation but also during the irrigation intervals. They observed that the vapour pressure deficit (VPD) and air temperature above the canopy were lower in the sprinkler irrigated field compared to surface irrigated fields throughout the irrigation interval where the effect on temperature lasted 2-3 days after the irrigation. They revealed that the evaporation over this period was about 3-11% lower in a sprinkler irrigated field compared to the surface irrigated field during three winter seasons. Similarly, Kang et al. (2002) found that the cumulative surface evaporation at the top of the canopy under sprinkler irrigation was 12% lower than that under surface irrigation.

It is generally believed that the evaporation losses/WDEL is not entirely loss since they partly contribute to decrease the crop water requirements (Tarjuelo et al. 2000). McNaughton (1981) indicated that the part of droplet and canopy evaporation replacing crop ET, should be regarded as consumptive and beneficial, whereas Burt et al. (1997) described it as consumptive but non beneficial.

2.3 Studies on evaporation losses during sprinkler irrigation – 1. Experimental

2.3.1 Irrigation measurement via ‘catch-cans’

The losses are conventionally determined in the field from volumetric or gravimetric measurement of water collected in ‘catch-cans’. These are difference of the depth of

water applied and the depth of water received in the catch-cans (Kohl et al. 1987) and their use is laborious labour intensive, and prone to error (Figure 2.2). An inherent problem in this method is that the evaporation loss also includes any water evaporated from the catch-cans during the irrigation. Accurate measurement of water that reaches the ground is also very difficult especially in windy conditions which increase the sampling area due to drift. To avoid these difficulties of measurement, wind drift losses are often included with the evaporation losses (McLean et al. 2000). Kohl et al. (1987) reported that measurements using catch-cans commonly have major experimental error. Seginer et al. (1991) also reported that catch-cans based measurement may be subjected to relevant measurement error and even evaporation from the catch-cans themselves during the experiments. Playan et al. (2005) stated that the diameter of the catch-cans used in experiment may have an effect on results. Since there are no alternative methods to measure the loss, most of the studies have been conducted by this method. However, they differed in the details of the method.

Figure 2.2: Measuring the volume of water in a catch-can using measuring cylinder (source: Smith, Cotton CRC Water Team)

Christiansen (1942) was the pioneer in both experimental and theoretical research concerning evaporation losses from sprinkler irrigation. He investigated the droplet evaporation losses from sprinklers by using mass-balance (catch-cans) technique under different climatic and operating conditions at Davis, California. He estimated from field tests that the losses ranged from less than 10 to 40% in the afternoon and approximately 4% in the morning, concluding that a significant amount of the loss was due to evaporation from the catchment devices. He also developed a theoretical equation to predict the evaporation losses during sprinkler irrigation on the basis of thermodynamic principles and reported that the evaporation loss from the droplets is negligible compared to the losses from crop canopy and soil.

Using the catch-cans technique, Frost & Schwalen (1955) estimated that the droplet evaporation losses were as high as 35-50% during the day time under extreme conditions of bright sunlight, high air temperature and low humidity which prevails in Arizona. Further investigation reported that the losses formerly attributed to the droplet evaporation actually occurred after water reaches the catch cans. After appropriate correction it was found to be 3 to 10% under most conditions. They also established a nomograph summarising the relationship between the spray losses and different operating as well as climatic factors based upon a large number of field trials.

2.3.2 Irrigation measurement via electrical conductivity

To minimize the errors in the catch-cans method, George (1957) used an electrical conductivity (EC) method to estimate the droplet evaporation loss. He found that the losses ranged from 2% at a relative humidity of 48% with wind velocity 1.79 m s^{-1} to 15% at a relative humidity of 14% and wind speed of 9.95 m s^{-1}. Accordingly, he stated that losses were highly correlated with relative humidity, but no correlation

was found with vapour pressure deficit. He estimated that up to 40% of the measured losses could be attributed to the total evaporation losses from the catch cans.

Using the same method (electrical conductivity) Kraus (1966), estimated the losses ranged from 3.4 to 17% after adjusting for catch can evaporation. To reduce the evaporation from the metal catch cans, cans were painted white and filled to a depth of 6 mm. He also mentioned that evaporation and total loss was approximately proportional to the vapour pressure deficit, but no apparent relationship with wind velocity.

Based on the George (1957) work, Hotes (1969) reported that the droplet evaporation losses during sprinkler irrigation was linearly related to wind speed and may be less than 4% under most operational conditions. Hermsmeier (1973) carried out an experiment in the Imperial Valley of California using the electrical conductivity method and placed oil in the catch cans to reduce the evaporation from the catch container. He determined that the evaporation was reduced by 17.2% from that measured without oil. He measured the evaporation losses to be 2 to more than 50% under a variety of climatic conditions ranging from temperatures between 21 – 42 ^{0}C, wind speed 8.1 m s^{-1} and relative humidity 11 – 87%.

Yazar (1980) quantified the evaporation losses which ranged from 1.5 to 16.8% of the sprinkled volume at Med, Nebraska, using an electrical conductivity method. He also found that the wind speed and vapour pressure deficit were the most significant factors in evaporation losses which increased exponentially. He also found that the least significant factor on evaporation losses was the operating pressure. Drift losses were measured as 1.5 to 15.1% which was increased with the second power of the wind velocity and decreased with increasing distance in downwind direction. The estimated combined losses varied from 1.7 to 30.7% of the applied water.

2.3.3 Irrigation measurement using other techniques

Myers et al. (1970) conducted an experiment in an environmental control chamber at Gaineville, Florida and estimated the losses as 0.2-1.1%, while the evaporation from the canopy surface varied from 3.5 to 60% of the total volume applied. They also observed that evaporation loss during flight would not be more than 5% under most conditions. Using potassium ion as a chemical tracer in the irrigation water, Kohl et al. (1987) measured the evaporation losses as 0.5 to 1.4% for smooth spray plates and 0.4 to 0.6% for coarse serrated plates in a low pressure sprinkler.

Clark & Finley (1975) studied the effect of climatic factors on evaporation losses using a mass balance technique (Plastic fuel funnels and bottles) to measure spray evaporation at Bushland, Texas and found that wind speed and vapour pressure deficit were the most influential climatic parameters in evaporation losses. For wind speed less than 4.5 m s^{-1}, vapour pressure deficit was the most dominant parameter and the losses increased exponentially between wind speeds of 4.5 and 8.5 m s^{-1}. They reported that the average loss in the Southern Plains was approximately 15 percent and that up to 79% of the evaporation losses could be attributed to the wind speed.

2.3.4 Experimental studies – Summary and conclusion

Reviewing the available literature, it is concluded that the experimental studies have the following limitations:

(i) there were differences in definition of the losses,
(ii) the accuracy of experimental techniques,
(iii) evaporation losses were over estimated due to inclusion of evaporation losses from catch-cans,
(iv) it was difficult or not possible to separate the different components, and
(v) laborious and time consuming.

2.4 Studies on evaporation losses during sprinkler irrigation – 2. Model-based

2.4.1 Modelling approaches

Various models from simple statistical regression equations to complex physical-mathematical models are available to quantify the droplet evaporation during sprinkler irrigation. Statistical models are adequate for describing bulk responses but provide limited detailed information. On the other hand, physical-mathematical models provide better information on individual parameters, although they need more extensive input parameters. Both modelling approaches have been used to describe and study evaporation losses during sprinkler irrigation and are reviewed below.

2.4.2 Statistical models

Recent studies, predominantly in Europe (e.g., Trimmer 1987, Keller & Bliesner 1990, Faci & Bercero 1991, Montero et al. 1999, Tarjuelo et al. 2000, Faci et al. 2001, Dechmi et al. 2003, Playan et al. 2004, Bavi et al. 2009,) have attempted to use the experimental data in regression models (Table 2.3) to quantify the interaction of the climatic and operating factors. However, quantifying the evaporation losses in sprinkler irrigation is very difficult due to a number of factors both climatic (air temperature, air friction, relative humidity, solar radiation, wind velocity etc.) and operating (droplet diameter, nozzle size, sprinkler height, operating pressure etc.). The problem is particularly acute with respect to separation of the components of losses. In that case, resorting to statistical (empirical) formulae often becomes the only way to circumvent the difficulties. However, the results from this approach are highly dependent on application of particular statistical techniques, which may vary from author to author. The statistical approach is adequate for describing empirical relationships but provides limited information on the physical processes involved.

Table 2.3: Empirical equations used for wind drift and evaporation losses (WDEL) estimation. The independent variables are: Specific heat of water (C_p, J kg^{-1} °C^{-1}), Latent heat of vapourization (kj kg^{-1}) (nozzle diameter (D_{nozzle}, mm), vapour pressure deficit (e_s-e_a, kPa), operating pressure (P, kPa), wind speed (W & U, m s^{-1}), evapotranspiration (ET_0, mm day^{-1}), air temperature (T_a, ^{O}C), and water temperature (T_w, ^{O}C)

Reference	Empirical equations
Christianse n (1942)	$E = \frac{100 C_p \Delta T}{L}\left[\frac{e_w - e_a}{e_w - e_a - 0.00067P(T_a - T_w)}\right]$
Mather (1950)	$E = \rho_a UH(W_{down} - W_{up})A1$ (For fixed overhead sprinkler) $E = \rho_a UB(W_{sat} - W_0)A\pi r^2$ (For rotating sprinkler)
Trimer (1987)	$E = \left[1.98 D_{nozzle}^{-0.72} + 0.22(e_s - e_a)^{0.63} + 3.6X10^{-4} h^{1.16} + 0.14W^{0.7}\right]^{4.2}$
Keller & Bliesner (1990)	$WDEL = \left[1 - \left(\begin{matrix}0.976 + 0.005ET_0 - 0.00017ET_0^{\ 2} + 0.0012U - \\ IG(0.00043ET_0 + 0.00018U + 0.000016ET_0U)\end{matrix}\right)\right]100$
Yazar (1984)	$E = 0.389\exp^{(0.18W)}(e_s - e_a)^{0.7}$
Seginer et al. (1991)	$Loss = \frac{Q_e}{Q_s} = 0.0087\exp^{0.213W}(T_a - T_w)^{0.58}$ $Loss = \frac{(Q_e + Q_d)}{Q_d} = 0.03222\exp^{0.075W}(T_a - T_w)^{0.69}$ (Semi arid condition)
Hussein (1993)	$E = 10.86 - 14.29D_{nozzle} - 0.79RH + 1.79T_a - 1.75U + 0.0031P$
Montero et al. (1999)	$WEDL = 7.63(e_s - e_a)^{0.5} + 1.62U$
Faci & Bercero (1991)	$WEDL = 20.44 + .75U$
Tarjuelo et al. (2000)	$WEDL = 0.007P + 7.38(e_s - e_a)^{0.5} + 0.844U$
Faci et al. (2001)	$WEDL = 0.74D_{nozzle} + 2.58U + 0.47T_a$
Dechmi et al. (2003)	$WEDL = 7.479 + 5.287U$
Bavi et al. (2009)	$E = 4.4\exp(0.66U)(e_s - e_a)^{-0.215} T_a^{-0.115} P^{0.381}$

2.4.3 Overview of physical-mathematical models

Physical-mathematical models are developed on the basis of mathematical equations representing the physical process. These experimentally verified models, although requiring more extensive input data, provide a much better means of predicting actual values. The advantages of physical modelling over other techniques (empirical equations) are: (i) it can minimize the knowledge gaps (ii) it can predict the value accurately by minimizing experimental errors, and (iii) a proven model can be a valuable engineering and research tool for the scientists. The physical-mathematical modelling approach of droplet evaporation is based on combining the equations accounting for the water droplet evaporation with particle dynamics theory.

2.4.4 Droplet trajectory models

The droplet evaporation-trajectory model is based mainly on mass and heat transfer and ballistic equations. Langmuir (1918) first proposed a differential equation for the rate of mass transfer from a still droplet, considering diffusion is the sole mechanism of vapour movement from the droplet, and that the droplet temperature is equal to the wet bulb temperature of ambient gas for an isolated droplet, which can be expressed as:

$$\frac{dm}{dt} = -\frac{4\pi r D_V M}{RT}(e_S - e_O) \qquad (2.1)$$

where m is the mass of the droplet (Kg),

t is the time (s),

r is the droplet radius (m),

D_v is the mass diffusion of vapour in the gas ($m^2\ s^{-1}$),

M is the gram molecular weight of vapour (Kg $mole^{-1}$),

R is the universal gas constant (J K^{-1} $mole^{-1}$),

T is the absolute temperature of the droplet (^{O}K),

e_s is the saturated vapour pressure of the droplet at the droplet temperature (kPa), and

e_o is the vapour pressure at some larger distance from the droplet (kPa).

Hardy (1947) presented a modified equation similar to that of Langmuir for the rate of evaporation from the surface of a sphere accounting for forced air convection as:

$$\frac{dD_p}{dt} = -2\left(\frac{D_v}{D_p}\right)\left(\frac{\rho_a}{\rho_1}\right)\left(\frac{M_v}{M_a}\right)\left(\frac{e_s - e_o}{P}\right)N_{Nu} \tag{2.2}$$

where D_p is the droplet diameter (m),

M_v and M_a are the molecular weight of vapour and air respectively (Kg mole^{-1}),

ρ_a and ρ_1 are the density of air and water droplet respectively (Kg m^{-3}),

$(e_s - e_0)$ is the difference in the saturation pressure at wet and dry bulb temperature (kPa),

P is the partial pressure of air (kPa), and

N_{Nu} is the Nusselt Number (dimensionless).

Hardy (1947) presented an expression for Nusselt Number given by Frossling (1938) to account for the mass transfer from a droplet under forced convection, for Reynolds number from 2 to 800, given as:

$$N_{Nu} = 2.0 + 0.552 N_{\mathrm{Re}}^{0.5} N_{Sc}^{0.33} \tag{2.3}$$

where N_{Nu} is the Nusselt No (dimensionless),

N_{Sc} is the Schmidt No (dimensionless),

N_{Re} is the Reynolds No (dimensionless),

ν_a is the kinematic viscosity of the air (m^2 s^{-1}), and

V_r is the relative velocity of the between droplet and air (m s^{-1}).

Seginer (1965) proposed the following differential equation, describing droplet ballistics in an original way using an empirical drag coefficient C_q and an empirical non-dimensional exponent q,

$$g - \frac{dV}{dt} = C_d V^q \tag{2.4}$$

where g is the acceleration of gravity (m s^{-2}),

V is the velocity (m s^{-1}),

t is time (s),

The drag coefficient, C_d for a sphere can be found in the literature to be a function of the Reynolds' number as shown in equation (2.5).

$$C_d = \frac{24}{R_e} + \frac{6}{R_e} + 0.4 \tag{2.5}$$

Various authors have developed droplet evaporation models based on the heat and mass transfer theory for numerous purposes such as chemical spray (application of hot gas through scattering a jet of droplets) drying, agricultural spray (application of pesticides through scatter in a mass or jet of droplets) as well as for sprinkler (an irrigation device that discharges water into the air forming a jet of water droplets) droplet evaporation. Ranz & Marshall (1952) first developed a model to estimate droplet evaporation using heat and mass transfer equations and presented an equation for molecular transfer rate during evaporation along the flight path of the droplet. They used the model in chemical spray drying for very small diameter droplets with low Reynolds Number (0-200). Most subsequent investigators have used the heat transfer theory to describe the evaporation from droplet and have referenced the work of Ranz & Marshal (1952). Starting from the equation of Marshall (1954), Goering et al. (1972) arrived at an equation similar to Hardy's for studying the change of diameter in smaller (15-135 μm) droplets.

Williamson & Threadgill (1974) also used the mass diffusion equation in a form similar to Ranz & Marshall (1952) for agricultural spray, considering diameters ranging from 0.1 to 0.2 mm. They concluded that the results of their model were accurate under experimental conditions, when compared to horizontal and vertical displacements and change in droplet diameter due to evaporation.

Kincaid & Longley (1989) theorized an empirical model based on the above theory to predict the droplet evaporation and assess the role of changes in water temperature in the evaporation process. They assumed, and proved that, the temperature of the droplet does not necessarily reach the wet bulb temperature of the air instantaneously as the droplet leaves the nozzle, which was assumed by most previous researchers. They reported that this assumption may be correct for the spraying of agricultural chemicals where the drops are small (<0.55 mm). They also considered that diffusivity is a function of air temperature and pressure while others considered temperature only. Model predictions were reasonably accurate but there was a tendency for the model to under-predict loss rates for the smallest drops measured (0.3 to 0.5 mm). Some of the difference may be due to experimental errors in measuring loss from the smaller drops.

Based on the principle of impulse momentum, Edling (1985) established a model for estimating kinetic energy, evaporation and wind drift of droplets from low pressure irrigation sprinklers in order to determine the influence of design and meteorological parameters on droplet behaviour. He concentrated mainly on the effect of droplet size and its impacts on soil erosion. He verified his predicted results with those of Williamson & Threadgill (1974) and observed a similar trend for small droplet diameter. However, he recommended that additional verification was needed for the model through appropriate experimentation.

2.4.5 Plant-environment energy balance models

To understand the physical and environmental effect of sprinkler irrigation, it is necessary to understand the interactions among the soil-plant-atmosphere system. These interactions can be solved by the different equations governing the energy and mass budgets of the soil-plant-atmosphere system and depend on atmospheric (air temperature, relative humidity, wind speed, solar radiation), plant (type, leaf angles, leaf area index, canopy structure & height) and soil factors (soil texture & structure, soil temperature etc).

Various plant- environment models are available and range from simple statistical regression equations to complex theoretical-physical mechanistic models. So far, numerous plant-environment models have been developed based on the same principles and differential equations. However, these models differ in various process and solving techniques.

Among these Stewart & Lemon (1969) first presented a model named SPAM to describe the plant canopy phenomenon neglecting soil-water processes. They considered the effects of radiation, turbulent convection, and stomatal characteristic of the plant to develop their model. However, the proposed model ultimately became unrealistic to simulate the canopy energy balance due to neglect of some phenomenon (i.e., condensation, precipitation interception etc.). The model also faced difficulties through the neglect of data like soil surface temperature, surface water content and water potential.

Thereafter, a model was presented by Goudriaan (1977) including below soil surface processes, but ignored precipitation-interception and bidirectional canopy reflectance. Also, the model was written in an old computer language which is unavailable today.

Norman (1982) developed a complete mechanistic model titled CUPID, describing the whole processes involved in soil-plant atmosphere system of evaporation in sprinkler irrigation. The CUPID model does consider precipitation-interception, as well as condensation, bidirectional canopy reflectance, and the heat and water flux with water storage below soil surface. CUPID is a comprehensive soil-plant atmosphere model that uses inputs of leaf physiological characteristics (photosynthesis, stomatal conductance, and respiration), canopy architecture, and soil characteristics (heat and water properties) with boundary conditions at the bottom of the root zone and above the canopy. Although it has some limitations, it is considered the most thorough model for simulating the water and energy budget during an irrigation cycle (Thompson 1986).

2.4.6 Combination trajectory/environment models

Thompson et al. (1993a) developed a unique comprehensive model named 'CUPID-DPEVAP' to assess water losses during sprinkler irrigation of a plant canopy under field conditions. The combination of equations governing water droplet evaporation based on the heat and mass transfer analogy used by Ranz & Marshall (1952) as reviewed in section 2.4.4, linked with temperature-droplet model presented by Longley & Kincaid (1989), and droplet ballistics equations (three dimensional) with the plant-environment energy model 'CUPID' created by Norman (1982), were used in their model. Further they included droplet heat and water exchange above the canopy, along with the energy associated with cool water impinging on the canopy and soil.

The CUPID-DPEVAP model was able to give results in reasonable agreement with field measurements carried out in experimental plots equipped with low pressure sprinkling systems and lysimeters. The model was also used to quantify the partitioning of water losses between droplet evaporation, evaporation from wetted

canopy and soil, and transpiration during irrigation. The model was verified through field water balance measurements using monolithic lysimeters.

(a)

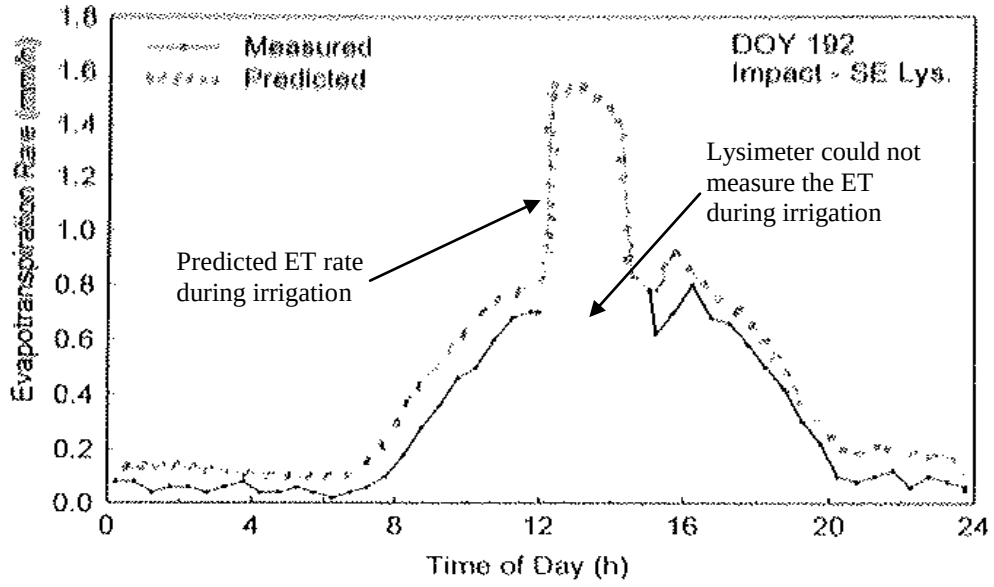

(b)

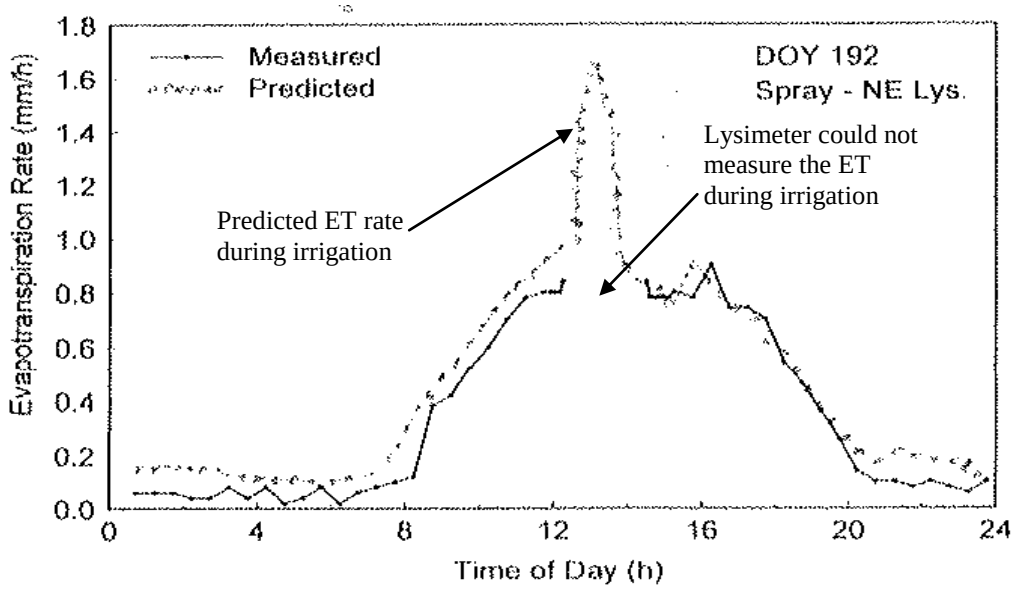

Figure 2. 3: Measured and predicted value of evapotranspiration during sprinkler irrigation for (a) impact sprinkler (b) spray nozzle (source: Thompson et al. 1997)

However, the experimental values of total ET were lower than the predicted values in the period with no irrigation. Most importantly, they could not verify the predicted values of model during the irrigation, because they were not able to measure the ET through lysimetry during the irrigation (Figure 2.3). They attempted to verify the model by comparing predicted air temperature and vapour pressure above the canopy during irrigation with measurements of these parameters and successfully predicted these climatic parameters using their model.

Most recently, Lorenzini (2004) developed an analytical model considering the effects of air friction (ignored in previous models) on droplet evaporation which is relevant in a turbulent flow (Reynolds Number >1000). He did not consider the physical (mass and heat transfer) changes of droplet to develop the model. The model proved to fully match the kinematic results obtained by more complicated procedures of Edling (1985) and Thompson et al. (1993b). He compared the field measurements and theoretical values in terms of travel distance for the model of Edling as well as Thompson et al. and for time-of-flight (Thompson et al. 1993b). The observed data of Lorenzini & Edling showed reasonable agreement in two cases (droplet diameter 1.5 mm and 2.5 mm), but poor agreement with droplet diameter of 0.5 mm. A comparative analysis based on data from Thompson et al. *(*1993b) in terms of travel distance and time-of-flight showed a difference with a droplet diameter of 0.3 mm. He recommended that the model still needs further verification to determine aerial water droplet evaporation and conscientiously obtained experimental evidence would also help in the full physical comprehension of the phenomenon.

2.4.7 Model-based studies – Summary and conclusion

Reviewing the comparative approaches, it is concluded that among the different procedures now available:

(i) the heat and mass transfer approach combined with ballistic theory offers a sound basis for the assessment of evaporation from falling droplets and the results are in reasonable agreement with experimental data for Reynolds Numbers (generally lower than 1000) that fall, mainly, under the laminar and/or intermediate flow laws,

(ii) the Lorenzini (2004) model has proved to be kinematically reliable to analyse the droplet evaporation losses from both a qualitative and quantitative point of view, particularly for small droplet diameters and large Reynolds Numbers (turbulent flow), and

(iii) considering all the parameters incorporated within the model CUPID-DPEVAP developed by Thompson et al. (1993a), it can be considered the most complete model available to quantify the evaporation losses in sprinkler irrigation.

However, these models should be validated through appropriate experimentation.

2.5 Evaluation of the methods to estimate evapotranspiration (ET) for partitioning

Evapotranspiration (ET) is a term used to describe the sum of evaporation and plant transpiration from the land surface, usually vegetated, to atmosphere. In environmental and agricultural usage the term ‘evaporation’ refers to the movement of water to the air from sources such as the soil, canopy interception, and water bodies. Transpiration is the movement of water within a plant and the subsequent loss of water as vapour through stomata in its leaves. Evapotranspiration is an important part of the water cycle. An element (such as a tree) that contributes to evapotranspiration can be called an evapotranspirator.

Li et al. (2008), for example, reviewed the numerous methods for measurement or estimation of evapotranspiration. These methods include: (i) empirical and semi-empirical; (ii) mass transfer; (iii) hydrological/water balance; and (v) micrometeorological/ energy balance. However, beyond the approximate physical simulation provided by an evaporation pan, the most common methods of estimating field ET are hydrological approaches (such as field water balance and weighing lysimetry), and micrometeorological methods, e.g. eddy covariance, Bowen Ratio – Energy Balance (BREB) (Singh & Xu 1997).

Jensen et al. (1990) analyzed the performance of 20 different methods against lysimeter measured ET for 11 stations around the world under different climatic conditions. The Penman–Monteith method ranked as the best method for all climatic conditions; however, the ranking of other methods varied with climatic condition. Several comparative studies have also confirmed the superiority in performance of the Penman–Monteith approach reported by Choisnel et al. (1992), Amatya et al. (1995), Chiew et al. (1995) and Evett et al. (1998).

2.5.1 Empirical and semi-empirical methods

Although empirical and semi-empirical methods relate pan evaporation (PE), actual evaporation or lysimeter measurements to meteorological factors (Li et al. 2008), they have a limited range of applicability because of (a) difficulty in measurement of variables at other places, (b) their limited range of accuracy in the model structure, (c) difficulty in comparing one method with another due to method-specific model variables. These methods were considered no further in this research.

2.5.2 Mass transfer methods

The mass transfer methods, developed on the basis of Dalton's Law using the concept of eddy motion transfer of the water vapour from the evaporating water surface to the atmosphere, provide satisfactory results in many cases (Thornthwaite & Holzman 1939, Jensen 1973). These methods are considered relatively accurate alternatives and less expensive than the energy budget methods (Harbeck 1962, Rosenberry et al. 1993). However, the success of these methods depends on the accuracy of the mass transfer coefficient, which is normally determined by calibration against an independent measurement of evaporation (Rosenberry et al. 1993).

2.5.3 Hydrological/water balance methods

The hydrological method is based on the law of conservation of mass: any change in the water content of a given soil volume during a specified period must equal to the difference between the amount of water added to the soil volume and the amount of water withdrawn from it can be expressed by general water balance equation for determining evaporative loss from soil, foliage, and sprinkler spray and transpiration is:

$$E + T = P + I + \Delta S - D - R \tag{2.6}$$

where E is the evaporation (mm day^{-1}),

T is the transpiration (mm day^{-1}),

P is the precipitation (mm day^{-1}),

I Irrigation (mm hr^{-1})

ΔS is the change in soil water storage for the medium of interest (mm day^{-1}),

D is the drainage for medium of interest (mm day^{-1}), and

R is the runoff losses for the medium of interest (mm day^{-1}).

E can be separated from evapotranspiration either by measuring E with microlysimeters, by measuring T with stem flow gauges, or by having no plants in the system. In this approach, ET is measured by determining all other components of the equation. This method can generally be used to calibrate other ET estimation methods but it also has some disadvantages. For example, canopy interception is not often considered in the water balance equation (Li et al. 2008) and the other components are not easily determined accurately in the actual application of the equation (Shi et al. 2008). In this method, measurements are typically representative of only a small area, and high spatial variability of soil water content results in sampling difficulties and problematic extrapolations to larger scales (Dunin 1991). The water balance methods are considered to be simple in theory, but rarely produce reliable results in the short period evaporation estimate (Singh 1989, Morton 1990, Singh & Xu 1997, Abtew 2001). Furthermore, it is not feasible to measure the ET during sprinkler irrigation with a lysimeter due to simultaneous addition of water (Thompson et al. 1997, Martinez-Cob et al. 2008). Lysimetry usually involves permanent installation, hence high cost and is less suitable for measuring short-time ET. However, for situations with well-defined surface and lower boundary conditions, it is still a reliable method.

2.5.4. Micrometeorological methods – Bowen Ratio Energy Balance (BREB) method

Micrometeorological methods are on the energy balance equation given by:

$$\lambda E = ET = R_n - H - G \tag{2.7}$$

where λE is the latent heat (W m^{-2}),

ET is the evapotranspiration (W m^{-2}),

R_n is the net radiation (W m^{-2}),

H is the sensible heat flux (W m^{-2}), and

G is the soil heat flux (W m^{-2}).

These methods have many advantages: (i) they are in situ measurements without disturbing the environment around the plant canopy (ii) these allow continuous measurements, and (iii) time-averaged measurements at a point provide an area-integrated, ensemble average of the exchange rates between the surface and the atmosphere (Baldocchi et al. 1988).

The method was first proposed by Bowen (1926) based on the energy balance equation (2.7) and the ratio $H/\lambda E$, known as the Bowen Ratio (β), gives information about the partition of the available energy at the surface between sensible (H) and latent heat (λE) fluxes. Starting with the basic energy balance equation (2.7), the latent and sensible heat can be estimated using the following equations:

$$\lambda E = \frac{R_n - G}{(1+\beta)} \tag{2.8}$$

$$H = \frac{\beta\left(R_n - G\right)}{\left(1+\beta\right)} \tag{2.9}$$

The parameters are described earlier.

The Bowen Ratio (β) is estimated from measurements of the temperature and vapour pressure deficits using the flux-gradient equations:

$$\lambda E = \frac{\rho_a C_p}{\gamma} K_w \, \Delta e / \Delta z \tag{2.10}$$

$$H = \rho_a C_p K_h \, \Delta T / \Delta z \tag{2.11}$$

where $\Delta e / \Delta z$ is the vapour pressure gradient (kPa),

$\Delta T / \Delta z$ is the temperature gradient (^{O}C),

γ is the psychrometric constant (k Pa $^{o}C^{-1}$),

C_p is the specific heat of the air (J kg $^{o}C^{-1}$),

ρ_a is the mean air density (kg m^{-3}),

K_w eddy transfer coefficient for latent heat, and

K_h eddy transfer coefficient for sensible heat.

Hence, assuming that K_h is equal to K_w the Bowen Ratio can be determined as:

$$\beta = eqn2.11 / eqn2.10 = \gamma \left(\Delta T / \Delta e \right) \quad (2.12)$$

This method is theoretically simple, but has two major limitations. Firstly the requirement for extensive upwind fetch distance is critical so that the temperature and water vapour profiles established in the airflow are representative of the evaporating surface: this requires a distance of at least 100 times the measurement height above the surface, i.e. typically at least 200 m of uniform surface (e.g. Craig & Hancock 2004). Secondly, the vapour pressure differences between two levels 1 m apart (typical for BREB instrumentation) are very small which requires a pair of high-cost psychrometers.

In addition, the basic assumption of equal eddy diffusivities for heat and water vapour is not always met under some atmospheric conditions (Barr et al. 1994, Gavilan & Berengena 2007). The method does not work under Bowen ratio values in the vicinity of -1 (Twine et al. 2000, Brotzge & Crawford 2003).

2.5.5. Micrometeorological methods – Eddy covariance (ECV) method

The Eddy covariance (ECV, also known as eddy correlation) method was developed utilizing the concepts of measurement of vertical transfer of heat and water vapour by eddies from the evaporative surface. The theoretical basis of the method allowing direct measurements of atmospheric turbulent fluxes to determine surface fluxes, namely the eddy covariance flux method, was presented by Swinbank (1951). However, prior to 1990, limitations in sensor performance and data acquisition systems restricted the duration of the eddy covariance studies to short campaigns during the growing season (Verma et al. 1986). However, during the past decade the eddy covariance method has emerged as an important tool for evaluating fluxes between terrestrial ecosystems and the atmosphere. At present, the method is being applied in a nearly continuous mode for the direct measurement of crop and grass land evaporation, forest evaporation and evaporation in irrigated fields.

ECV is now generally considered as a standard direct micrometeorological method to measure the surface flux (Baldocchi 2003, Yu et al. 2006), which can be used for comparing with the other methods or models. It can measure water vapour and heat fluxes simultaneously while avoiding the large fetch requirement. The method offers an attractive alternative to other more cumbersome and limited methods such as BREB or weighing lysimeter (Craig & Hancock 2004).

Although it has some limitations such as relatively high equipment cost, complexity in use and requires steady environmental conditions, ECV is gaining popularity over other methods such as lysimeters and Bowen Ratio-Energy Balance (BREB) method because:

i. it is the most reliable and accurate direct measuring method (Wang et al. 2007),

ii. it offers several advantages over lysimetry by providing more areal integration, finer temporal resolution, less site disruption and by eliminating the need to estimate other terms of a water budget (precipitation, deep percolation, runoff, and storage etc.) (Sumner 2001),

iii. unlike BREB, eddy covariance needs much less demanding fetch requirements and rapid development of modern electronics makes the equipment a potentially standard tool for researchers (Craig & Hancock 2004),

iv. sonic anemometers make it possible to measure the sensible heat flux in wet conditions and to calculate evaporation as a residual of the energy balance (Gash et al. 1999),

v. this technique emphasizes the influence of additional climatic factors on the intensity of the process (Assouline & Mahrer 1993),

vi. the microcomputer data acquisition system has real time data processing of the digital turbulence data (Baladocchi 2002),

vii. all the components of the energy budget can be measured simultaneously and thus errors can be identified, quantified and corrected by closing the energy balance (Villalobos et al. 2009),

viii. averaging flux measurements over long periods reduces the random sampling error to relatively small values (Baladocchi 2002), and

ix. ET can be measured for short times as well as on a seasonal basis (Sammis et al. 2004).

An alternative flux measurement technology is Large Aperture Scintillometer (LAS) and this is generally used over large path lengths (several kilometres). However the principal sensitivity of the technique is to the sensible heat energy flux with evaporative energy flux being derived via Bowen Ratio estimation. In addition this technology is still expensive and complex to use (Meijininger et al. 2006).

One limitation of the eddy covariance technique is that the size and shape of the representative region contributing to the measured flux, the flux 'footprint", is not fixed in time (Horst & Weil 1992, Baldocchi, 1997). Also, eddy covariance measurements are sometimes difficult to interpret during weakly-turbulent periods, usual1y at night (Lee et al. 1996, Paw et al. 2000, Baldocchi et al. 2000). The technique also cannot directly account for advection in areas of significant heterogeneous or complex terrain, limiting its applicability in some locations.

2.5.6. Micrometeorological methods – Penman-based methods

Although a variety of weather parameter (radiation-temperature) based energy balance models (Jensen & Haise 1963, Priestley & Taylor 1972, Jensen et al. 1990) have been developed in the past, over the past 20 years the emphasis has been on the Penman method, modified Penman methods, and the Penman-Monteith methods. This is because the Penman method (Penman 1948), and modified Penman method (Du & Pruitt 1975) utilize the solar radiation, relative humidity, wind speed, and air temperature to estimate evaporation using ‘combination’ of energy budget and aerodynamic transport approaches. The principal advantage arising from this combination is that measurements are required at only level in the atmosphere, rather than the difference between measurements at two levels as required for each of the energy budget and aerodynamic transport approaches independently (e.g. Monteith & Unsworth, 1990).

The Penman-Monteith method (Monteith 1965) extends the method with the inclusion of a bulk stomatal resistance parameter for a vegetated surface to estimate the evapotranspiration (also called the ‘actual evaporation’) from that surface. However, the necessary bulk stomatal resistance values for most vegetation types are not readily available.

Allen et al. (1998) changed some variables of the basic Penman–Monteith method to constants by simplifying it to calculate a reference evaporation ET_o from a standard (theoretical but grass-like) reference surface. The final form is known as the 'FAO-56 PM' model. Comparative studies performed by Allen et al. 2000, Walter et al. 2000, Itenfisu et al. 2003 and Temesgen et al. 2005 after the development of the FAO-56 PM method recognized FAO-56 PM as the international standard ET_o estimation method.

When combined with a crop coefficient, the reference crop ET_o can be used to estimate crop ET_c. The most common and widely used method is generally referred to as the "FAO-56 Method" which is described by Allen et al. (1998).

Despite the convenience of Penman-Monteith-based approaches, accurate measurement still requires a representative air flow for the surface and hence a long upwind fetch, i.e. strictly at least 100 times the measurement height (as with the Bowen Ratio – Energy Budget method).

2.5.7 Conclusions

Reviewing the comparative methods, it is concluded that eddy covariance (ECV) will be the most appropriate and reliable direct method for measuring evapotranspiration during sprinkler irrigation. Moreover, the limitations of other field measurements methods like minimum requirements of 100 m fetch in BREB method restrict to use this method in a small scale (50 m circle) area under this study. Unable to monitor the water balance in lysismeter due to continuous addition of water during irrigation also restrict using lysimeter to measure the total ET during irrigation. The limitations of these mostly used field methods suggest ECV is the only option to measure the total ET during irrigation and subsequent periods.

2.6 Eddy covariance system

2.6.1 Theory

The atmosphere contains turbulent motions of upward and downward moving air (Figure 2.4) that transport trace gases including water vapour. Eddy covariance theory describes the relationship between samples of these turbulent motions and the trace gases at certain point, using time series of multiple measurements (at least ten per second) from fast-response sensors. These sensors are usually a sonic anemometer to measure instantaneous vertical airspeed; and simultaneously a thermistor to measure instantaneous air temperature and an open-path infrared gas analyzer (together at one physical point on the tower) to measure water vapour density (Figure 2.5). In practice this task is accomplished by statistical analysis of the instantaneous vertical flux density, using Reynolds' rules of averaging (Reynolds 1985).

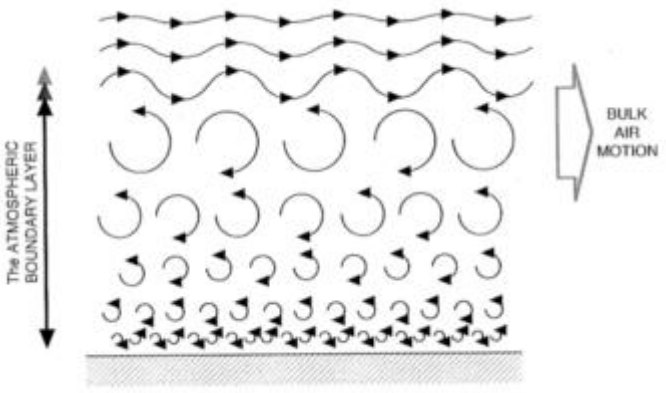

Figure 2.4: Classical view of the structure of eddies in the atmospheric boundary layer over a uniform vegetated surface (source: Hancock 2008)

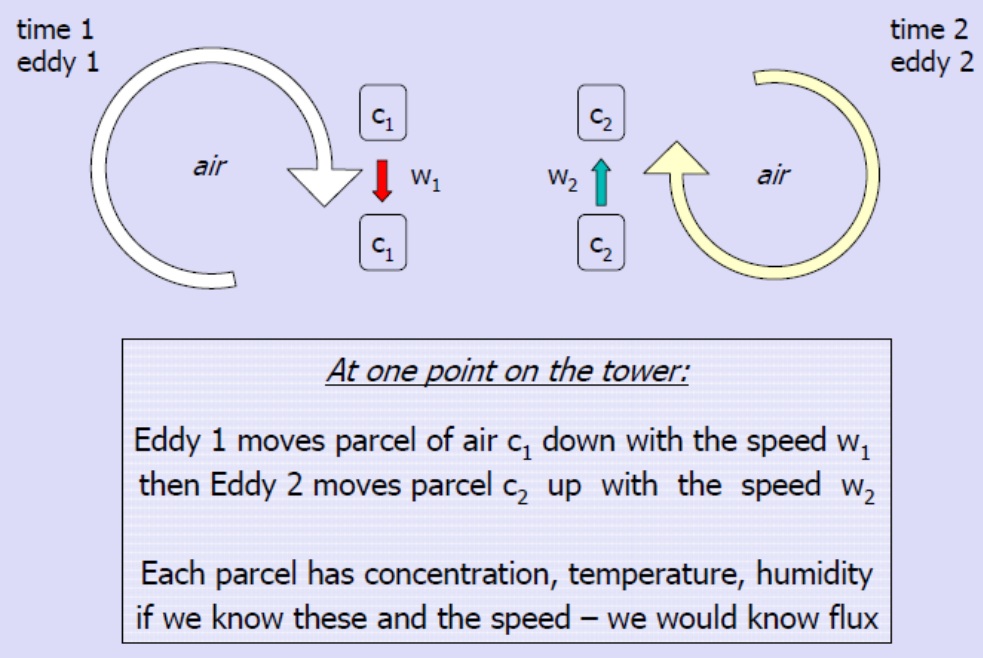

Figure 2.5: Eddies at one imaginary point imaginary eddies at measurements height of the ECV station (source: Burba & Anderson n.d.)

According to Reynolds convention, each parameter can be split into its mean value plus an instantaneous deviation from the mean (i.e. $\overline{X} = \bar{x} + x'$). The long-term mean vertical wind velocity over a flat uniform surface can be assumed to have a value of zero. Applying these assumptions and the rules of statistical averaging, the mean vertical flux for an averaging period longer than a few seconds can be obtained with the eddy covariance technique, which involves the covariance between the vertical wind velocity and the vapour concentration to compute the latent heat flux (λE). Sensible heat flux (H) can likewise be determined by this system using the covariance of vertical wind velocity and air temperature. From turbulent transport theory the sensible and latent heat fluxes for any averaging period are calculated as follows:

$$H = \rho_a c_p \overline{w'T'} \tag{2.13}$$

$$\lambda E = \rho_a \lambda \overline{w'q'} \tag{2.14}$$

where H is the mean sensible heat flux (W m^{-2}),

ρ_a is the instantaneous air density (kg m^{-3}),

C_p is the specific heat of air (J kg^{-1} K^{-1}),

$\overline{w'T'}$ is the covariance of vertical airspeed w and temperature T (m s^{-1})

λE is the latent heat flux (W m^{-2}),

λ is the latent heat of vaporisation of water (J g^{-1}), and

$\overline{w'q'}$ is the covariance of vertical wind speed and specific humidity q.

2.6.2 Errors and corrections

Besides careful instrument maintenance and periodic calibration, higher quality data are obtained through rigorous post processing. ECV data processing involves despiking, lag time correction, converting sonic temperature into actual temperature, coordinating rotation using planar fit method, correction for density fluctuations (WPL-correction) and frequency response correction. Each is described in the following subsections.

In general, the ECV technique is assumed to be the most accurate method for the estimation of turbulent fluxes. However, as a result of limitations in, for example, sensor design, finite flux averaging and processing methods, turbulent fluxes measured using the eddy covariance technique have a tendency to underestimate the true atmospheric fluxes (Massman & Clement 2004). Several reasons for this underestimation have been discussed by Mahrt (1998) which include: (i) the lack of coincidence of the source areas for the various flux components measured very near

a surface such as evaporation coming from leaves and sensible heat from a hot, dry soil surface; (ii) flux divergence arising from transport that is one-dimensional such as insufficient fetch; (iii) non-stationarity of measured time series over the typical 30 mins averaging periods so that covariance arising from very low frequency fluctuations is missed; (iv) turbulent dispersive fluxes arising from organized planetary-boundary-layer circulations that may have preferred locations so that the mean vertical velocities at an instrument location may be systematically different from zero giving rise to a vertical advective flux and (v) measurements errors related to sensor separation, frequency response alignment problems and interference from tower or instrument-mounting structures. Consequently, several authors have proposed correction algorithms in order to correct for this underestimation (e.g., Schotanus et al. 1983, Moore 1986, Horst 2000, Wilczak et al. 2001,Van Dijk et al. 2003). The resulting ECV measured turbulent flux consists of the covariant term and the various correction terms. The resulting ECV measured turbulent flux consists of the covariant term and the various correction terms.

2.6.2.1 Despiking and low pass filtering

Sometimes sensors are subject to spikes (high frequency instantaneous data) in the signal time series due to both electronic and physical noise that are unrelated to the desired signal. Although their effect on fluxes may be small, it is recommended that these spikes to be removed early in the data processing stream to avoid cross-contamination of signals through correction or other signal manipulations. Spikes should be removed and erroneous data should be replaced with running means to avoid errors in further calculations. Despiking and low pass filtering may be required on any or all signals and it is the user's responsibility to determine the necessity for application of these processing items.

The despike criterion could be set to remove signals that are more than six times the standard deviation for a given averaging period so that all outliers are considered spikes and removed (Burba & Anderson n.d.). Mauder & Foken (2004) recommended that any values, which exceed 5.5 times standard deviations in a window of 10 values, are labelled as spikes. However, if this spike criterion is fulfilled by 4 or more values in a row, they will not be considered as spikes. They are supposed to be 'real' in this case. Values, which are detected as spikes, can be excluded for later calculations or replaced linearly by interpolated values.

2.6.2.2 Lag removal

There is a possibility that a time delay occurs between two time series, if two different instruments used (Mauder & Foken 2004). Since, without correcting for this delay, fluctuations in vertical wind velocity (w') will not correlate with fluctuations in gas concentration resulting in underestimation of flux ranging from 5 to 15%, Matching the time series from a sonic anemometer and from gas analyser requires compensating for time delays in the signal acquisition from these instruments and this is crucial for the closed path system (Burba & Anderson n.d.).

2.6.2.3 Determining appropriate averaging period

An optimal averaging period for eddy flux computation is critical for avoiding low-frequency or high-frequency losses (Finnigan et al. 2003, Sun et al. 2006). Many flux sites adopted a 30 min averaging period for the flux computation (Baldocchi et al. 2003, Sun et al. 2006). However, a 10 min interval was also used by many scientists (Twine et al. 2000, Testi et al. 2004, Kumagai et al. 2005).

It should be pointed out that the choice of averaging period is an additional facet of the ECV processing that can have a substantial effect on the observed energy balance

(Finnigan et al. 2003, Cava et al. 2008), because short averaging intervals act as a high pass filter that can remove low-frequency components of the turbulent flux under certain circumstances. The potential for loss of flux is particularly high over rough canopies, such as forests, and when measuring at a substantial height relative to the canopy. These measurement conditions lead to a shift in the turbulent cospectrum toward lower frequencies, with consequently greater potential for loss due to short averaging interval.

The averaging interval must also not be too short. If it is too short it could lead to an effect similar to a high pass filter that will result in missed contributions from lower frequencies, and finally to underestimation of the measured flux. There are several ways to choose an averaging time. The most widely used approaches are labelled 'mandatory', 'empirical' and 'ogives'.

- The mandatory approach simply uses standard averaging times of 30 min or 1 hour. It is easy to execute, and it works well for many traditional settings, but it may not be best for all conditions.
- The empirical approach analyses the data with different (reasonable) averaging times (e.g., 10 min, 30 min, 1 hr, 2 hrs, 4 hrs), and chooses the one with the largest flux.
- The ogives method relies on cumulative co-spectra constructed over a range of frequencies. At some points the accumulated period is lengthened, no more flux is added. This then becomes the best averaging time. This is, perhaps, the most flexible and justified approach, but it requires substantial data processing and analysis (e.g. Lee et al. 2004).

2.6.2.4 Coordinate rotation

When a sonic anemometer cannot be levelled perfectly, such that its *w* axis is always perpendicular to the mean flow/mean wind streamlines, the *w*-signal will likely be

contaminated by the other two of the 3D wind components (Burba & Anderson n.d.). Therefore, coordinate rotation should be applied to satisfy the assumption that the time average of vertical wind speed is zero in ECV measurements. Two methods are available to make the *w* value zero, one is classical coordinate rotation methods (double rotation and triple rotation) and another one is the planar fit. Planar fit method is most suitable for gently sloping grassland and flat farmland (e.g. Paw et al. 2000, Finnigan et al. 2003).

2.6.2.5 Conversion of fluctuations of sonic temperature into actual temperature

Sonic anemometers measure temperature using the speed of sound between the transducers. As the speed of sound depends on the air temperature and also to a minor part on the water vapour content of the air, the temperature should be corrected for air density or humidity fluctuations. To obtain the fluctuations of the actual temperature instead of the fluctuations of sonic temperature the humidity correction is applied (Schotanus et al. 1983).

2.6.2.6 Frequency response corrections

Frequency response corrections are required to account for the inability of the measurement system to capture very high frequency or low frequency fluctuations in signals. Frequency response corrections are a family of corrections that compensate for the flux losses at different frequencies of turbulent transport. There are a number of separate reasons for these losses, but all of them are related to the sensor performance and to the response of the eddy covariance system. According to Burba & Anderson (n.d.) the main frequency response corrections include:

i. time response corrections: To compensate for the loss of flux due to inability of sensors to respond fast enough to small fluctuations which contribute to the flux
ii. sensor separation: To compensate for the loss of flux due to mismatch of the two sensors.
iii. scalar/vector path averaging: To compensate for the loss of flux due to loss of very small eddies.
iv. tube attenuation: To compensate for the loss of flux due to the fact that sampling air through the inlet tube attenuates (dampens) small fluctuations.
v. high pass filtering: To compensate for the loss of flux in low frequency part of co spectrum due to averaging, linear de-trending or non-linear filtering.
vi. low pass filtering : To compensate for the loss of flux in low frequency part of co spectrum mostly due to use of the anti-aliasing filters.
vii. digital sampling : To compensate for the aliasing during the digital sampling.

2.6.2.7 Correction for density fluctuations (WPL-correction)

The Webb-Pearman-Leuning term (often referred as WPL or density term) is used to compensate for the fluctuations of temperature and water vapour that affect the measured fluctuation in CO_2, H_2O and other gases. To determine turbulent fluxes of air constituents like H_2O and CO_2 the correction described by Webb et al. (1980) is necessary. It corrects for two aspects: the first is the conversion of the volume related measurement of the content of a scalar quantity, e.g. absolute humidity (gm m^{-3}) into a mass-related parameter like specific humidity or mixing ratio. The second aspect is the correction of a positive vertical mass flow, which results from the mass balance equation, because vertical velocities of ascending parcels have to be different from descending ones due to density differences (Webb et al. 1980, Fuehrer & Friehe 2002).

2.6.3 Footprint analysis for ECV measurements

The flux 'footprint' is the upwind area on the crop surface or ground where the atmospheric flux measured by ECV sensors (at a particular height) is generated; and therefore for which the calculated heat, water, gas and momentum transport is registered by the instruments. This is different to the frequently used term 'fetch' which is the upwind extent of the crop or surface over which the measurement are being taken by an instrument.

Eddy-covariance measurements are being widely used in continuously monitoring turbulent exchanges of mass and energy at the vegetation–atmosphere interface (Aubinet et al. 1999, Baldocchi et al. 2001). However, the reliability and accuracy of these measurements depends on certain theoretical assumptions of the eddy-covariance technique (Kaimal & Finnigan 1994, Foken & Wichura 1996, Baldocchi 2002), the most important of which is horizontal homogeneity, stationarity and mean vertical wind speed equal to zero during the averaging period.

The proliferation of eddy-covariance flux systems often violating some of the theoretical requirements of this methodology in a variety of conditions and ecosystems has created an increasing interest in footprint analysis. In fact, in a heterogeneous landscape the ecosystems contributing to the flux may change with wind direction, atmospheric stability, measuring height and surface roughness (Schmid 1997, Rannik et al. 2000). Since the footprint of a turbulent flux measurement defines the ''field of view'' of the measuring system, its estimation is essential for data interpretation when measurements are performed in non-uniform conditions of source/sink distribution and a problem of flux measurement representativeness arises (Finn et al. 1996, Schmid 2002, Schmid & Lloyd 1999).

The term footprint was coined by Schuepp et al. (1990), who explored several approaches to the advection–diffusion equation, and then further developed the

approximate solution by Calder (1952) as proposed by Gash (1986). Since then, the footprint problem has been studied using three different model formulations:

(i) analytical solutions by the advection–diffusion equation (Horst & Weil 1992, Schmid, 1994, Haenel & Grunhage 1999, Korman & Meixner 2001),

(ii) Lagrangian stochastic models describe the defusion of a scalar by a stochastic differential equation (Leclerc & Thurtell 1990, Kurbanmuradov et al. 1999, Rannik et al. 2000, Markkanen et al. 2003), and

(iii) large-eddy simulations (Leclerc et al. 1997).

Analytical solutions are elegant but limited in their range of applicability; however, they are suitable for short vegetation canopies (Finn et al. 1996). Lagrangian stochastic and large-eddy simulations are more flexible and robust than analytical ones as they can be applied to any turbulence regime. Regardless of their versatility and physically grounded description of diffusion, Lagrangian models and LES are used less often in field measurement design and data interpretation, mainly due to their complexity and computational requirements.

Despite the large availability of footprint models, there is a general need for experimental validation of model outputs (Schmid, 2002, Leclerc et al. 2003b, Foken & Leclerc, 2004). In several studies, analytical footprint model predictions have been compared with footprint estimates of the Lagrangian type taken as a reference (Horst & Weil 1992, Leclerc & Thurtell 1990, Kljun et al. 2003). Contrarily, few in situ validation experiments, which focus on one-dimensional validation of flux footprints assuming a crosswind infinite line source configuration, are available (Leclerc et al. 1997, Finn et al. 1996, Copper et al. 2003). The primary reason for this lack of footprint experimentation is largely due to the constraints imposed by model assumptions (Kljun et al. 2004). Measurements in complex flow fields, as dispersion inside and above high vegetation canopy, may not be ideal for evaluation and

validation of footprint models. For this reason, Kljun et al. (2004) suggest the validation under ideally controlled conditions that can be reproduced in wind tunnels or watertank experiments. Foken & Leclerc (2004) discussed and compared the effectiveness and applicability of three validation methods:

(i) the use of artificial trace gases,

(ii) the use of natural sources of scalars, and

(iii) the presence of obstacles in the flow field. Although they give no general guidelines for footprint model validation and pointed out that validation conditions should respect model assumptions.

2.7 Atmospheric stability analysis

Integral turbulence characteristics are statistical measures describing atmospheric turbulence in the surface layer. They are defined as the normalised standard deviations of fluctuating turbulent parameters (Tillmann 1972). Integral turbulence characteristics have been widely used in a variety of applications, such as an instrument for quality assessment of turbulence data (Wichura & Foken 1995), in accumulation methods assuming flux variance similarity (e.g. Businger & Oncley 1990), for the direct determination of turbulent fluxes (Foken 1990, Wyngaard et al. 1971), in air pollution models (e.g. Blackadar 1997), or in applications representing the influence of surface properties on turbulent fluxes as for example in footprint models (Schmid 1997). The Atmospheric stability was analysed using the general form of integral turbulence characteristics equation expressed as:

$$\frac{\sigma_x}{X_*} = \phi_x\left(\frac{z-d}{L}, \frac{z_i}{L}, \frac{(z-d).f}{u_*}\right) \tag{2.15}$$

where x is the fluctuating parameter,

X_* its corresponding normalising factor derived from its characteristic turbulent flux,

φ_x a function scaling with different parameters such as:

the aerodynamical height $(z-d)$, the mixing layer height z_i, the Coriolis parameter f, the friction velocity u_* and the Obukhov-length L.

Integral turbulence characteristics were observed to scale with local and non-local parameters. The locally influencing parameters include atmospheric stability and surface properties. Atmospheric stability, commonly expressed in terms of the dimensionless height $(z - d)/L$ following from the Monin-Obukhov similarity theory (Monin & Obukhov 1954), was used by many authors to formulate parameterisations for integral turbulence characteristics of wind components, the temperature and humidity (e.g. Foken et al. 1991, Panofsky et al. 1977, Tillmann 1972, Wyngaard et al. 1971).

Surface properties such as distribution of aerodynamic obstacles, roughness length, water saturation and canopy height were found to have a considerable effect on turbulent fluxes, and therefore on the general applicability of the concept of integral turbulence characteristics (De Bruin et al. 1991). The non-local influencing parameters, including geographical latitude and mixing layer height, were regarded as having no significant influence on integral turbulence characteristics by most authors.

2.8 Energy balance over a crop/soil surface

The main source of energy in the atmospheric surface layer region is solar radiation. The energy absorbed by the surface is primarily partitioned into sensible, latent and soil heat fluxes. Other energy terms to be considered include advection of sensible and latent heat, storage terms and energy consumed in metabolic and photosynthetic process termed as biomass heat storage (Anderson 1983).

The surface energy balance over a crop/soil surface is conventionally expressed in terms of energy transfer into and out of a control volume including the vegetation, canopy-air space and a layer of soil deep enough to exclude the heat transfer through its bottom. Following (Oke 1987, Hancock 2008):

$$\lambda E = R_n - H - D - G - J - \mu A \tag{2.16}$$

where, λE is the latent heat (W m^{-2}),

R_n is the net radiation (W m^{-2}),

H is the sensible heat flux (W m^{-2}),

D is the advective energy removed horizontally by advection (W m^{-2}),

G is the soil heat flux (W m^{-2}),

J is the flux of energy into physical storage (W m^{-2}), and

μA is the flux of energy into biochemical (W m^{-2}).

Table 2.4: (Thom 1975) sets out typical magnitudes of energy budget in W m^{-2} for each component for thriving plant community of moderate height (about 1m) in cloudless, summer conditions in middle latitudes at four times of day

Times of day	R_n	D	G	J	μA	H
Near sun rise	0	±5	-5	+10	+3	-8
Midday	+500	±25	+25	+2	+12	+461
Near sunset	0	±15	+5	-10	+2	+3
Midnight	-50	±10	-25	-2	-3	-20

2.8.1 Radiation at the earth surface

Solar radiation is the primary source of energy for evaporation. Radiation transfers energy by means of electromagnetic waves characterised by wavelengths. The wavelengths important for calculation of water use are those in which the sun, the earth and the atmosphere radiate (Burman & Pochop 1994). Radiation from the sun, which is at a much higher temperature than the earth, has a higher intensity and is of

shortwave length (0.15 to 4 microns). Radiation from the earth and atmosphere, or terrestrial radiation is referred to as longwave radiation.

All objects emit radiation at intensities proportional to the fourth power of their temperature at temperatures above absolute zero. Therefore the flux of radiation R over all wavelengths from an object is calculated from the Stefan-Boltzmann Law:

$$R = \varepsilon \sigma T^{4} \quad (2.17)$$

where ε is the emissivity of the object (dimensionless),

σ is the Stefan-Boltzmanns constant,

$= 5.6703 \times 10^{-8}$ W m^{-2} K^{-4}, and

T is the absolute temperature (K).

2.8.1.1 Extraterrestrial radiation

The solar radiation striking the top of the earth's atmosphere is called the extraterrestrial (solar) radiation, R_a. When the incident radiation is perpendicular to the surface, R_a = 0.082 MJ m^{-2} min^{-1} (the 'solar constant' R_{sc}), however, extraterrestrial radiation varies depending on the locality and the angle of incidence, and is therefore a function of latitude, date and time of day.

2.8.1.2 Solar ('shortwave') radiation

Solar radiation passes through the atmosphere and reaches the earth's surface. Part of this shortwave radiation is reflected back to the atmosphere and is known as albedo, α. The albedo varies with the surface type, slope and the angle of incidence. For short green vegetation cover albedo is assumed to be in the range 0.20 to 0.25 (Du & Pruitt 1975). The net solar radiation is the solar radiation (R_{sn}) that is not reflected from the surface and is calculated as:

$$R_{sn} = (1 - \alpha)R_s. \quad (2.18)$$

2.8.1.3 Terrestrial ('longwave') radiation

Longwave radiation is the radiant flux resulting from emission of energy from gases and particles in the atmosphere, and by vegetation and the ground surface. The incident shortwave radiation reaching the earth is radiated back to the atmosphere with a longer wavelength. Part of this longwave radiation comes back again to the earth surface. The difference between the two sets of emissions, the downwelling and emitted longwave radiation is called net longwave radiation.

2.8.1.4 Net radiation

Net radiation (R_n) is the amount of energy available at the surface for energy consuming processes such as evapotranspiration ET and heating of soil and atmosphere. It is the difference between the net shortwave radiation (R_{ns}), and the outgoing net longwave radiation (R_{nl}) can be expressed by:

$$R_n = SR_{in} - SR_{out} + lR_{in} - lR_{out} \quad (2.19)$$

where R_n is the net radiation (W m^{-2}),

SR_{in} is the incoming shortwave radiation (W m^{-2}),,

SR_{out} is the outgoing shortwave radiation (W m^{-2}),

lR_{in} is the incoming longwave radiation (W m^{-2}), and

lR_{out} is the outgoing longwave radiation (W m^{-2}).

During the day net radiation is a positive value as incoming radiation exceeds outgoing radiation allowing the surface to gain energy. At night with no incoming solar radiation there is more outgoing radiation than incoming creating a negative value for net radiation.

2.8.2 Latent heat flux (λE)

Latent heat flux is the flux of heat from the Earth's surface to the atmosphere that is associated with evaporation or transpiration of water at the surface. It is an important component of Earth's surface energy budget. In this process water is transferred into the atmosphere through conduction and convection. The heat energy then can move horizontally advection (atmospheric circulation). Under specific conditions, latent heat flux may be measured with the Bowen Ratio technique (section 2.5.4 above), or by eddy covariance (section 2.5.5 above). When evaporation is taking place the energy transport is upward and the flux is defined as positive. On the other hand, condensation is the phase change from a gas to a liquid.

2.8.3 Sensible heat flux (H)

Sensible heat flux is the process where heat energy is transferred from the Earth's surface to the atmosphere by conduction and convection. In this process, heat is initially transferred into the air by conduction as air molecules collide with those of the surface. As the air warms it circulates upwards via convection, both 'fully forced' convection due to eddies generated by the drag of the surface against the prevailing wind (e.g. Oke 1987), and as (i.e. enhanced by) natural convection when the atmosphere is unstable.

2.8.4 Soil heat flux (G)

The third major use of radiant energy is the soil heat flux to warm the subsurface of the earth. Heat is transferred in this process from the surface downwards via conduction. Like in the case of sensible heat transfer, a temperature gradient must

exist between the surface and the subsurface for heat transfer to occur. Heat is transferred downwards when the surface is warmer than the subsurface (positive ground heat flux). If the subsurface is warmer than the surface then heat is transferred upwards (negative ground heat flux).

A review of published energy balance studies shows considerable variation in the chosen reference depths. Recent studies have used reference depths ranging from 1 mm (Heusinkveld et al. 2004) to 10 cm (Tanaka et al. 2003). Shallow reference depths are sometimes chosen with the intent of minimizing heat storage so that it might be neglected (Baldocchi et al. 2000, Wilson et al. 2000, da Rocha et al. 2004). A shallow reference depth, however, may create the potential for large errors in soil heat flux measurements (Buchan 1989). Neglecting heat storage above the reference depth may also lead to significant errors in soil heat flux (Mayocchi & Bristow 1995).

The energy is distributed over the three major categories of energy use, λE, H, and G. During the day, the available radiant energy is used to evaporate water into the air, raising the humidity of the air. Sensible heat is transferred upwards to warm the air above the surface. Heat is also conducted down into the subsurface. At night the processes reverse. At night with no incoming solar radiation there is more outgoing radiation than incoming creating a negative value for net radiation. Under these circumstances the surface cools due to a loss of energy and heat is transferred from the air toward the surface. As air cools through the evening the loss of energy allows condensation to occur, so long as the air's humidity is at or near saturation. Williams et al. (2004) reported that in the case of a dense close canopy structure, the soil evaporation can be neglected during irrigation as well as under dry conditions.

Besides the major categories of energy, there are additional energy fluxes in the energy balance system, namely advected energy and changes in biomass stored

energy. These are usually considered 'minor' but may be significant in certain circumstances (e.g. Oke 1987)

2.8.5 Advected energy

Advection is usually defined as the horizontal divergence of sensible heat flux when it is large enough to produce a downward sensible heat flux close to the ground (McNaughton & Jarvis 1983, Diaz-Espejo et al. 2005). However, advected energy can also include latent heat (Thom 1975). Advection can play a significant role in the energy exchange over large inhomogeneous surfaces. Hence, where there is selective watering, i.e. irrigation, some local advection also can occur. The magnitude of local advection depends on wind speed, wind direction, fetch and temperature difference, e.g. between two adjacent fields which are differently treated, and also the spatial location of the field (Xiaomin et al. 2001).

In general advected energy can be expressed as follows (Thom 1975):

$$D = D_H + Dv \tag{2.20}$$

where D_H and D_V are the respective divergences of the horizontal fluxes of sensible and latent heat integrated between the soil surface $(z = o)$ and the reference level $z = z_R$, i.e:

$$D_H = \int_0^{z_R} \frac{\partial}{\partial x}\left(\rho c_p u T\right) dz \tag{2.21}$$

and:

$$D_V = \int_0^{z_R} \frac{\partial}{\partial x}\left(\frac{\rho c_p}{\gamma} ue\right) dz \tag{2.22}$$

from which a useful approximation is (Thom 1975):

$$D = \rho c_p u z_R . \frac{\partial}{\partial x}\left(T + \hat{e}/\gamma\right) \tag{2.23}$$

where ρ is the average density of air,

C_p is the specific heat of air at constant temperature and pressure,

u, T and $\hat{e}$ are the average values of u, T and e for the layer $0 \rightarrow z_R$.

The total rate at which energy is stored physically within a column of unit cross-sectional area extending from the soil surface to the level $z = z_R$ (the height at which the R_n is measured):

$$J = J_H + J_V + J_{veg} \tag{2.24}$$

where $$J_H = \int_0^{z_R} \rho c_p \frac{\partial T}{\partial t} \partial z \tag{2.25}$$

$$J_V = \int_0^{z_R} \frac{\rho c_p}{\gamma} \frac{\partial e}{\partial t} \partial z \tag{2.26}$$

in which J_H and J_V are the respective rates of change of sensible and latent heat contents of the air within the column and

$$J_{veg} = \int_0^{z_R} \rho_{veg} c_{veg} \frac{\partial T_{veg}}{\partial t} \partial z \tag{2.27}$$

where J_{veg} is the rate of change of the heat content of the vegetation itself, and

ρ_{veg}, c_{veg} and T_{veg} are the density, specific heat and temperature, respectively.

As Thom (1975) stated J_H and J_V are usually negligible unless z_R is much in excess of a metre or two. Therefore the above equation can be approximated by the following:

$$J = J_{veg} \tag{2.28}$$

Assuming $\frac{\partial T_{veg}}{\partial t}$ is adequately approximated by $\frac{\partial T}{\partial t}$ and that c_{veg} is roughly 70% of the value of the specific heat of water (4.2 x 10^3 J kg^{-1} $^0C^{-1}$) it can be deduced from equation (2.27) that:

$$J_{veg} = 0.8 m_{veg} \delta T_1 \tag{2.29}$$

where m_{veg} is the mass of vegetation over unit horizontal area from a height $z = 0$ to z = h expressed as $m_{veg} = \int_0^h \rho_{veg} dz$ and ∂T_{veg} and δT_1 is again the representative air temperature change in ^{0}C per hour.

2.8.6 Biomass storage heat flux

Biomass stores two types of energy:

- physical heat energy storage due to changes in biomass temperature (enthalpy) and
- biochemical energy storage in chemical bonds and its release due to processes of photosynthesis and respiration, respectively (Gu et al. 2007).

There is evidence indicating that biomass heat and biochemical energy storages are not insignificant components of the surface energy budget. For example, Samson & Lemeur (2001) found that biomass heat storage and biochemical energy storage were up to 60 and 20 W m^{-2}, respectively, in a mixed deciduous forest while Meyers & Hollinger (2004) reported that the two energy storage terms could each be over 20 W m^{-2} for maize and soybean canopies which are not negligible in comparison to net radiation.

On the other hand, McCaughey (1985) reported that the storage term is the most difficult term in the energy balance equation to measure and that it has often been

neglected. He also stated that when a canopy is dry and net radiation is high, the daily total storage seldom exceeds 2–3% of R_n, and thus can safely be ignored. Oliphant et al. (2004) reported that biomass heat storage flux magnitude in a temperate deciduous forest is too small, so that it can be ignored.

2.9 Canopy interception and evaporation

Canopy interception can be defined as the amount of water stored temporarily during sprinkler irrigation. It is often considered as a loss under sprinkler systems (Wang et al. 2006). During the irrigation, some portion of water is intercepted by the crop and accumulates until the plant's storage capacity is reached. This water evaporates (but is continually replenished) during irrigation, and then continues evaporating following irrigation until the foliage is dry (Tolk 1992). The portion of water droplets that evaporate during sprinkling as labelled 'in-canopy evaporation'. The water which stays on leaves to be evaporated later is called 'interception loss'. In sprinkler irrigation these two combined (canopy evaporation during irrigation and intercepted water losses after irrigation) losses are considered as part of 'evaporation loss' (Other components of 'evaporation loss' include droplet evaporation loss.)

Interception by the canopy is governed by the specific water interception capacity on the surfaces of leaves, twigs, branches and trunks (Wanqin et al. 2004). On the other hand, wet canopy evaporation in sprinkler irrigation is a continuous and dynamic process controlled directly by a combination of meteorological variables (e.g., radiant energy supply, air temperature, atmospheric humidity deficit and atmospheric turbulence) and canopy structure (Monteith & Unsworth 1990). Since it has been difficult to measure during sprinkler irrigation, wet canopy evaporation has been neglected in many studies in the past.

Rutter (1975) reported that the interception storage capacities of plant leaves ranged from 1.2 mm for Douglas fir to 0.4 mm for oak coppice in winter. Available literature has reported that canopy interception varied from 1.8 to 2.7 mm for corn (Seginer 1967, Smajstrla & Hanson 1980, Steiner et al. 1983, Lamm & Manges 2000). Norman & Campbell (1983) suggested that the canopy interception with small leaves, such as wheat might be as much as 10 mm for a single event under high evaporative condition. Amount of intercepted water in corn was less than 8% of the total water applied by impact sprinkler irrigation in day (Tolk et al. 1995), 25–30% of total water applied on early days (Du et al. 2001) and 24–28% of the total applied seasonal water (Li & Rao 2000). Thompson et al. (1988b) predicted that the canopy interception loss was 3.2 mm (at more than 60%) is the main contributor to the evaporation during sprinkler irrigation. Wang et al. (2006) estimated the average depth of canopy interception as 1.62 mm using a water-wiping method, whilst using a rain gauge method it was found to be 0.18 mm for winter corn canopy in China. Kang et al. (2005) reported that the maximum value of winter wheat canopy interception was not more than 1.0 mm and that this was 1.3% of the total irrigation amount.

Some investigators have proposed that canopy interception offsets evapotranspiration loss which would have occurred in an unsprinkled field (Mather 1950, Frost 1963). On the other hand, intercepted water might be an important factor to influence the field microclimate (Tolk et al. 1995, Du et al. 2001, Kang et al. 2002) and to improve environmental conditions inside the canopy for crop growth (Yang et al. 2000). A growing crop canopy has the potential to modify distribution of water applied during irrigation.

Although there are several methods that measure the rate of evaporation of intercepted water such as weighing (Teklehaimanot & Jarvis 1991), by eddy covariance method (Van der Tol et al. 2003), water volume balance (Aboal et al.

1999) or by Leyton's method (Leyton 1967), the wet canopy evaporation rate has previously and almost always been estimated using meteorological variables and Penman-Monteith equation (Monteith 1965, Monteith & Unsworth 1990, He et al. 2003). A major advantage of Penman's equation is that it requires measurement (or estimation) of only net radiation (*G* is typically small for a day), plus air temperature, relative humidity and wind speed at a single elevation (Tolk 1992).

2.10 Transpiration

2.10.1 Introduction

According to U.S. Geological Survey (2011) the transpiration may be defined as the process by which water that is absorbed by plants, usually through the roots, is evaporated into the atmosphere from the plant surface, such as leaf pores. Leaf surfaces are dotted with openings which are collectively called stomata, and in most plants they are more numerous on the undersides of the foliage. The stomata are bordered by guard cells that open and close the pore. Cummins (2007) stated that leaf transpiration occurs through stomata, and can be thought of as a necessary "cost" associated with the opening of the stomata to allow the diffusion of carbon dioxide gas from the air for photosynthesis. Transpiration also cools plants and enables mass flow of mineral nutrients and water from roots to shoots. Mass flow of liquid water from the roots to the leaves is caused by the decrease in hydrostatic (water) pressure in the upper parts of the plants due to the diffusion of water out of stomata into the atmosphere. Water is absorbed at the roots by osmosis, and any dissolved mineral nutrients travel with it through the xylem. Although the transpiration naturally occurs in vegetative plants the total amount will decrease as evaporation of water from the wetted canopy increases (Norman and Campbell, 1983). Kume et al. (2006) reported that most of the water losses during sprinkler irrigation are due to evaporation of water intercepted and held on the. The water vapour-exchange processes, which

consist mainly of wet canopy evaporation and dry canopy transpiration, are quite different depending on whether the canopy is wet or dry. In dry condition, transpiration is the major part of evepotranspiration over the crop surface while during irrigation canopy evaporation dominates the evapotranspiration due to the free water available to evaporate on the canopy (Kume et al. 2006, Bosveld & Bouten 2003) and the stomatal pores were impeded by liquid water on the leaf surfaces (Ishibashi & Terashima 1995, Brewer et al. 9991, Forseth 1990).

The ability for independent and adequate measurement of canopy transpiration T is important when examining energy and water balance in vegetation (Ham et al. 1990). Two types of approach have so far been developed to measure the quantity of water transpired by a plant canopy (Chabot et al. 2005).

The first approach includes calculating 'climatic demand' (or 'evaporative demand') to estimate the reference evapotranspiration and combine it with a crop coefficient function dependent on the type of the crop. As reviewed in section 2.5.6 above, the FAO-56 Penman-Monteith method (Allen et al. 1998) sets out the different formulae and methods to determine both reference evapotranspiration and crop coefficients used to estimate the evapotranspiration of canopies.

The second approach is the direct measurement of the transpiration of the plant. These measurements can be carried out with different systems and time scales (Wilson et al. 2001). Some measurement methods have the disadvantage of disturbing the natural environment, such as weighing lysimeters, which disturb the soil; or the field chamber methods which deduce the crop transpiration from the variation of the air humidity measurement but which also modify the microclimate (Reicosky, 1985). Chemical and isotopic tracers (Bariac et al. 1994) have also been used to measure the transpiration of the plants although the data can be difficult to interpret and these tracers do not permit continuous measurement. The eddy

covariance technique (Tanner 1987), Bowen Ratio (Heilman & Brittin 1989, Prueger et al. 1997) and the aerodynamic combined method (Perrier & Tuzet 1991) do not modify the natural environment and permit good temporal resolution. However, these methods are complex and require expensive equipment (sections 2.5.5 and 2.5.4 above, respectively).

Transpiration rates for whole plants as well as individual branches can also be determined by techniques which measures the rate at which sap ascends stems. The 'sap flow method' has been used successfully for several years to determine the transpiration of canopies due to its several advantages including relatively easy, easily automated, continuous monitoring over a period of time as short as necessary along with their capacity to measure the transpiration term only (Chabot et al. 2005).

Several sap flow measurement methods have been developed like heat pulse velocity (HPV) method and heat balance (HB) method using heat as a tracer for sap movement. In heat pulse method short pulses of heat are applied rather than continuous supply of heat. Among these, the heat balance method developed by Sakuratani (1981) is seen to have some advantages over other methods. The stem heat balance approach requires no calibration or stem intrusion by temperature probes are the two significant advantages over HPV method. However, there are two types of uncertainty related to the sap flow method have been mentioned (Chabot et al. 2005) namely:

(i) direct uncertainties due to sap flow sensor measurements and

(ii) uncertainties related to the extrapolation of the flow from a sample of stem to the transpiration of the entire canopy. This second source is mainly dependent on the heterogeneity of the crop's development (Cermak & Kucera 1990).

Sampling can be achieved easily in homogeneous canopies where the crops are all at the same stage of development and where the contributions of radiant energy and soil humidity are uniform.

2.10.2 Theory of heat balance method

The method is developed on the basis of heat balance of stem. The stem is heated electrically and the heat balance is solved for the amount of heat taken up by the moving sap stream which is then used to calculate the mass flow of sap in the stem.

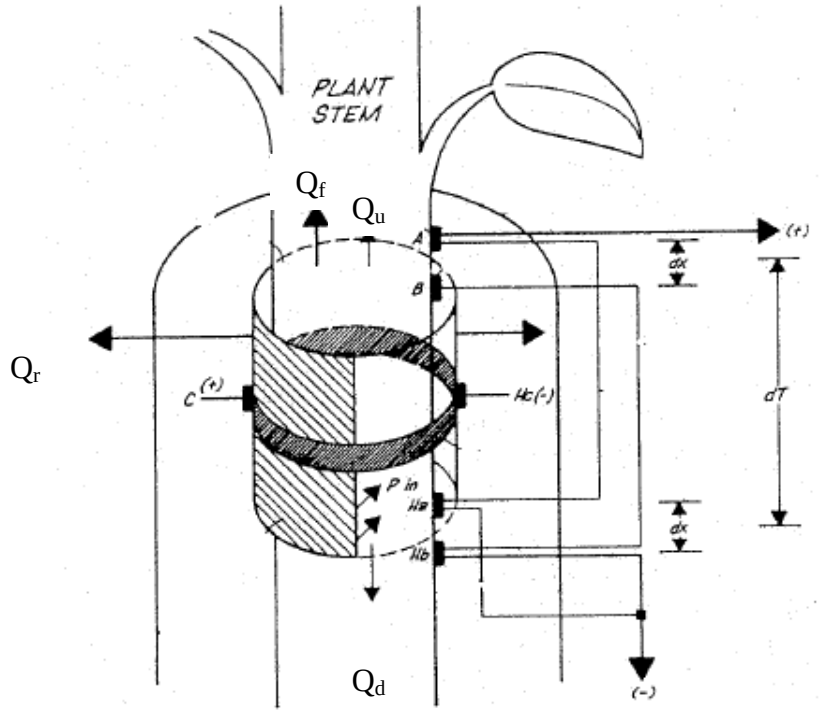

Figure 2.6: Stem gauge schematics with two differentially wired thermocouples where channel AH measures difference in temperature A-H_a and channel BH measures the difference in temperature B-H_b (source: Dynagage Sap Flow Sensor User Manual, 2005, Dynamax Inc.)

The method uses a measurement technique which is non-invasive of the stem and does not require an empirical calibration. Mass flow is calculated by balancing the heat into and out of a stem. Gentle heating (P_{in}) is applied continuously from a flexible heater that encircles the stem. Heat losses include vertical ($Q_v = Q_u + Q_d$) and radial conduction (Q_r) and transport by the flow.

According to Baker & van Bavel (1987) the xylem mass flow rate can be calculated using the energy balance equation:

$$P_{in} = Q_v + Q_r + Q_f \tag{2.30}$$

where P_{in} is the input power (W),

Q_v is the vertical or axial heat conduction through the stem $(\mathrm{W\ m^{-1}\ K^{-1}})$,

Q_r is the vertical or axial heat conduction through the stem (W $\mathrm{m^{-1}\ K^{-1}}$), and

Q_f is the heat convection carried by the sap$(\mathrm{W\ m^{-1}\ K^{-1}})$.

The flow through the stem can be estimated by rearranging the equation (2.30) to give:

$$Q_f = P_{in} - Q_v - Q_r \tag{2.31}$$

The input power is calculated from the electrical resistance and voltage across the heater using the Ohm's law as presented below.

$$P_{in} = \frac{V^2}{R} \tag{2.32}$$

The Q_v and Q_r are determined from the measurements of and dt_u and dt_r. Finally, Q_f is converted to the mass flow rate of sap.

The vertical conduction Q_v is calculated by measuring the upward and downward temperature gradients away from the heater using Fourier's equation (Baker & van Bavel 1987, Sakuratani 1981). The sum of the gradients is algebraically equivalent to ($dt_u - dt_d$) (Steinberg et al. 1990), so that Q_v is obtained from:

$$Q_v = K_{st} A(dT_u - dT_d) / dx(0.04) \quad (2.33)$$

where A is the cross-sectional area of the heated section of the stem (m^2),

K_{st} is the conductivity of the stem (W m^{-1} K^{-1}),

dt_u is the temperature difference of two thermocouple above the heater (^{O}C),

dt_d temperature difference of two thermocouple below the heater (^{O}C),

dx is the distance between two thermocouple junctions on each side of the heater (Figure 2.6) and

0.04 is the factor to convert the thermocouple differential signals to degree C.

The radial component of stem heat balance Q_r is determined from the measurements of temperature gradient dt_r using the equation:

$$Q_r = K_{sh} dt_r \quad (2.34)$$

where K_{sh} is the effective thermal conductance of the sheath of materials surrounding the heater (W m^{-1} K^{-1}), the value of K_{sh} is unknown and depends on the thermal conductivity of the insulating sheath and stem diameter and dt_r is the temperature difference of two thermocouple in radially (^{O}C).

Once the all the components of the stem heat balance equation (2.31) are known, the mass flow rate of sap per unit time through stem is determined by difference and the mass flow rate of sap (*F*) as described by (Baker & Bavel, 1987, Sakuratani, 1981, Steinberg et al. 1990):

$$F = (P_{in} - Q_v - Q_r) / (CpdT) \quad (2.35)$$

Substituting the values or Q_v and Q *the* equation 2.35 can be written as:

$$F = \frac{P_{in} - K_{st} A(dt_u + dt_d) - (K_{sh} dt_r)}{C_p dT} \quad (2.36)$$

where C_p is the specific heat of water (4.186 J g^{-1} ^{O}C) and dT is the temperature difference between upper and lower junctions expressed as:

$$dT = (dt_u + dt_d) \big/ 2(0.04) \quad (2.37)$$

On the basis of literature, it is found that the heat balance sap flow method would be the appropriate method to measure the transpiration during sprinkler irrigation.

2.11 Conclusions and summary

The conclusions drawn from this review are as follows:

(1) There are major differences among researchers regarding the magnitude of evaporation losses during sprinkler irrigation; and this is principally due to the limitation of measurement techniques used.

(2) There is a wide range of factors which influence evaporation losses but it would appear that climatic (evaporative demand) and operating (sprinkler choice and use) factors are the major contributors to evaporation losses.

(3) The great effect of sprinkler irrigation is a significant increase of ET and reduction of transpiration. It also decreases the atmospheric demand modifying the microclimate of the irrigated area.

(4) Among the field experimental methods, the traditional catch-can method only can estimate the droplet evaporation losses with limited accuracy.

The limitations include overestimation of losses due to inclusion of evaporation losses from catch-can itself. Although, the lysimeter method can measure the total evapotranspiration during the nonirrigation period, this method could not measure the evapotranspiration during the period of irrigation due to the continuous addition of water.

(5) Although the statistical regression models can quantify the interaction of climatic and operating factors, these could not separate the components of the losses. Almost all the mathematical models have been confined on droplet evaporation losses. The only complete physical-mathematical (CUPID-DPEVAP) has been developed to predict the different components of evaporation losses. However, this model could not be verified during the period of irrigation due to limitations of measurement technique.

(6) The eddy covariance (ECV) method would be the most reliable and appropriate method to measure the evapotranspiration during the sprinkler irrigation. It can operate in continuous mode for either short or long duration irrigation trials and therefore can overcome the principal limitations of current measurement techniques for ET during irrigation.

(7) In energy balance equation, the major components of fluxes are the net radiation, latent heat flux, sensible heat flux and soil heat flux. Although advected energy can sometimes be dominant in a sprinkler-irrigated field, the other terms physical storage and biochemical energy flux are negligible. Also, in fully closed canopy condition, the soil heat flux can be considered as negligible.

(8) Heat balance sap flow method would be most reliable and convenient method to measure the transpiration rate of the plant for continuous monitoring during irrigation as well as during nonirrigation periods.

In summary, the review of past research reveals it was not possible to measure the total evaporation loss and its components during sprinkler irrigation due to the lack of appropriate instruments and measurement techniques. The recent development of the eddy covariance (ECV) system has provided a tool which is being routinely used for other evaporation research including measuring evaporation from natural and agricultural plant communities. However, a review of the literature provided no instances of it being used to measure evaporation losses occurring during sprinkler irrigation. Instead, research has focused on using traditional methods acknowledged to have many limitations. Hence the specific objectives of this research are to:

1. Use the eddy covariance technique (ECV) to measure the total evaporation occurring during sprinkler irrigation over a range of surfaces.
2. Through complementary measurements, partition the total evaporation into the canopy evaporation, soil evaporation, crop transpiration, canopy interception and droplet evaporation components.
3. Demonstrate how ECV data can be aid in management of sprinkle irrigation.

Chapter 3: Methodology

3.1 Introduction

The literature review (Chapter 2) highlighted the limitations of the traditional methods of lysimeters and catch-cans to measure the evaporation losses during sprinkler irrigation as well as the potential of the eddy covariance (ECV) system to measure the evaporation during sprinkler irrigation. Although eddy covariance has been used successfully to measure evaporation from natural and agricultural plant communities, a review of the literature provided no instances of it being used to measure evaporation losses occurring during sprinkler irrigation. The literature review also demonstrated that simultaneous measurement of sap flow using the heat balance sap flow method could give an indication of the transpiration which is a major component in evapotranspiration.

Preliminary measurements using the ECV system over the grass showed that this system is able to measure the additional evaporation occurring during sprinkler irrigation (Chapter 4). To provide better understand of this technique, and its feasibility, a series of field experiments were conducted over different surfaces like bare soil and different stages of crop including measurements of major energy fluxes and sap flow (Chapter 4 & 5). This present chapter provides details of the methodology used in the field experiments.

The data from these experiments were used to calculate the additional evaporation and reduction of sap flow, during irrigation events and subsequent period (Chapter 5). The data under these experiments were also used to determine the total additional volume of water required due to the evaporation losses in sprinkler irrigation and to separate its components. The data were also used to develop regression equations to

predict the additional evaporation under arbitrary sprinkler irrigation on the basis of climatic data for cotton growing areas in Australia (Chapter 6).

3.2 Study site

The experimental trials were carried out at the agricultural experimental station ('Agplot') situated at the University of Southern Queensland (USQ), Toowoomba, Queensland (Qld) 4350, Australia. The geographic location of the site is 27º36'00"S, 151º54'00"E and the altitude is 693 m above sea level (Figure 3.1). The surface of the site is free draining clay textured red Kraznozem soil (NCEA 2005) surrounded by few buildings at north and west. The soil contains high amounts of iron that help to maintain their highly permeable structure and generally deeper with soil depths reaching in excess of 2.0 m. The p^H of the soils is acidic to neutral.

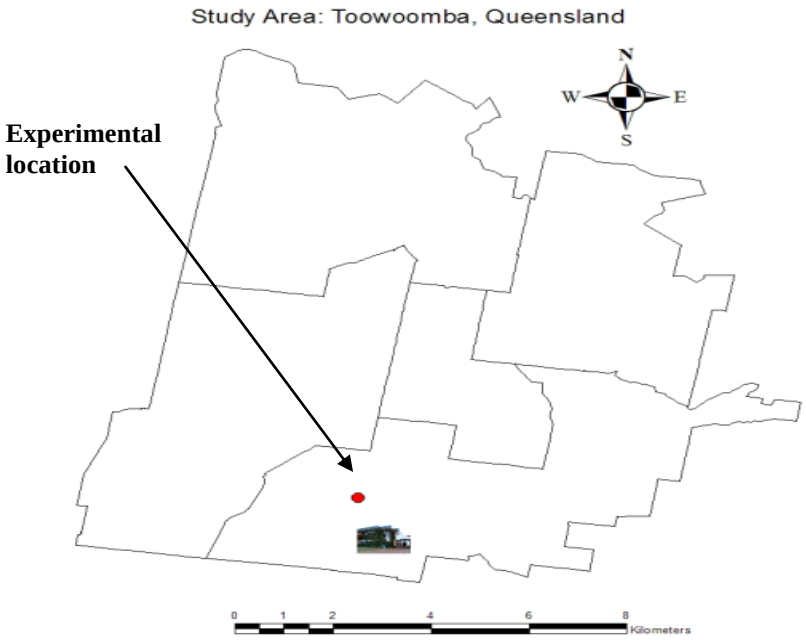

Figure 3.1: Map of the study site

3.3 Climate and weather

The climate of the study site is sub-tropical with long, hot summers and short, mild to cold winters. The mean daily maximum temperature reaches its maximum value in January with approximately 28.2 ^{0}C, while the mean daily minimum temperature reaches its minimum value in July (6.4 ^{0}C). The relative humidity (RH) presents the inverse behavior reaching a maximum of typically 65% in June and minimum of 51% in September. The region is characterized by irregular rainfall, particularly in the summer when the climate is sub-tropical and rainfall is dominated by discrete cumulonimbus storms. The annual average is approximately 700 mm. The monthly maximum (114 mm) typically occurs in February and minimum (27 mm) in April (Figure 3.2).

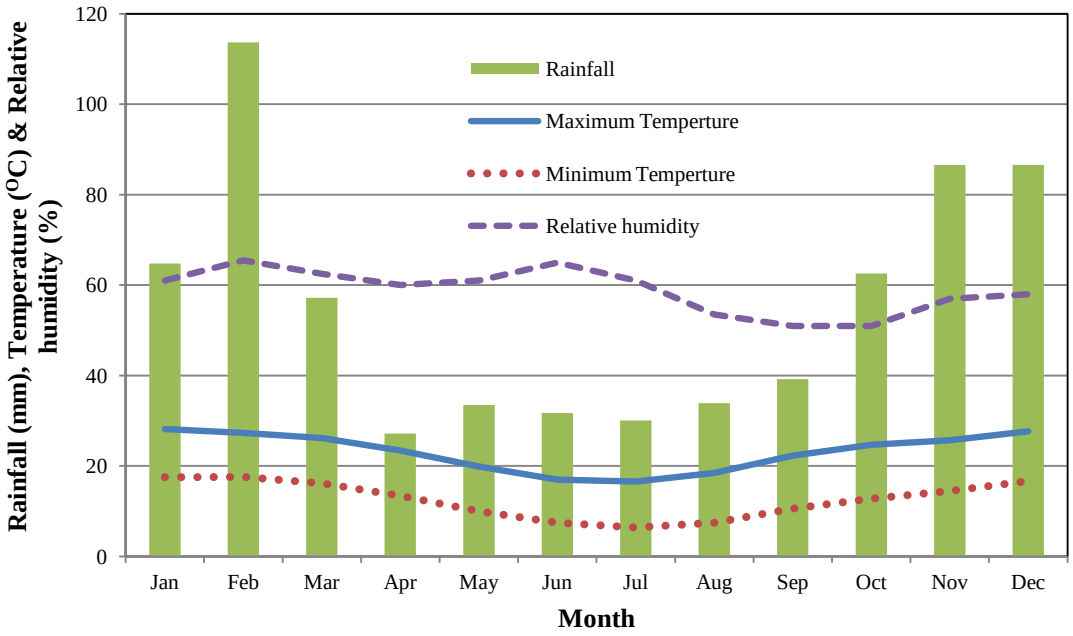

Figure 3.2: Long term monthly average data of Toowoomba Airport near to study site (1998-2010) (source: Bureau of Meteorology, Australian Government)

3.4 Crop establishment and agronomic practices

The study site was 109 x 54 m in size making two plots one (52m x 52 m) is for main crop and another (24m x 24m) for refuge crop (Figure 3.3). The main plot was planted with genetically modified (GM) cotton (71BRF) variety and the other plot with general cotton variety (71RRF) as an insect refuge crop (Figure 3.4). The seeds were planted at 0.75 m row-to-row and 0.07 m plant-to-plant in both cases on 8 October 2010. The seeds were planted into dry soil and irrigated after planting to ensure adequate soil moisture and crop establishment. First and second round of herbicides (Roundup Ready Flex) were applied on 21 December 2010 and 24 March 2011 respectively to kill the weeds. Fertilizer was applied on 24 February 2011 at the mid stage of the crop to ensure adequate nutrients in the soil.

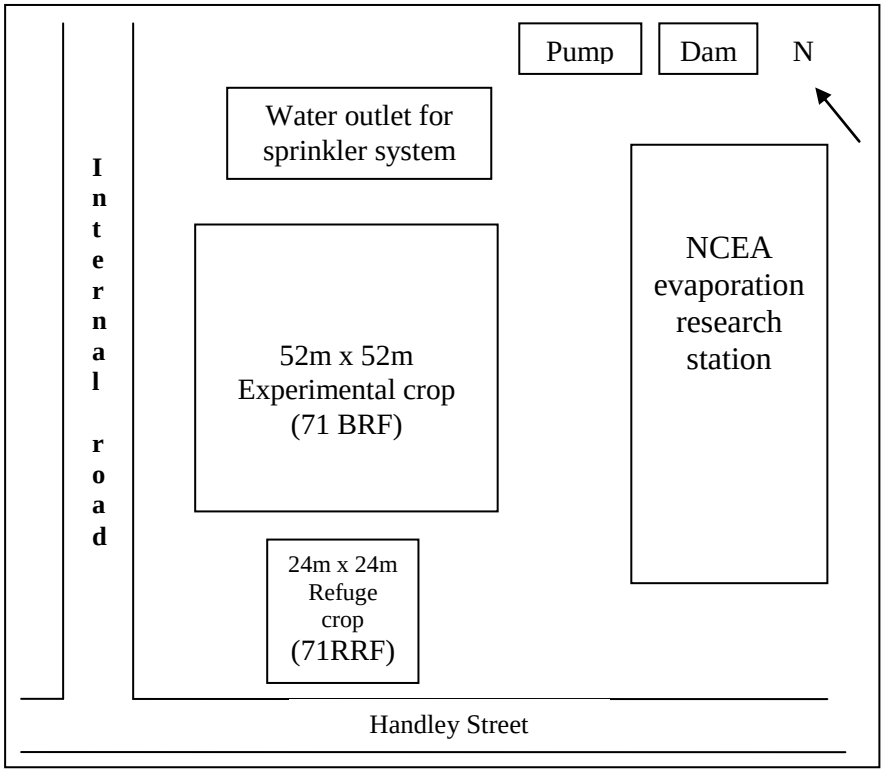

Figure 3.3: Schematic layout of the experimental site (not to scale)

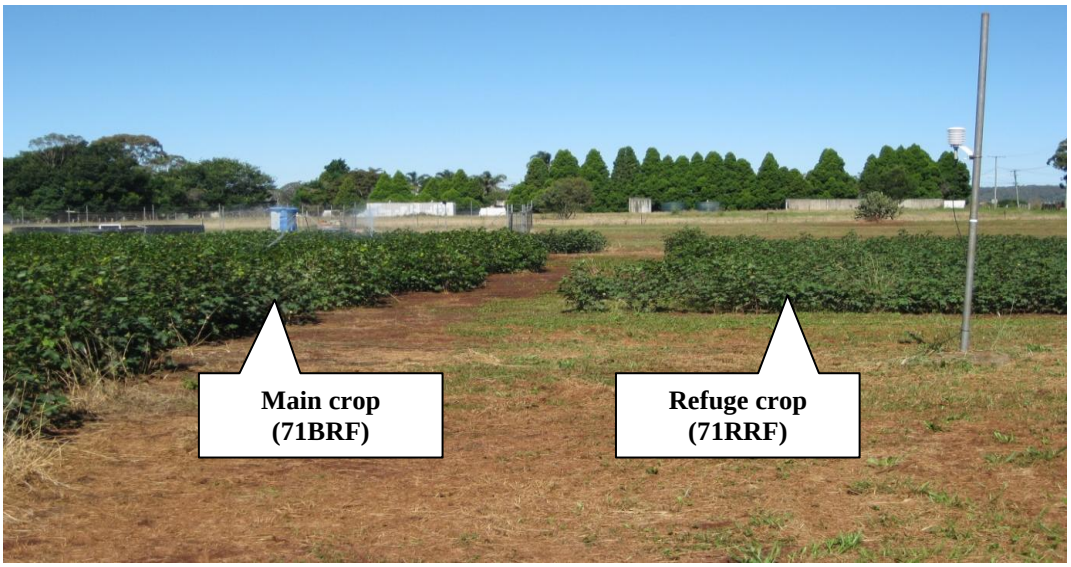

Figure 3.4: Crops at early and mature stage at the experimental field

3.5 Irrigation system and instruments layout

A movable sprinkler irrigation system was used consisting of 23 lengths of 50 mm diameter aluminium pipes and 24 sprinklers. Two sizes of plastic low volume, low angle (9^o) and low pressure impact sprinklers (e.g., model 5024, Naan Dan Jain

Irrigation Ltd.) and spray type sprinkler (R3000, Nelson Irrigation Corporation of Australia Pty. Ltd.) were used in irrigation experiments. The irrigation system was installed in a way to make a circle of 50 m with an area of 0.2 ha (Figure 3.5) for all trials. The spacing of laterals and nozzles was 9 m. The height of the sprinklers was varied from 0.2 m to 0.95 m depending on the height of the crop.

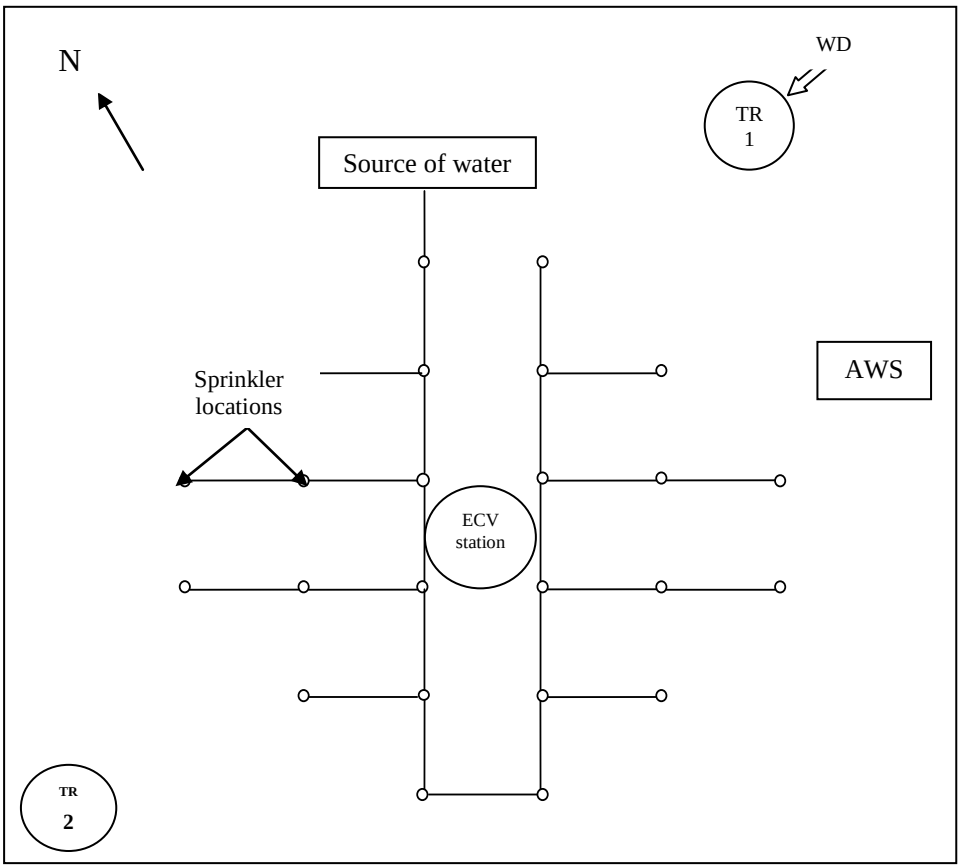

Figure 3.5: Sprinkler layout to form a 50 m irrigated circle with the ECV system at the centre along and other instrument in different locations. TR1 and TR2 represent the position of the measurement of temperature and relative humidity at upwind and downwind position, respectively and AWS represents the position of automatic weather station.

According to the footprint analysis (Appendix A), the ECV station showed that the effective fetch influenced the measurements was about 70 m towards the upwind

distance. It was observed from the analysis that measurements at a height of 2 and 2.5 m were mainly affected by fluxes coming from an upwind area at a distance of about 8-15 m (Figure A.2, Appendix A) in the representative days over the crop. On the other hand, from the cumulative flux it is seen that about 80% flux came from the crop area (Figure A.2, Appendix A).

The system was normally operated at 300-350 kPa with each sprinkler rotation set to full circle. During the irrigation the pressure was measured at the nozzle using pressure gauge (Figure 3.6). The source of the water was a dam located around 150 m from the study site through an underground supply line using a high pressure pump. Multiple trials were undertaken in which irrigations were applied for different durations, 30, 60, 120 and 180 mins, and at the 30, 60, 120 and 180 mins intervals at the middle part of the day (when the sun was high in the sky and a substantial evaporative flux expected). For short duration (30 mins) irrigation, several irrigations were conducted in a day and then combined (using a nondimensionalisation technique set out in Section 3.11). Experiments were conducted in different periods of the 2010-2011 season, according to the weather conditions. The sap flow was measured only at mature crop canopy conditions starting from the experiment IV. The general characteristics of the experiments are listed in Table 3.1.

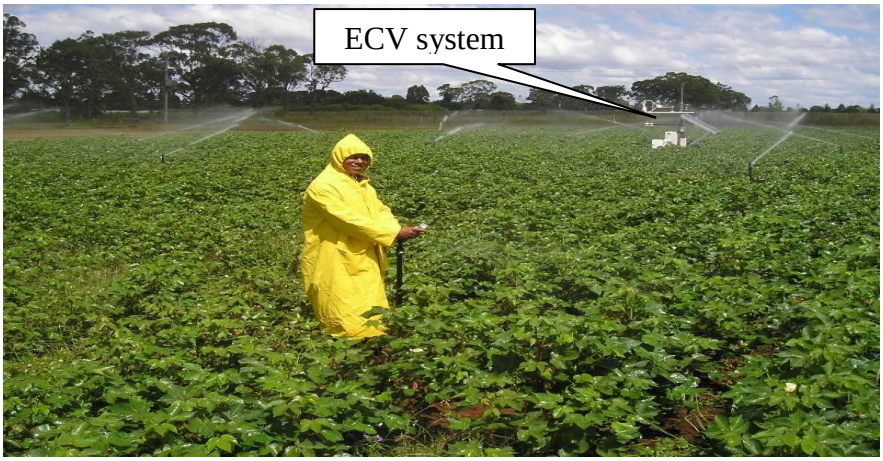

Figure 3.6: The author measuring nozzle pressure during irrigation

Table 3.1: General characteristic of the experiments

Experiment	Surface	Period	Combination of irrigation trials in hour			Sprinkler system			Pressure	Application rate
			Pre	Irri	Post	Type	Size (mm/No)	Height (m)	kPa	mm/hr
Experiment I	Grass	18 Mar. – 30 Apr. 2010	1/2	1/2	1/2	Impact	3.2	0.20	350	9.25
Experiment II	Bare soil	25 -30 Nov. 2010	1/2	1/2	1/2	Impact	3.2	0.20	350	9.25
Experiment III	Partial (50%) coverage of crop canopy	19 Feb. – 1 Mar. 2011	1/2	1/2	1/2	Impact	3.2	0.95	300-350	8.64 - 9.25
Experiment IV	Partial 75% coverage of crop canopy	16 Mar.– 6 Apr. 2011	1	1/2	1			0.95		
Experiment V	Full canopy coverage	8 Apr. 2011	1	1	1			0.65 - 0.95	300	8.64
Experiment VI	Full canopy coverage	7 Apr. 2011	2	2	2			0.95		
Experiment VII	Full canopy coverage	9- 17 Apr. 2011	3	3	3			0.95		
Experiment VIII	Full canopy coverage	21- 24 Apr. 2011	3	3	3	Spray	14	0.95	300	9.20
Experiment IX	Full canopy coverage	25 Apr. - 1 May 2011	3	3	3	Impact	2.5	0.95	300	5.30
Experiment X	Full canopy coverage	5 - 7 May 2011	3	3	3	Spray	14	0.95	300	9.20

3.6 Measurements

3.6.1 Energy flux measurement

The sensible and latent heat fluxes H and λE respectively, were as the residual of the energy budget for the plant/soil cropping system:

$$H + \lambda E = R_n - G - D - J - \mu A \quad (3.1)$$

Ignoring the minor terms the equation 3.1 becomes:

$$H + \lambda E = R_n - G \quad (3.2)$$

where, λE is the latent heat flux (W m^{-2}),

R_n is the net radiation (W m^{-2}),

H is the sensible heat flux (W m^{-2}),

D is the advective energy removed horizontally by advection (W m^{-2}),

G is the soil heat flux (W m^{-2}),

J is the flux of energy into physical storage (W m^{-2}), and

μA is the flux of energy into biochemical process (W m^{-2}).

The partitioning of the total flux H and λE was determined by the Bowen Ratio β:

$$\beta = \frac{H}{\lambda E} \quad (3.3)$$

Section 2.6 determined instantaneously using the eddy covariance (ECV) system placed at the centre of the irrigation system (Figure 3.5). As reviewed in section 2.6.2, although the ECV system provides direct measurements of both H and λE

these measurements do not include the entire flux of H and λE at this point because the ECV measurement footprint (section 2.6.3) extends to some extent beyond the experimental area. However, following Twine et al. (2000) the error in both H and λE is in proportion such that an accurate Bowen Ratio is measured.

The ECV system (Figure 3.7) comprised a fast-response three dimensional sonic anemometer (model CSAT3, Campbell Scientific, Inc., Logan, UT, USA) to measure the velocity and temperature, coupled with open path infrared gas analyzer (model LI7500, Licor, Inc., Lincoln, NE, USA – Figure 3.8) to measure the vertical water vapour flux in the atmosphere. The CSAT3 sensor was oriented toward the predominant wind direction for the day of the trials. The height of the instruments was increased from 2.0 to 2.5 m above the ground depending on the height of the crop. The height of the ECV system was also maintained depend on sprinkler height to keep the sensors out of water droplet or wetting. The separation between sensors was of 15 cm as recommended by Campbell Scientific Inc. The ECV system logger (CR3000, Campbell Scientific, Inc., Logan, UT, USA) recorded signals from these instruments at high frequency of 10 and 20 Hz and averaged over 5 min intervals.

The net radiation (R_n) in equation 3.1 was measured using a four component net radiometer (NR01, Hukseflux Thermal Sensors B.V, The Netherlands) through the equation 2.19 under the section 2.8.1.4 in chapter 2. The net radiometer was placed in the ECV tower at the centre of the irrigated field maintaining the height 1.5 m above the ground level

The soil heat flux (G) was measured with two heat flux plates (HFP01, Campbell Scientific, Inc., Logan, UT, USA) buried in the ground at 5 cm depth, at two locations (one between the rows and another one between plants) of the irrigated area. The values of G were obtained as the average of the two measurements using the same data logger.

The temperature and relative humidity at the experimental site were measured using a temperature and relative humidity probe (HMP 45c, Campbell Scientific, Inc., Logan, UT, USA) placeing at two locations on the periphery of the irrigated plot, one upwind and one downwind as shown in Figure 3.3. The air temperature and relative humidity was measured every 0.1 sec and the 5 min averages were recorded in the same data logger used for the flux measurements.

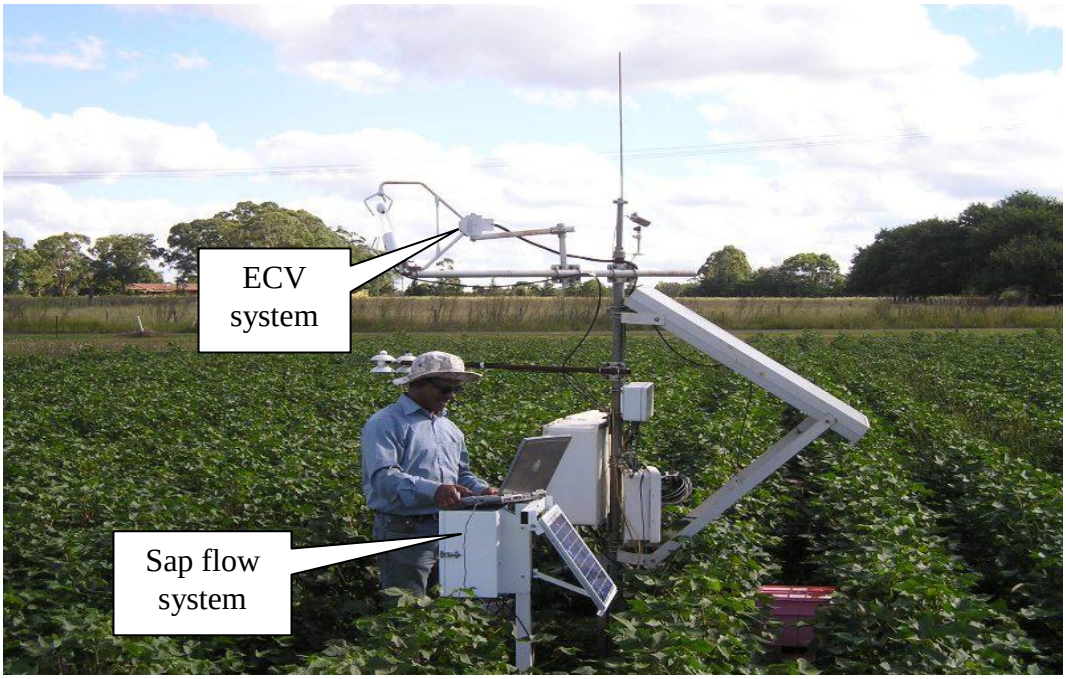

Figure 3.7: Installed ECV and sap flow system at the centre of the field for continuous measurements

The crop canopy temperature in the experimental field was measured using an infrared thermometer (Model 4000L, Everest Interscience Inc., USA, factory-calibrated) that was installed on a bracket of the eddy covariance system (Figure 3.8) such that its viewing centreline was at an angle 15 degree from the horizontal. Canopy temperature was also measured every 0.1 sec and the 5 min averages were

recorded in the same data logger used for flux measurements. The canopy temperature was measured only after the development of plant canopy to avoid the problems with soil in the field of view. Measurements were taken from a height of about 1 m above the crop.

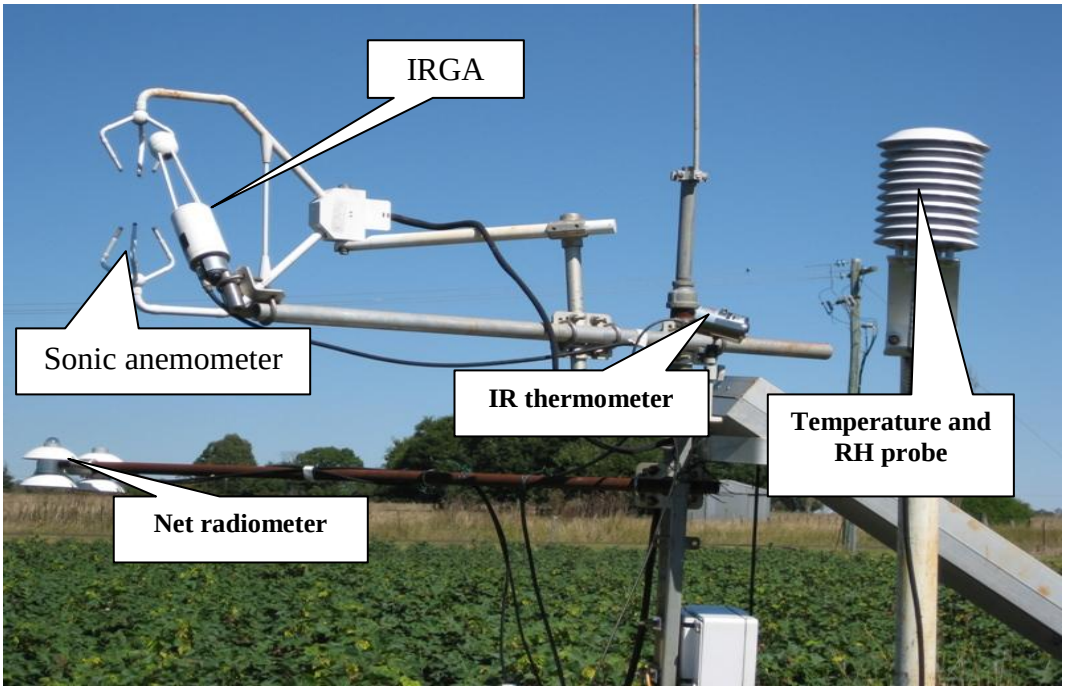

Figure 3.8: Sonic anemometer, infrared gas analyser (IRGA), four-component net radiometer, temperature, relative humidity probe and infrared thermometer installed at the experimental site

3.6.2 Sap flow measurements

The sap flow system consisted of six dynagauge sap flow sensors (model SGC10, ICT International Pty. Ltd, Australia), each with a digital interface, a hub to connect the sensors to the data logger, and a data logger (Smart data-logger, ICT International Pty. Ltd, Australia) shown in Figure 3.9. The sensors were installed on six randomly-

selected plants of 10 to 13 mm stem diameter within the irrigated area. The gauge sensors were protected from corrosion by an electrical insulating compound placed between the gauge interior and the plant stem, and the exterior of the gauge was covered with additional foam insulation, plastic wrap, and aluminium foil for thermal insulation.

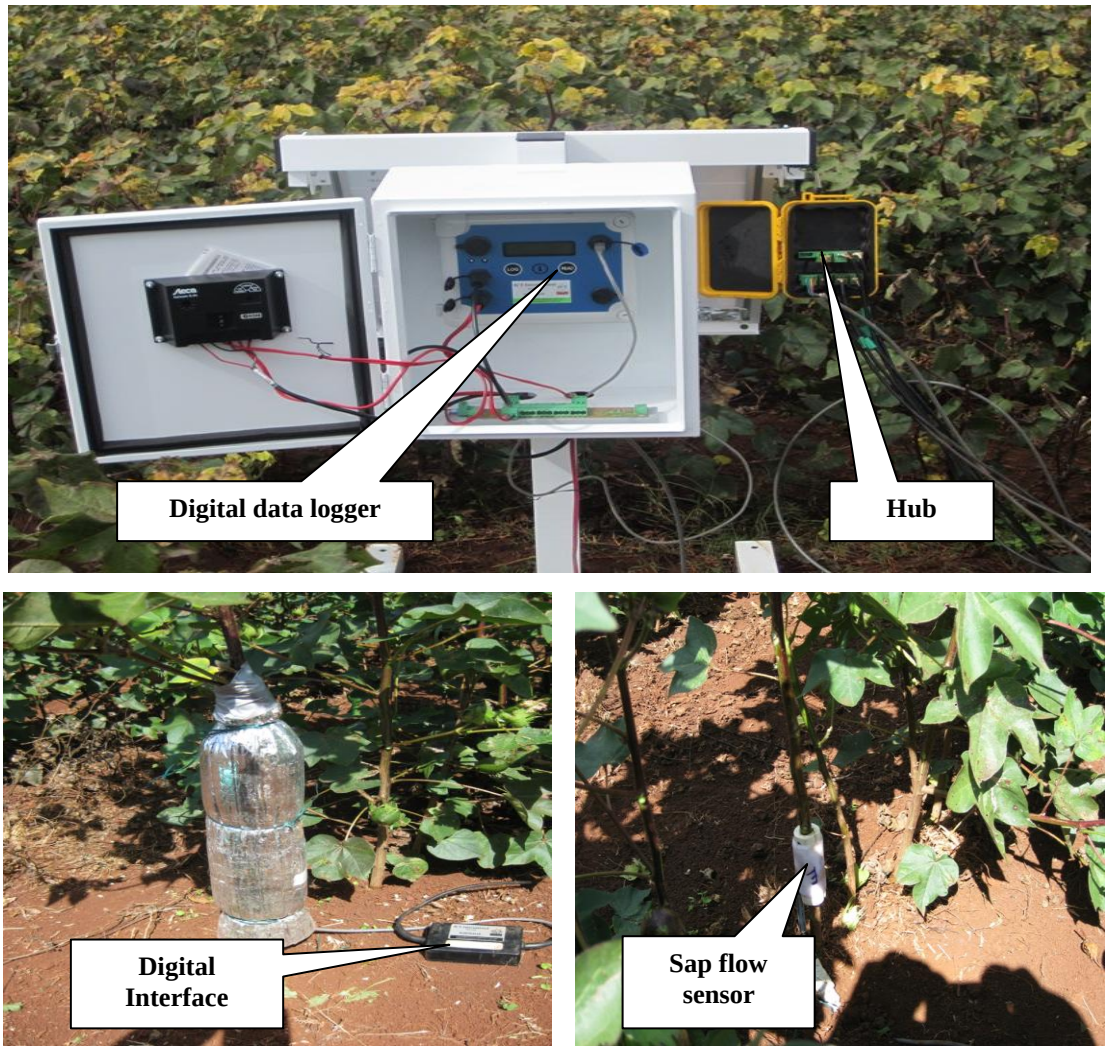

Figure 3.9: Sap flow system installed in the field

The gauges were reinstalled weekly to remove moisture build-up and to assess damage to plant stems and/or gauges. The auto calculation and adjustment option for wound correction factors (sheath conductance factor) of the smart data logger were used to adjust this factor in sap flow measurements. Sap flows (gm hr^{-1}) were sampled every minute (minimum as specification) and averaged over every 5 min similar to the eddy covariance system for easy comparison. The sap flow of six plants was then averaged to obtain flow rates in mm hr^{-1} considering plant densities of 18 plants per square metre.

3.7 Data processing analysis and corrections

In general, the ECV technique is assumed to be the most accurate method for the estimation of turbulent fluxes. However, as a result of footprint limitations (as noted above, section 3.6.1), and other recognised limitations, for example sensor design shortcomings and non-coincident location, finite flux averaging, and processing methods, the eddy covariance tends to underestimate the true atmospheric fluxes (e.g. Massman & Clement 2004). In order to minimize this underestimation, several authors have proposed correction algorithms which are provided in section 2.6.2.

According to Mauder & Foken (2006), the Webb, Pearman & Leuning (WPL) correction (Webb et al. 1980) is the vital correction for eddy covariance flux data and can correct the errors of up to 50% of error flux. Accordingly, the raw data were corrected for effects of density fluctuations induced by heat fluxes on the eddy fluxes of water vapour measured using the LI-7500. Leuning (2007) provided a detailed description of the principles and theory of the WPL correction. No corrections were made to account for sensor separation because the sensors (CSAT3 and LI-7500) were maintained at the distance (15 cm from centre to centre) recommended by Campbell Scientific Ltd. and the field was mostly homogeneous (having small

spatial variability, judged by visual assessment). Moore (1986) indicated that when close to ideal sensor separation is achieved, coordinate rotation corrections may result in flux adjustments of less than 3%. Thus, considering the previous statement and the fact that the field was practically flat, coordinate rotation was not performed in data processing and corrections. Data de-trending was not also pursued because the 5-min averaging period was considered short such that the risk of non-stationarity was low.

Based on these assumptions, the high frequency raw flux data were processed and corrected using the 'EdiRe' software (http://www.geos.ed.ac.uk/abs/research/micromet/EdiRe), which contains sonic temperature correction according to Schotanus et al. (1983) and correction for density fluctuations (WPL correction, section 2.6.2.7) according to Webb et al. (1980). With values calculated in data logger confirming that the data logger program was calculating the values correctly.

3.8 Data quality assessment

Closure of energy balance is considered as an important measure for evaluating eddy covariance measurements of the latent and sensible heat fluxes (Twine et al. 2000, Wilson et al. 2002). Although closure was not expected due to the constraints on the ECV footprint, the magnitude of non-closure was calculated by using the equation 3.4.

Ignoring all other sink and sources of fluxes as small, the energy balance was studied by using the following equation (Wilson et al. 2002):

$$EBR = \frac{\sum(\lambda E + H)}{\sum(R_n - G)} \tag{3.4}$$

where EBR is the energy balance ratio (which, when not equal to unity, indicates imperfect closure.

The data quality assessment in terms of energy balance closure shows that the eddy covariance method underestimated the latent and sensible heat flux by about 50% (Figure B.1 & B.2, Appendix B). This confirmed the need to use the ECV flux measurements solely to calculate the (instantaneous) Bowen Ratio.

Flux data were also tested using integral turbulence and stationarity tests following Foken and Wichura (1996). The integral turbulence test is based on the Monin-Obukhov hypothesis according to which various atmospheric parameters and statistics, when normalised by appropriate powers of the scaling velocity, u_* become universal functions of the stability parameter ξ. Here the stability function for vertical wind velocity following Panofsky et al. (1977) was employed:

$$\frac{\sigma_w}{u_*} = 1.3\left(1 - 2\frac{(z-d)}{L}\right)^{1/3} \qquad -3 < (z-d)/L < -0.2 \tag{3.5}$$

where σ_w is the standard deviation of the vertical wind velocity w,

u_* is the friction velocity (m s^{-1}),

z is the measurement height (m),

d is the zero plane displacement (m), and

L is the Monin-Obukhov length (m).

From the atmospheric stability analysis it was found that the data (nondimensional standard deviation of vertical speed as a function of $(z - d)/L$) lie in the stability

range $-0.5 \leq (z - d)/L \geq + 0.5$. However, most of the data points are within the range $-0.5 \leq (z - d)/L \geq + 0$ which indicates that unstable atmospheric conditions prevailed during the measurements. Stability analyses for the period of 28 February – 01 March (Experiment III) are presented in Appendix B (section B.3.1) as an example.

3.9 Calculation of sensible and latent heat flux

Despite eddy covariance being among the most advanced ‘‘in situ’’ measurement technologies that directly provide λE, it is widely known to underestimate the latent heat flux resulting in failure to achieve closure of the energy balance (Foken 2008). Twine et al. (2000) suggested that when the available energy ($AE = R_n - G$) measurement errors are known, ECV measurements of sensible and latent heat fluxes should be calculated for closure by maintaining the Bowen Ratio (BR). A preferred method of energy budget closure was suggested by Twine et al. (2000), supported by Ding et al. (2010) and Chavez et al. (2009), and labeled the ‘Bowen-Ratio (BR) closure method’: this was followed to calculate the sensible and latent heat flux using:

$$\lambda E = \frac{R_n - G}{1 + \beta} \tag{3.6}$$

and

$$H = \frac{\beta(R_n - G)}{1 + \beta} \tag{3.7}$$

where β is the Bowen ratio $\left(H \big/ \lambda E\right)$ and is calculated from the raw (uncorrected) values of H and λE.

After calculation of ET maintaining Bowen Ratio, the EC based ET improved significantly on the agreement between and ET_{ref}. Statistical analysis shows that

measurements error also reduced remarkably by calculating the evapotranspiration using Bowen Ratio method (Section B.3.2, Appendix B).

3.10 Calculation of actual evapotranspiration (ET_{ecadj})

The latent heat flux (λE) in W m^{-2} measured by the eddy covariance technique was converted into evapotranspiration termed ET_{ecadj} and converted into a water depth equivalent expressed as mm hr^{-1} in order to permit easy comparison. This was done using the following equation:

$$ET_{ecadj} = \frac{\lambda E}{(28.36_x 24)} \tag{3.8}$$

where ET is evapotranspiration (mm hr^{-1}) converted from EC measured λE (W m^{-2}). The numerical divisor (28.36 x 24) is the conversion of λE from W m^{-2} to mm hr^{-1}.

3.11 Nondimensionalisation of ET and sap flow

To overcome the difficulties in comparison and to quantify the relative magnitude of evapotranspiration changes during irrigation periods, a nondimensionalisation technique was employed. A dimensionless variable R_{et} was calculated as the ratio of actual evapotranspiration measured by the eddy covariance technique (ET_{ecadj}) to the reference evapotranspiration (ET_{ref}) estimated by FAO Penman-Monteith equation.

This technique will allow the trends in the variation of ET in different phases of irrigation to be shown more clearly, removing the variation caused by net radiation (R_n) as the effect of solar zenith angle and cloud cover and evaporative demand (Figure B.6 - B.8 in Appendix B). This technique also removes many random fluctuations resulting from sampling error. More importantly, nondimensional

technique would be the best suited technique to compare the data for different times and periods as well as to estimate the additional evaporation that occurs during the irrigation compared to the nonirrigated (pre-irrigation) period. Hence, the presentation of the trend of ET during irrigation and nonirrigation period and estimation of additional evaporation is done on the basis of nondimensional ET.

Similarly, the sap flow was also nondimensionalized as the ratio of sap flow F to the reference evapotranspiration ET_{ref} and is termed R_f.

Using this Nondimensionalisation technique, the dimensionless ET and F for different trials in a day were then averaged to convert them to a 'single' irrigation.

3.12 Calculation of reference evapotranspiration

The reference evapotranspiration (ET_{ref}) used in the process of nondimensionalisation is essentially a measure of evaporative demand. It is defined as the ET calculated for a dry canopy using the FAO Penman-Monteith equation according the Allen et al. (1998).

ET_{ref} was calculated using the climatic data measured at the experimental site. However it was necessary to use an adjusted net radiation (R_n) in the calculation because the measured values were altered by the irrigation wetting the canopy. The adjustment removed the effect of the wetting.

Wetting of the canopy causes a reduction in the albedo and temperature of the canopy (Figure 3.10). These in turn cause a decrease in the reflected shortwave radiation and a decrease in the longwave radiation emitted by the canopy. The result is an increase in net radiation (R_n) during the irrigation.

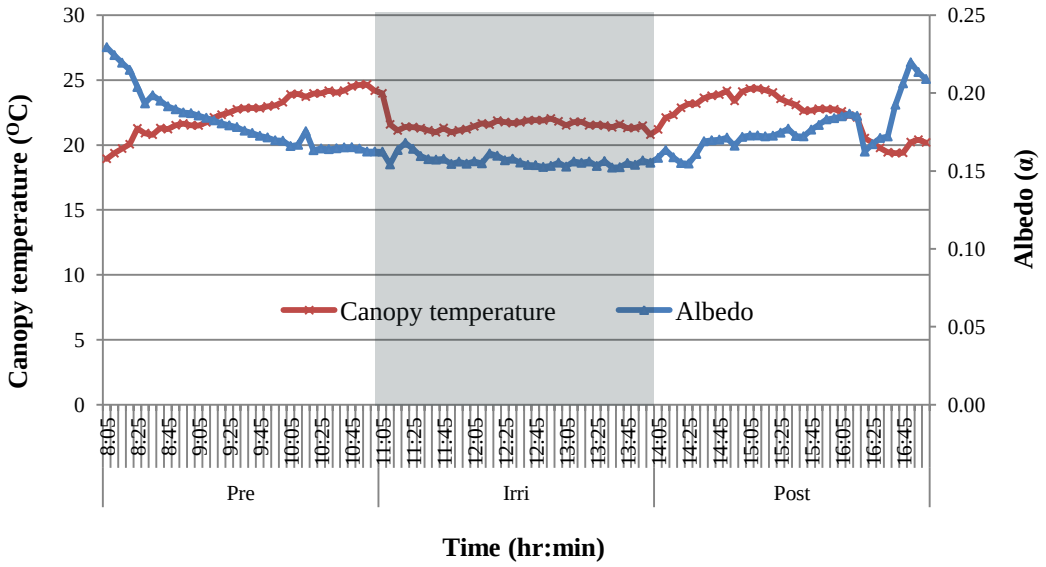

Figure 3.10: Effect of irrigation on surface temperature and albedo on 15 April 2011

The net radiation was adjusted by using the canopy albedo from the pre-irrigation period to calculate the outgoing shortwave radiation and hence the adjusted R_n.

The error of adjustment was calculated on the basis of canopy surface temperature at before and during period using the Stefan-Boltzmann law expressed as:

$$\frac{(lR_{out})_{irri}}{(lR_{out})_{pre}} = \frac{\sum T_{irri}^{4}}{\sum T_{pre}^{4}} \qquad (3.9)$$

where $(lR_{out})_{irri}$ is the outgoing longwave radiation in W m^{-2} during irrigation,

$(lR_{out})_{pre}$ is the outgoing longwave radiation in W m^{-2} before irrigation,

T_{irri} is the absolute canopy temperature in ^{O}K during irrigation, and

T_{pre} is the absolute canopy temperature in ^{O}K before irrigation.

Considering the canopy temperature before (24 ^{O}C) and during (21 ^{O}C) irrigation on a clear day (15 April 2011, DOY 105), the decrease in IR_{out} during irrigation was calculated as 4% with respect to the pre irrigation period. Given that IR_{out} is a very small components of R_n it was assumed reasonable to ignore this change.

Chapter 4: Preliminary measurements over bare soil and grass

4.1 Introduction

The literature review in Chapter 2 reported that eddy covariance (ECV) is a direct, accurate and reliable micrometeorological mass transfer method for measuring evaporation and evapotranspiration (ET). It has been used successfully for the last decade to measure evaporation from natural and agricultural plant communities, including surface irrigated fields and has major advantages over other ET assessment methods. However, the review provided no instances of it being used to measure evaporation losses occurring during sprinkler irrigation. Instead, sprinkler irrigation research has focused on using traditional methods acknowledged to have many limitations. It is hypothesized that these limitations can be overcome by adopting this new technique. Hence, preliminary measurements of total evaporation in sprinkler irrigation experiments were conducted to evaluate the capability of ECV technique to estimate the additional evaporation occurring during sprinkler irrigation. This chapter includes the measurements of total evapotranspiration before, during and after irrigation as well as the estimation of additional evaporation during the irrigation over bare soil and grass.

4.2 Methodology

The experimental trials were carried out at the agricultural experimental station (‘Agplot’) situated at the University of Southern Queensland (USQ), Australia. The

preliminary measurements were conducted over grass during the period March – April 2010 (Figure 4.1) and over bare soil during the period 25 – 29 November in the same year (Figure 4.2). Due to adverse weather conditions and lack of available water, more trials could not be conducted over the bare soil.

(a)

(b)

Figure 4.1: Measurement of evapotranspiration over (a) grass and (b) bare soil

On the basis of the quality of the data and weather condition, averages of the results for three days (DOY 78, 105 & 120) for grass and two days (DOY 329 & 333) for bare soil are presented. Several trials for short (30 mins) intervals were conducted in a day and then averaged the values of different trials averaged. All the measurements, data processing and analysis were done following the methodology described in the Chapter 3, with the exception that sap flow and canopy temperature measurements were not taken. The 15 mins averaged climate data were collected from the automatic weather station installed at the study site. The data were then converted into 5 mins averages using a linear interpolation technique.

4.3 Evaporation over grass

The total actual evapotranspiration (ET_{ecadj}) before (pre), during (irri) and after (post) irrigation, measured over the grass using eddy covariance (ECV) technique on relatively clear days are presented in Figure 4.2. The figures show that during the irrigation the evapotranspiration was measurably greater than the pre and post irrigation period in every trial. During each irrigation the actual ET (ET_{ecadj}) increased and was followed by declining evaporation as the surface (grass) dried. This was particularly evident in the first irrigation in the middle of the day where the radiation (evaporative demand) was relatively constant and at a maximum. During the second and third irrigations each day, although the net radiation decreased, the trends in ET_{ecadj} are still evident. In comparison with the reference evapotranspiration (ET_{ref}), the actual evapotranspiration (ET_{ecadj}) was less than the ET_{ref} in the pre and post irrigation periods in all cases. However, during the irrigation the ET_{ecadj} was close to ET_{ref} on DOY 78 & 105 (Figure 4.2a & b and exceeded the ET_{ref} on DOY 120 (Figure 4.2c). This indicates that some additional evaporation occurred during the irrigations as the direct effect of sprinkler irrigation. As the soil was covered by grass, this additional evaporation can be considered as the sum of the droplet evaporation during the flight and evaporation from the grass surface.

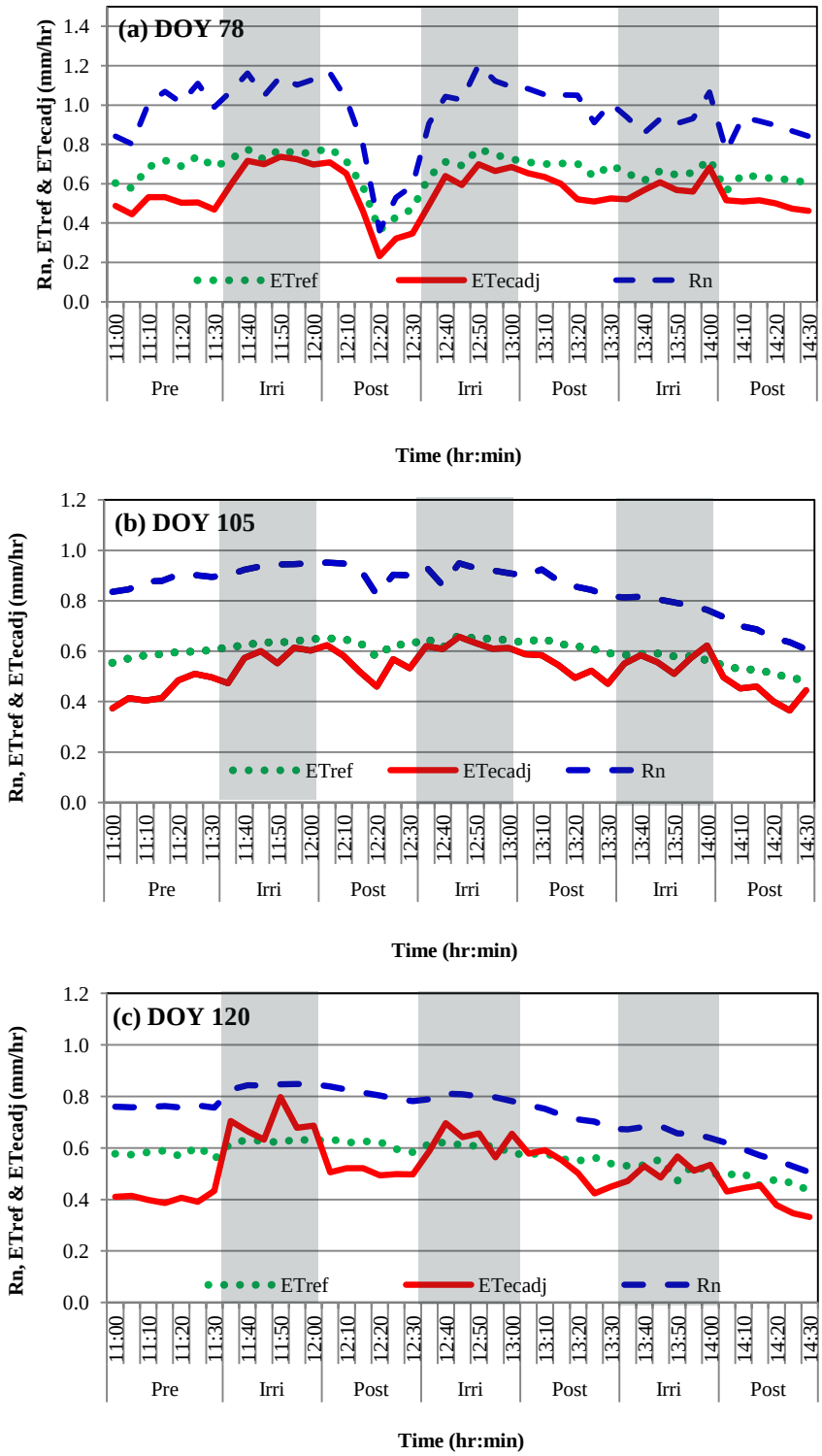

Figure 4.2: Reference evapotranspiration (ET_{ref}), actual evapotranspiration (ET_{ecadj}) and net radiation (R_n) on different days

From the analysis of the data it was found that, evapotranspiration measured by the ECV system fluctuated over the time due to the fluctuation of radiation. The effect of fluctuations still remained after averaging all the irrigation trials from a single day, which made it difficult to compare the data from irrigation the nonirrigation periods. To overcome this problem, nondimensional averaging of ET was used to compare the trend of actual evapotranspiration in different periods in a clearer way. The nondimensional curves of ET for individual days are shown in Appendix E. The curves illustrate that the data followed the similar trend in all cases (Appendix E.1a-E.1c) representing greater values during the irrigation than pre and post irrigation period, which indicates that the rate of evapotranspiration was greater during the irrigation in all irrigations.

The average nondimensional curves for three days (Figure 4.3) also show a similar trend. During the pre irrigation period the values of nondimensional ET were almost constant around the value 0.8 as the reference ET was greater than the actual ET (Figure 4.3). On the other hand, during the irrigation, the values rose rapidly after starting the irrigation and reached at steady state after about 10 mins due to increased actual ET as the direct effect of irrigation. This increased rate of ET represents the total additional evaporation which includes evaporation from the grass surface, soil evaporation and droplet evaporation. However, from the Figure (4.4), it is seen that there was no significant effect of irrigation on soil evaporation and it can be neglected as the soil was covered by the grass. Therefore it can be assumed that the total evaporation was the sum of evaporation from the grass surface and droplet evaporation. During the post (after) irrigation period, dimensionless ET was greater at the start of the period and gradually decreased over the time. This reflects the fact that after stopping the irrigation there was still some intercepted water on the grass which was evaporated over the time.

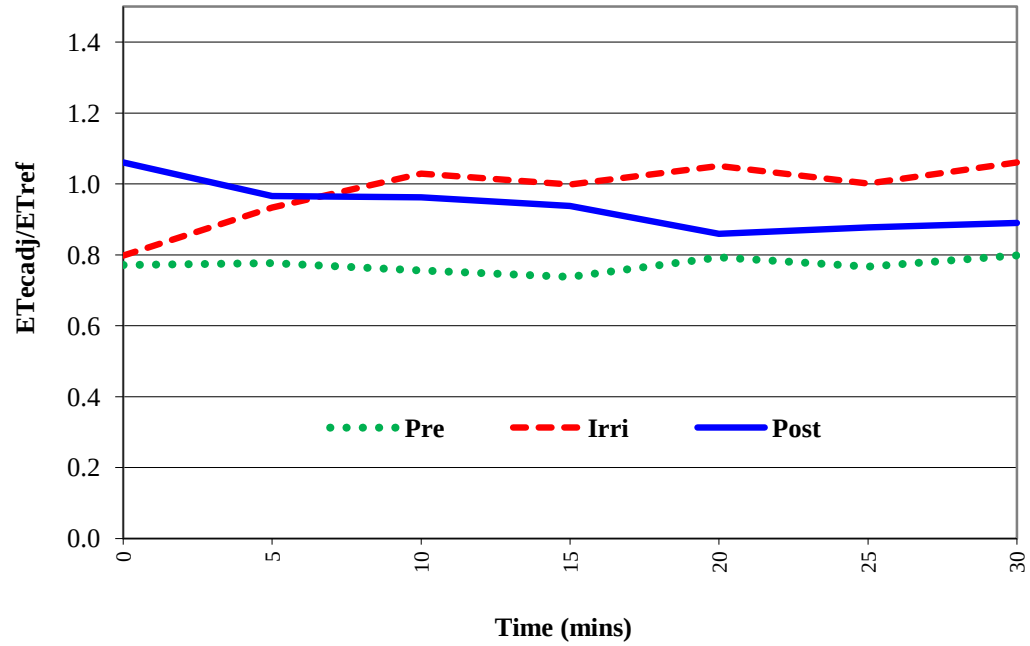

Figure 4.3: Nondimensionalised ET for grass surface

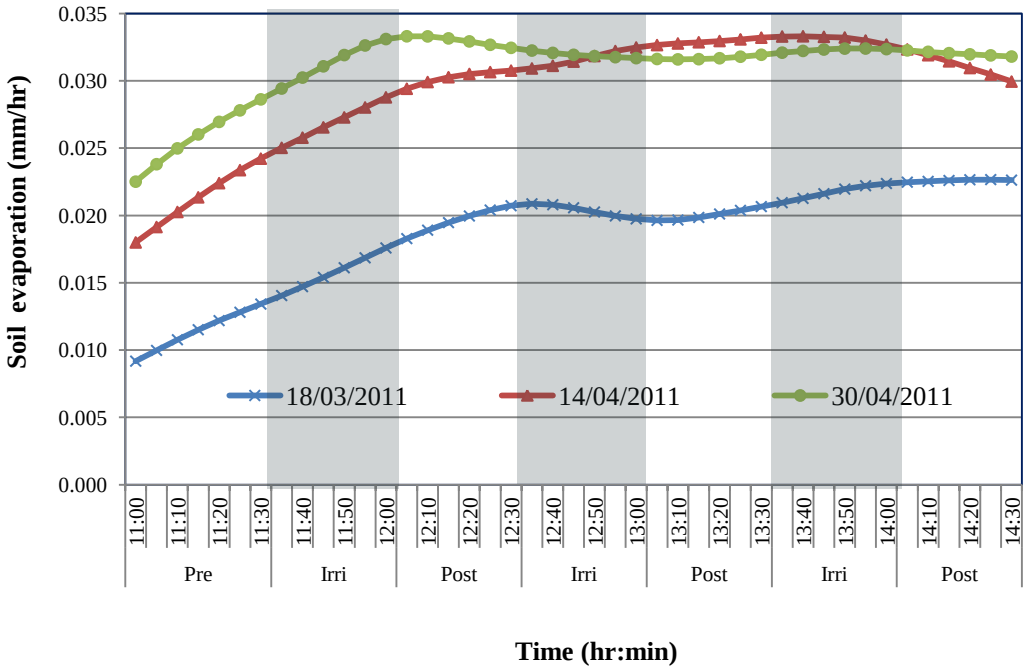

Figure 4.4: Soil evaporation under the grass surface

The additional evaporation defined as the difference of wet canopy ET during irrigation and dry canopy ET prior to irrigation was estimated on the basis of nondimensional ET before and during irrigation is presented in Table 4.1. The average value of nondimensional ET during the irrigation periods was considerably higher (0.96) than the pre irrigation period (0.73), which represents 32% additional evaporation. The maximum amount of additional evaporation (50%) was measured on a relatively clear and sunny day on 30 April 2010 (DOY 120), when the relative humidity was significantly lower compared to the other days (Figure 4.5). The average value of dimensionless ET during the post irrigation period was 0.85, slightly greater than the pre irrigation period, due to the wetness of the surface which caused some additional evapotranspiration until complete drying of the grass.

Table 4.1: Additional evaporation during sprinkler irrigation over the grass

DOY	Date	Combination of irrigation (hr)			Average ET_{ecadj}/ET_{ref}			Increment of ET_{ecadj}/ET_{ref} with respect to pre irrigation period	
		Pre	Irri	Post	Pre	Irri	Post	R_{et}	%
78	18/3/10	1/2	1/2	1/2	0.73	0.89	0.81	0.16	22
105	14/4/10	1/2	1/2	1/2	0.77	0.95	0.87	0.18	23
102	30/4/10	1/2	1/2	1/2	0.70	1.05	0.88	0.35	50
Average					**0.73**	**0.96**	**0.85**	**0.23**	**32**

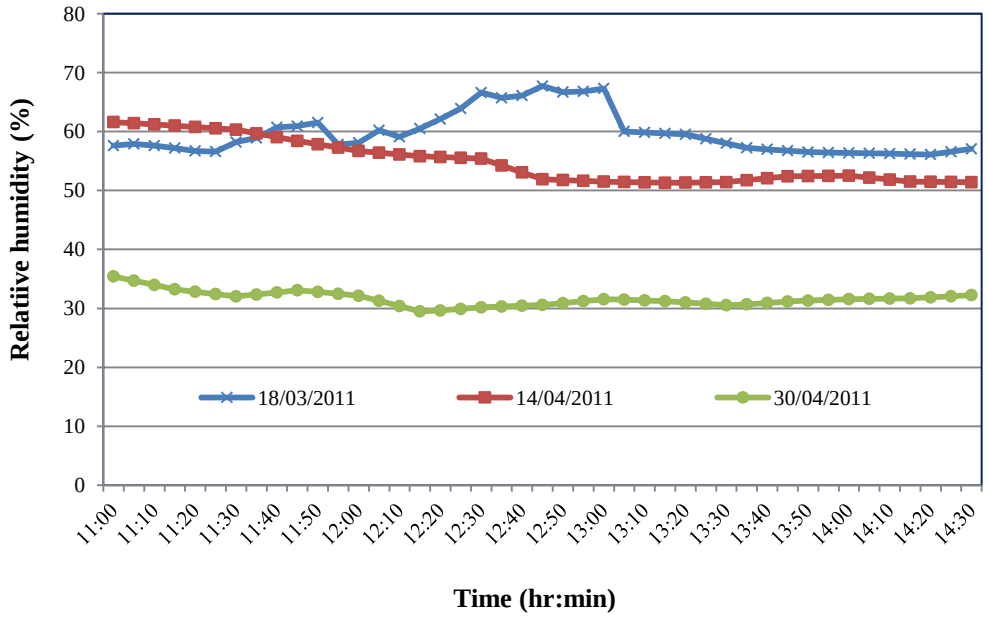

Figure 4.5: Comparison of relative humidity (RH) for three trial days

4.4 Evaporation over bare soil

Comparison of actual and reference ET in Figure (4.6), shows that over the bare soil there was no discernable difference between actual and reference ET during irrigation in both trials, although during the pre irrigation period ET_{ref} was slightly higher than actual ET in both cases. This might be due to the high atmospheric demand. But in case of grass, during the irrigation actual ET was found to be significantly greater than the reference ET (Figure 4.2). It means that over the bare soil there was little additional evaporation during irrigation.

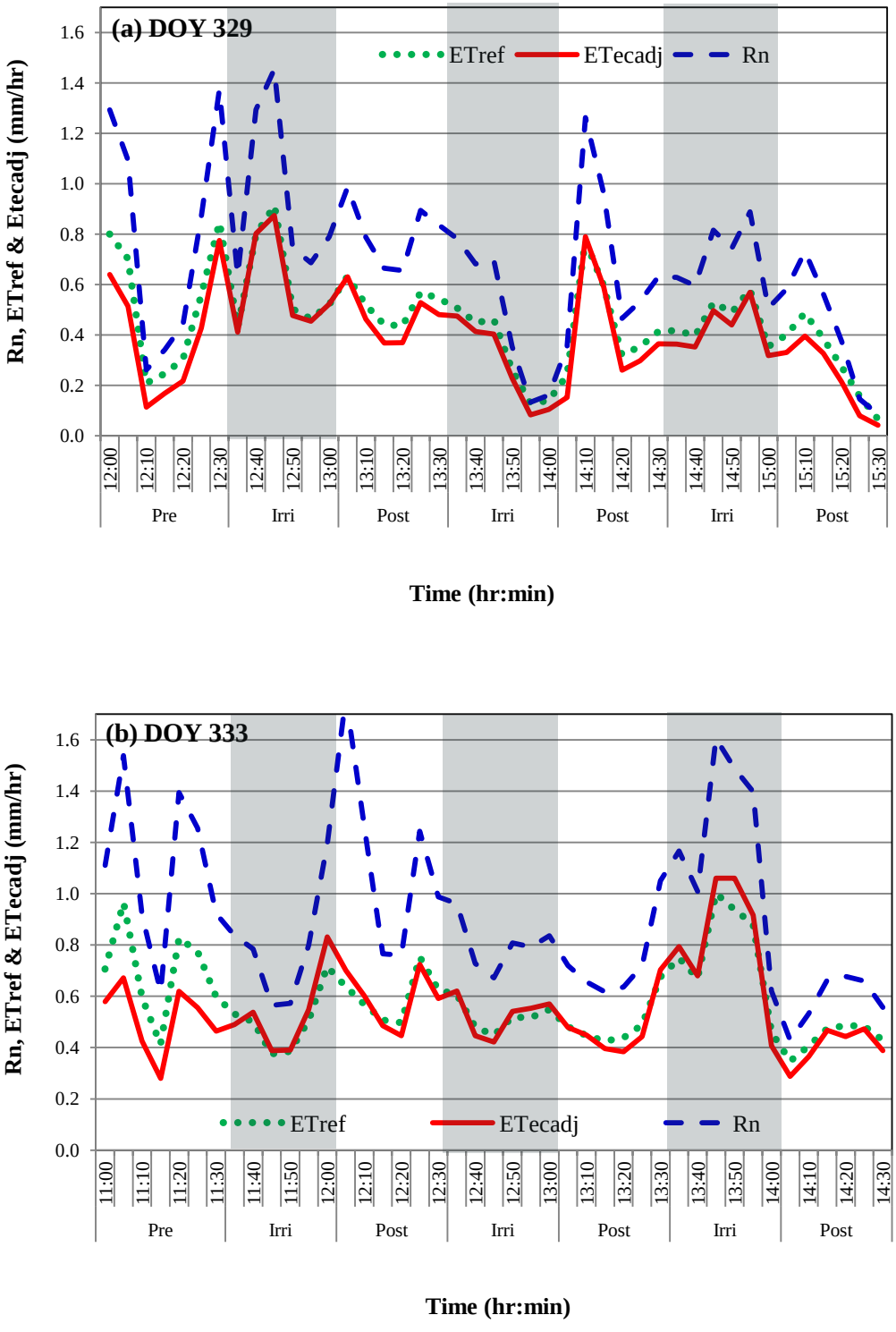

Figure 4.6: Comparison of reference and actual ET before, during and post irrigation for the trials over bare soil

The nondimensional curves of the two days averaged values over the bare soil are also different than for the grass surface. In this case, after starting the irrigation there was only a slight increase in dimensionless values compared to the initial values of the irrigation (Figure 4.7). Most interesting is that there was no significant difference between the irrigation and post irrigation periods which indicated that there was no intercepted water to evaporate after stopping the irrigation.

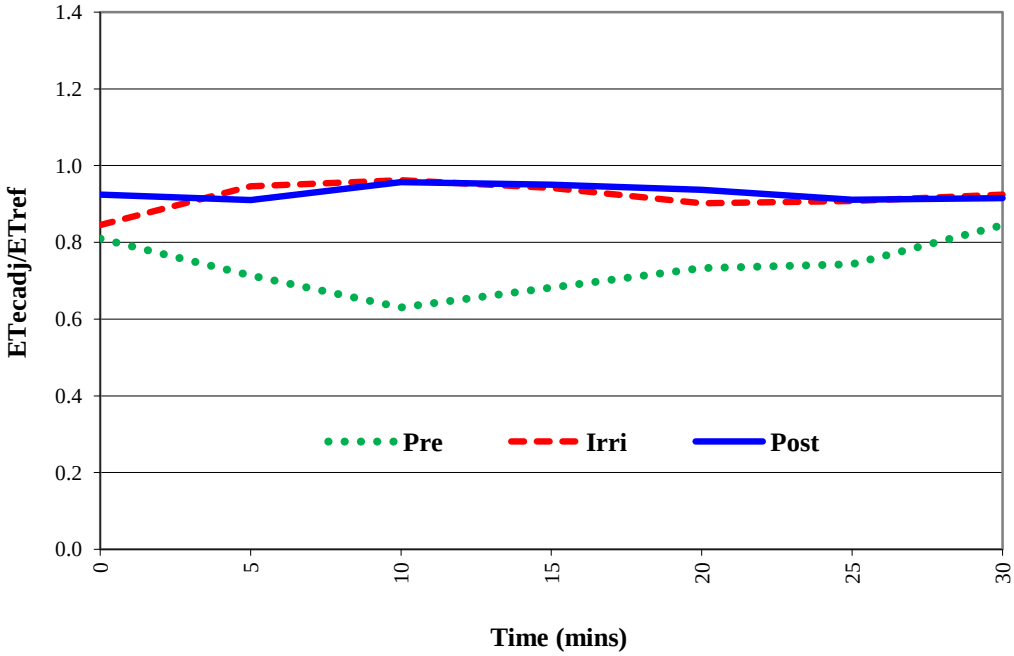

Figure 4.7: Nondimensionalised ET for bare soil

The average increment of ET during the irrigation was estimated as 27% (Table 4.2), most of which might be due to effect of the soil evaporation. The evaporation from the soil varied according to the time of the day (Figure 4.8). At mid day the rate of soil evaporation was higher than the morning and afternoon. The additional evaporation on DOY 333 (29 Nov 2010) was found to be almost double DOY 329 (25 Nov 2010). The soil evaporation on DOY 333 was considerably (on average

97%) greater than the DOY 329 (Figure 4.8). It indicates that over the bare soil, the soil evaporation was the dominant component in the total evaporation.

Table 4.2: Additional evaporation during sprinkler irrigation over the bare soil

DOY	Date	Combination of irrigation (hr)			Average ET_{ecadj}/ET_{ref}			Increment of ET_{ecadj}/ET_{ref} with respect to pre irrigation period	
		Pre	Irri	Post	Pre	Irri	Post	R_{et}	%
329	25/11/10	1/2	1/2	1/2	0.74	0.89	0.83	0.15	20
333	29/11/10	1/2	1/2	1/2	0.75	1.01	0.97	0.26	35
Average		**0.44**	**0.41**	**0.345**	**0.75**	**0.95**	**0.90**	**0.21**	**27**

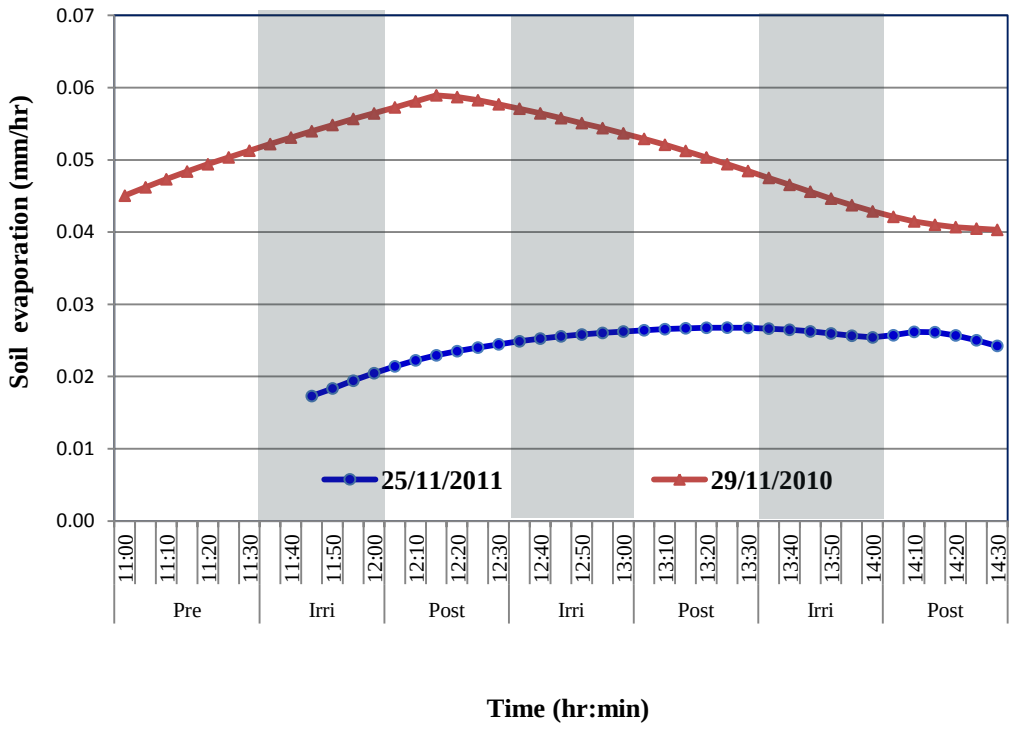

Figure 4.8: Comparison of soil evaporation on different days

4.5 Conclusions

The significant increment of nondimensional ET during irrigation over the grass indicates that additional evaporation occurred during irrigation. Average additional evaporation over the grass was estimated as 32%. The decreasing trend of ET during the post irrigation period was an indication of evaporation of the intercepted water from the grass surface. However, in the case of bare soil it was observed that there was no significant change in ET in comparison with reference ET during the irrigation. However, in terms of nondimensional ET the additional evaporation was estimated as 27% mostly due to variation of soil evaporation at different time of the day. Similar values of nondimensional ET during and after the irrigation period illustrates that there was no intercepted water on the bare soil surface but that evaporation from the moist soil continued at the maximum rate.

The preliminary results obtained from the preliminary measurements have shown that the ECV technique was able to measure the total evaporation and additional evaporation during sprinkler irrigation. The results are sufficiently encouraging to suggest this (ECV) technique can be used to measure the additional evaporation and its components during irrigation of field crops. This study also suggests that the estimation of additional evaporation using the nondimensional technique would be the best technique to estimate the additional evaporation minimizing the effect of climatic factors on the different days and at different times.

Chapter 5: Measurements of total evaporation during sprinkler irrigation of cotton – Results and discussion

5.1 Introduction

The literature review in Chapter 2 reported that the evaporation losses during sprinkler irrigation are still a vital issue to the irrigation community all over the world. Experimental results reviewed showed that they may vary from 0 to 45% of the applied water. For this reason, growers are less likely to adopt sprinkler irrigation and often cited these evaporation losses. However, theoretical studies reported that the losses should be much less. Due to the limitation of the available methodologies and techniques the losses could not be quantified reliably. But it is important in the determination of strategies for the optimal design and management of sprinkler irrigation systems, as well as for irrigation scheduling, to understand the application efficiency of the system. It is also important to provide accurate information regarding the evaporation losses which can help farmers to choose a suitable irrigation system.

The preliminary measurements of total and additional evaporation during sprinkler irrigation over grass and bare soil (Chapter 4) and Uddin et al. (2011) demonstrated that the ECV technique is capable of measuring total evaporation during the sprinkler irrigation. Hence, a series of experiments was conducted in a cotton crop throughout the season 2010-11 at different stages of crop maturity.

This chapter provides the results and discussion of the data obtained from the spray irrigation experiments conducted in the cotton crop following the methods described

in Chapter 3. The results are discussed in context of the objectives: (i) observation of the trend of evapotranspiration and sap flow before, during and after irrigation; (ii) estimation of the additional evaporation and (iii) reduction of sap flow during irrigation. The effect of operational and climatic factors was also assessed and the results are presented at the end of this chapter.

5.2 Effect of sprinkler irrigation on evapotranspiration

5.2.1 General trend of evapotranspiration

The measured actual evapotranspiration ET_{ecadj} on some relatively clear irrigated days (Figure 5.1b-5.1f) represents a distinct picture of the change of rate of ET as a result of irrigation, distinguishing three periods 'pre' (before), 'irri' (during) and 'post' (after) irrigation. The reference evapotranspiration ET_{ref} is used to compare the trend of actual ET during the different periods. For the purpose of comparison the value of ET_{ecadj} and ET_{ref} on a representative unirrigated day are also presented in the Figure (5.1a).

On the unirrigated day (DOY 57, Figure 5.1a) the actual and reference ET were almost same throughout the day, although there were some fluctuations in ET_{ecadj} due to fluctuations in the radiation. However, on irrigated days (Figure 5.1b – 5.1f), the actual evapotranspiration increased sharply during irrigation in every trial and decreased smoothly after stopping the irrigation in comparison with reference evapotranspiration. A similar trend was predicted by Thompson et al. (1997) using their model for both impact sprinkler and spray irrigation. They stated that the sharp increase in ET was due primarily to canopy evaporation from the wetted leaves. From the results of the current work it is clear that during the irrigation some degree of extra evaporation occurs due to the combined effects of canopy evaporation and droplet evaporation.

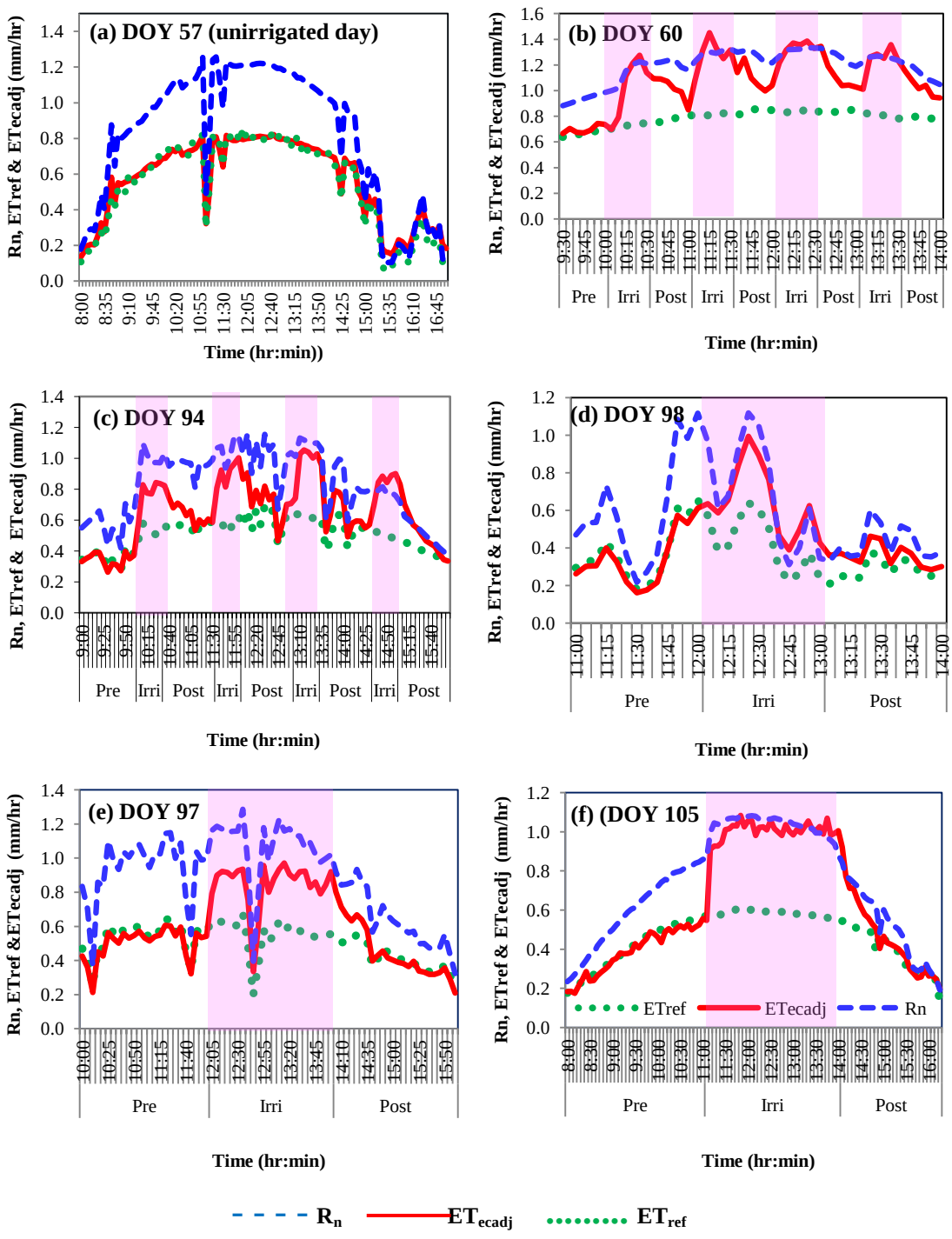

Figure 5.1: Reference evapotranspiration ET_{ref}, actual evapotranspiration ET_{ecadj} and net radiation R_n on representative days for different combinations of irrigation trials. In each the periods of irrigation are shown shaded in pink. (a) unirrigated; (b) 30 mins irrigation and 30 mins interval; (c) 30 mins irrigation and 60 mins interval; (d) 60 mins irrigation and 60 mins interval; (e) 120 mins irrigation; and (f) 180 mins irrigation

Before starting the first irrigation in the morning, the reference evapotranspiration ET_{ref} and actual evapotranspiration ET_{ecadj} were of similar magnitude in all cases (Fig 5.1b - 5.1f). During the irrigations the ET rates were significantly greater than before and after irrigation although the net radiation was almost same as the nonirrigated day. After stopping the irrigation, the ET_{ecadj} decreased smoothly until it matched or tended to match with ET_{ref} (Figure 5.1b – 5.1f) except in the case of the short (30 mins) drying periods (Figure 5.1b). For the short irrigation intervals (30 mins), it was observed that ET_{ecadj} was greater than ET_{ref} in all trials. The reason behind this might be the leaves of the plants did not fully dry within the 30 mins time interval. However, for longer (60, 120 & 180 mins) irrigation intervals it was found that the reference and actual ET matched each other after a certain time (approximately 60 mins) of ceasing irrigation (Figure 5.1d – 5.1f), indicating that the canopy was fully dry after that time.

5.2.2 Inspection of evapotranspiration flux magnitudes

In general, under calm or light wind conditions, it is to be expected that daily ET cannot exceed the net radiation R_n. However, on some days (DOY 94 and 98, Figure 5.1c and 5.1e respectively), it was found that the actual evapotranspiration ET_{ecadj} was close to and on some other days (DOY 60 and 105, Figure 5.1b – 5.1f) exceeded the available energy R_n. Tolk et al. (2006) and De Bruin et al. (2005) reported that this may happen in irrigation under advective conditions where the sensible heat flux is negative and the air close to the ground is stable and becomes stratified. These negative conditions buoyancy is suppress and turbulent motion, driven by wind is the only mechanism that can generate the turbulence required for the transport of heat and moisture (De Bruin et al. 2005).

De Bruin et al. (2005) also reported that under the condition $\lambda E > R_n$ and with G negligible, the additional energy needed to maintain the high evaporation rate must be supplied by extracting sensible heat H from the lower atmosphere. This results in a negative value of H.

Table 5.1 sets out five days in which irrigation trials were conducted in different combinations. Of these it is seen that on the two days of highest during-irrigation evaporation (Irri), the sensible heat flux H during irrigation was negative which indicates that there was some extra heat supplied.

Table 5.1: Averaged meteorological data recorded during five days in which irrigation trials were conducted in different combinations: average air temperature (T_a), relative humidity (RH), wind speed (WS), vapour pressure deficit (VPD), adjusted latent heat flux (λE_{adj}), adjusted sensible heat flux (H_{adj}), actual net radiation (R_n), and soil heat flux (G)

DOY	Date	Condition	T_a	RH	WS	VPD	λE_{adj}	H_{adj}	R_n	G
			°C	%	m/s	kPa	W/m^2	W/m^2	W/m^2	W/m^2
60	1/3/11	Pre	25.5	60	2.2	1.3	479	140	643	24
		Irri	28.2	50	1.8	1.9	814	**-40**	839	65
		Post	28.7	46	1.6	2.1	721	33	822	69
94	4/4/11	Pre	19.3	78.1	4.7	0.5	265	181	447	1
		Irri	19.9	75.1	3.7	0.6	366	86	470	18
		Post	19.1	80.4	3.9	0.5	298	71	391	22
97	7/4/11	Pre	18.7	68.0	4.8	0.7	343	273	642	26
		Irri	18.7	67.6	4.2	0.7	570	125	726	32
		Post	19.7	62.0	3.6	0.9	307	110	436	19
98	8/4/11	Pre	18.4	68.1	4.0	0.7	261	105	380	15
		Irri	18.6	65.6	4.1	0.7	427	45	490	18
		Post	18.3	68.4	3.4	0.7	244	19	278	15
105	15/4/11	Pre	19.8	69.5	1.7	0.7	268	133	410	9
		Irri	21.4	48.0	1.8	1.3	678	**-15**	701	39
		Post	22.0	41.6	2.6	1.5	237	16	271	18

Potential sources of additional energy and which would result in negative *H* are:

(i) release of thermal energy stored in the biomass (*J* of equation 2.16);

(ii) by local advection (to be anticipated as the irrigated area was small.

The example of upwind and downwind temperatures and relative humidity plotted in Figure 5.2 show that there was a difference in RH between the upwind and downwind positions during the irrigations: this also indicates an advective situation.

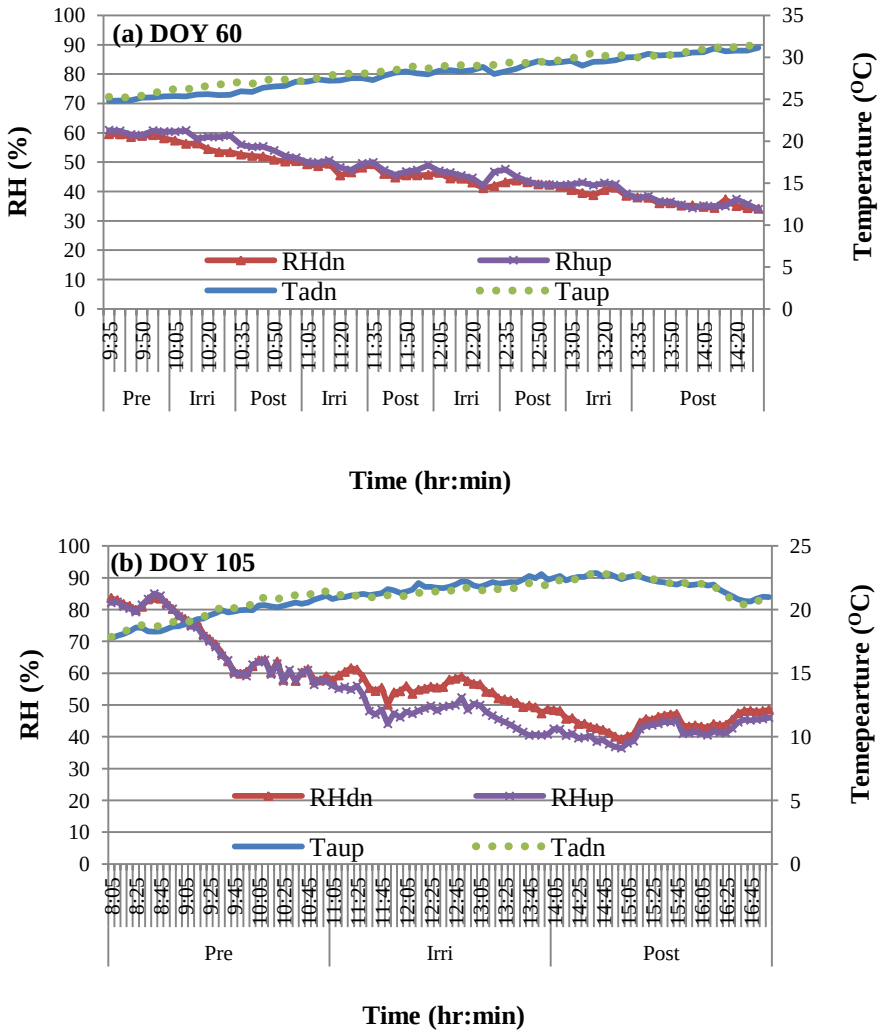

Figure 5.2: Temperature and relative humidity 25 m upwind and 25 m downwind of the ECV measurement site at the irrigated plot measured on DOY 60 and 105

5.2.3 Overview of nondimensionalised ET results

Previously (Chapter 4) it was found that nondimensionalising and averaging represents the trends of the rate of change of ET in different phases of irrigation more clearly removing the day-to-day and during-day variation of net radiation (R_n) and evaporative demand. This technique also removes many random fluctuations, particularly those caused by intermittent cloud cover. More importantly, nondimensionalisation of ET was also found to be the best suited technique to compare the data for different time and periods as well as to estimate the additional evaporation that occurs during the irrigation. Hence, the presentation of the trend of ET during irrigation and nonirrigation periods and estimation of additional evaporation is done on the basis of nondimensionalised ET.

The nondimensional values illustrate that the trend of actual ET is similar in all irrigation trials showing significantly greater values during irrigation than the pre and post irrigation periods (Appendix L). However, the values of increment of nondimensional ET during irrigation were not same. At the initial stage (50% cover) of crop under the experiment III (Table 3.1, section 3.5), the value of dimensionless ET was found approximately 1.4 times higher than the reference ET (Figure 5.3) which was less than the values for 75% and 100% crop canopy coverage. It is noticeable that, in the case of short (30 mins) drying periods, the nondimensional curve for the post-irrigation period did not match with pre-irrigation period due to the same reason (wetness of the canopy) mentioned earlier (section 5.2.1). This figure also support the observation presented in Figure (5.1b) that the leaves of the plants did not fully dry within the 30 mins time and gave the greater value of actual ET resulting in a comparatively higher nondimensional number.

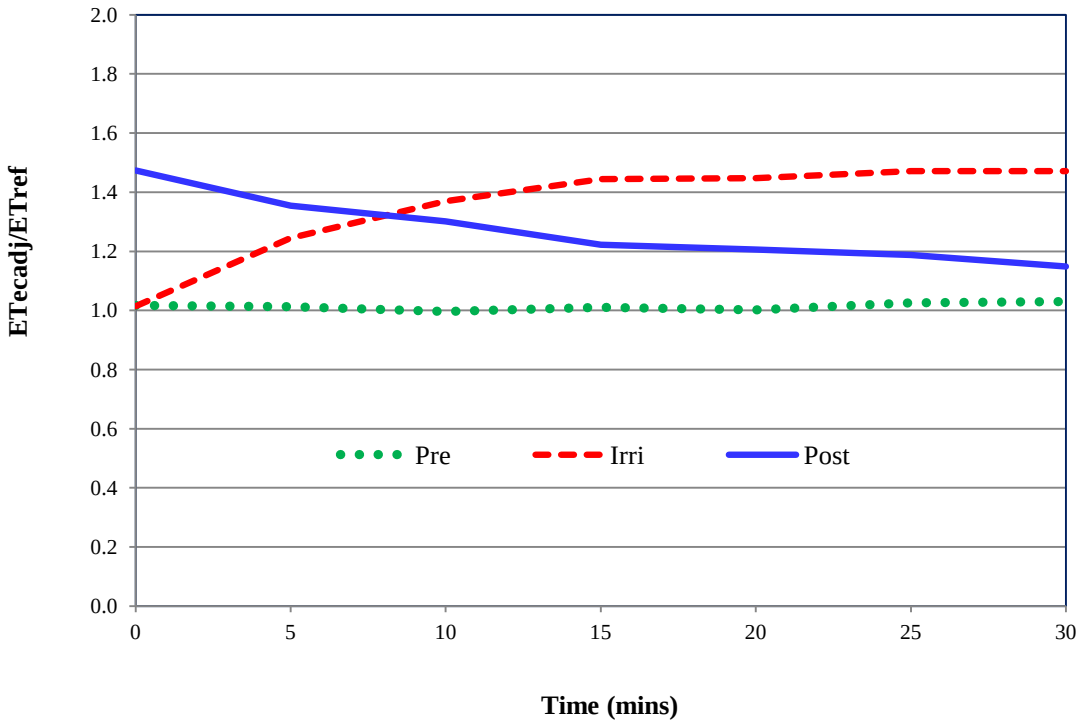

Figure 5.3: Nondimensionalised ET curves for the combination of 30 mins irrigation and 30 mins interval at the initial stage (50% cover) of crop

To observe the effect of a longer time drying period on ET during the post irrigation period, another experiment was conducted under the combination of 30 mins irritation and 60 mins interval at the partial (75%) crop canopy coverage (Experiment IV, Table 3.1, section 3.5). In that case, the value of nondimensional ET during irrigation was also found to be higher (about 1.6 times of ET_{ref}) than the pre irrigation period (Figure 5.4). Interestingly, in that case the magnitude of the nondimensional values during the irrigation was higher compared to the values for 50% crop canopy coverage and slightly less than for the full canopy coverage. It means that the rate of ET increased on the basis of crop canopy coverage. The higher values were observed for higher crop canopy coverage. Drying (post irrigation) curve (Figure 5.4) shows that still there was a gap between actual and reference ET, although the drying period

was increased. However, the gap between the pre- and post-irrigation values at the end of the period was less than for the 30 mins drying period which indicates that the canopy was still drying.

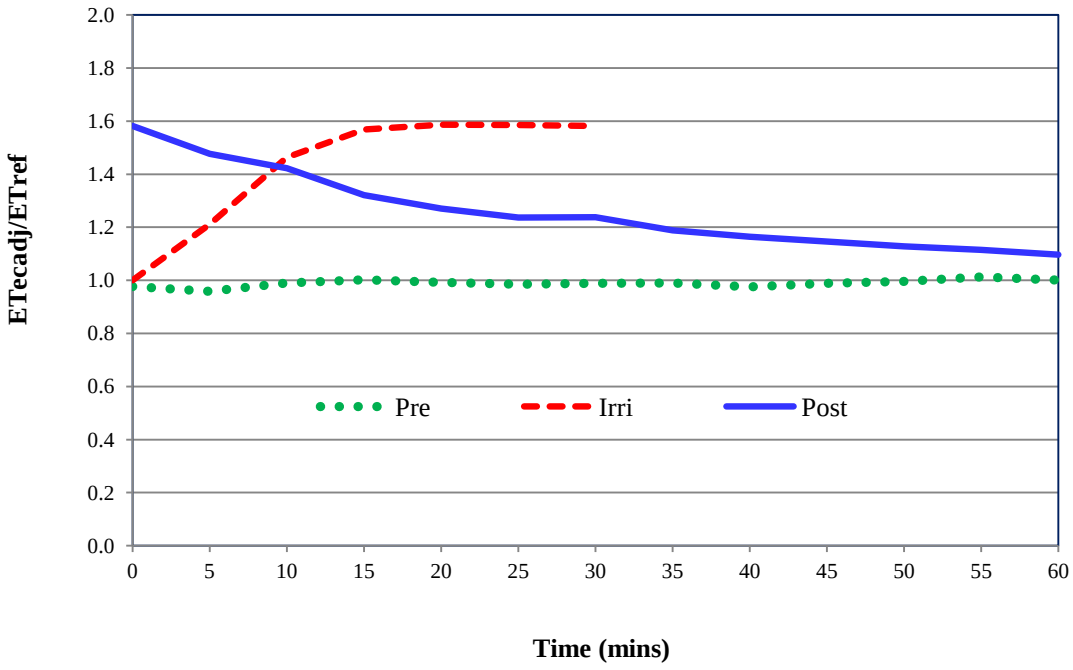

Figure 5.4: Nondimensionalised ET curves for the combination of 30 mins and 60 mins interval at 75% crop canopy coverage

Following the experiments for longer (60 mins and 120 mins) irrigation durations under the experiment V & VI (Table 3.1, section 3.5), a similar trend of drying was found in case of 60 mins trial (Figure 5.5). However, in the case of the 120 mins trial (Figure 5.6) under Experiment VI, the drying curve was found to be aligned with pre-irrigation curve after about 60 mins (marked by a vertical bar) and followed the similar path of reference ET after that. Under those trials the values of dimensionless ET were relatively less in all (pre-, during- and post-) periods. The reason might be that the crop was suffering some degree of moisture stress on that day resulted the lower value of nondimensional ET.

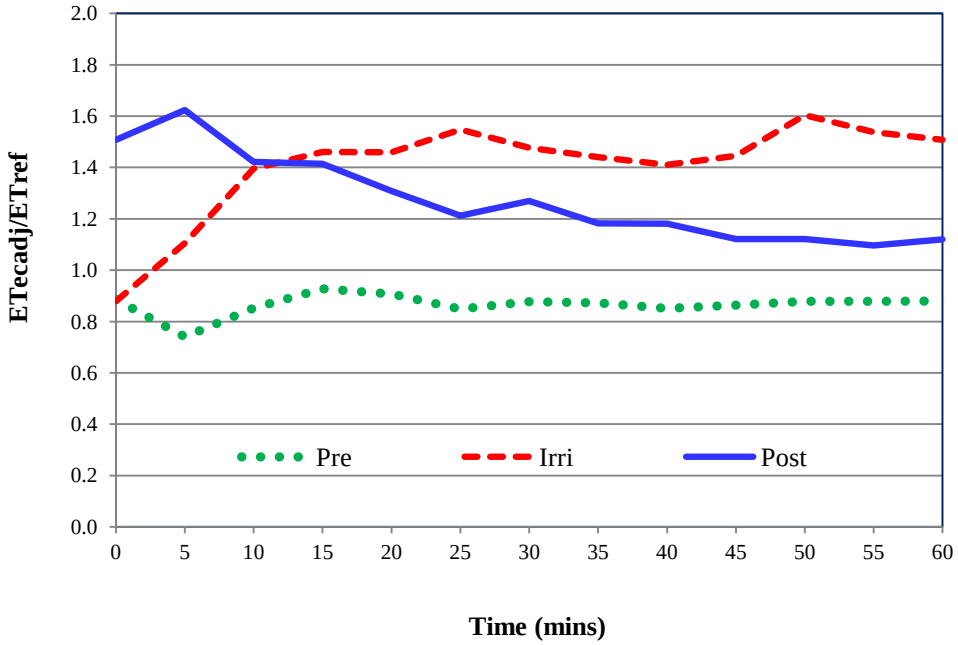

Figure 5.5: Nondimensionalised ET curves for 60 mins irrigation trial at full crop canopy condition

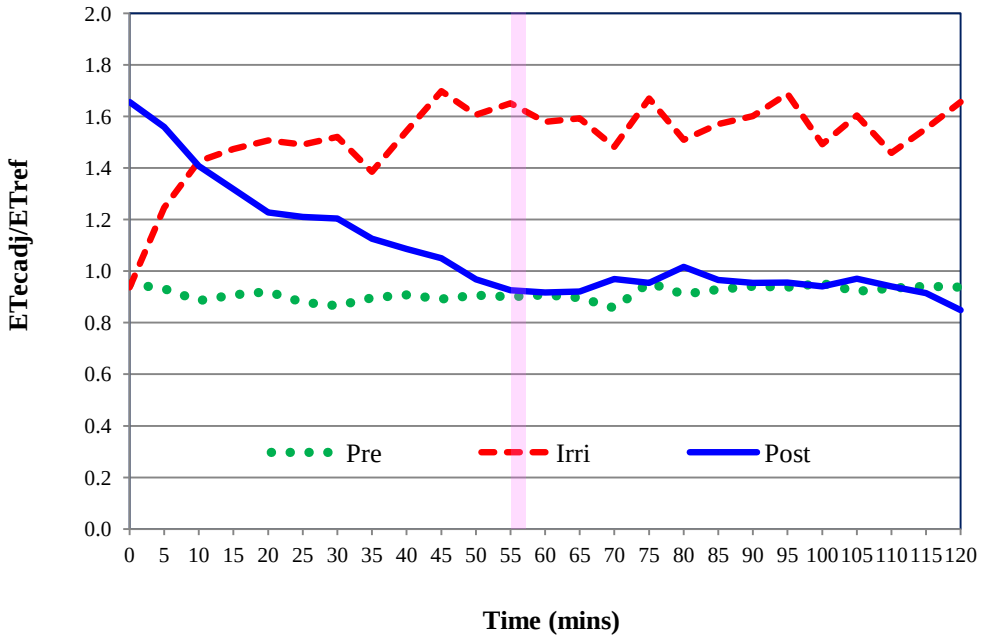

Figure 5.6: Nondimensionalised ET curves for 120 mins irrigation trial at full crop canopy condition (with the pink bar indicating approximate alignment of Pre/Post ET results)

Continuing the experiments, several trials were carried out for 180 mins irrigation under full crop canopy conditions (Experiment VII). The average values of nondimensional ET are presented in Figure 5.7. The figure shows that the magnitude of the values during irrigation was highest among the three conditions of crop and was about 1.6 times greater than the pre-irrigation period. The drying curve followed the similar path as earlier and matched with pre-irrigation curve at about 60 mins, which was similar to the 120 mins irrigation trial (Figure 5.6).

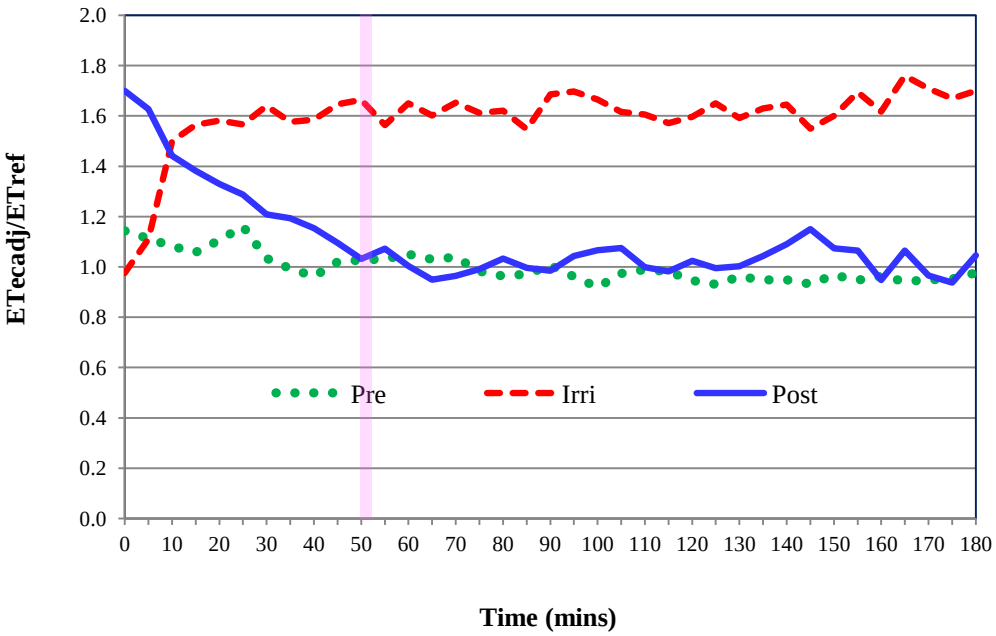

Figure 5.7: Nondimensional curves for 180 mins irrigation trial at full crop canopy condition (with the pink bar indicating approximate alignment of Pre/Post ET results)

Plots of nondimensional ET for individual days are presented in Appendix (L). The figures show that the trend was almost the same for individual days, but there were fluctuations in the data which were largely removed by the averaging. The data for longer trials (Appendix L) show that the drying (post irrigation) curve matched with pre irrigation values after 60 mins of ceasing irrigation in most cases. Therefore, it

can be approximated that the drying time is about 60 mins, although this will vary with evaporative demand.

5.2.4 Additional evaporation during irrigation at 50% crop canopy

The average value of dimensionless ET, calculated on the basis of several individual trials conducted at the initial stage of the crop under the experiment-I (Table 3.1, section 3.5), are illustrated in Table 5.2. The data indicate that during the irrigation, the estimated average nondimensional values were significantly higher in all trials compared to the pre irrigation period. It is noticeable that the overall average value of nondimensional ET (e.g. time from 0 mins - 180 mins in Figure 5.7) was smaller compared to the average value of dimensionless ET during the period of steady state (e.g. time from 10 mins -180 mins in Figure 5.7). Prior to irrigation the average value of the dimensionless ET was 1.01 and varied from 0.92 to 1.08, while during the irrigation the value was estimated as 1.38 and ranged from 1.25 to 1.53. The average increment of nondimensional ET was calculated as 37% with the range 20% - 53% (Table 5.2). The average value of dimensionless ET post irrigation was slightly higher than the pre irrigation period and lower than during irrigation in every single day trial as a result of evaporation of intercepted water after irrigation.

Table 5.2: Average values of ET_{ecadj}/ET_{ref} at pre-, during- and post-irrigation periods for partial (50%) crop canopy condition during 19 February – 01 March 2011

DOY	Date	Average ET_{ecadj}/ET_{ref}			Increment of ET_{ecadj}/ET_{ref} during irrigation with respect to pre irrigation period	
		Pre	Irri	Post	R_{et}	%`
50	19/2/11	1.08	1.30	1.20	0.22	20
51	20/2/11	1.07	1.29	1.20	0.22	21
55	24/2/11	0.92	1.25	1.07	0.33	36
56	25/2/11	0.94	1.35	1.17	0.41	44
59	28/2/11	1.00	1.53	1.17	0.53	53
60	01//3/11	1.05	1.53	1.32	0.48	46
Average		**1.01**	**1.38**	**1.19**	**0.37**	**37**

Although the equipment related factors (e.g. nozzle size, pressure and height) were similar for all trials, the amount of additional evaporation varied considerably with an increasing trend from day to day. At the beginning of the experiments (DOY 50 & 51), the additional evaporation was estimated as 20-21%, while on DOY 55 & 56, it was 36-45% (Figure 5.8). At the last stage, it was 46-53%. Since, the major climatic factors were minimized using the nondimensional technique and the equipment related factors were the same, crop growth and advection would be the other factors which most likely influenced the amount of extra evaporation.

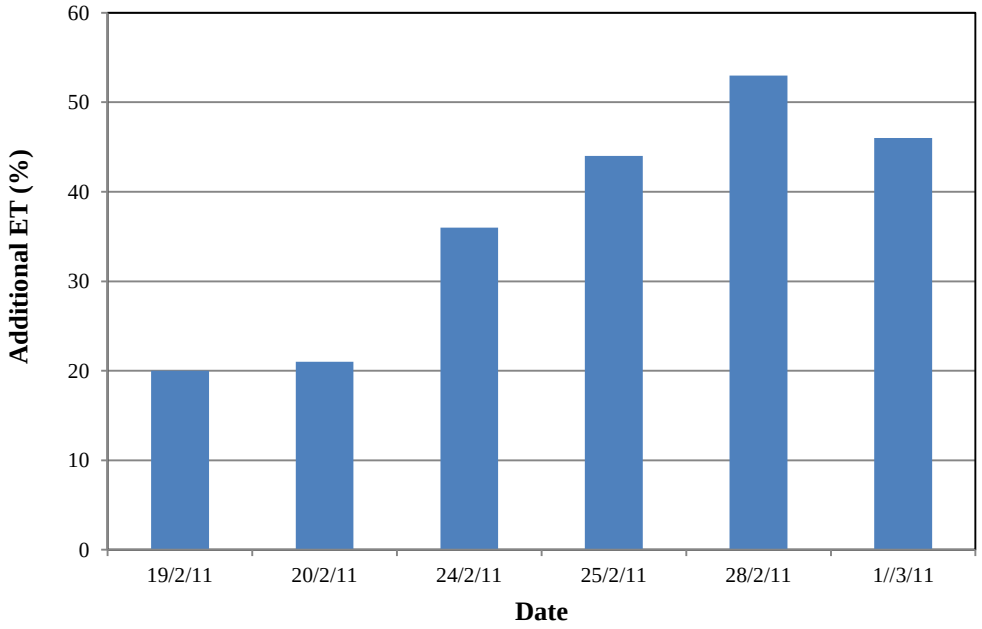

Figure 5.8: Comparison of additional evaporation at 50% crop canopy condition

Todd et. al. (2000) provided an index termed the advection index (*AI*) as the ratio of latent heat flux λE_{adj} and the difference between net radiation (R_n) and soil heat flux (G) to measure the advection effect expressed as:

$$AI = \frac{\lambda E_{adj}}{(R_n - G)} \tag{5.1}$$

According to Todd (2000), when $AI > 1$ there will be significant advection. Since AI was equal to or less than 1 in every trial (Table 5.3), it is most likely that increasing crop coverage during the trials caused the increase in the additional evaporation. From the meteorological data (Table 5.3), it is seen that during the irrigation the vapour pressure deficit (VPD) was higher on DOY 59 and 60 than the other days and negative (-40 Wm^{-2}) value of H on DOY 60 may also influenced the rate of evaporation.

Table 5.3: Computation of the Todd et al. (2000) Advection Index *AI* from meteorological data recorded during the period 19 Feb – 1 March 2011

DOY	Condition	T_a	RH	WS	VPD	λE_{adj}	H_{adj}	R_n	G	AI
		(^oC)	(%)	m/s	kPa	W/m^2	W/m^2	W/m^2	W/m^2	
50	Irri	24.6	70	3.2	0.9	681	107	823	35	0.9
51	Irri	29.6	53	1.3	2.0	793	1	857	63	1.0
55	Irri	22.3	56	3.2	1.2	594	97	743	53	0.9
56	Irri	22.4	59	2.6	1.1	600	132	788	56	0.8
59	Irri	27.8	51	0.9	1.8	593	30	683	61	1.0
60	Irri	28.2	50	1.8	1.9	814	**-40**	839	65	1.0

The average values of actual evapotranspiration (ET_{ecadj}) for each day are also presented in Table 5.4. From the table it is seen that average value of ET pre irrigation was 0.68 mm/hr and ranged from 0.56 – 0.87 mm/hr, while during irrigation it was 1.04 mm/hr (0.81 to 1.22 mm/hr) which was significantly higher that pre irrigation period. During the post irrigation period the value was 0.94 but varied from 0.69 to 1.11 mm/hr.

Table 5.4: Average values of actual evapotranspiration (ET_{ecadj}) in the pre, during and post irrigation periods for partial (50%) crop canopy condition during 19 February –1 March 2011

DOY	Date	Combination of irrigation			Average ET_{ecadj} (mm/hr)		
		Pre	Irri	Post	Pre	Irri	Post
50	19/2/11	1/2	1/2	1/2	0.67	1.05	0.96
51	20/2/11	1/2	1/2	1/2	0.87	1.16	1.01
55	24/2/11	1/2	1/2	1/2	0.65	0.81	0.69
56	25/2/11	1/2	1/2	1/2	0.56	0.87	0.77
59	28/2/11	1/2	1/2	1/2	0.65	1.15	1.11
60	01/3/11	1/2	1/2	1/2	0.70	1.22	1.07
Average					**0.68**	**1.04**	**0.94**

5.2.5 Additional evaporation during irrigation at 75% crop canopy

At this crop stage, the nondimensional ET was also significantly higher during irrigation. The average value of dimensionless ET at pre irrigation period was 0.99 (0.84 to 1.08), while during the irrigation the average value was 1.53 and ranged from 1.35 to 1.74. This corresponded to an increment of 56% with the range of 33% - 69% (Table 5.5). The increment of evaporation varied substantially due predominately to the effect of climatic factors (Table 5.5 & Appendix K). According to the advection index (Table 5.5), advection was present on DOY 81 and 84, where the increment of evaporation was higher than the average value. On DOY 84 the effect was strong (AI = 1.3 and H = –195 Wm^{-2}) and resulted in the highest (69%) extra evaporation. Although, the AI index was less than 1 on DOY 93, 94 and 96, the additional evaporation was higher than the average value due to high wind speed (Figure 5.9). Lower vapour pressure deficit (0.6 kPa) than the average value 0.96

(Appendix K) might be another reason for the higher rate of evaporation. Higher values of dimensionless ET during the post irrigation period than the pre irrigation period also represents the evaporation of intercepted water. It is interesting to observe that the values of post irrigation nondimensional ET (average 1.39) at this stage (75% covered) were greater than at 50% cover (1.19). This illustrates the increase in interception capacity of the canopy with increasing crop canopy coverage. Note that the nondimensional ET varies (decreases) continuously throughout this period and the average does represent any particular state or stage of the drying process.

Table 5.5: Average values of ET_{ecadj}/ET_{ref} and the Todd et al. (2000) Advection Index *AI* pre-, during- and post-irrigation during 16 March - 6 April 2011

DOY	Date	Average ET_{ecadj}/ET_{ref}			Increment of ET_{ecadj}/ET_{ref} during irrigation with respect to pre irrigation period		*AI*
		Pre	Irri	Post	R_{et}	%	
75	16/3/11	0.96	1.35	1.18	0.39	41	0.96
81	22/3/11	1.00	1.57	1.28	0.57	57	1.11
84	25/3/11	1.03	1.74	1.49	0.71	69	1.32
86	26/3/11	1.03	1.37	1.17	0.34	33	0.93
90	31/3/11	1.03	1.60	1.28	0.57	55	0.99
91	01/4/11	1.00	1.43	1.27	0.43	43	0.89
92	02/4/11	1.08	1.58	1.28	0.50	46	0.90
93	03/4/11	1.00	1.59	1.29	0.59	59	0.91
94	04/4/11	0.96	1.57	1.21	0.61	64	0.94
96	06/4/11	0.84	1.43	1.17	0.59	70	0.95
Overall		**0.99**	**1.52**	**1.26**	**0.53**	**54**	
Average	**Nonadvective**	**0.99**	**1.49**	**1.23**	**0.50**	**51**	
Average	**advective**	**1.02**	**1.66**	**1.39**	**0.64**	**63**	

De Bruin et al. (2005) reported that, for a small field of finite size, the latent heat flux is expected to increase with increasing wind speed due to fact that dry air is forced to flow over the wet irrigated surface. They also suggest that, the evaporation losses during sprinkler irrigation can be significant at high wind speed and recommended not to irrigate if high wind speed is expected.

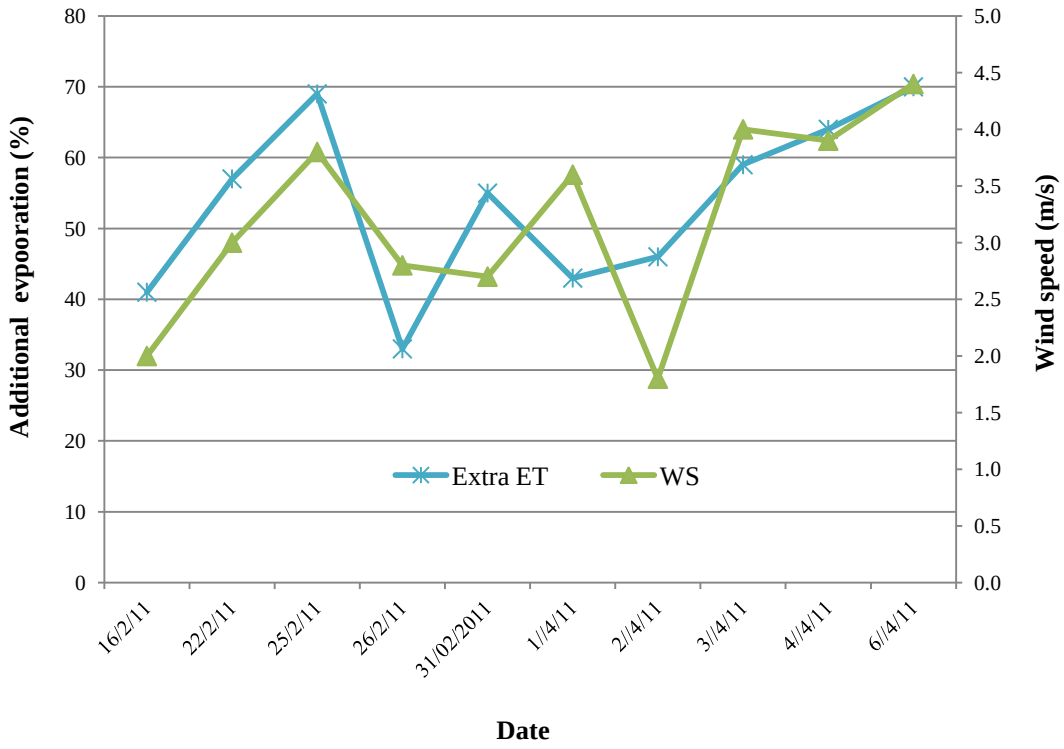

Figure 5.9: The comparison of additional evaporation and wind speed during irrigation

The average increment of nondimensional ET during the irrigation for nonadvective days was 51% compared to the pre irrigation period. In advective conditions the increment was 63% which was 12% greater than the nonadvective days (Figure 5.10).

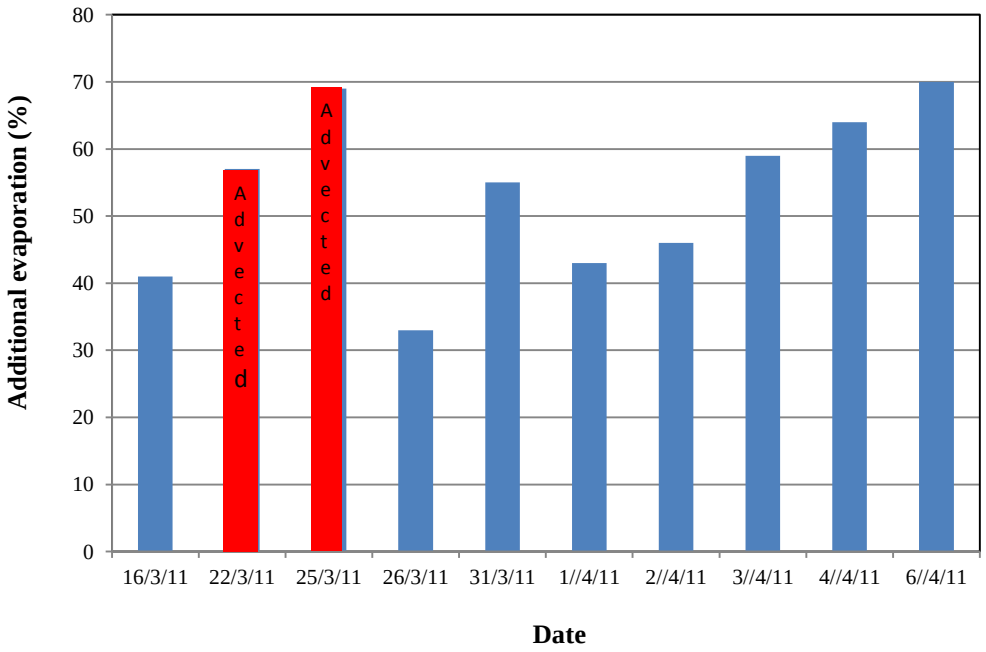

Figure 5.10: Additional evaporation for partial (75%) crop canopy condition on individual days

The average values of actual evapotranspiration (ET_{ecadj}) for each day are presented in Table 5.6. From the table it is seen that average values of ET during irrigation were also significantly higher than pre irrigation period. At the pre irrigation period the average value was 0.45 mm/hr ranged from 0.33 – 0.61 mm/hr, while during irrigation it was 0.86 mm/hr (0.55 to 1.19 mm/hr). Following post irrigation the value was 0.66 varied and varied from 0.44 to 0.95 mm/hr.

Table 5.6: Average values of actual ET **(ET_{ecadj}) pre, during and post irrigation for partial (75%) crop canopy condition during 16 March - 6 April 2011**

DOY	Date	Combination of irrigation (hr)			Average ET_{ecadj} (mm/hr)		
		Pre	Irri	Post	Pre	Irri	Post
75	16/3/11	1	1/2	1	0.43	0.86	0.64
81	22/3/11	1	1/2	1	0.45	0.91	0.79
84	25/3/11	1	1/2	1	0.59	1.19	0.95
86	26/3/11	1	1/2	1	0.57	0.98	0.70
90	31/3/11	1	1/2	1	0.61	0.88	0.53
91	01/4/11	1	1/2	1	0.39	0.55	0.44
92	02/4/11	1	1/2	1	0.47	0.96	0.72
93	03/4/11	1	1/2	1	0.41	0.73	0.60
94	04/4/11	1	1/2	1	0.34	0.88	0.64
96	06/4/11	1	1/2	1	0.33	0.64	0.58
Average					**0.45**	**0.85**	**0.66**

5.2.6 Additional evaporation during irrigation at full canopy

At the full canopy condition, the nondimensional ET was higher than for the partial canopy coverage. During the irrigation the values were significantly higher compared to the pre irrigation period. During the pre irrigation period the average value of dimensionless ET was 0.95 varied from 0.79 to 1.08, while during the irrigation the average value was 1.73 (1.54 to 2.08). The average increment was estimated as 84% within the range from 47% - 123% (Table 5.7). The trend in the post irrigation period was similar to that observed previously (higher than pre and smaller than irrigation period) with ET ranging from 0.98 to 1.28 again indicating the existence of intercepted water on the canopy after irrigation. The tabulated data illustrate that

there was a significant variation in additional ET. As the crop was at its mature stage, the variability of the daily results was due to the variability of climatic factors and the effect of advection.

Table 5.7: Average values of ET_{ecadj}/ET_{ref} pre, during and post irrigation at full crop canopy condition during 7-17 April 2011

DOY	Date	Average ET_{ecadj}/ET_{ref}			Increment of ET_{ecadj}/ET_{ref} during irrigation with respect to pre irrigation period		*AI*
		Pre	Irri	Post	R_{et}	%	
97	07/4/11	0.91	1.54	1.06	0.63	69	0.8
98	08/4/11	0.86	1.58	1.14	0.72	84	0.9
99	09/4/11	0.79	1.76	0.98	0.97	123	1.0
102	12/4/11	1.04	2.04	1.09	1.00	96	1.2
103	13/4/11	0.91	1.57	1.14	0.66	73	1.1
104	14/4/11	1.02	2.08	1.28	1.06	104	1.4
105	15//4/11	0.96	1.71	**1.12**	0.75	78	1.0
107	17/4/11	1.07	1.57	1.12	0.50	47	0.9
Average	**Overall**	**0.95**	**1.73**	**1.12**	**0.79**	**84**	
	Nonadvective	**0.93**	**1.65**	**1.09**	**0.72**	**80**	
	Advective	**1.03**	**2.06**	**1.19**	**1.03**	**100**	

In some trials the ratio of ET_{eacadj} to ET_{ref} was very low due to the difference between the actual and reference ET (Figure 5.11). The figure represents the higher reference *ET* on DOY 97, 98 & 99 as the result of higher net radiation at pre irrigation period (Appendix K) resulted in the lower value of nondimensional ET.

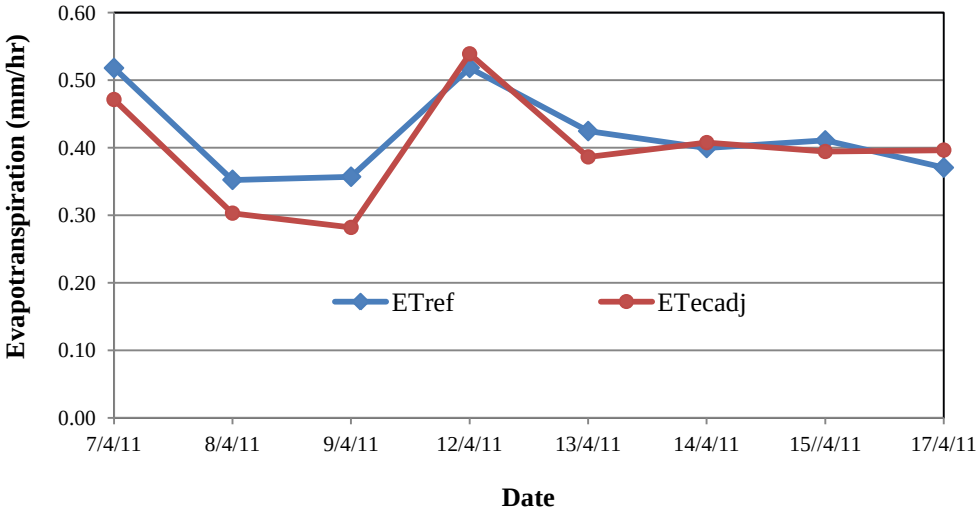

Figure 5.11: Comparison of reference and actual ET during the pre irrigation period

The energy balance components and daily advection index or evaporative fraction are provided in Table 5.8. According to the advection index, most of the days were advection free, except DOY 102 and DOY 104. On DOY 102 the effect was moderate where the advection index was 1.2 and the sensible heat flux was -142 W m^{-2}. On DOY 104, the phenomenon was severe where the index was 1.4. This means that about 40% of the additional energy used to evaporate water was supplied by the advected heat.

Table 5.8: Meteorological data recorded during the period 7 – 17 April 2011

DOY	Condition	T_a	RH	WS	VPD	λE_{adj}	H_{adj}	R_n	G	T_c	AI
		(^{o}C)	(%)	m/s	kPa	W/m^2	W/m^2	W/m^2	W/m^2	(^{o}C)	
97	Irri	18.7	67.6	4.2	0.7	570	125	726	32	19.8	0.8
98	Irri	18.6	65.6	4.1	0.7	427	45	490	18	18.9	0.9
99	Irri	19.3	63.4	3.3	0.8	480	42	554	32	19.7	1.0
102	Irri	19.6	54.1	2.7	1.1	831	**-148**	707	24	18.1	**1.2**
103	Irri	22.0	45.6	1.7	1.4	289	373	702	39	18.5	1.1
104	Irri	23.1	43.3	2.6	1.6	814	**-213**	631	30	18.7	**1.4**
105	Irri	21.4	48.0	1.8	1.3	678	**-15**	701	39	21.6	1.0
107	Irri	19.0	73.5	3.5	0.6	436	61	528	31	19.4	0.9

As the result of severe advection, the latent heat flux was significantly higher than the net radiation with negative values of sensible heat flux (Figure 5.12) on that day. The negative sensible heat flux indicates that the additional energy required to maintain the high evaporative rate was supplied by the sensible heat flux. De Bruin et al. (2005) reported that when $\lambda E > R_n$, the sensible heat (H) must be negative to supply the additional required energy. Due to this reason the additional evaporation was very high (104%) on that day compared to the average (84%). The figure also shows that the soil evaporation is about 4% of net radiation which is slight lower than the soil evaporation (about 6% of net radiation) under nonadvective condition. This may also be the effect of advection.

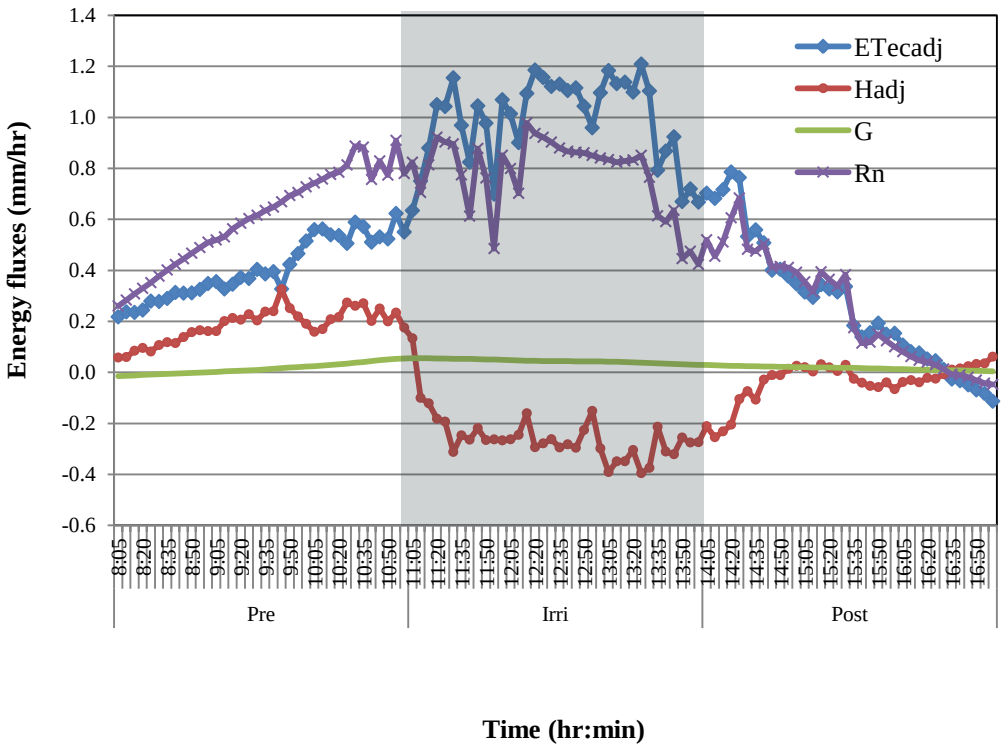

Figure 5.12: Components of energy fluxes under advective condition (DOY 104, 14 April 2011)

On DOY 105, although the advection index was 1.0, the sensible heat flux was negative (-15 Wm^{-2}) shown in Table 5.8, which indicates that some energy consumed by latent heat (λE) was supplied by sensible heat flux which increased the ET rate. In this regard, Brakke et al. (1978) reported that sensible heat supplied from 15 to 50% of energy consumed by λE of alfalfa in Nebraska, USA. Abdel Aziz et al. (1964) found that measured ET of alfalfa reached maximum of 71% more than measured R_n in Utah due to advected heat.

Although, there was no significant impact of advection on DOY 99, the percentage of extra evaporation was very high. The reason is that the low value of actual ET during the irrigation period (Figure 5.11 & Appendix G) led to a higher estimate of additional evapotranspiration. At the pre irrigation period (morning) on DOY 99, the sensible heat flux H was higher than λE (Appendix K), which was the reverse of normal ($\lambda E > H$), resulting in the severe underestimation of ET ratio (Table 5.7). The minimum value of additional evaporation was found on DOY 107 might be due to the lowest vapour pressure deficit among the trial days (Table 5.8).

The average increment of dimensionless ET on nonadvective days was 80%. On the other hand, on advective days the increment was 100% which was 21% greater than the nonadvective day (Figure 5.13). In this regard, Tolk et al. (2006) reported that advective enhancement of crop evapotranspiration occurs when drier, hotter air is transported into the crop by wind, and can be an important factor in the water balance of irrigated crops in a semiarid climate. They indicated that advected atmospheric deficits and sensible heat flux H added as much as 10.5 mm d^{-1} to ET, with H providing an average of 42% of the energy used in ET. Li and Yu (2007) mentioned that due to enhanced advection, the percentage of latent and sensible heat flux exchange contribution to the total water loss from the fields through evapotranspiration can exceed 50%.

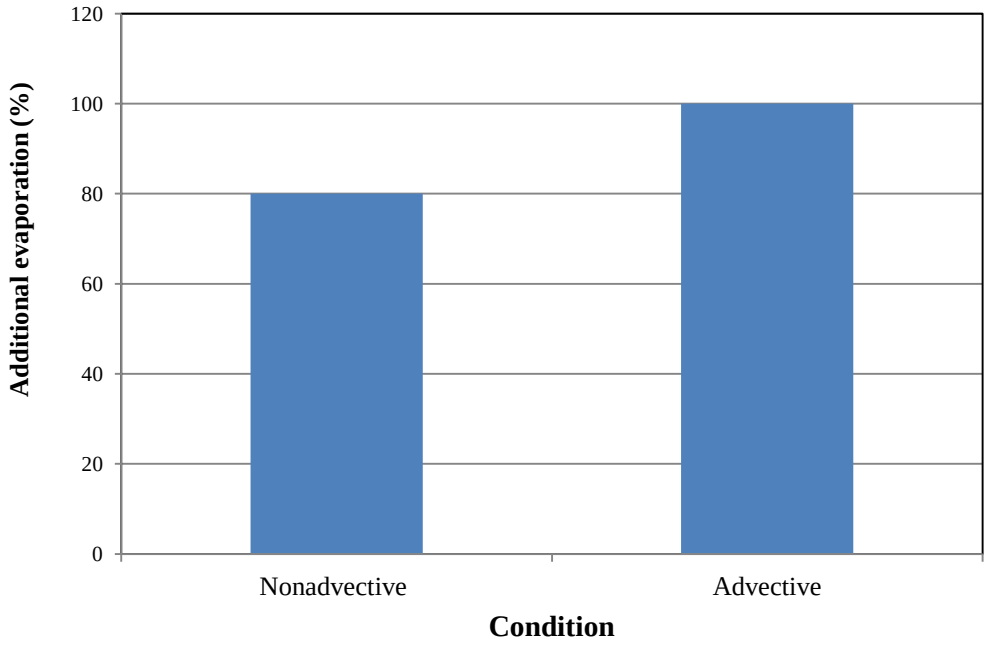

Figure 5.13: Additional evaporation at advective and nonadvective condition at full crop canopy coverage

Theoretically it is well documented that rate of evaporation from a wet canopy is higher than under dry canopy conditions reported by Rutter (1967), Stewart (1977) and Calder (1979). However, limited studies have so far been done in this regard to measure the ET rates during irrigation due to the lack of appropriate method and instruments. Although Thompson et al. (1997) predicted that during sprinkler irrigation ET rates went up to 100% greater (approximated from graph) than the nonirrigation period (for mature corn canopy condition in USA), the theoretical results could not be verified experimentally due to the lack of appropriate instruments. Waggoner et al. (1969) found short-term ET rates from wet corn canopies to be more than double that of dry corn canopies during typical summertime conditions in Connecticut (USA).

5.2.7 Idealized ET curves

Using data from the three hour (180 mins) irrigation period the idealized pictures of evapotranspiration for advective and nonadvective conditions were drawn using the average nondimensional values of ET shown in Figure 5.14a & 5.14b .

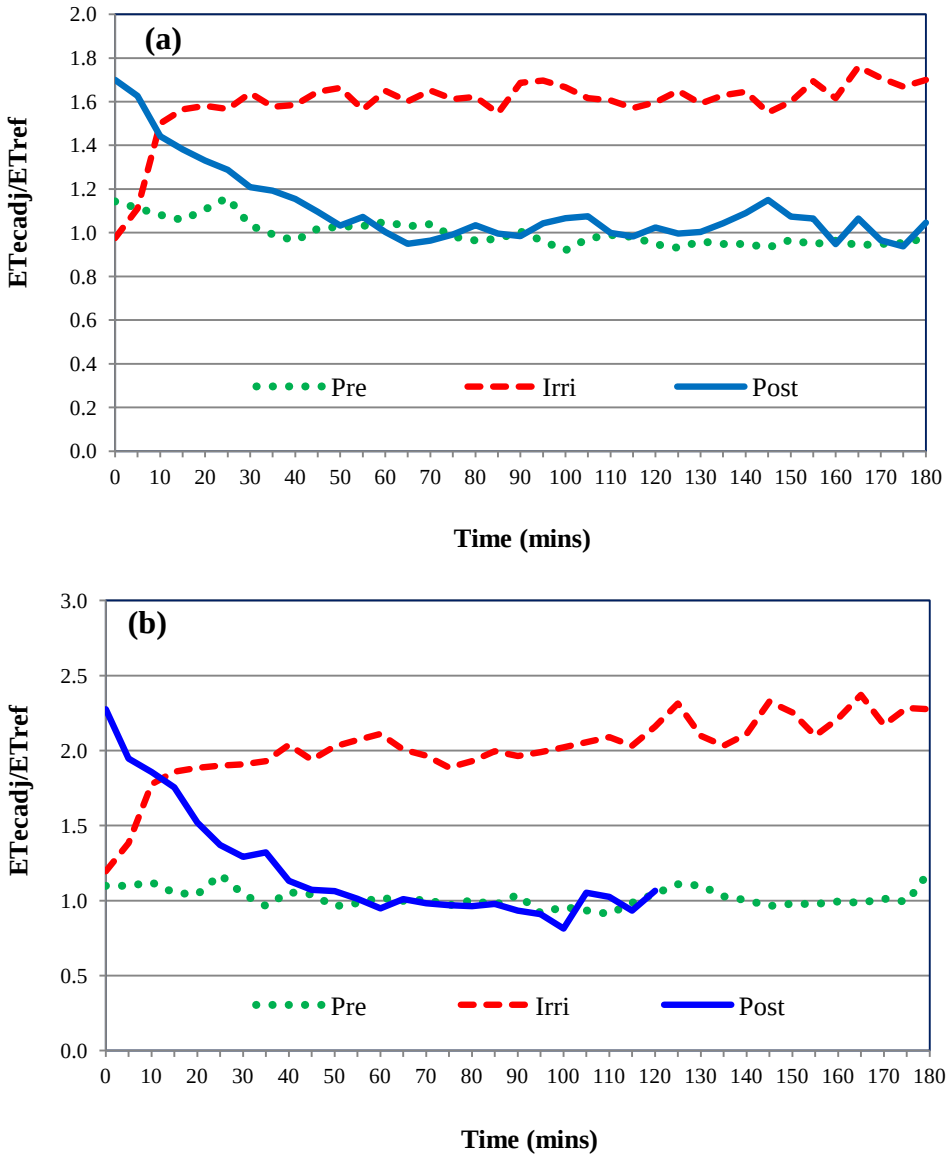

Figure 5.14: Idealized curves of evapotranspiration (ET) for sprinkler irrigation during (a) nonadvective and (b) advective condition

From the above idealized curves, five distinct phases can be distinguished shown in Figure 5.15: (i) a period of more or less constant value of nondimensional ET prior to irrigation, (ii) a period of rapid increase of ET just after starting irrigation, (iii) more or less stable ET during irrigation, (iv) a period of declining rate of ET post irrigation (drying), followed by (iv) a more or less constant rate of ET in terms of nondimensional value.

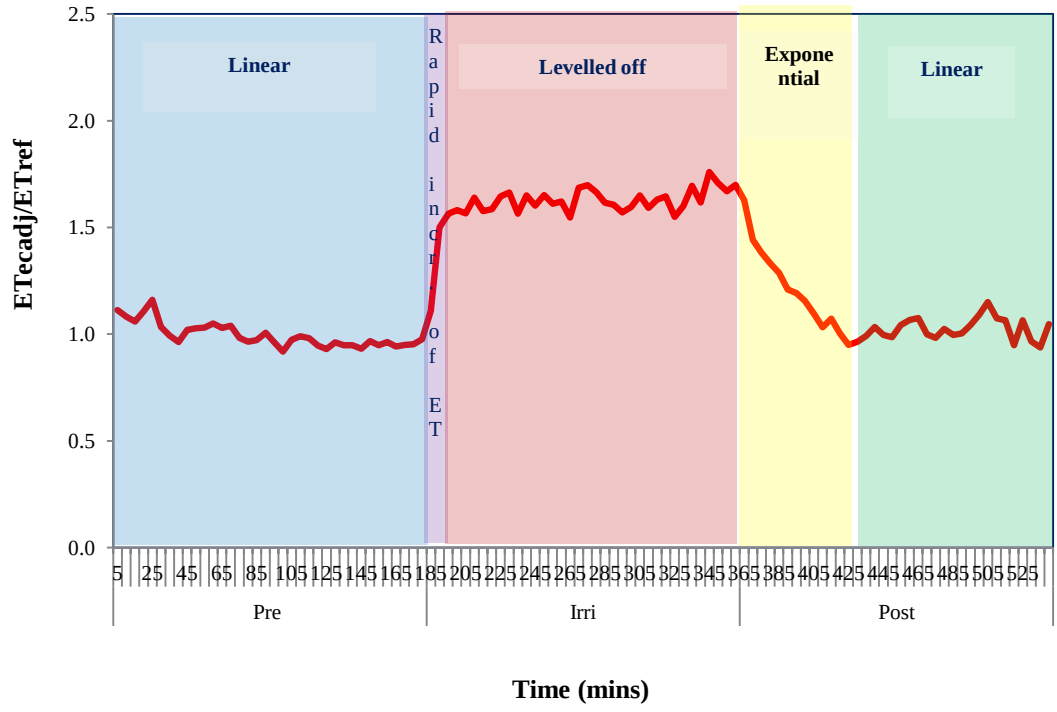

Figure 5.15: Schematic representation of the different phases of irrigation in terms of dimensionless ET

Functions for different the phases were obtained using regression analysis. The equations were fitted to the nondimensional values of ET (ET_{ecadj}/ET_{ref}) during different irrigation periods. Various mathematical regression equations were investigated including the simple linear, quadratic, exponential, power and

logarithmic (Details are provided in Appendix D). The best fitting equations are provided in Table 5.9. From the analysis it is seen that the at the pre irrigation period the data followed a linear relationship. During the irrigation, the wetting curve quickly jumps to the potential rate of evaporation under a steady wet canopy condition which followed a linear relationship with time. The drying curve (ET rate) post irrigation, however, is an exponential decay for evapotranspiration until fully dry and nearly constant following a linear relationship after that.

Table 5.9: Best fitting regression equations of nondimensional ET for different phases of irrigation under advective and nonadvective conditions (where R_{et} is the nondimensional ET and t is the time)

Phase	Best fitted equations	
	Nonadvective	Advective
Pre irrigation	$R_{et} = -0.0009t + 1.0804$	$R_{et} = -0.0002t + 1.0387$
During irrigation	$R_{et} = 0.0006t + 1.5737$	$R_{et} = 0.0024t + 1.8318$
First stage of post irrigation	$R_{et} = 1.6332\exp(-0.009t)$	$R_{et} = 2.0412\exp(-0.013t)$
Second stage of post irrigation	$R_{et} = 0.0003t + 1.0013$	$R_{et} = 0.0018t + 0.9718$

5.3 Effect of irrigation on sap flow

5.3.1 General characteristics of sap flow

The measured rates of sap flow F from different trials and the diurnal pattern of sap flow on a non-irrigated day are shown in Figure 5.16. These results are judged to be representative of those for the rest of the days. On the non-irrigated day the sap flow

followed the diurnal variation in ET, producing a symmetrical curve about early afternoon with a rapid increase after sunrise and a rapid decrease in the late afternoon (Figure 5.16a). On the other hand on days where irrigation was applied the sap flow rates greatly reduced during the irrigation because the evaporative energy was fully consumed to evaporate the intercepted water on the canopy (Kume et al. 2006, Bosveld & Bouten 2003) and the stomatal pores were impeded by liquid water on the leaf surfaces (Ishibashi & Terashima 1995, Brewer et al. 9991, Forseth 1990). For example on DOY 84 (Figure 5.16b), before the irrigation events, the sap flow and reference evapotranspiration were similar. As soon as irrigation started, the sap flow rates decreased sharply continuing at a low flow rate up to the end of the irrigation event. Once the irrigation stopped, the sap flow rate progressively increased until it matched the reference ET after about 35 mins.

A similar trend was observed for longer irrigation periods and intervals (Figure 5.16c and 5.16d). However, in this case, the sap flow reached at its minimum value at about 35 mins after the onset of the irrigation. Because of the longer time (more than 30 mins) to reach its minimum value, the average rate of sap flow was less in the longer irrigation trials. The recovery period (35 mins) was same as previous (short duration) trials.

Thompson et al. (1997) measured a similar trend of sap flow in full canopy corn. However, they predicted a more rapid decrease in transpiration with the onset of irrigation and faster recovery of transpiration after completing irrigation. The reason behind this phenomenon might be due to the sap flow lagging behind transpiration as a result of water storage in the biomass of the plants. Steinberg et al. (1989) indicated that in woody plants, sap flow and transpiration may differ appreciably due to the water stored in the stem and branches of plants. The time lag between transpiration

and sap flow has also been attributed to the capacitance or water buffering capacity of the plants (Schulze et al. 1985, Fichtner & Schulze 1990, Kostner et al. 1998).

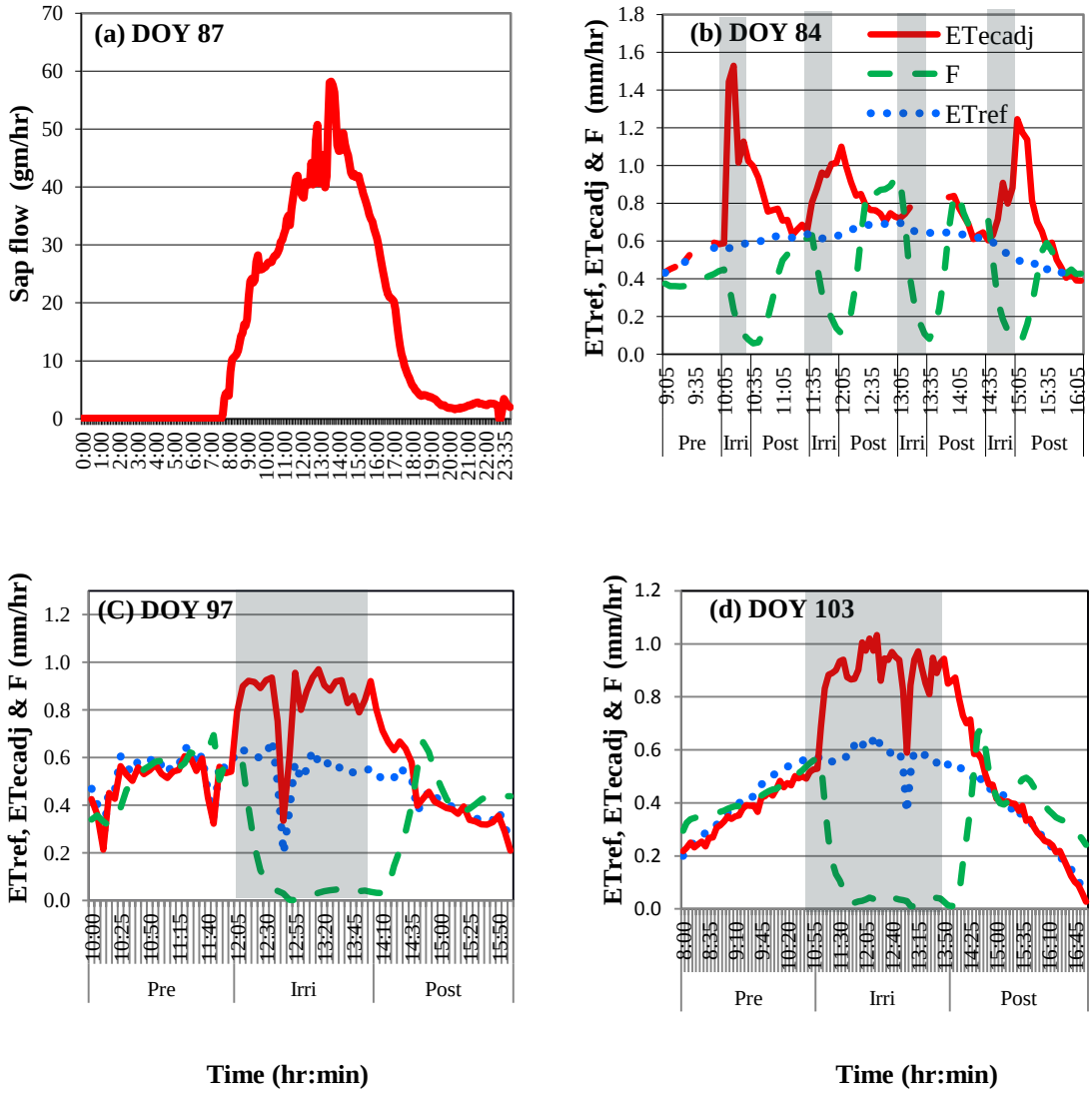

Figure 5.16: Sap flow *F*, reference evapotranspiration ET_{ref} and actual evapotranspiration ET_{ecadj} on selected days for different trials. Periods of irrigation are shown shaded. (a) non-irrigated day; (b) 30 mins irigation trails; (c) 120 mins irrigation trials; and (d) 180 mins irrigation trials

Two other features are evident from the sap flow plots, particularly Figures 5.16 c & d. First is the increased sap flow (relative to ET_{ecadj} and ET_{ref}) early morning and late afternoon. This has been observed in other studies, for example, Tomo'omi Kumagai et al. (2009) who showed that sap flow in woody plants exceeded transpiration from late afternoon through the night to early morning to replace moisture lost from the plant tissue during the high evaporative demand period through the middle of the day.

The second feature is the spike of sap flow that ocurs toward the end of the drying period as crop transpiration re-establishes. The cause of this is not known but it appears to be a response to the relatively rapid increase in transpiration that occurs during this period. This phenomenon also has been observed in other studies (Thompson et al. 1997).

The nondimensional curves produced from the nondimensional values of sap flow (F/ET_{ref}) following the same procedure used for ET, are presented in Figure 5.17. Figures show that nondimensional curves followed the same trend in all trials. However, the increased sap flow in the early morning and late afternoon is now more obvious (Figure 5.17a and 5.17b). This is due largely to the very low values of ET_{ref} at these times.

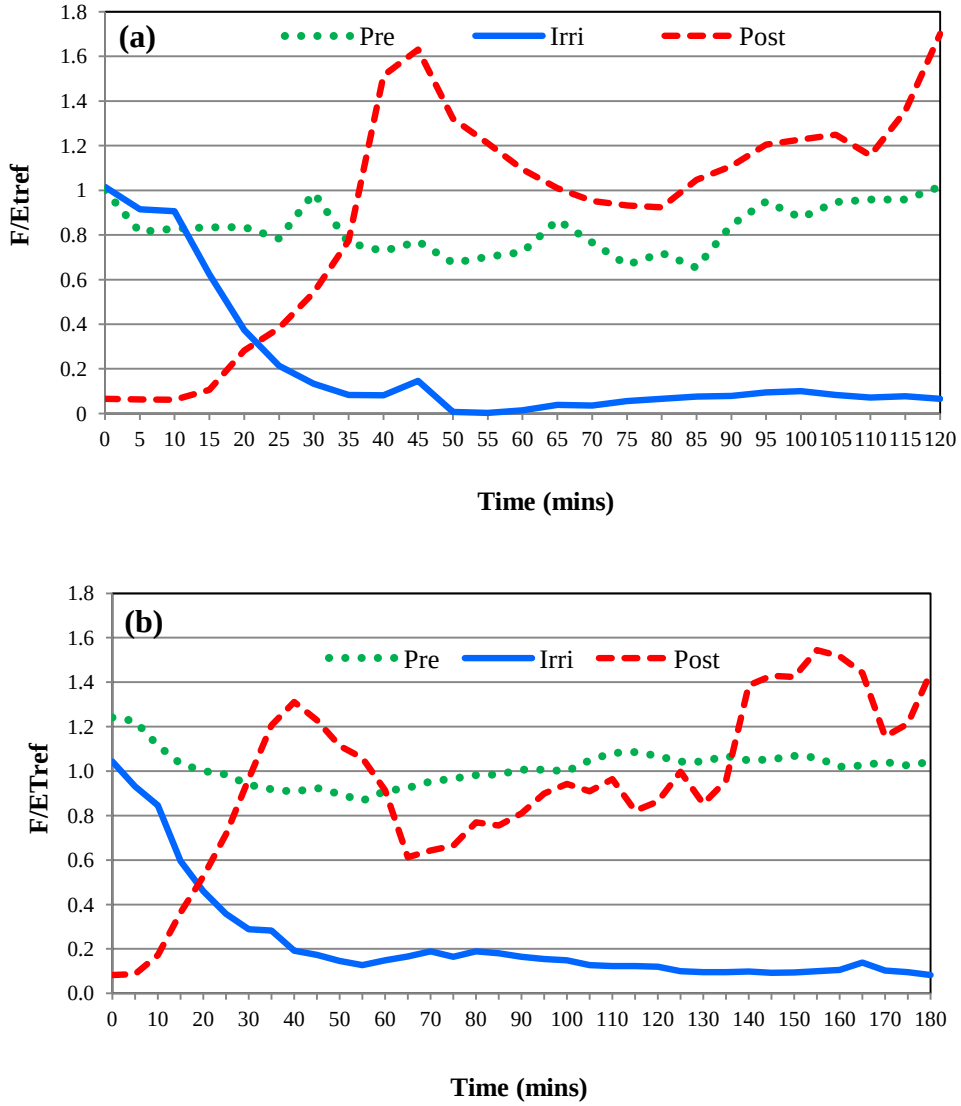

Figure 5.17: Nondimensionalised curves of sap flow *F* for (a) 120 mins and b) 180 mins irrigation trials

For short time (30 mins) irrigation (Figure 5.18), it is observed that the minimum value of sap flow was reached at the end of irrigation period and was still reducing. In comparision with the 60 mins irrigation it is revealed that the 30 mins irrigation was not sufficient for the sap flow to reach its minimum level (Figure 5.19).

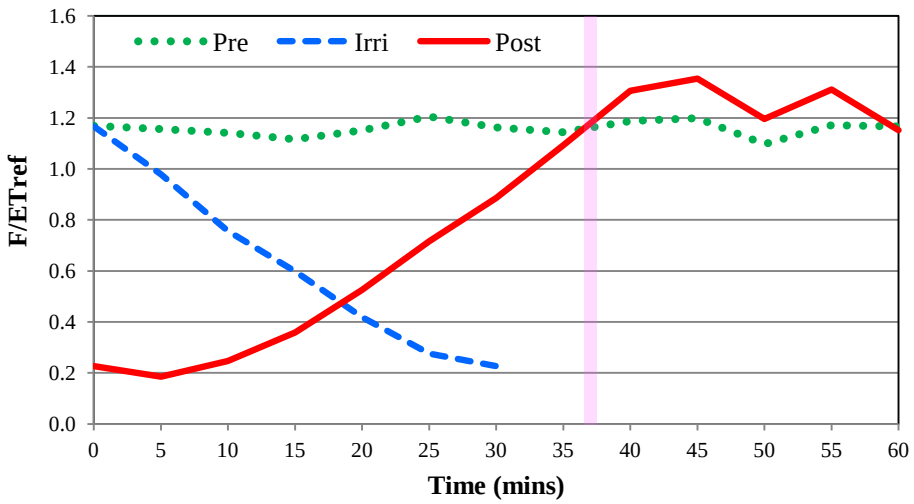

Figure 5.18: Nondimensionalised curves of sap flow *F* for 30 mins irrigation trials (with the pink bar indicating approximate alignment of Pre/Post *F* results)

Increasing the irrigation time, it was found that the sap flow reached at its miniimum value at around 35 mins after commencing the irrigation and continued at this value until irrigation ceased (Figure 5.19).

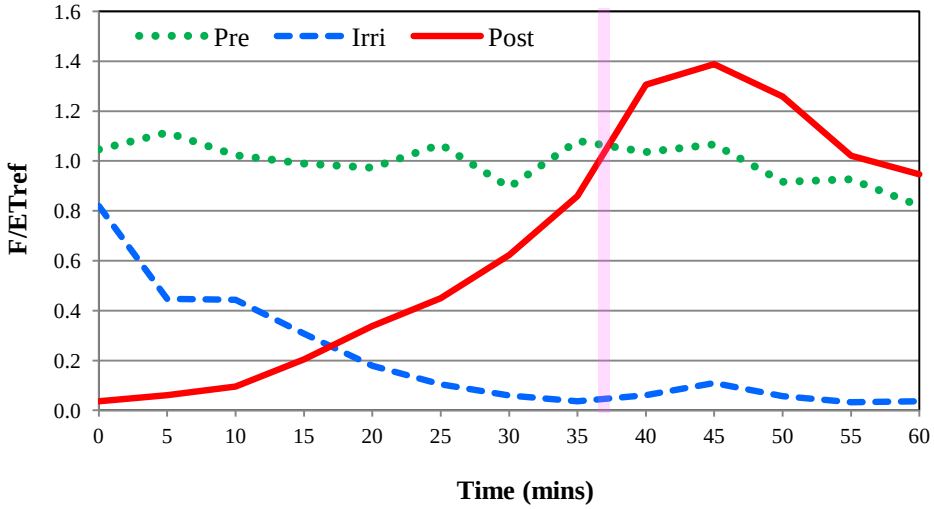

Figure 5.19: Nondimensionalised curves of sap flow *F* for 60 mins irrigation trials

From the long (120 & 180 mins) irrigation trials, it was found that most of the cases the sap flow reached at its minimum value at around 35 mins (Figure 5.20). Due to this reason the average value of sap flow for long duration irrigation trial was less than the short time irrigation trial (Table 5.10). Accordingly, average suppression of sap flow was calculated on the basis of long irrigation trials. On the other hand, the recovery time was about 35 mins (indicated by a bar line) in most of the cases.

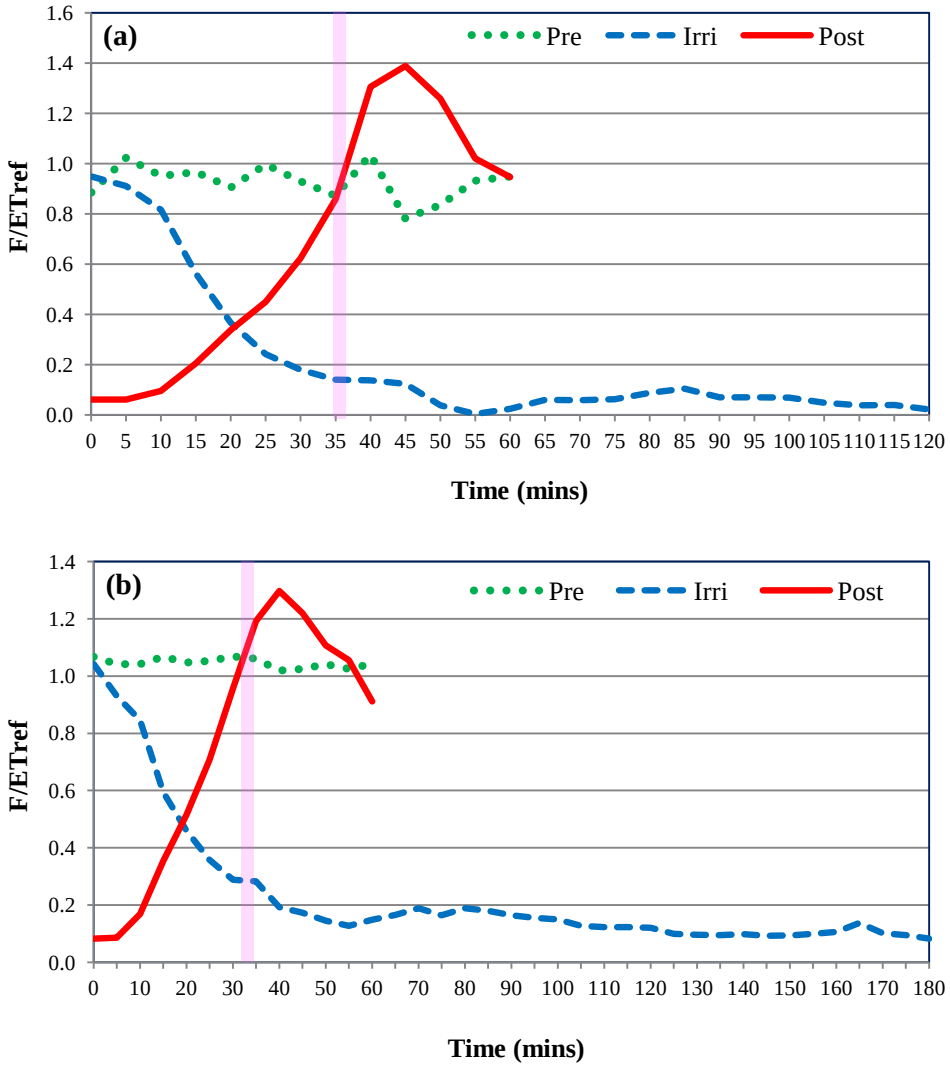

Figure 5.20: Nondimensionalised curves of sap flow (*F*) for long irrigation trials (a) 120 mins (b) 180 mins (with the pink bar indicating approximate alignment of Pre/Post *F* results)

5.3.2 Reduction of sap flow during irrigation

Similar to the evapotranspiration, the reduction of sap flow was determined on the basis of nondimensionalised values of sap flow and the values for each day trial are provided in Appendix J. As the magnitude of the reduction depends on the duration of irrigation, the results are provided according to the duration of irrigation.

The average nondimensional values for all trials during the period 25 March – 13 April 2011, are presented in Table 5.10. In the long irrigation trials (DOY 98–103), the average reduction of sap flow was 82% and varied from 81% to 97% (Table 5.10). As indicated previously the sap flow could not reach its minimum value in the short (30 mins) irrigations and resulted in a higher average value of nondimensional sap flow (0.60) than the average value (0.14) for the longer irrigations.

The overall reduction of sap flow (82%) in full crop canopy condition measured under this study was similar to that of Thompson et al. (1997) conducted in USA in corn crop using the same (sap flow) method. They predicted that the overall reduction of transpiration was 80% during irrigation and measured 83% both in case of impact and spray nozzles.

The average value of nondimensional *F* at post-irigation period was found to be less than the pre-irrigation period and greater than during irrigation. It was just reverse of evapotranspiration, where sap flow recovered to its normal flow with drying of the canopy.

Table 5.10: Average values of F/ET_{ref} pre-, during- and post-irrigation during 25 March – 13 April 2011

DOY	Date	Combination of irrigation (hr)			Average F/ET_{ref}			Reduction of F/ET_{ref} during irrigation		Average
		Pre	Irri	Post	Pre	*Irri*	Post	R_f	%	%
84	25/3/11	1	1/2	1	0.77	0.37	0.81	0.40	52	
91	1/4/11	1	1/2	1	1.05	0.42	1.00	0.63	60	
92	2/4/11	1	1/2	1	1.25	0.62	0.82	0.63	50	
93	3/4/11	1	1/2	1	1.13	0.69	0.89	0.44	39	**45%**
94	4/4/11	1	1/2	1	1.23	0.64	0.89	0.59	48	
97	6/4/11	1	1/2	1	1.07	0.86	0.63	0.21	20	
98	7/4/11	1	2	1	0.96	0.18	0.75	0.78	81	
99	9/4/11	1	3	1	0.86	0.03	0.54	0.83	97	**82%**
102	12/4/11	1	3	1	1.06	0.21	0.9	0.85	80	
103	13/4/11	1	3	1	0.93	0.13	0.84	0.80	86	

The average actual sap flow for short duration irrigations was 0.33 mm/hr (0.17–0.38 mm/hr), while for long duration irrigation the value was 0.17 mm/hr with the variation from 0.01- 0.12 mm/hr (Table 5.11).

Table 5.11: Average values of actual sap flow *F* pre-, during- and post-irrigation during 25 March – 17 April 2011

DOY	Date	Combination of irrigation (hr)			Average sap flow (*F*) (mm/hr)			Average sap flow *F* during irrigation
		Pre	Irri	Post	Pre	Irri	Post	(mm/hr)
84	25/3/11	1	1/2	1	0.39	0.33	0.48	
91	1/4/11	1	1/2	1	0.4	0.17	0.34	
92	2/4/11	1	1/2	1	0.53	0.38	0.46	
93	3/4/11	1	1/2	1	0.46	0.37	0.38	0.33
94	4/4/11	1	1/2	1	0.42	0.38	0.46	
97	6/4/11	1	1/2	1	0.41	0.37	0.25	
98	7/4/11	2	2	2	0.59	0.11	0.34	
99	9/4/11	2	2	2	0.35	0.01	0.31	0.08
102	12/4/11	2	2	2	0.56	0.12	0.42	

In a comparison trial (15 April 2011), carried out to better illustrate the sap flow dynamics during irrigation, three gauges were installed on plants inside the irrigation area and another three on plants outside the irrigated area. The Figure 5.21 illustrates that the sap flow during irrigation was slightly higher than the other trials. Because, in that case three sensors were used for irrigated plot and three were used for the nonirrigated area which may have influenced the average values.

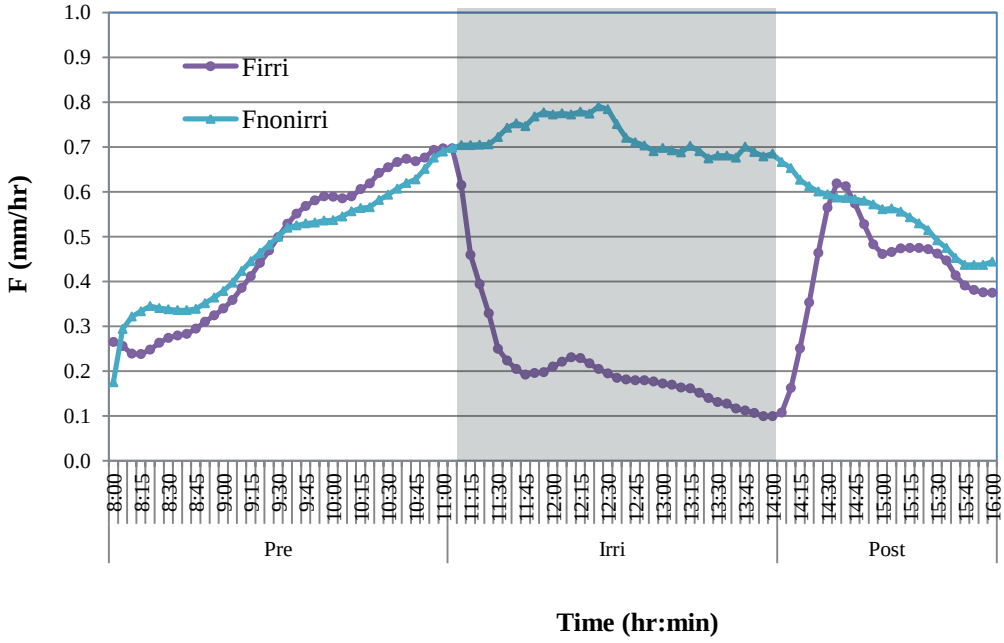

Figure 5.21: Comparison of sap flow in an average of three irrigated 'F_{irri}' and three non-irrigated '$F_{nonirri}$' plants on a clear day (15 April 2011; DOY 105)

Considering the average value of the nondimensionalised sap flow for the irrigated (0.41) and non-irrigated (1.24) condition, the average reduction of sap flow was found to be 67%. Using the same method, Tolk et al. (1995) estimated that the suppression of transpiration to be more than 50% for a corn crop. Most recently, Martinez-Cob et al. (2008) found that reduction of transpiration for the irrigated

treatment was 58% in corn. However, there are no published measurements for cotton with which to compare the observed results.

5.3.3 Idealized curves for sap flow

The idealized curves of sap flow at pre-, during- and post-irrigation period were established using the average nondimensionalised values of sap flow and are shown in Figure 5.22.

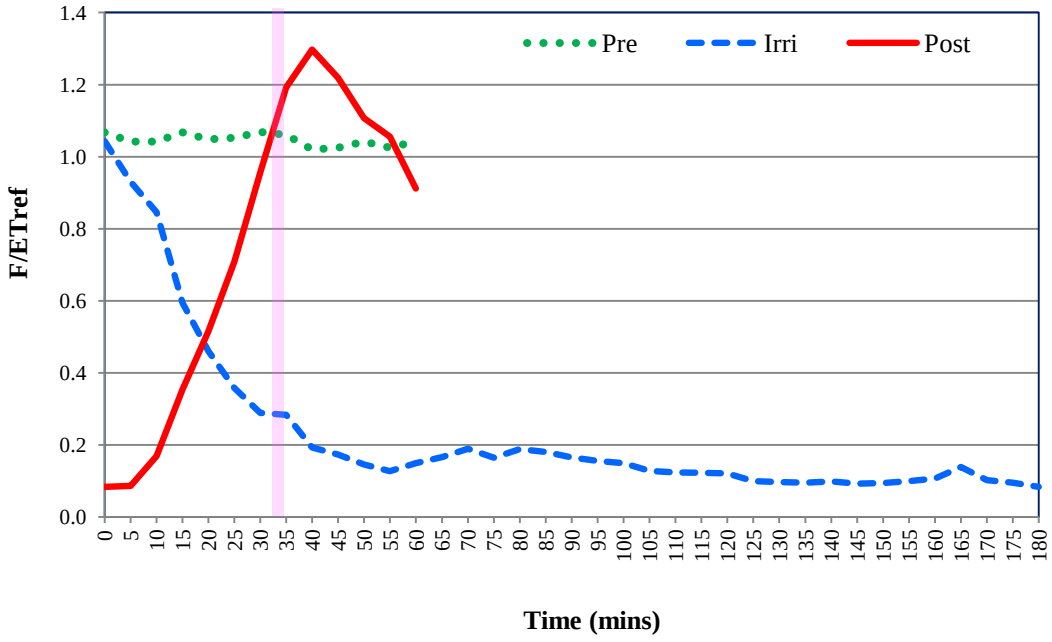

Figure 5.22: Idealized curves of sap flow for different phases of irrigation (with the pink bar indicating approximate alignment of Pre/Post *F* results)

Similar to the evapotranspiration, the equations for different phases were obtained using regression analysis. The equation were fitted to the nondimensionalised values

of F (= F/ET_{ref}) and the best fitting equations were obtained on the basis of statistical criterion provided in Appendix D. These are presented in Table 5.12.

Table 5.12: Best fitting regression equations of sap flow for different phases of irrigation (where R_f is the nondimensionalised value of sap flow and t is time)

Phase	Best fitted equation
Pre irrigation	$R_f = 0.00004t + 1.0572$
First stage of irrigation	$R_f = -0.387 \ln t + 1.5572$
Second stage of irrigation	$R_f = -0.0001t + 0.1042$
First stage of Post irrigation	$R_f = 0.0053t^{1.56}$
Second stage of Post irrigation	$R_f = -0.209 \ln t + 1.5809$

From the regression analysis it is revealed that at the pre-irrigation period the data followed a linear relationship. During the irrigation, values decreased logarithmically until reaching the minimum value. After that it followed polynomial relationship. For the post-irrigation period, the rate of sap flow F progressively increased following polynomial relationship with time and matched with pre-irrigation period after 35 mins.

5.4 Effect of sprinkler parameters on ET and sap flow

In later trials under experiments VII, VIII, IX and X (Table 3.1, section 3.5) during the period 21 April – 07 May 2011, the effect of nozzle size and type on evapotranspiration during irrigation was studied. The variation of pressure and height of sprinkler could not be studied due to the limitation of the height of the ECV station (which could not be raised above 2.5 m without its measurement footprint exceeding the 50 m diameter irrigated area). At high pressure the sensors did not function reliably due to the wetness from the spray.

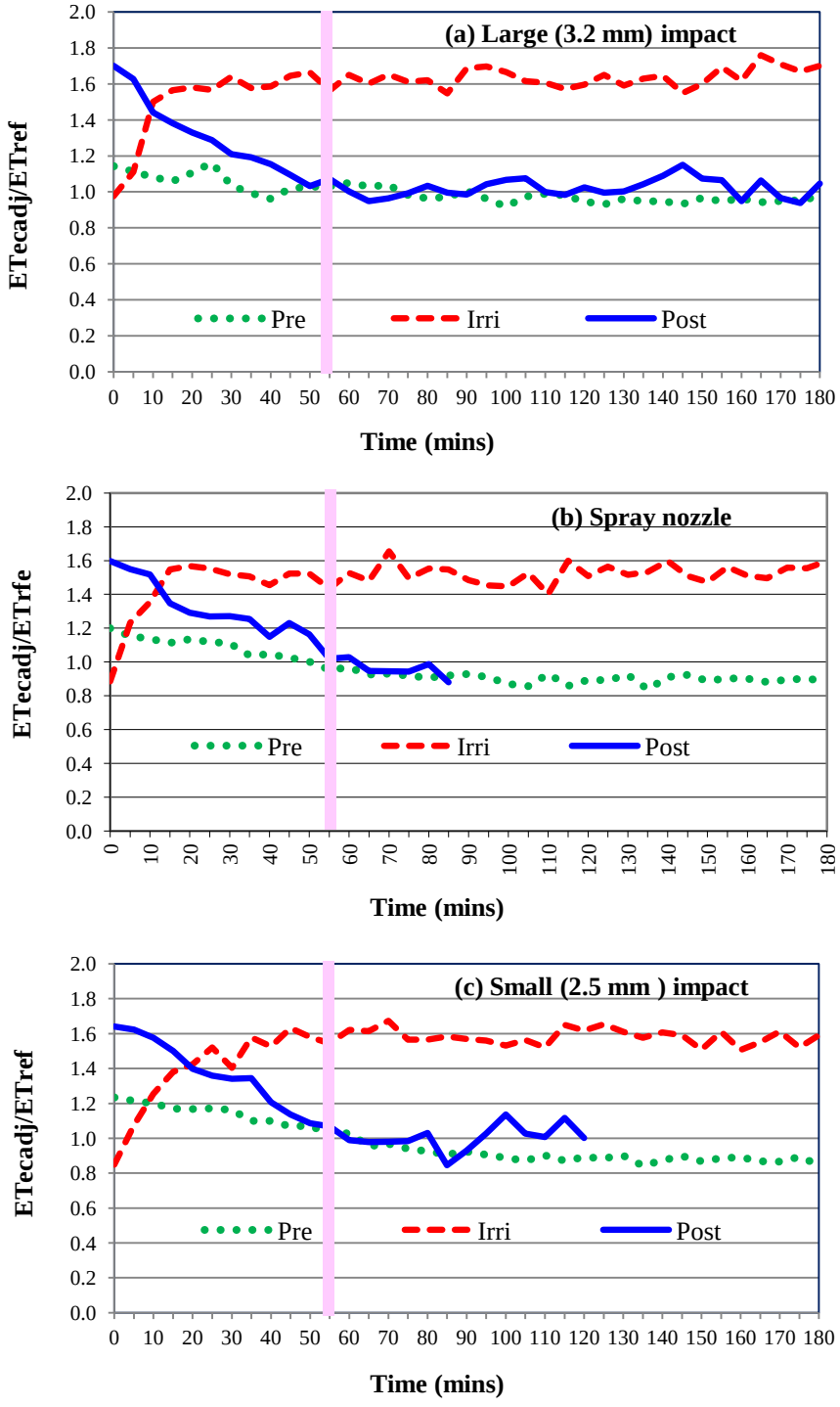

Figure 5.23: Nondimensionalised ET for three types of nozzle (with the pink bar indicating approximate alignment of Pre/Post *F* results) (a) large (3.2 mm) impact (b) spray and (c) small (2.5 mm) impact

From the plots of nondimensionalised ET for nonadvective condition shown in Figure 5.23, it is revealed that the curves followed the same trend as before. However, the increase in evaporation was different for each type and size of sprinkler.

Table 5.13: Additional evaporation (nondimensionalised) for different types of sprinkler at full crop canopy condition

Type of sprinkler	Average ET_{ecadj}/ET_{ref}		Increment of ET_{ecadj}/ET_{ref} during irrigation with respect to pre irrigation period	
	Pre	Irri	R_{et}	%
Impact (3.2 mm)	0.93	1.65	0.72	80
Impact (2.5 mm)	0.92	1.51	0.60	66
Spray (size 14)	0.93	1.48	0.55	59

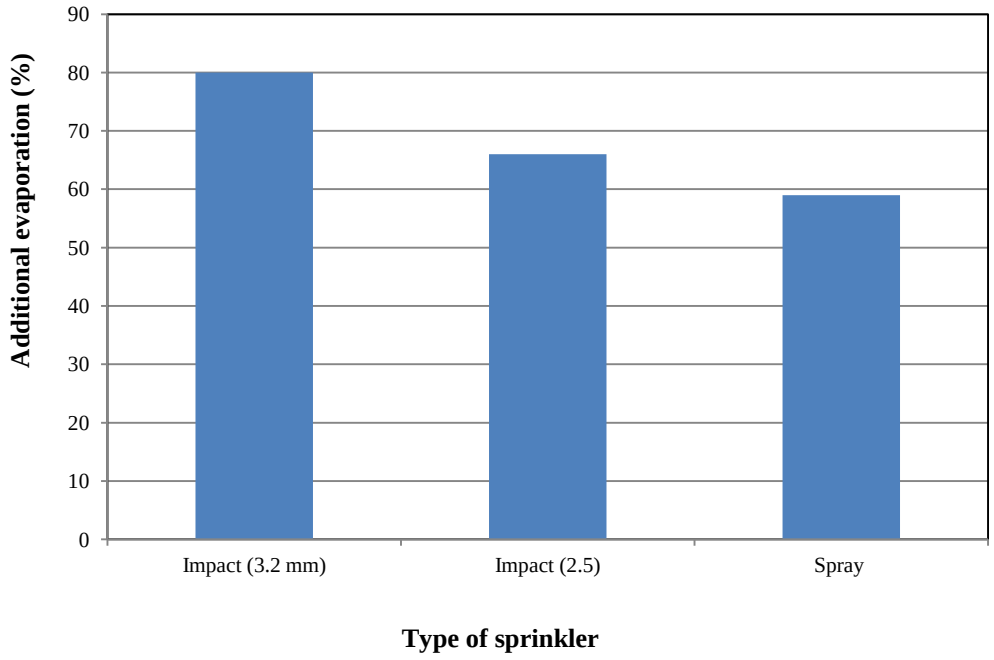

Figure 5.24: Additional evaporation for different types of sprinkler

The additional evaporation (80%) was greater for the larger size impact sprinkler rather than small size impact sprinkler (66%). The additional evaporation was lowest (59%) for the spray nozzle (Figure 5.24) possibly due to the fact that the low-angle impact sprinklers keep the plant canopy wet longer than spray heads, allowing more opportunity for evaporation (Yonts et al. 2007). Yonts et al. (2007) reported the similar results in terms of evaporation losses (3.81%) which include droplet evaporation, canopy evaporation, plant interception and soil evaporation in low angle impact sprinkler compared to the spray nozzle (2.08%). A smaller amount (20%) of additional evaporation occurred in spray nozzle than impact sprinkler also reported by Thompson et al. (1993b).

The wetting pattern of plants was studied using different types of nozzles with variable size. The graph produced from average of several day trials for different sprinkler is presented in Figure 5.25. The figure represents that there is no significant difference among the nozzles in terms of time to reach the sap flow at its minimum level.

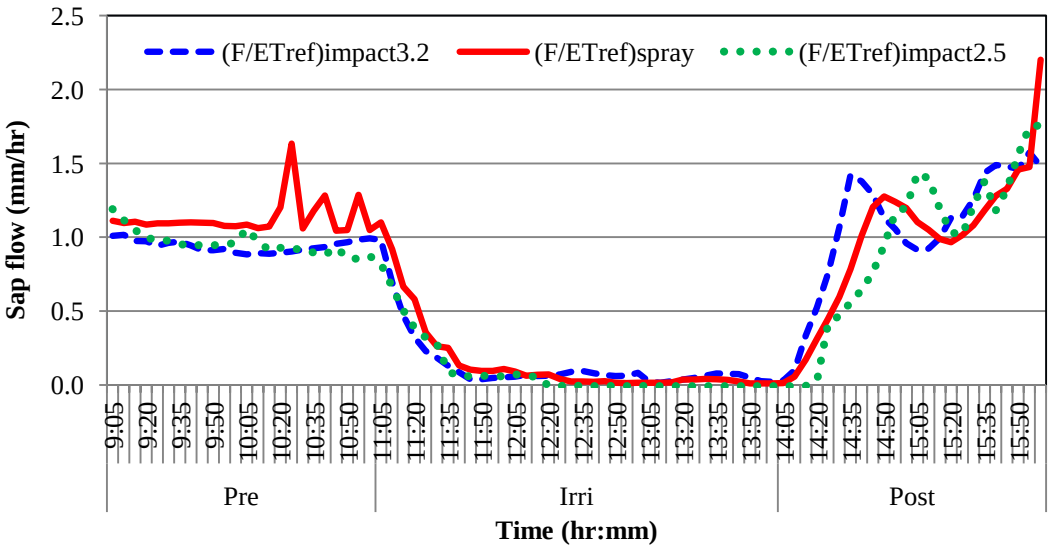

Figure 5.25: Comparison of sap flow for three types of nozzle under experiments VII, VIII, IX and X (Table 3.1, section 3.5)

5.5 Uncertainty in measurement

Although the measurements were done with great care, there was an uncertainty in evapotranspiration and sap flow measurements due to systematic and random errors. If it may be reasonably assumed that any systematic errors associated with the ECV-based measurement technique will be the same, proportionally, for all experimental periods, the uncertainty associated with the ET and sap flow differences may be estimated from the distribution of random fluctuations observed across all comparable trials.

Hence this uncertainty was determined on the basis of statistical characteristics (mean and standard error) of nondimensional values of ET and sap flow under conditions when each can reasonably be assumed to be in 'steady state' and therefore repeat measurements of the same (normalised) quantity. To estimate the uncertainty, measured data from the total of nine hours of nonadvective irrigation trials under full crop canopy condition were combined. The analysis was carried out separately for the aggregated periods (3 hours each, approximately) of pre-irrigation and 'levelled-off' period during irrigation (i.e. after initial wetting of the canopy was complete). The mean and standard error of the averaged values of nondimensional ET and sap flow were calculated and are presented in Table 5.14.

Table 5. 14: Uncertainty in evapotranspiration and sap flow measurements

Parameter	Evapotranspiration (mm/hr)		Sap flow (mm/hr)	
	Pre irrigation	During irrigation	Pre irrigation	During irrigation
No. of data values (*n*)	36	33	36	29
Mean	0.99	1.62	1.05	0.15
Standard error	0.06	0.05	0.04	0.02

The results indicate that the absolute error in ET measurements varied little (from 0.05 mm/hr to 0.06 mm/hr) whereas error in sap flow measurements was 0.02 mm/hr to 0.04 mm/hr (Table 5.14). Compared to the mean, the average relative error in ET measurements was 5% which ranged from 3% to 6%. On the other hand, relative error in sap flow measurements varied from 4% to 13%. During the irrigation relative error in sap flow measurements was comparatively higher (13%). Braun & Schmid (1999) reported that the highest error may occur predominantly at low flow rates where *dT* (temperature difference between upper and lower junctions of the sensor) approaches to zero.

Furthermore, the results of Table 5.14 indicate that for the mean ET difference, 0.63 mm/hr, the ECV-based measurement system developed in this research has resolved this with a discrimination of order ±11% (= 0.63/0.055) overall (for the nonadvective irrigation trials under full crop canopy condition). Likewise for these trials, the sapflow change during irrigation has been resolved with a discrimination of order ±30% (= 0.90/0.03) for these results.

5.6 Effect of irrigation on microclimate

To observe the effect of irrigation on microclimate, the meteorological parameters vapour pressure deficit VPD, relative humidity RH and air temperature T_a were measured upwind, within and downwind of the irrigated plot. A considerable difference in RH and VPD was observed between upwind and downwind position during irrigation, although the values were same at pre and post irrigation period. At the downwind position the relative humidity was higher due to the modification of climate by increasing the moisture in the atmosphere thus reducing the VPD (Figure 5.26). The effect continued to some extent until the canopy dried. The same pattern was observed from upwind to the middle of the irrigated plot (Figure 5.27). There

was no significant difference found in temperature during the irrigation at those two positions.

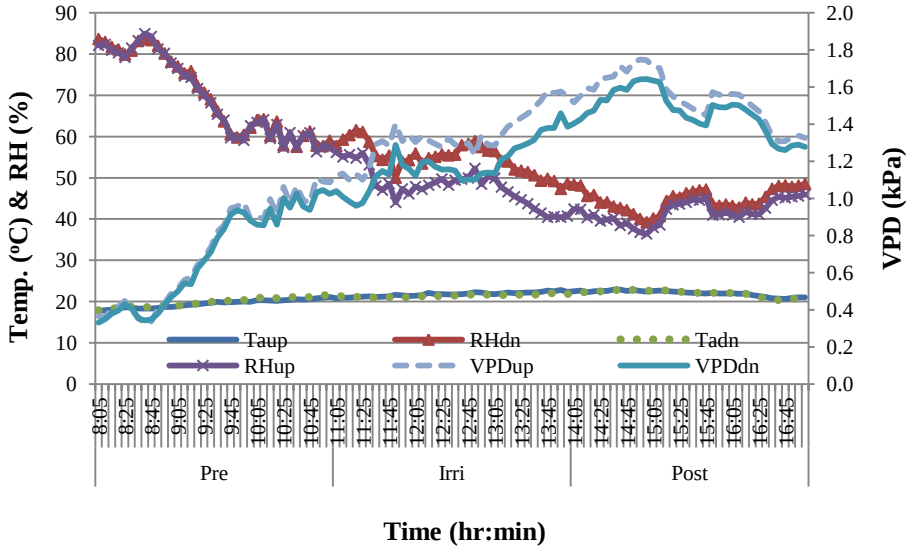

Figure 5.26: Air temperature, RH and VPD upwind and downwind of the plot on a clear day (DOY 105, 15 April 2011)

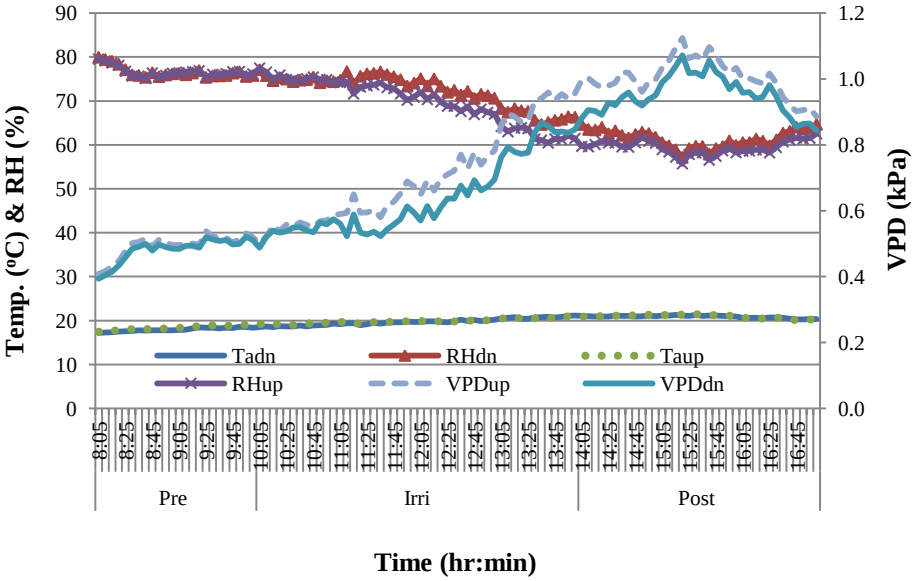

Figure 5.27: Air temperature, RH, VPD upwind and within the plot on a clear day (DOY 114, 24 April 2011)

During the irrigation the canopy temperature was significantly lower in almost all trials in compared with the pre and post irrigation periods. A representative plot of canopy temperature is presented in Figure 5.28. This shows that before the irrigation the canopy temperature was higher than the air temperature. Soon after starting the irrigation, the canopy temperature decreased rapidly and matched with air temperature during the irrigation. After completion of irrigation, the canopy temperature rose and reached a steady state level after about 60 mins. As with the nondimensionalised ET, recovery time of canopy temperature also indicates that the drying time might be about 60 mins.

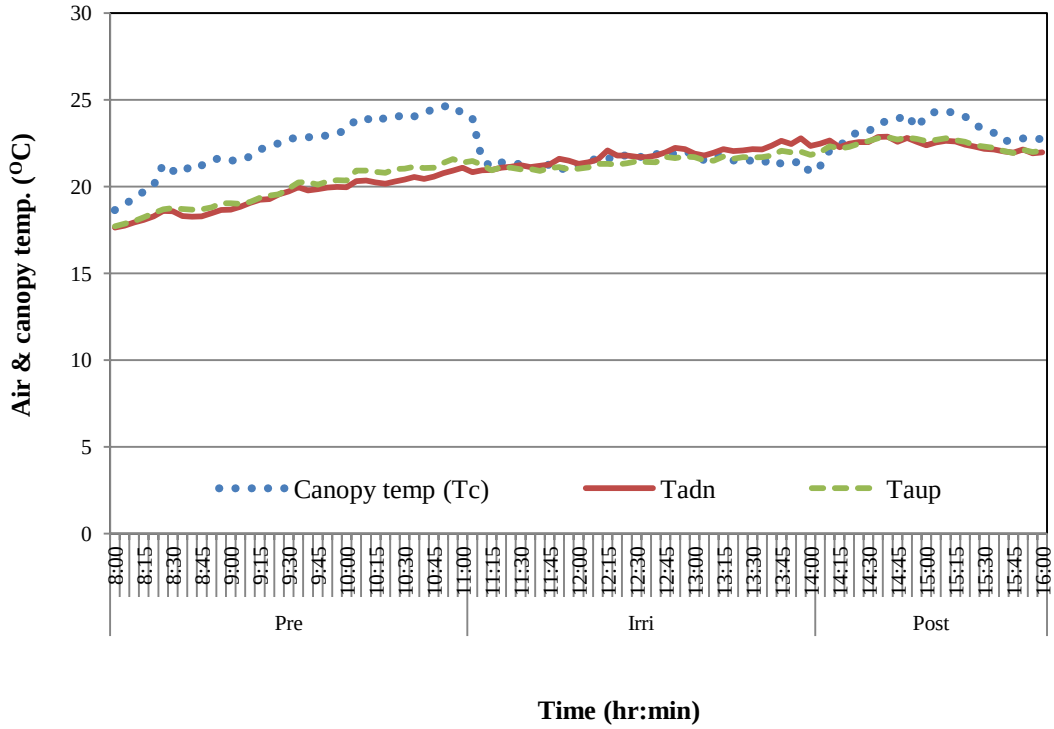

Figure 5.28: Air and canopy temperature during the irrigation trials (DOY 105, 15 April 2011)

By studying the downwind effect of droplets evaporation in sprinkler irrigation, Kohl & Wright (1974) showed that the air temperature generally reduced to less than 1 ^{O}C and vapour pressure deficit by 0.8 kPa. Chen (1996) reported that the day time average VPD decreased and RH increased while air and canopy temperature decreased in a sprinkled irrigated field. Cavero et al. (2009) reported that maize canopy temperature reduced significantly during day time sprinkler irrigation event from 6.1 ^{O}C to 4.3 ^{O}C.

It is well documented that during irrigation, the atmospheric demand in the irrigated area is suppressed significantly due to modification of microclimate. Similar results were found in this study as shown in Figure (5.29). Figure 5.29 illustrates that the atmospheric demand was lower within the irrigated plot than upwind during the irrigation, while it was same pre and post irrigation period.

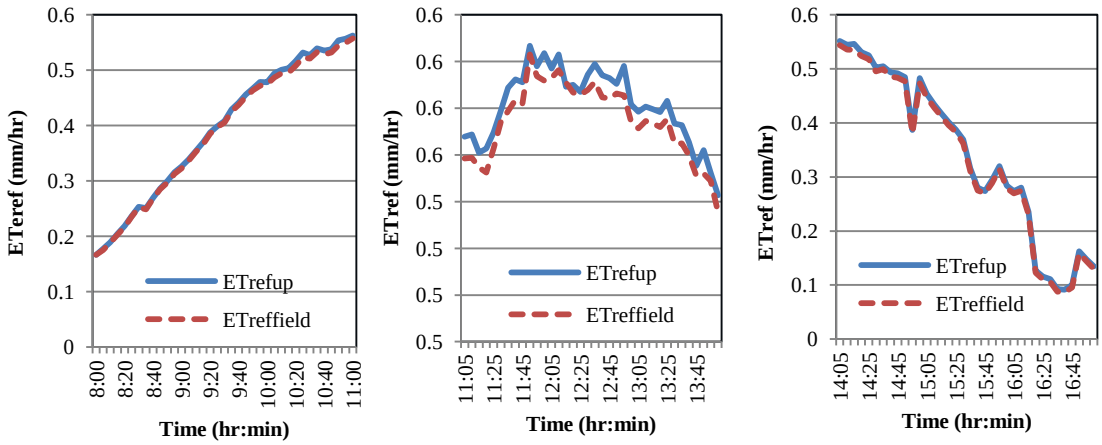

Figure 5.29: Comparison of evaporative demand (reference ET) upwind and within the crop (a) pre- (b) during (c) post-irrigation condition on a clear day 15 April 2011 (DOY 105)

Recently Martinez-Cob et al. (2008) reported estimated ET rates during sprinkler irrigation (calculated using the Penman-Monteith equation) that were significantly lower than those for the same crop when not being irrigated. They concluded that evaporation decreases during irrigation which is incorrect. In essence they calculated the evaporative demand, which as shown above reduces during irrigation but actual evaporation increases. Most probably they were in error in their study by not changing the values for the stomatal resistance r_s, and the atmospheric resistance r_a used in the Penman-Monteith equation to account for the canopy wetness due to the effect of irrigation.

5.7 Conclusions

Nondimensionalisation using ET_{ref} and averaging results from multiple trials gave idealized curves of the total evapotranspiration for each stage, i.e pre-, during and post-irrigation. These curves provide measurements of total evaporation during irrigation which permits calculation of the additional evaporation caused by irrigation. The principal features are:

- The rate of total evapotranspiration varied significantly according to crop growth stage and climatic factors, especially advection.
- The significant increase of total ET from partial canopy to full canopy indicates that canopy evaporation was higher in full canopy due to the greater area of canopy surface in full crop canopy condition and hence greater interception capacity.
- The decreasing value of nondimensional ET during post irrigation period represents the evaporation of intercepted water from the canopy.
- Significantly higher values of total evapotranspiration were measured during irrigation in advective condition, which illustrates the increased additional evaporation to some extent under advected irrigation.

Observations of the entire phenomenon occur during irrigation and subsequent period over the crop using nondimensionalisation of total ET measured by the energy balance (using ECV for energy flux partition) confirmed that this method was able to measure the total ET as well as additional evaporation during the irrigation. (This is consistent with the results of the preliminary measurements, as reported in Chapter 4).

The measurements of total ET at different stages of crop will allow quantifying the volume of additional water required in sprinkler irrigation to meet the additional evaporation (Chapter 6). The measured ET data at different phases of irrigation event can also be used to predict the total additional evaporation in sprinkler irrigation in cotton growing areas of Australia using the local climatic data (Chapter 6).

It is also concluded that:

1. Sap flow measurements showed the strong reduction in transpiration during irrigation with a lag in response of sap flow to canopy wetting and drying. The bulk evaporation during irrigation was from the water intercepted by the canopy.
2. A smaller amount of additional evaporation was found using spray nozzles compared to impact sprinklers, perhaps due to the fact that low-angle impact sprinklers keep the plant canopy wet longer than spray heads, allowing more opportunity for evaporation.
3. Considerable difference in relative humidity and vapour pressure deficit was observed between upwind and downwind locations as well as at the middle of the irrigated plot during irrigation. However, no significant difference was found in temperature during the irrigation at those positions, which might be due to the small size of the irrigated plot. As the effect of the modification of the microclimate, the atmospheric demand (reference ET) within the irrigated

plot was found lower than the outside, although the actual ET measured by the energy budget / ECV method was much greater, due to the effect of direct evaporation from the canopy surface.

4. The uncertainty analysis in ET and sap flow measurements showed that the error in ET measurements varied little (from 0.05 mm/hr to 0.06 mm/hr) whereas error in sap flow measurements was 0.02 mm/hr to 0.04 mm/hr. The analysis indicates that ECV-based measurement system developed in this research has been resolved with ±11% discrimination and sap flow change during irrigation has been resolved with a discrimination of ±30%.

Chapter 6: Irrigation implications of experimental results

6.1. Introduction

The literature review (Chapter 2) demonstrated that in many previous studies all other components except droplet evaporation were ignored due to difficulties in measurement. However, separation of these components is essential for design and management of efficient sprinkler irrigation systems. Nevertheless, measurement of major components (evaporation and transpiration) of ET in different crop stages (Chapter 5) indicates that the components of total ET can be separated using these measurements. Hence, the potential implication of the experimental data under this study would be the estimation of total volume of canopy evaporation and to separate this amount into its different components including additional evaporation in sprinkler irrigation, soil evaporation, droplet evaporation, canopy interception capacity etc. Another implication of these experimental data would be the prediction of additional evaporation under sprinkler irrigation at other times and places.

This research presented in this chapter has focused on demonstration of: (i) separation of total amount of canopy evaporation into its components in sprinkler irrigation; (ii) prediction of the actual ET under sprinkler irrigation for different times and places using climatic data; and (iii) estimation of amount of canopy evaporation and its major components from the predicted ET. It illustrates how the ECV measurements can be used to predict the additional volume of water required in a range of irrigated regions of different climate and irrigation system on the basis of local climatic data. This will allow farmers and researchers to get an idea about the additional evaporation in sprinkler irrigation according to the local climatic and

operational conditions and hence the additional water that needs to be applied in each irrigation to satisfy this evaporative loss.

It needs to noted that the prime purpose of this chapter is to demonstrate how the ECV data can be used for these predictions, and that data for that purpose will need to be collected for the range of irrigated region, climates crops, and sprinkler irrigation systems.

6.2 Total canopy evaporation and its components

The different components of total evaporation measured by the ECV technique in Chapter 5 were separated by using the areas between the actual ET, reference ET and sap flow curves (Figures 6.1 & 6.2). In this case the measured data for two relatively clear days, DOY 103 for impact sprinkler and DOY 114 for spray type sprinkler are shown in Figure 6.1a and Figure 6.1b respectively as representative of other days.

The values of ET during irrigation and subsequent periods for different types of nozzles show that during the irrigation the values of ET increased significantly due to the direct effect of irrigation for both impact and spray sprinklers in terms of actual ET (Figure 6.1a-b) and nondimensional ET (Figure 6.2a-b). At the same time, a significant reduction of transpiration occurs, reflected in the measurements of sap flow (Figure 6.1a, 6.1b, 6.2a & 6.2b).

From the figures it is seen that total depth of canopy evaporation, soil and droplet evaporation during and immediately following an irrigation is the summation of:

- additional evaporation during irrigation (C),
- reduction of transpiration during irrigation in terms of sap flow (D) from the rates which would have occurred without irrigation, and

- canopy interception capacity which includes additional evaporation during drying (E) and reduction of transpiration in terms of sap flow during drying (F).

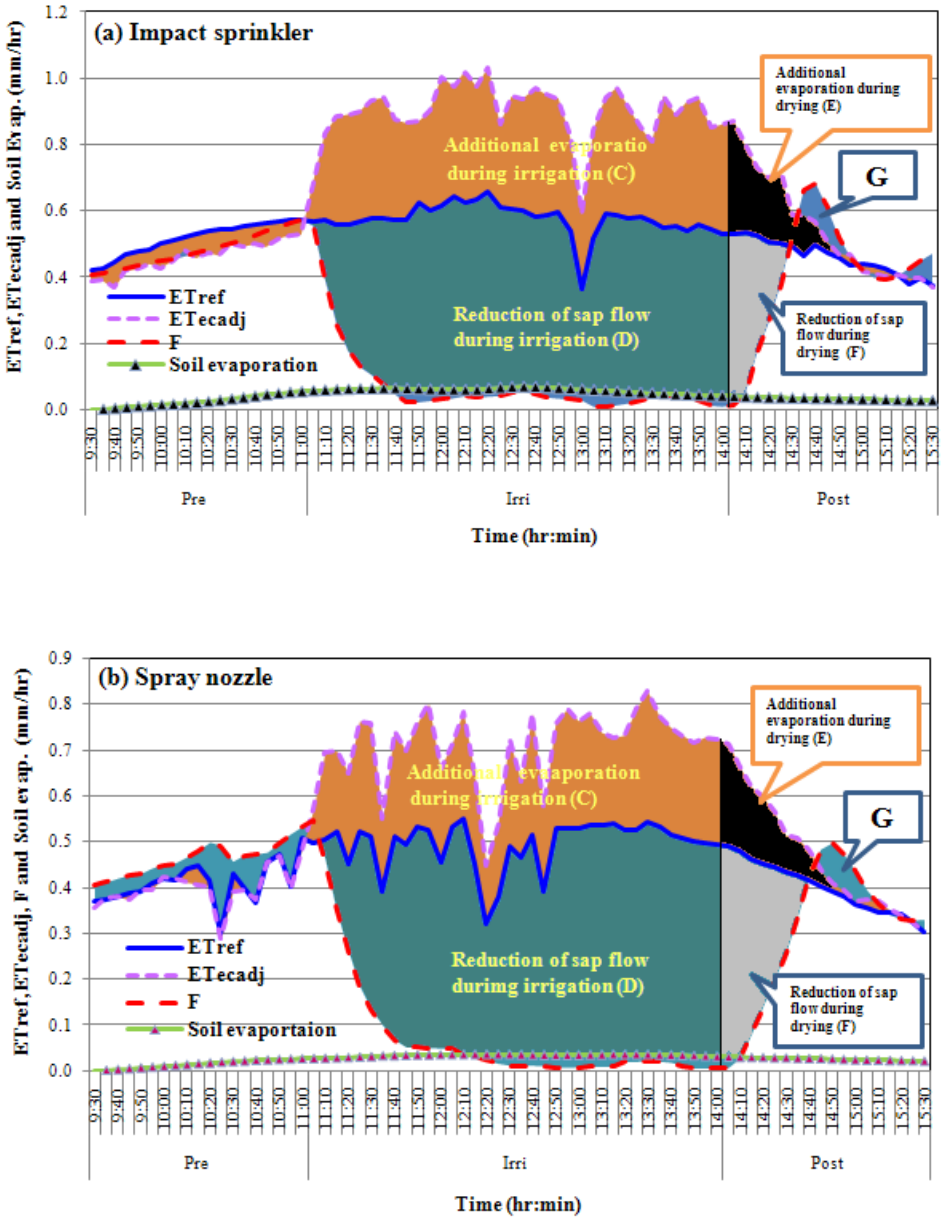

Figure 6.1: Reference ET (ET_{ref}), actual ET (ET_{ecadj}) and sap flow (F) in different types of sprinklers on different days (a) DOY 103 and (b) DOY 114

The soil evaporation represented by line graph at the bottom of the Figure 6.1a & 6.1b is included in the total evaporation and hence in the summation of the above areas.

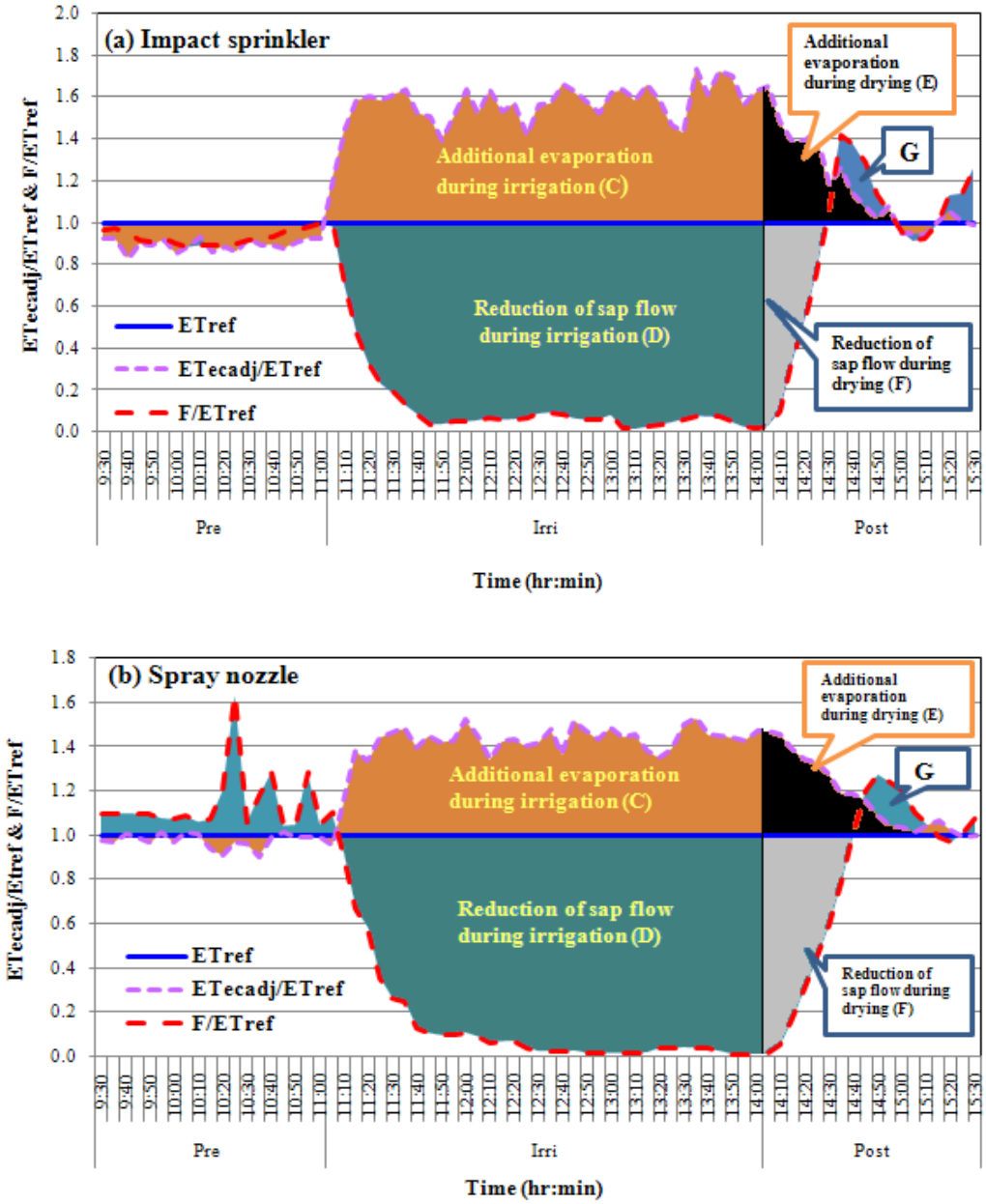

Figure 6.2: Nondimensionalised evapotranspiration (ET) and sap flow (*F*) for different types of nozzles

From the experimental data it was observed that at the end of the post irrigation (drying) period (14:30 15:00 PM) the sap flow continued to rise beyond the reference and actual ET and then decreased until it matched the reference and actual ET. The area under this curve denoted by 'G' in Figure 6.1a & 6.1b could not be explained reasonably under this study. Since the area of the part is small, it was ignored in the calculations in this Chapter.

The figures show that a significant amount of additional evaporation (C) occurs during irrigation as the effect of canopy evaporation and droplet evaporation. Although, the droplet evaporation could not be quantified due to technical limitations, the preliminary measurements over the bare soil (Chapter 4) under this study indicated that it would be negligible. Thompson et al. (1997) also predicted that droplet evaporation is negligible compared to the canopy evaporation. On the contrary, a remarkable amount of sap flow (sum of D & F) was suppressed due to the wetness of the canopy which would have occurred without irrigation. Since, it was not possible to identify the lag between sap flow and transpiration in the field measurements, sap flow was considered to represent the transpiration. Evaporation of intercepted water (sum of E & F) continued after irrigation ceased. This was assumed to give a measure of the canopy interception capacity of the crop, and can be identified using the same data. However, a negligible amount (0.1% of applied water) of soil evaporation was measured in both cases under closed (mature) canopy condition. In this regard, Williams et al. 2004 reported that in a closed canopy crop, the soil evaporation can be neglected both in irrigated and non-irrigated conditions. Yonts et al. (2007) also reported that the evaporation from the soil during irrigation is assumed to be negligible for the low angle impact sprinkler as a result of evaporation demands being met by the water evaporating from plant leaves. Hence, the soil evaporation was neglected in further estimation.

The separation of the components of total canopy evaporation into its different components in this section allowed to predict the total depth of canopy evaporation and its major components for different times and places through predicting actual ET.

6.3 Idealized model

To predict the actual ET and sap flow in nonadvective and advective irrigation conditions, idealized models for both conditions were developed using the equations developed in Chapter 5 (Table 5.9 & Table 5.12) under full crop canopy conditions. These are shown in Figure 6.3.

Under advective irrigation conditions the nondimensionalised values of ET were comparatively higher (Figure 6.3b) in comparison with nonadvective condition (Figure 6.3a) due to the reasons described in section 5.2.2. However, there was no significant difference was found in nondimensional *F* because the canopy was fully wetted in both cases and hence suppressed the sap flow similarly.

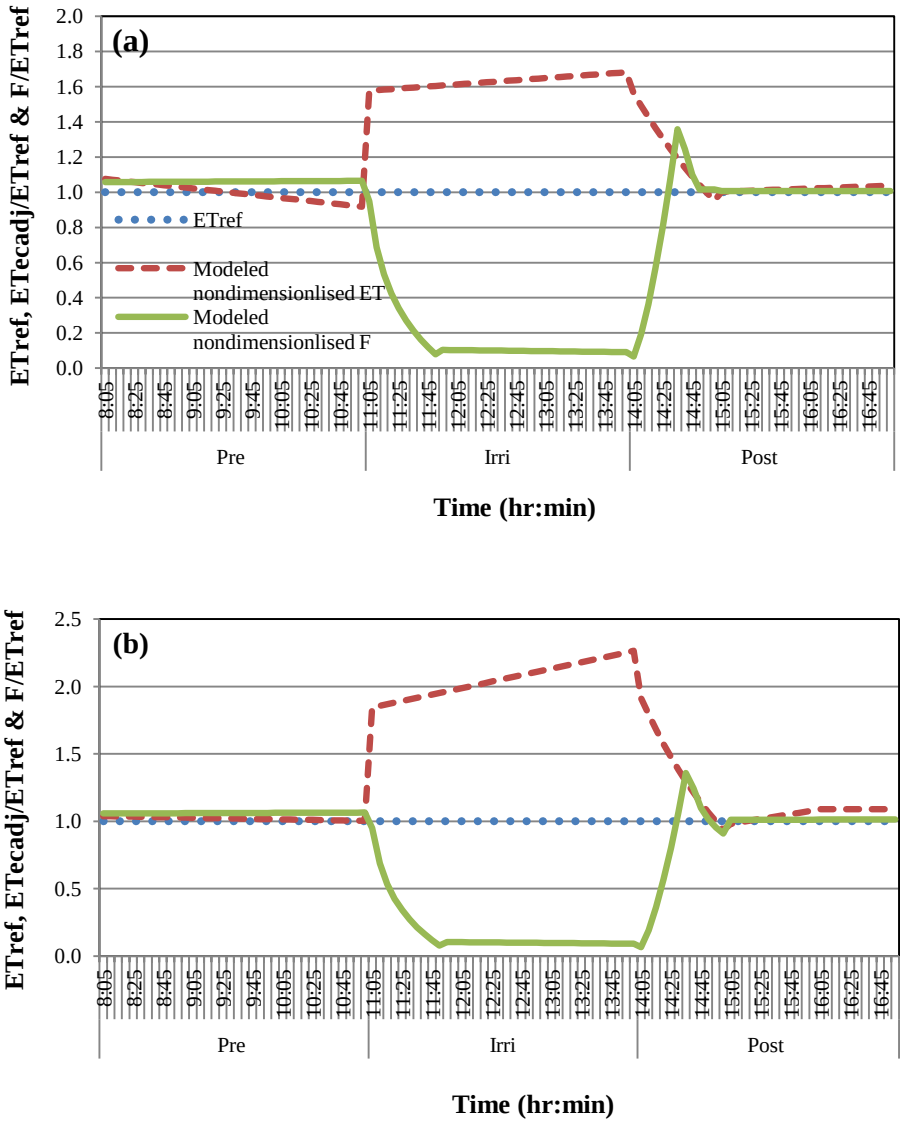

Figure 6.3: Idealized model for ET and sap flow (*F*) in (a) nonadvective and (b) advetcive conditions

6.4 Validation of model

Comparisons of actual and predicted evapotranspiration (ET) and sap flow (*F*) using the idealized model for two selected days for two conditions are presented in Figure 6.4a & b. From the figures it is seen that the regression models predicted the actual value of ET and *F* quite reasonably for different periods of the irrigation trials in both

conditions. However, in advected condition the predicted value was slightly overestimated due to the reason of limited number of trails.

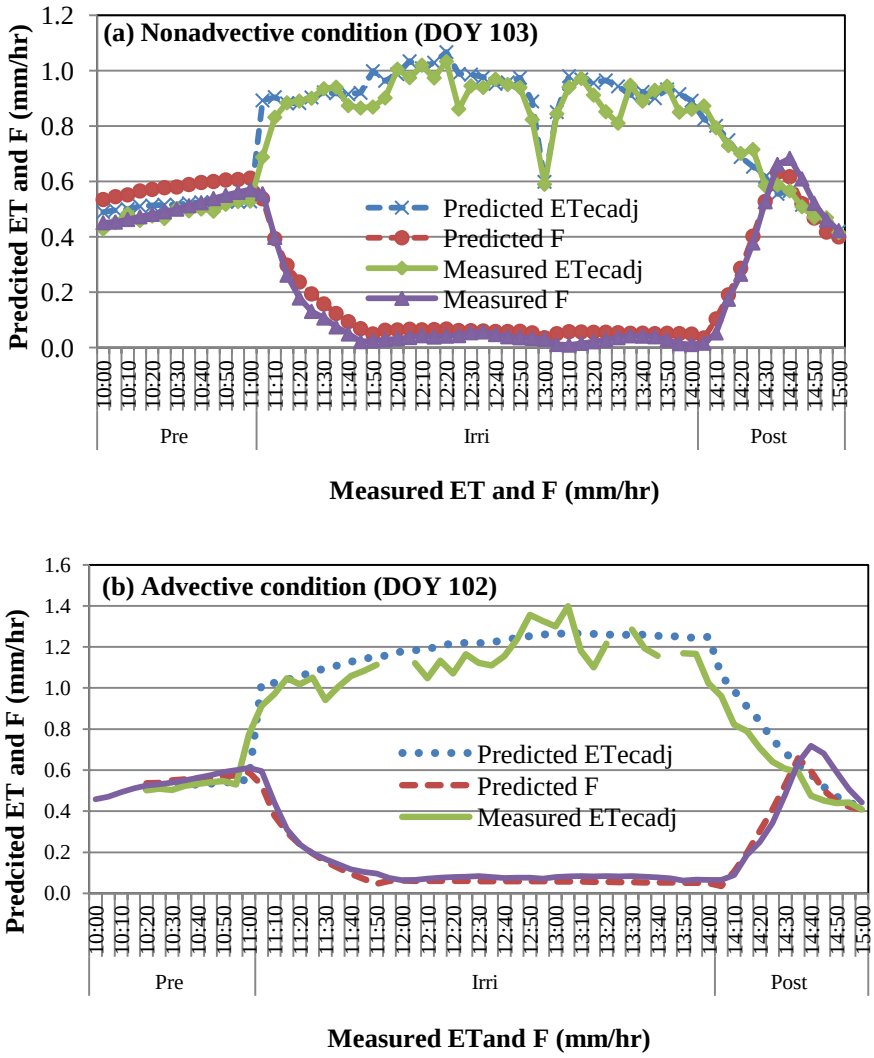

Figure 6.4: Comparison of measured and predicted evapotranspiration and sap flow

Statistical analysis also demonstrated the agreement between predicted and observed values of ET and *F* was quite good in all cases with slope and coefficient of determination (R^2) close to unity in most of the cases (Figure 6.5 & 6.6). The lower value of RMSE (0.054 – 0.09 mm/hr) also indicates that the model predicted the ET

rates reasonably. The error in terms of RMSE observed in advective conditions (10%) was slightly higher compared to nonadvective conditions (7%). Relatively higher errors were found in sap flow prediction which was 0.047 – 0.048 mm/hr (18% -21% errors in terms of RMSE).

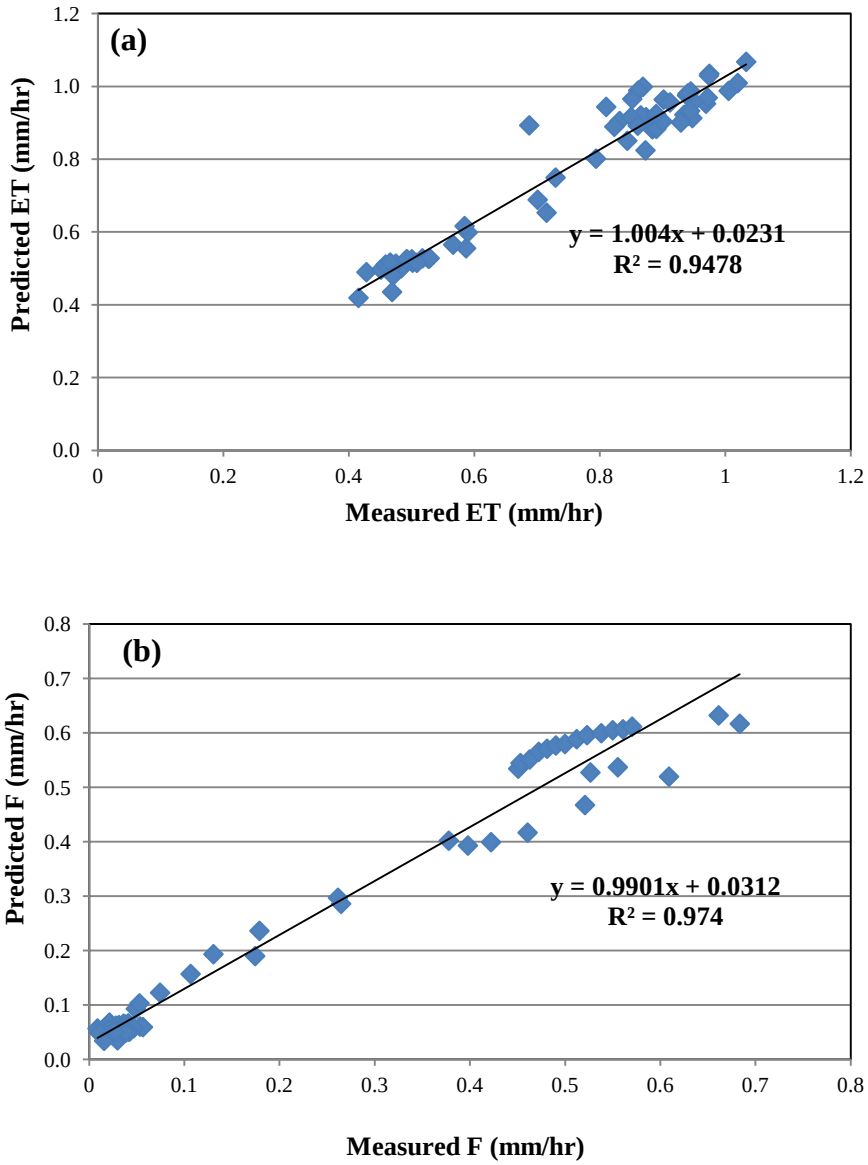

Figure 6.5: Comparison of measured and predicted actual evapotranspiration and sap flow in nonadvective condition (a) evapotranspiration (b) sap flow

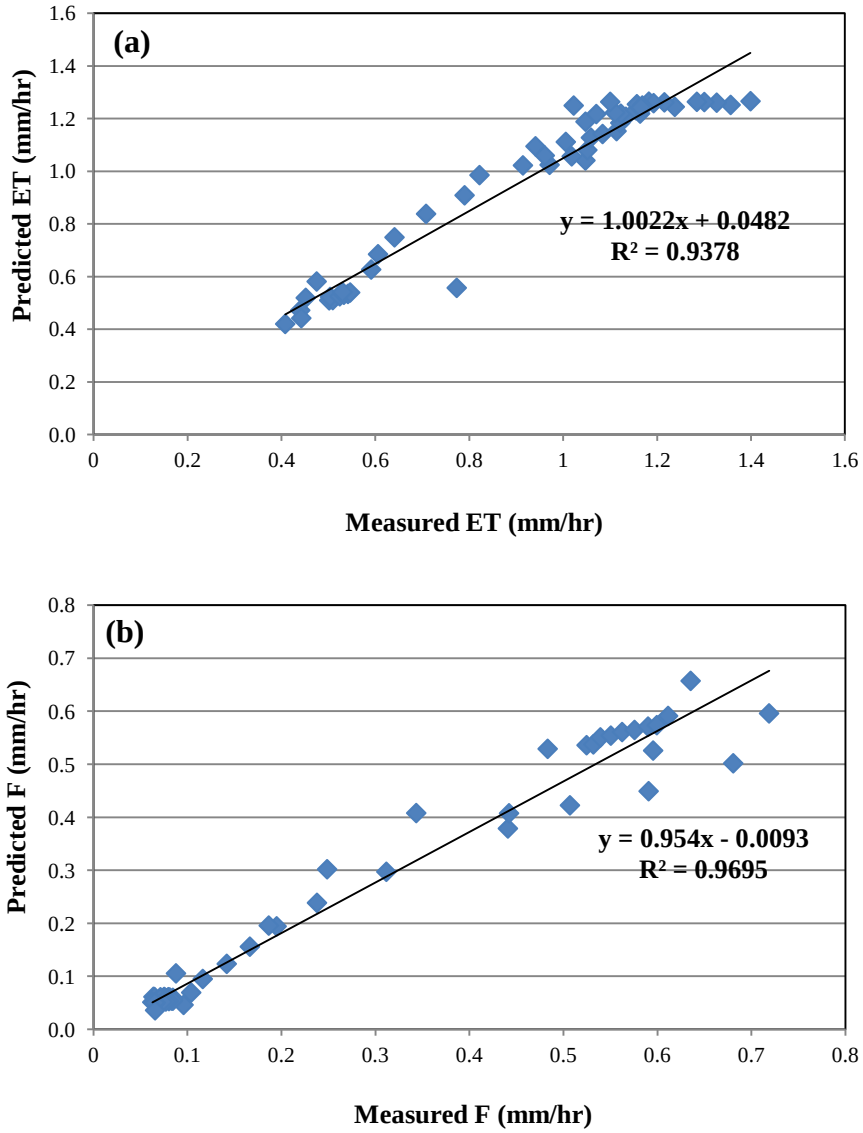

Figure 6.6: Comparison of measured and predicted actual evapotranspiration and sap flow in advective condition (a) evapotranspiration (b) sap flow

6.5 Climate and irrigation case study data

The depth of total canopy evaporation and its components under nonadvective and advective conditions was predicted for some selected cotton growing areas in

different locations of Australia (Table 6.1) as a case study adopting the regression models presented in Figure 6.3. The actual evapotranspiration (ET_{act}) in this case was calculated using the values of nondimensionalised ET (R_{et}) and the estimated reference ET of those selected places (i, e. $ET_{act} = (R_{et})_{modelled}$ x ET_{ref}). Similarly, the transpiration (T) was calculated using the values of nondimensionalised sap flow (R_f) and the estimated reference ET (i, e. $T = (R_f)_{modelled}$ x ET_{ref}). The reference ET (ET_{ref}) was estimated on the basis of weather data (Appendix M) of nearby weather station of those areas collected from the Australian Bureau of Meteorology. The estimation was demonstrated for an arbitrary 3 hour irrigation event in the middle of a typical cloud free (sunny) summer day (15 January 2009; DOY 15) for low angle sprinkler nozzles under nonadvective and advective irrigation conditions. The depth of evaporation was calculated through calculating the area under predicted actual ET and transpiration (T) curves using Simpson's rule (Basak 2008).

Table 6.1: Details of the weather station of the selected areas

Station	State	Latitude	Longitude	Altitude (m)
Emerald Airport	Queensland	23.95^{O} S	148.18^{O} E	189.4
St. George Airport	Queensland	28.049^{O} S	148.59^{O} E	198.5
Bourke Airport	New South Wales	30.04^{O} S	145.95^{O} E	107.3
Griffith Airport	New South Wales	34.25^{O} S	146.05^{O} E	134.0
Trangie Research Station	New South Wales	31.99^{O} S	147.95^{O} E	215.0

The predicted values of actual ET and T for different locations are provided in Figures 6.7 & 6.8. The Figures illustrate that the total evaporation on the given day was lower in the cotton growing areas in Queensland (Figure 6.7) than in New South Wales (Figure 6.8). The figures also illustrate that under advective irrigation conditions the amount was considerably higher in all places (Figure 6.7 & 6.8).

The additional evaporation is slightly higher in St. George than Emerald in Queensland due to the higher average temperature and lower relative humidity at St. George (Table 6.2). Among the cotton growing areas in New South Wales the additional evaporation is higher in Trangie (Figure 6.8e & f) due to slightly higher net radiation (R_n) and significantly higher air temperature on that day (Table 6.4). The similar amount of additional evaporation in Bourke and Hillston (Figure 6.8a, 6.8b, 6.8c & 6.8d) is due to the similar weather (T_a and R_n) conditions (Table 6.2).

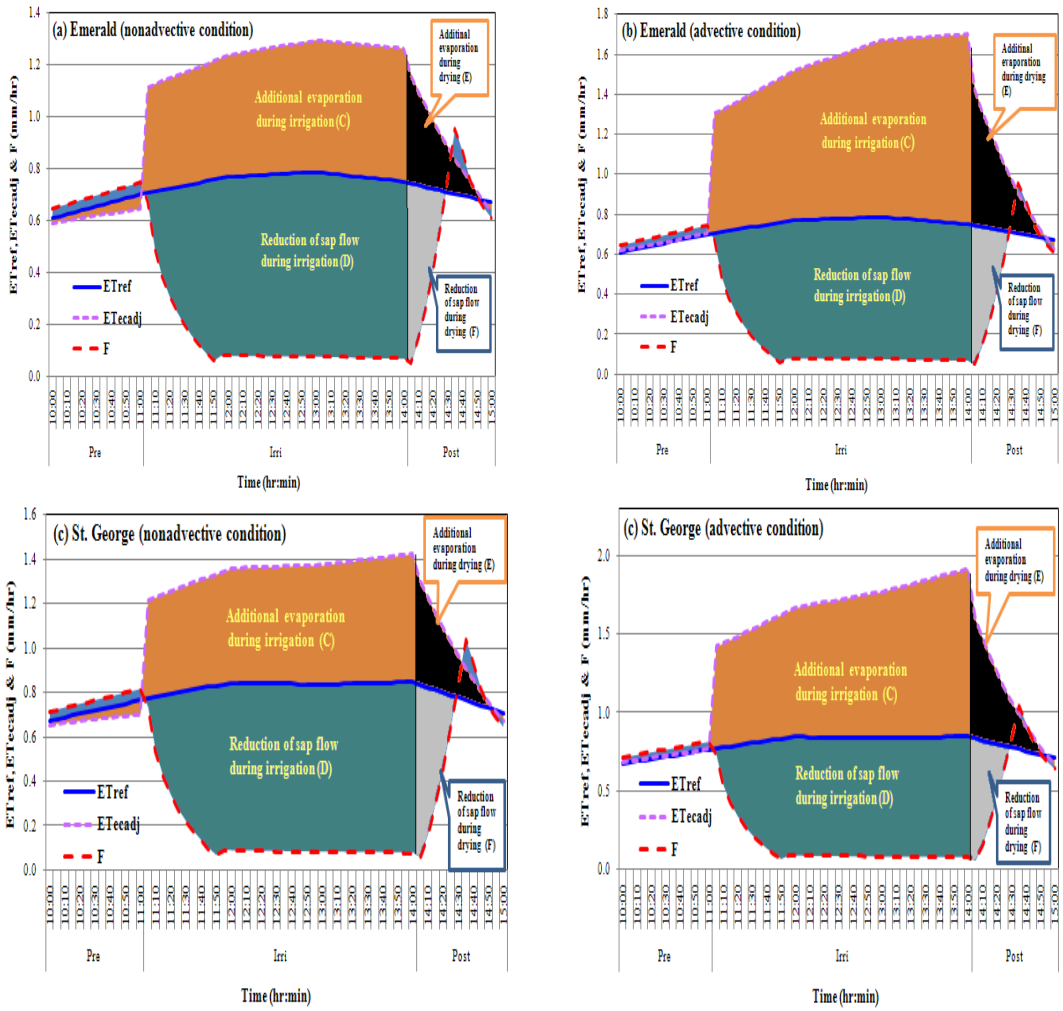

Figure 6.7: Prediction of actual ET and sap flow at different locations of Queensland

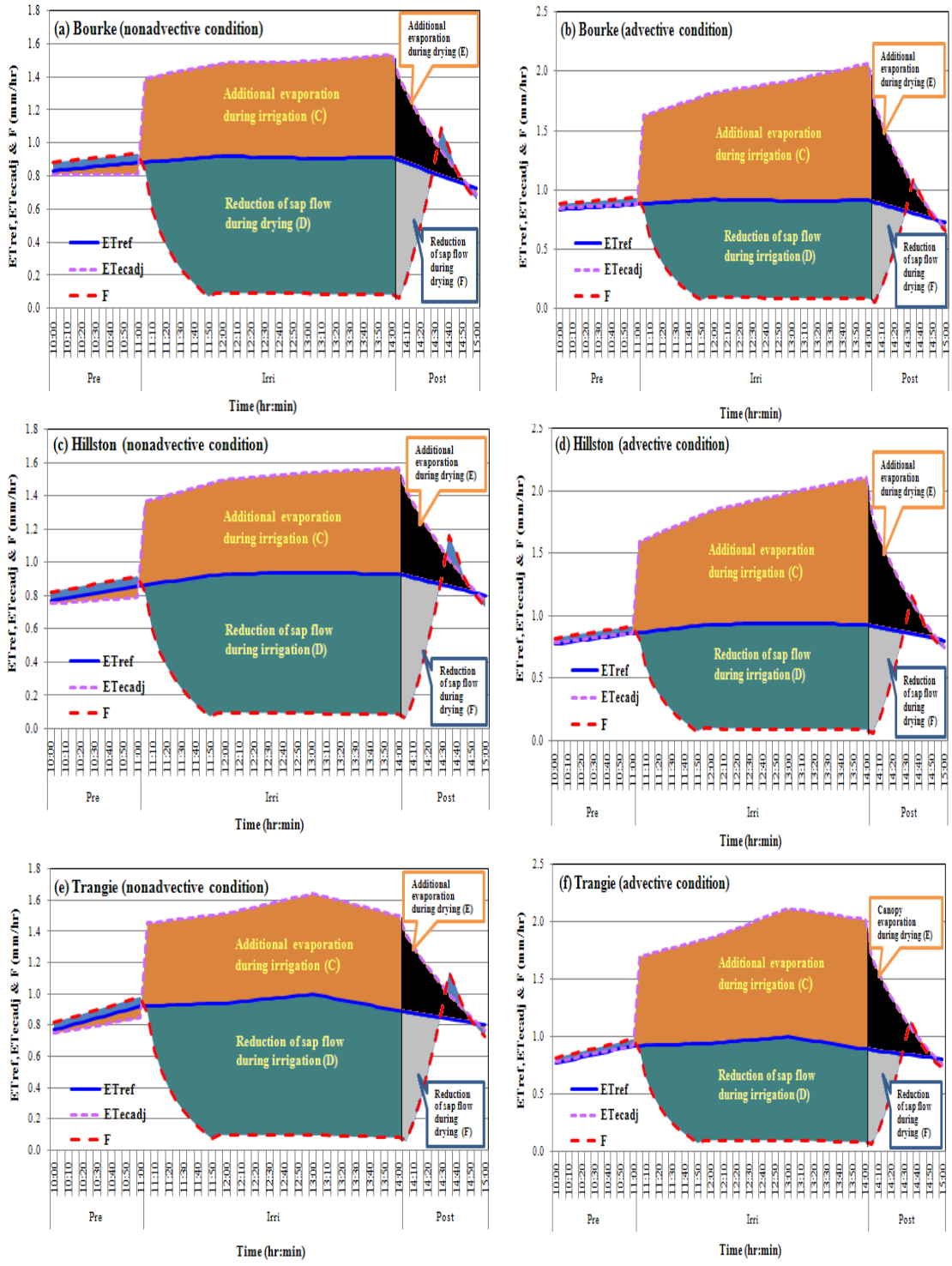

Figure 6.8: Prediction of actual ET and sap flow at different locations of New South Wales

Table 6.2: Day time (8:00 AM – 17:00 PM) average value of weather variables on 15 January 2009

Station	T_a	RH	WS	Calculated R_n
	^{O}C	%	m/s	W/m^2
Emerald Airport	29.1	48	17	561
St. George Airport	32.0	32	16	548
Bourke Airport	29.1	48	17	522
Griffith AirPort	31.1	19	27	523
Trangie Research Station	36.4	20	23	533

6.6 Total canopy evaporation

Total estimated depth of canopy evaporation (includes the canopy evaporation during irrigation (C), reduction of sap flow during irrigation (D), additional evaporation during drying (E), intercepted water during drying (F)) for the three hour irrigation event in each location is presented in Table 6.3. The tabulated values show that total depth of canopy evaporation was comparatively higher in New South Wales (NSW) compared to Queensland (QLD). The depth of canopy evaporation varied from 3.66 mm at Emerald to 4.15 mm at Trangie under nonadvective conditions. Under advective conditions the variation was 4.39 mm to 5.44 mm (Table 6.3).

Assuming an application rate of 10 mm/hr for the three hours, these canopy evaporations represent 11% to 13% of applied water in nonadvective conditions, while it was 14% to 18% in advective conditions (Table 6.3). A similar result (about 13% of applied water applied by overhead impact sprinkler) was predicted by Thompson et al. (1997) while Yonts et al. 2007 measured 15% for corn canopy in USA.

The predicted values show that irrigation under advective conditions can increase the canopy evaporation on average about 30% in comparison with nonadvective

conditions. Li & Yu (2007) mentioned that due to enhanced advection, the percentage of latent and sensible heat flux exchange contribution to the total water loss from the fields through evapotranspiration can exceed up to 50%.

Table 6.3: Total canopy evaporation (sum of part C, D, E & F in figures) for different locations (the value within the bracket represents the percentage of applied water)

State	Cotton growing areas	Total depth of applied water (mm)	Total canopy evaporation		% of additional evaporation due to advection
			Nonadvective condition (mm)	Advective condition (mm)	
QLD	Emerald	30	3.36(11)	4.39(15)	31
	St. George		3.67(11)	4.80(16)	31
NSW	Bourke		4.00(11)	5.23(17)	30
	Hillston		4.00(13)	5.33(18)	33
	Trangie		4.15(14)	5.44(18)	31

6.7 Additional evaporation

Similarly, the total amount of additional evaporation during irrigation (C) was also calculated for each place which is provided in the Table 6.4. Likewise, a higher amount was predicted in New South Wales compared to Queensland. The total amount of additional evaporation varied from 1.55 mm at Emerald to 1.92 mm at Trangie which was 5% to 6% of applied water (30 mm) in nonadvective irrigation. In advective conditions it was estimated as 2.17 mm (7% of applied water) to 2.71 mm (9% of applied water).

The increment of evaporation due to advection was almost same in all places which was about 40% compared to the nonadvective condition (Table 6.4). The effect of advection on additional evaporation (which is mostly canopy evaporation) during

irrigation was relative higher than for total canopy evaporation. The reason in this case might be the lower, sometimes negative, values of sensible heat flux (*H*) during irrigation compared to nonirrigation period (Appendix K).

Table 6.4: Additional evaporation during irrigation (part C in Figures) in different locations (the value within the bracket represents the percentage of applied water)

State	Cotton growing areas	Total depth of applied water (mm)	Additional evaporation		% of additional evaporation due to advection
			Nonadvective condition (mm)	Advective condition (mm)	
QLD	Emerald	30	1.55(5)	2.17(7)	40
	St. George		1.69(6)	2.37(8)	40
NSW	Bourke		1.85(6)	2.59(9)	40
	Hillston		1.88(6)	2.63(9)	40
	Trangie		1.92(6)	2.71(9)	41

6.8 Canopy interception capacity

The calculated depths of intercepted water evaporated during drying (includes additional evaporation during drying and reduction of sap flow during drying) varied slightly depending on location and weather conditions. It also slightly influenced by advection. The values varied from 0.41 mm to 0.51 mm under advective condition, while it was higher in advective condition ranged from 0.50 mm to 0.62 mm (Table 6.5).

The fact that these values vary is a weakness of the drying model because the interception capacity is a feature of the crop canopy and should be constant for a

given canopy condition. If the evaporative demand changes then the rate and time of drying will change accordingly.

Regardless, the average value of interception capacity of the mature cotton canopy was estimated as about 0.5 mm which was about 2% of the applied water. Yonts et al. 2007 also reported the amount of intercepted water lost is about 4% of applied water for low-angle impact sprinklers in mature corn canopy with no wind conditions. The difference of the might be due to the different leaf area index of two crops.

Table 6.5: Canopy interception capacity of cotton (sum of part E & F in figures) calculated for different locations

State	Cotton growing areas	Canopy interception capacity	
		Nonadvective condition (mm)	Advective condition (mm)
QLD	Emerald	0.41	0.50
	St. George	0.46	0.56
NSW	Bourke	0.49	0.59
	Hillston	0.51	0.62
	Trangie	0.49	0.60

6.9 Partition of total additional evaporation

From the above discussions the components of total additional evaporation in sprinkler irrigation can be summarised in Table 6.6. The table indicates that canopy evaporation including droplet evaporation during irrigation is the dominant component (about 80%) in additional evaporation calculated as the ratio of additional evaporation during irrigation to the total depth of additional evaporation (i.e.

(C/(C+E+F))*100 followed by the canopy interception calculated as the ratio of canopy interception capacity to the total depth of additional evaporation (i.e ((E+F)/(C+E+F))*100 which was 20%. The average amount of additional evaporation would be about 6% of applied water under normal conditions and about 8% in advective conditions. It means that irrigators in those places may need to apply 6-8% of additional water.

Table 6.6: Components of total additional water evaporation during irrigation and subsequent (drying) period for low angle types impact sprinkler for 30 mm of applied water

Additional water	Nonadvective condition		Advective condition	
	(mm)	%	(mm)	%
Canopy and droplet evaporation during irrigation	1.80	6	2.50	8
Canopy interception capacity	0.47	2	0.57	2
Evaporation from Soil	negligible	negligible	negligible	negligible
Total additional water	2.27	8%	3.07	10%

6.10 Conclusions

Demonstration to separate the components of total canopy evaporation into its different components shows that this approach successfully enabled separation of the components of total canopy evaporation including beneficial suppressed transpiration as the result of overhead irrigation.

Demonstration of the process to predict the total depth of canopy evaporation including its major components via predicting ET through ECV data under this study also showed that the prediction of additional amount of water requirements in sprinkler irrigation irrespective of time and place is possible using the local climatic data.

The estimation of additional evaporation in different locations illustrated that the amount varied from 1.55 mm (5% of applied water) to 1.92 mm (6%) depending on the local weather conditions. This study reported that the additional amount of evaporation would be comparatively higher in New South Wales than Queensland.

Among the components of additional evaporation, additional evaporation during irrigation (includes canopy and droplet evaporation) was the dominant (about 80%) in total additional evaporation, while the additional evaporation during drying (canopy interception) was about 20%. The soil evaporation was negligible in close canopy condition.

Chapter 7: Conclusions and recommendations

7.1 Summary

The study investigated the additional evaporation/additional depth of water required in sprinkler irrigation as the result of evaporation losses during and following irrigation, adopting the eddy covariance-sap flow methods over a range surfaces from bare soil to a mature cotton crop in a small scale at the USQ agricultural experimental station, Queensland Australia. A detailed methodology was developed under this study provided in Chapter 3. The capability of sap flow gauges (sensors) to measure the sap flow and hence transpiration during wetting (sprinkler irrigation) and drying period was evaluated in a glass house before undertaking the field experiments (Appendix C). Preliminary measurements of total evapotranspiration (ET) were conducted over bare soil and grass to evaluate the capability of the eddy covariance (ECV) technique to measure the total ET during irrigation (Chapter 4). This was followed by a series of experimental trials at different stages of a cotton crop throughout the growing season to estimate the additional evaporation that occurs due mostly to canopy evaporation (Chapter 5). Measurements of sap flow under those experiments also allow estimation of the reduction of transpiration during irrigation (Chapter 5). The data obtained from these extensive irrigation trials were then use to calculate the total depth of additional water required to meet the evaporation losses (canopy and interception) during irrigation and subsequent periods as well as to separate these two components including their contribution to the total losses (Chapter 6). These data were also used to develop regression models to predict the additional evaporation that may occur in sprinkler irrigation events in other parts of cotton growing areas of Australia using local climatic data (Chapter 6).

The methodology developed under this study would allow anyone interested to quantify the depth of additional water requirements due to the additional evaporation that occurs as the direct effect of sprinkler irrigation in any location for their site-specific environmental, climatic and operational conditions. It also allows separation of the major components (canopy and interception) of additional evaporation including the interception capacity of the plants. The results obtained from this study provide important information to farmers regarding the additional amount of water that would be required to meet the evaporation losses. Reported results about the additional evaporation and its components under this study are important information to the designer as well as manufacturer for further improvements of sprinkler irrigation system. The nondimensional technique introduced in this study is an important tool to compare the ET data in irrigation research, minimizing the affect of climatic factors. Estimation of the interception capacity of a canopy using the nondimensional ET from the ECV established drying curve is a new dimension to determine the canopy interception capacity of not only crop canopies but also forest canopies. The regression models,determined on the basis of experimental data, can aid irrigators to get an indication of the additional evaporation which may occur in any other location of not only Australia but also around the world on the basis of local climatic data, and thus help to estimate the depth of additional water requirements.

This chapter contains the conclusions from the research, with respect to the objectives, set out in sections 7.2, 7.3 and 7.4 and section 7.5 contains the recommendation for further research.

7.2 Evaluation of eddy covariance technique to measure the total ET

Measurements of total evapotranspiration (ET) during sprinkler evaporation over bare soil and grass using the eddy covariance technique (Chapter 4) following the methodology (Chapter 3) showed that eddy covariance was able to measure the total ET during irrigation, clearly demonstrating the rate of change of ET according to the irrigating conditions. The measurements over grass provided a significant increment of ET during irrigation as the result of canopy and droplet evaporation in comparison with the nonirrigation period. The decreasing trend of ET post irrigation represents the drying characteristics of wet canopy quite reasonably. In the case of bare soil it was observed that there was no significant change in ET in comparison with reference ET during the irrigation. Similar values of nondimensional ET during and after irrigation illustrates that there was no intercepted water on the bare soil surface. The results suggested that the eddy covariance technique could be used to measure the additional evaporation and its components during irrigation over the crop (Chapter 5) which satisfied the hypothesis (i) in section 1.2 and objective 1 in section 2.11.

This study also suggests that the estimation of additional evaporation using nondimensional technique would be a best technique minimizing the effect of climatic factors in different time. Measurements over the bare soil indicate that droplet evaporation during sprinkler irrigation might be negligible. However, detailed investigations over the broad ranges of surfaces are required to achieve more conclusive results.

7.3 Measurements of total evaporation during sprinkler irrigation

The greatest effect of overhead sprinkler on water losses was the increase in evapotranspiration (ET) as mostly canopy evaporation and reduction in sap flow, which answered the question about the phenomena that occur during in sprinkler irrigation. The successful application of nondimensionalisation of ET and sap flow (*F*) using reference ET provided the idealized curves of total ET and sap flow for each stage, i.e pre-, during and post-irrigation periods. These curves allowed estimation of the total evaporation occuring during irrigation as well as the total reduction of sap flow. The idealized nondimensionalised ET curves permit calculation of the additional evaporation caused by irrigation, including the principal features which are:

- The rate of total evapotranspiration varied significantly according to crop growth stage and climatic factors, especially advection.
- The significant increase of total ET from partial canopy to full canopy indicates that canopy evaporation was higher in full canopy due to the greater area of canopy surface in full crop canopy condition and hence greater interception capacity. These results answered the question about the major component of evaporation losses during sprinkler irritation indicating that canopy evaporation would be the dominant component in sprinkler irrigation.
- Significantly higher values of total evapotranspiration were measured during irrigation in advective conditions, which answered the question regarding the advection effect on irrigation showing that advective conditions can increase the additional evaporation substantially on the basis of climatic conditions especially wind speed.
- The decreasing value of nondimensional ET during the post irrigation period represents the evaporation of intercepted water from the canopy which

allowed calculation of the interception capacity of the canopy (Chapter 6) supporting the hypothesis (ii) set out in section 1.2 that total evaporation during sprinkler irrigation can be partitioned into the different components using eddy covariance-sap flow data.

The strong reduction in transpiration during irrigation (indicated by the sap flow) in response to canopy wetting indicates that the bulk of evaporation during irrigation was from the water intercepted by the canopy, which allowed separating the components of additional evaporation in Chapter 6.

Reduction of atmospheric demand through modification of microclimate as the result of canopy and droplet evaporation could be beneficial in irrigated cropping andsupports the hypothesis (ii), that beneficial evapotranspiration can be portioned using eddy covariance-sap flow method.

A smaller amount of additional evaporation caused by spray nozzles compared to impact sprinklers indicates that precision nozzles can minimize the additional evaporation in sprinkler irrigation, although it needs further investigation.

The measurements of total ET illustrate that the amount of additional evaporation mainly depends on crop canopy condition, equipment related factors and climatic factors especially on advection. Therefore, further research needs to be done for a range of variable climatic and operational factors in different crops.

7.4 Implications of experimental results

Measurements of total evaporation using eddy covariance and reduction of transpiration using sap flow in Chapter 5 provided the opportunity to estimate the total depth of canopy evaporation during irrigation and subsequent periods, including

separation of its components in Chapter 6. The data also permitted estimation of the additional evaporation in different places and times.

Successful separation of the components of total canopy evaporation into its different components including additional evaporation during irrigation and canopy interception capacity using the idealized nondimensional ET and sap flow satisfied the hypothesis (ii) set out in section 1.2 and objective 2 in section 2.11. However, the droplet evaporation could not be separated due to the limitations of the instrument under this study which can be studied in future research.

Illustration of the process to predict the additional evaporation in sprinkler irrigation using ECV-sap flow data for different places and times showed that ECV-sap flow data can be used to predict the magnitude of additional evaporation for different regions in various operating and climatic conditions and satisfied the hypothesis (iv) and objective 3.

7.5 Recommendations for future research

This work has been conducted in a small scale within a single irrigated field on a single crop type. It should be noted that the specific results and conclusions might be expected to be impacted by the agronomic and climatic factors as well as the irrigation management practices adopted within the trials. However, this work has identified several areas of research which could be addressed in future studies including:

- Application of the ECV technique in large scale crops under real irrigation (especially mostly used lateral move and centre pivot) system.

- Conducting extensive research using this technique under various operational conditions, especially different types of sprinkler ranging from Low Energy Precision Application (LEPA) to large size impact sprinkler and various climatic conditions.
- Development of a rigorous, accurate technique for the measurement of droplet evaporation.
- Detailed investigation of droplet evaporation for various sprinklers over a range of surfaces and climates.
- Measurements of transpiration were not possible. Future research should focus on this and in particular the relationship between transpiration and sap flow during dynamic conditions such as during sprinkler irrigation.
- Verification of the technique to determine interception capacity of the canopy with other methods.
- Evaluation of predictive models to measure the additional evaporation during irrigation and subsequent periods by conducting experiments in real field conditions.
- Verification of a physical-mathematical model (for example CUPID-DPEVAP) using ECV-sap flow data.
- Application of ECV-sap flow method to measure the additional evaporation during night time sprinkler irrigation.

List of references

Abdel-Aziz, M. H., S.A. Taylor, & Ashcroft., G. L. (1964). Influence of advective energy on transpiration. *Agron. J., 56*, 139-142.

Aboal, J. R., Jimenez, M. S., Morales, D., & Hernandez, J. M. (1999). Rainfall interception in laurel forest in the Canary Islands. *Agricultural and Forest Meteorology, 97*(2), 73-86.

ABS. (2006). *Water account Australia*, 2004-05, ABS Catalogue No. 4610. Australian Bureau of Statistics. Commonwealth of Australia.

ABS. (2010). *Water account Australia*, 2008-09, ABS Catalogue No. 4610. Australian Bureau of Statistics. Commonwealth of Australia.

Abtew, W. (2001). Evaporation estimation for Lake Okeechobee in south Florida. *Journal of irrigation and drainage engineering, 127*(3), 140-147.

Abu-Ghobar, H. M. (1993). Evaporation and drift losses in sprinkler irrigation under hot and dry conditions. *Journal of King Saud University, 5*(2), 153-164.

Allen, R. G., Pereira, L. S., Raes, D., & Smith, M. (1998). *Crop evapotranspiration-Guidelines for computing crop water requirements-FAO Irrigation and drainage paper 56*. Rome: FAO.

Allen, R. G., Walter, I. A., Elliott, R., Mecham, B., Jensen, M. E., Itenfisu, D., et al. (2000). *Issues,requirements and challenges in selecting and specifying a standardized ET equation.* Proc., 4th National Irrigation Symp., Am. Soc. Agric. Engrs. (ASAE), St. Joseph, MI, USA.

Amatya, D., Skaggs, R., & Gregory, J. (1995). Comparison of methods for estimating REF-ET. *Journal of irrigation and drainage engineering, 121*(6), 427-435.

Anderson, D. E. (1983). *Turbulent exchange of carbon dioxide water vapour heat and nmomentum over crop surface,* (Doctoral dissertation), University of Nebraska, Lincoln.

Assouline, S., & Mahrer, Y. (1993). Evaporation from Lake Kinneret: 1. Eddy correlation system measurements and energy budget estimates. *Water Resources Research, 29*(4), 901-910.

Aubinet, M., Grelle, A., Ibrom, A., Rannik, U., & Moncrieff, J. (1999). Estimates of the annual net carbon and water exchange of forests: The EUROFLUX methodology. *Adv. Ecol. Res, 30*, 113–175.

Baker, J., & Bavel, C. H. M. (1987). Measurement of mass flow of water in the stems of herbaceous plants. *Plant, Cell & Environment, 10*(9), 777-782.

Baladocchi, D. D. (2002). *Assessing the eddy covariance technique for evaluating the carbon balance of ecosystem*. Berkeley Ecosystem Science Division, Department of Environmental Science, Policy and Management, University of California.

Baldocchi, D. D. (1997). Flux footprints within and over forest canopies. *Boundary-Layer Meteorology, 85*(2), 273-292.

Baldocchi, D. D. (2003). Assessing the eddy covariance technique for evaluating carbon dioxide exchange rates of ecosystems: past, present and future. *Global Change Biology, 9*(4), 479-492.

Baldocchi, D. D., Falge, E., Gu, L., Olson, R., Hollinger, D., Running, S., et al. (2001). FLUXNET: A new tool to study the temporal and spatial variability of ecosystem-scale carbon dioxide, water vapor, and energy flux densities. *Bulletin of the American Meteorological Society, 82*(11).

Baldocchi, D. D., Hincks, B. B., & Meyers, T. P. (1988). Measuring biosphere-atmosphere exchanges of biologically related gases with micrometeorological methods. *Ecology*, 1331-1340.

Baldocchi, D. D., Law, B. E., & Anthoni, P. M. (2000). On measuring and modeling energy fluxes above the floor of a homogeneous and heterogeneous conifer forest. *Agricultural and Forest Meteorology, 102*(2-3), 187-206.

Bariac, T., Jamil-Gonzalez, D., Richard, P., Brisson, N., Keterji, N., Be´thenod, O., et al. (1994). *Evapotranspiration re´elle et bilans isotopiques de l'eau dans le continuum sol-plante-atmosphe`re. Ecosyste`me et changements globaux.* . France.: Dourdan.

Barr, A. G., King, K., Gillespie, T., Hartog, G., & Neumann, H. (1994). A comparison of Bowen ratio and eddy correlation sensible and latent heat flux measurements above deciduous forest. *Boundary-Layer Meteorology, 71*(1), 21-41.

Basak, N. N. (2008). *Surveying and levelling*. New Delhi: Tata McGrow Hill Publishing Company.

Bavi, A., Kashkuli, H., Boromand, S., Naseri, A., & Albaji, M. (2009). Evaporation losses from sprinkler irrigation system under various operating conditions. *Journal of Applied Sciences, 9*(3), 597-600.

Benjamin Cummins (2007), *Biological Science* (3 ed.), Freeman, Scott, p. 215

Blackadar, A. K. (1997). *Turbulence and Diffusion in the Atmosphere*, Springer-Verlag.

Bosveld, F. C., & Bouten, W. (2003). Evaluating a model of evaporation and transpiration with observations in a partially wet Douglas-fir forest. *Boundary-Layer Meteorology, 108*(3), 365-396.

Bowen, I. S. (1926). The ratio of heat losses by conduction and by evaporation from any water surface. *Physical review, 27*(6), 779.

Brakke, T. W., Verma, S. B., & Rosenberg, N. J. (1978). Local and Regional Components of Sensible Heat Advection. *Journal of Applied Meteorology, 17*, 955-963.

Braun, P. & Schimd, J. 1999. Sap flow measurements in grapevines (Vitis vinifera L.) 2. Granier measurements. *Plant and soil,* 215**,** 47-55.

Brewer, C., Smith, W., & Vogelmann, T. (1991). Functional interaction between leaf trichomes, leaf wettability and the optical properties of water droplets. *Plant, Cell & Environment, 14*(9), 955-962.

Brotzge, J. A., & Crawford, K. C. (2003). Examination of the surface energy budget: A comparison of eddy correlation and Bowen ratio measurement systems. *Journal of Hydrometeorology, 4*(2), 160-178.

Buchan, G. (1989). *Soil heat flux and soil surface energy balance: a clarification of concepts.* Paper presented at the Australasian Conf. Heat Mass Transfer, 4th, Univ. of Canterbury, Christchurch, New Zealand.

Burba, G., & Anderson, D. (n.d.). *Introduction to the Eddy Covariance Method.general guidelines and convential workflow.* LI-COR Biosciences.

Burman, R. D., & Pochop, L. (Eds.) (1994). *Evaporation, evapotranspiration and climatic data*. Elsevier Science Ltd. .

Burt, C. M., Clemmens, A. J., Strelkoff, T. S., Solomon, K. H., Bliesner, R. D., Hardy, L. A., et al. (1997). Irrigation performance measures: efficiency and uniformity. *Biological Systems Engineering: Papers and Publications*, 38.

Businger, J. A., & Oncley, S. P. (1990). Flux measurement with conditional sampling. *J. Atmos. Oceanic Tech., 7*, 349-352.

Calder, I. (1979). Do trees use more water than grass. *Water Services, 83*, 11-14.

Calder, K. (1952). *Some recent British work on the problem of diffusion in the lower atmosphere,*. Paper presented at the Proc. U.S. Tech. Conf. Air Poll., New York.

Cava, D., Contini, D., Donateo, A., & Martano, P. (2008). Analysis of short-term closure of the surface energy balance above short vegetation. *Agricultural and Forest Meteorology, 148*(1), 82-93.

Cavero, J., Medina, E., Puig, M., & Martínez-Cob, A. (2009). Sprinkler Irrigation Changes Maize Canopy Microclimate and Crop Water Status, Transpiration, and Temperature. *Agronomy Journal, 101*(4), 855.

Cermak, J., & Kucera, J. (1990). Scaling up transpiration data between trees, stands and watersheds. *Silva Carelica (Finland), 15*.

Chabot, R., Bouarfa, S., Zimmer, D., Chaumont, C., & Moreau, S. (2005). Evaluation of the sap flow determined with a heat balance method to measure the transpiration of a sugarcane canopy. *Agricultural Water Management, 75*(1), 10-24.

Chavez, J. L., Howell, T. A., & Copeland, K. S. (2009). Evaluating eddy covariance cotton ET measurements in an advective environment with large weighing lysimeters. *Irrigation Science, 28*(1), 35-50.

Chavez, J. L., Neale, C. M. U., Hipps, L. E., Prueger, J. H., & Kustas, W. P. (2005). Comparing aircraft-based remotely sensed energy balance fluxes with eddy covariance tower data using heat flux source area functions. *Journal of Hydrometeorology, 6*(6), 923-940.

Chaya, L., & Hills, D. (1991). Droplet size and drift potential from micro-sprayer irrigation emitters. *Transactions of the Asae, 34*(6), 2453-2459.

Chen, Z. (1996). Analysis on agro-meteorological effect on mulberry field under sprinkler irrigation condition. *J. Hangzhou Univ. (Nat. Sci. Div.), , 23*(1), 92-99.

Chiew, F., Kamaladasa, N., Malano, H., & McMahon, T. (1995). Penman-Monteith, FAO-24 reference crop evapotranspiration and class-A pan data in Australia. *Agricultural Water Management, 28*(1), 9-21.

Choisnel, E., de Villele, O., Lacroze, F., & Européenne, C. (1992). *Une approche uniformisée du calcul de l'évapotranspiration potentielle pour l'ensemble des pays de la Communauté Européenne*: Office des publications officielles des communautés européennes.

Christiansen, J. (1942). Irrigation by sprinkling. *California Agricultural Experimental Station Bulletin 670', University of California, Berkeley, California.*

Clark, R. N., & Finley, W. W. (1975). Sprinkler evaporation losses in the Southern Plains. *ASAE Paper No. 75-2573, American Society of Agricultural Engineers, St. Joseph, Mich.*

Copper, D. I., W.E., E., J, A., L, H., J, K., M.Y., L., et al. (2003). Special source-area analysis of three-dimensional moisture field from lidar, eddy covraiance, and a footprint model *Agricultural Forest Meteorology, 114*, 213-234.

Craig, I., & Hancock, N. (2004). *Methods for Assessing Dam Evaporation – An Introductory Paper,* : National Centre for Engineering in Agriculture (NCEA), University of Southern Queensland (USQ), Toowoomba, Australia.

Da Rocha, H. R., Goulden, M. L., Miller, S. D., Menton, M. C., Pinto, L. D. V. O., de Freitas, H. C., et al. (2004). Seasonality of water and heat fluxes over a tropical forest in eastern Amazonia. *Ecological Applications, 14*(4), 22-32.

Dadiao, C., & Wallender, W. (1985). Droplet size distribution and water application with low-pressure sprinklers. *Transactions of the Asae, 28*(2), 511-516.

De Bruin, H., Bink, N., & Kroon, L. (Eds.). (1991). *Fluxes in the surface layer under advective conditions*. New York: Springer Verlag.

De Bruin, H. A. R. D., Hartogensis, O. K., R. G. Allen, & Kramer, J. W. J. L. (2005). Regional Advection Perturbations in an Irrigated Desert (RAPID) experiment. *Theor. Appl. Climatol, 80*, 143–152.

De Wrachien, D., & Lorenzini, G. (2006). Modelling spray flow and waste in sprinkler irrigation practice: An overview. *Actual Tasks on Agricultural Engineering, Proceedings, 34*, 227-250.

Dechmi, F., Playan, E., Cavero, J., Faci, J., & Martínez-Cob, A. (2003). Wind effects on solid set sprinkler irrigation depth and yield of maize (Zea mays). *Irrigation Science, 22*(2), 67-77.

Diaz-Espejo, A., Verhoef, A., & Knight, R. (2005). Illustration of micro-scale advection using grid-pattern mini-lysimeters. *Agricultural and Forest Meteorology, 129*(1-2), 39-52.

Ding, R., Kang, S., Li, F., Zhang, Y., Tong, L., & Sun, Q. (2010). Evaluating eddy covariance method by large-scale weighing lysimeter in a maize field of northwest China. *Agricultural Water Management, 98*(1), 87-95.

Du, Y., Wan Doorenbos, J., & Pruitt, W. O. (1975). Guidelines for predicting crop water requirements. *Irrigation and Drainage Paper (FAO).*

Du, Y., Wang, J., Liu, Z., & Cai, C. (2001). Water distribution and microclimatic effects of sprinkler irrigation on spring wheat field. *Chinese Journal of Applied Ecology, 12, 398-400*.

Dugas, W. (1990). Comparative measurement of stem flow and transpiration in cotton. *Theoretical and Applied Climatology, 42*(4), 215-221.

Dugas, W., Fritschen, L., Gay, L., Held, A., Matthias, A., Reicosky, D., et al. (1991). Bowen ratio, eddy correlation, and portable chamber measurements of sensible and latent heat flux over irrigated spring wheat. *Agricultural and Forest Meteorology, 56*(1-2), 1-20.

Dunin, F. (1991). Extrapolation of 'point'measurements of evaporation: some issues of scale. *Plant Ecology, 91*(1), 39-47.

Edling, R. (1985). Kinetic energy, evaporation and wind drift of droplets from low pressure irrigation nozzles *Transactions of the ASAE, 28*(5), 1543 – 1550.

Ertekin, C., & Yaldiz, O. (2004). Drying of eggplant and selection of a suitable thin layer drying model. *Journal of food engineering, 63*(3), 349-359.

Evett, S., Howell, T., Todd, R., Schneider, A., & Tolk, J. (1998). *Evapotranspiration of irrigated alfalfa in a semi-arid environment, Paper No 982123, An ASAE Meeting Presentation.*

Faci, J., Salvador, R., Playan, E., & Sourell, H. (2001). Comparison of fixed and rotating spray plate sprinklers. *Journal of irrigation and drainage engineering, 127*, 224.

Faci, J. M., & Bercero, A. (1991). Efecto del viento en la uniformidad y en las pe´rdidas por evaporacio´n y arrastre en elriego por aspersio´n. *Inv. Agric. Prod. Prot. Veg, 6*(2), 171–182.

Fairweather, H., Austin, N., & Hope, M. (2003). *Water use efficiency, Land & Water Australia, National Programme for Sustainable Irrigation*.

Fichtner, K., & Schulze, E. D. (1990). Xylem water flow in tropical vines as measured by a steady state heating method. *Oecologia, 82*(3), 355-361.

Finn, D., Lamb, B., Leclerc, M., & Horst, T. (1996). Experimental evaluation of analytical and Lagrangian surface-layer flux footprint models. *Boundary-Layer Meteorology, 80*(3), 283-308.

Finnigan, J., Clement, R., Malhi, Y., Leuning, R., & Cleugh, H. (2003). A re-evaluation of long-term flux measurement techniques part I: averaging and coordinate rotation. *Boundary-Layer Meteorology, 107*(1), 1-48.

Foken, T. (1990). Turbulenter Energieaustausch zwischen Atmosphäre und Unterlage - Methoden, meßtechnische Realisierung sowie ihre Grenzen und Anwendungsmöglichkeiten. *Berichte des Deutschen Wetterdienstes, 180,* 287.

Foken, T. (2008). The energy balance closure problem: an overview. *Ecological Applications, 18*(6), 1351-1367.

Foken, T., & Leclerc, M. (2004). Methods and limitations in validation of footprint models. *Agricultural and Forest Meteorology, 127*(3-4), 223-234.

Foken, T., Skeib, G., & Richter, S. (1991). Dependence of the integral turbulence characteristics on the stability of stratification and their use for Doppler-Sodar measurements. *Z. Meteorol., 41*, 311-315.

Foken, T., & Wichura, B. (1996). Tools for quality assessment of surface-based flux measurements. *Agricultural and Forest Meteorology, 78*(1-2), 83-105.

Foley, J., & Raine, S. (2001). *Centre pivot and lateral move machines in the Australian cotton industry* (NCEA Publication No 1000176), Australia: National Centre for Engineering in Agrculture, University of Southern Queensland.

Foley, J., & Raine, S. (2002). Overhead irrigation in the Australian cotton industry. *The Australian Cottongrower, 23*(1), 40.

Forseth, I. N. (1990). Function of leaf movements. In R.L. Satter, H.L. Gorton & T.C. Vogelman, *The pulvinus: motor organ for leaf movement* (pp. 238-261). Rockville: The American Society of Plant Physiologists.

Froessling, N. (1938). Ueber die verdunstund fallender tropfen. *Gerlands, Beitr, Geophysics, 52*, 170-190.

Frost, K. (1963). Factors affecting evapotranspiration losses during sprinkling. *Trans. ASAE, 6*(4), 282-283.

Frost, K. R., & Schwalen, H. C. (1955). Sprinkler evaporation losses. *Agricultural Engineering, 36*, 526-528.

Frost, K., & Schwalen, H. (1960). Evapotranspiration during sprinkler irrigation. *Transactions of the Asae, 3*(1), 18-20.

Fuehrer, P., & Friehe, C. (2002). Flux corrections revisited. *Boundary-Layer Meteorology, 102*(3), 415-458.

Gao, Z., Bian, L., & Liu, S. (2005). Flux measurements in the near surface layer over a non-uniform crop surface in China. *Hydrology and Earth System Sciences Discussions, 2*(3), 1067-1085.

Gash, J. (1986). A note on estimating the effect of a limited fetch on micrometeorological evaporation measurements. *Boundary-Layer Meteorology, 35*(4), 409-413.

Gash, J., Valente, F., & David, J. (1999). Estimates and measurements of evaporation from wet, sparse pine forest in Portugal. *Agricultural and Forest Meteorology, 94*(2), 149-158.

Gavilan, P., & Berengena, J. (2007). Accuracy of the Bowen ratio-energy balance method for measuring latent heat flux in a semiarid advective environment. *Irrigation Science, 25*(2), 127-140.

George, T. J. (1957). *Evaporation from irrigation sprinkler sprays as determined by an electrical coductiveity method* (Unpublished M.S. Thesis), University of California, Berkley.

Georing, J. T., Bode, L. E., & Gebhardt, R. M. (1972). Mathematical modelling of spray droplet declaration and evaporation. *Trans. ASAE, 15*(2), 220-225.

Goudriaan, J. (1977). *Crop micrometeorology: a simulation study*, Centre for Agricultural Publishing and Documentation. Wageningen. NL.

Goyne, P., & McIntyre, G. (2003). Stretching water- Queensland's water use efficiency cotton and grains adoption program. *Water Science & Technology, 48*(7), 191-196.

Gu, L., Meyers, T., Pallardy, S. G., Hanson, P. J., Yang, B., Heuer, M., et al. (2007). Influences of biomass heat and biochemical energy storages on the land surface fluxes and radiative temperature. *J. Geophys. Res.,112,* 2007.

Haenel, H. D., & Grünhage, L. (1999). Footprint analysis: a closed analytical solution based on height-dependent profiles of wind speed and eddy viscosity. *Boundary-Layer Meteorology, 93*(3), 395-409.

Ham, J., & Jay, M. (1990). Determination of soil water evaporation and transpiration from energy balance and stem flow measurements. *Agricultural and Forest Meteorology, 52*(3-4), 287-301.

Hancock, N. (2008). ENV4106 Irrigation Science: *Study book (2008)*. Toowoomba, Australia: University of Southern Queensland.

Harbeck, E. (1962). *A practial field techniqu for measuring reserviour evaporation utilizing mass transfer theory* (Paper No 272). USA: US Geological Survey Professional.

Hardy, J. (1947). *Evaporation of drops of liquid (*Reports and Memoranda, No. 2805), Great Britain Aeronautical Research Council.

He K. N., Tian Y., & C., Z. G. (2003). Modeling of the daily transpiration variatonin locust forest by Penman-Monteith equation. *Acta Ecologica Sinica 23*(2), 251-258.

Heilman, J., Brittin, C., & Neale, C. (1989). Fetch requirements for Bowen ratio measurements of latent and sensible heat fluxes. *Agricultural and Forest Meteorology, 44*(3-4), 261-273.

Hermsmeier, L. (1973). Evaporation during sprinkler application in the desert climate, *Unpublished Paper No. 73-216, presented at the Summer Meeting, ASAE*, Lexington KY, 14.

Heusinkveld, B., Jacobs, A., Holtslag, A., & Berkowicz, S. (2004). Surface energy balance closure in an arid region: role of soil heat flux. *Agricultural and Forest Meteorology, 122*(1-2), 21-37.

Hills, D., & Gu, Y. (1989). Sprinkler volume mean droplet diameter as a function of pressure. *Transactions of the ASAE, 32*(2), 471-476.

Horst, T. (2000). On frequency response corrections for eddy covariance flux measurements. *Boundary-Layer Meteorology, 94*(3), 517-520.

Horst, T., & Weil, J. C. (1992). Footprint estimation for scalar flux measurements in the atmospheric surface layer. *Boundary-Layer Meteorology*, *59*(3), 279-296.

Hotes, F. L. (1969). Analysis of sprinkler irrigation losses. *Journal of the Irirgation and Drainage Div. of ASCE, 95*, 218-223.

Inoue, H., & Jayasinghe, S. (1962). On size distribution and evaporation losses from spray droplets emitted by a sprinkler. *Technical Bulletin of Faculty of Agriculture, Kagawa University*, 202-212.

Ishibashi, M., & Terashima, I. (1995). Effects of continuous leaf wetness on photosynthesis: adverse aspects of rainfall. *Plant, Cell & Environment, 18*(4), 431-438.

Itenfisu, D., Elliott, R. L., Allen, R. G., & Walter, I. A. (2003). Comparison of reference evapotranspiration calculations as part of the ASCE standardization effort. *Journal of irrigation and drainage engineering, 129(*6), 440-448.

Jensen, M. E. (1973). *Consumptive use of water and irrigation water requirements* (Manual No. 70), Irrig. Drain. Div., Am. Soc. Civ. Engr.

Jensen, M. E., Burman, R. D., & Allen, R. G. (1990). *Evapotranspiration and irrigation water requirements* (Manual No. 70), American Society of Civil Engineers (ASCE).

Jensen, M. E. E. (1980). *Design and operation of farm irrigation systems,* American Society of Agricultural Engineers, St. Joseph, MI, U.S.A: Michigan.

Kaimal, J. C., & Finnigan, J. J. (Eds.) (1994). *Atmospheric boundary layer flows: their structure and measurement*: USA: Oxford University Press.

Kang, Y., Liu, H. J., Liu, S. P., & Lou, J. (2002). *Effect of sprinkler irrigation on field microclimate,* Proceedings of the 2002 ASAE Annual International Meeting/XVth CIGR World Congress, ASAE Paper Number 022285.

Kang, Y., Wang, Q. G., & Liu, H. J. (2005). Winter wheat canopy interception and its influence factors under sprinkler irrigation. *Agricultural Water Management, 74*(3), 189-199.

Keller, J., & Bliesner, R. D. (Eds.) (1990). *Sprinkle and trickle irrigation*. New York: Van Nostrand Reinhold.

Kincaid, D. (1996). Spraydrop kinetic energy from irrigation sprinklers. *Transactions of the Asae, 39*(3), 847-853.

Kincaid, D., & Longley, T. (1989). A water droplet evaporation and temperature model. *Transaction of the ASAE, 32*(2), 457-463.

Kincaid, D., Nabil, M. & Busch, J. (1986). Spray losses and uniformity with low pressure center pivots. ASAE Paper No. 86-2091. St. Joseph, MI: ASAE, American Society of Agricultural Engineers.

Kincaid, D., Solomon, K., & Oliphant, J. (1996). Drop size distributions for irrigation sprinklers. *Transactions of the Asae, 39*(3), 839-845.

Kljun, N., Kastner-Klein, P., Fedorovich, E., & Rotach, M. (2004). Evaluation of Lagrangian footprint model using data from wind tunnel convective boundary layer. *Agricultural and Forest Meteorology, 127*(3-4), 189-201.

Kljun, N., Kormann, R., Rotach, M., & Meixer, F. (2003). Comparison of the Langrangian footprint model LPDM-B with an analytical footprint model. *Boundary-Layer Meteorol, 106*(2), 349-355.

Kohl, K., Kohl, R., & De Boer, D. (1987). Measurement of low pressure sprinkler evaporation loss. *Transactions of the ASAE, 30*, 1071-1074.

Kohl, R., & Wright, J. (1974). Air temperature and vapor pressure changes caused by sprinkler irrigation. *Agronomy Journal, 66*, 85-88.

Kohl, R. A., & DeBoer, D. W. (1985). Drop size distributions for a low pressure spray type agricultural sprinkler. *Transactions of the Asae, 27*(6), 1836-1840.

Kormann, R., & Meixner, F. X. (2001). An analytical footprint model for non-neutral stratification. *Boundary-Layer Meteorology, 99*(2), 207-224.

Kostner, B., Granier, A., & Cermak, J. (1998). Sapflow measurements in forest stands: methods and uncertainties. *Ann Sci. For., 55*, 13-27

Kovoor, G. M., & Nandagiri, L. (2007). Developing Regression Models for Predicting Pan Evaporation from Climatic Data—A Comparison of Multiple Least-Squares, Principal Components, and Partial Least-Squares Approaches. *Journal of irrigation and drainage engineering, 133*(5), 444-454.

Kraus, J. (1966). Application efficiency of sprinkler irrigation and its effects on microclimate. *Transactions of the Asae, 9*(5), 642-645.

Kumagai, T., Saitoh, T. M., Sato, Y., Takahashi, H., Manfroi, O. J., Morooka, T., et al. (2005). Annual water balance and seasonality of evapotranspiration in a

Bornean tropical rainforest. *Agricultural and Forest Meteorology, 128*(1-2), 81-92.

Kume, T., Kuraji, K., Yoshifuji, N., Morooka, T., Sawano, S., Chong, L., et al. (2006). Estimation of canopy drying time after rainfall using sap flow measurements in an emergent tree in a lowland mixed dipterocarp forest in Sarawak, Malaysia. *Hydrological processes, 20*(3), 565-578.

Kurbanmuradov, O., Rannik, U., Sabelfeld, K., & Vesala, T. (1999). Direct and adjoint Monte Carlo algorithms for the footprint problem. *Monte Carlo Methods and Applications, 5*(2), 85-112.

Lamm, F., & Manges, H. (2000). Partitioning of sprinkler irrigation water by a corn canopy. *Trans. ASAE, 43*(4), 909-918.

Langmuir, I. (1918). The evaporation of small spheres. *Physical review, 12*(5), 368.

Leclerc, M., Meskhidze, N., & Finn, D. (2003b). Comparison between measured tracer fluxes and footprint model predictions over a homogeneous canopy of intermediate roughness. *Agricultural and Forest Meteorology, 117*(3-4), 145-158.

Leclerc, M., & Thurtell, G. (1990). Footprint prediction of scalar fluxes using a Markovian analysis. *Boundary-Layer Meteorology, 52*(3), 247-258.

Leclerc, M. Y., Shen, S., & Lamb, B. (1997). Observations and large-eddy simulation modeling of footprints in the lower convective boundary layer. *Journal of Geophysical Research, 102*(D8), 9323-9334.

Lee, X., Black, T. A., den Hartog, G., Neumann, H. H., Nesic, Z., & Olejnik, J. (1996). Carbon dioxide exchange and nocturnal processes over a mixed deciduous forest. *Agricultural and Forest Meteorology, 81*(1-2), 13-29.

Lee, X., Massman, W., & Law, B. E. (Ed.) (2004). *Handbook of micrometeorology: a guide for surface flux measurement and analysis*. Kluwer Academic Publishers.

Leyton L., Reynolds R. C., & B., T. F. (1967). *Rainfall interception in forest and moorland.* In: Sopper, W.E., Lull, H.W. (Eds.), Forest Hydrology (pp 163-179). Oxford: Pergamon Press

Li, J., & Rao, M. (2000). Sprinkler water distributions as affected by winter wheat canopy. *Irrigation Science, 20*(1), 29-35.

Li, L., & Yu, Q. (2007). Quantifying the effects of advection on canopy energy budgets and water use efficiency in an irrigated wheat field in the North China Plain. *Agricultural Water Management, 89*(1-2), 116-122.

Li, S., Kang, S., Zhang, L., Li, F., Zhu, Z., & Zhang, B. (2008). A comparison of three methods for determining vineyard evapotranspiration in the arid desert regions of northwest China. *Hydrological processes, 22*(23), 4554-4564.

Liebethal, C., & Foken, T. (2003). On the significance of the Webb correction to fluxes. *Boundary-Layer Meteorology, 109*(1), 99-106.

Liu, H. J., & Kang, Y. (2006). Effect of sprinkler irrigation on microclimate in the winter wheat field in the North China Plain. *Agricultural Water Management, 84*(1-2), 3-19.

Leuning, R. (2007). The correct form of the Webb, Pearman and Leuning equation for eddy fluxes of trace gases in steady and non-steady state, horizontally homogeneous flows. *Boundary-Layer Meteorology, 123*(2), 263-267.

Lorenzini, G. (2002). Air temperature effect on spray evaporation in sprinkler irrigation. *Irrigation and Drainage Systems, 51*(4), 301-309.

Lorenzini, G. (2004). Simplified modelling of sprinkler droplet dynamics. *Biosystems Engineering, 87*(1), 1-11.

Lorenzini, G., & De Wrachien, D. (2005). Performance assessment of sprinkler irrigation systems: a new indicator for spray evaporation losses. *Irrigation and Drainage, 54*(3), 295-305.

Lorenzini, G., & De Wrachien, D. (2005). Spray evaporation losses in sprinkler irrigation systems: A new performance indicator. *Actual Tasks on Agricultural Engineering, 33*, 199-213.

Mahrt, L. (1998). Flux sampling errors for aircraft and towers. *Journal of Atmospheric and Oceanic technology, 15*(2), 416-429.

Markkanen, T., Rannik, U., Marcolla, B., Cescatti, A., & Vesala, T. (2003). Footprints and fetches for fluxes over forest canopies with varying structure and density. *Boundary-Layer Meteorology, 106*(3), 437-459.

Marshall, W. R. (1954). *Atomization and spray drying, Chemical Engineering Progress* (Monograph Series 4.2, Vol 5). New York: American Institute of Chemical Engineers.

Martinez-Cob, A., Playan, E., Zapata, N., Cavero, J., Medina, E., & Puig, M. (2008). Contribution of evapotranspiration reduction during sprinkler irrigation to application efficiency. *Journal of irrigation and drainage engineering, 134*(6), 745-757.

Massman, W., & Clement, R. (2004). *Uncertainty in eddy covariance variance flux estimates resulting from spectral attenuation.* In X. Lee, W. Massman, and B. Law (Eds), Handbook of Micrometeorology—A Guide for Surface Flux Measurement and Analysis (pp 67-99): Kluwer Academic Publisher.

Mather, J. (1950). An investigation of evaporation from irrigation sprays. *Agricultural Engineering, 31*(7), 345-348.

Mauder, M., & Foken, T. (2004). *Documentation and instruction manual of the eddy covariance software package TK2*. Work Report University of Bayreuth, Dept. of Micrometeorology, 26, 44.

Mauder, M., & Foken, T. (2006). Impact of post-field data processing on eddy covariance flux estimates and energy balance closure. *Meteorologische Zeitschrift, 15*(6), 597-609.

Mayocchi, C., & Bristow, K. (1995). Soil surface heat flux: some general questions and comments on measurements. *Agricultural and Forest Meteorology*, *75*(1-3), 43-50.

McCaughey, J. (1985). Energy balance storage terms in a mature mixed forest at Petawawa, Ontario—a case study. *Boundary-Layer Meteorology, 31*(1), 89-101.

McLean, R. K., Ranjan, R., & Klassen, G. (2000). Spray evaporation losses from sprinkler irrigation systems. *Canadian Agricultural Engineering*, *42*(1), 1-8.

McMillan, W., & Burgy, R. (1960). Interception loss from grass. *Journal of Geophysical Research*, *65*(8), 2389-2394.

McNaughton, K. (1981). Net interception losses during sprinkler irrigation. *Agricultural Meteorology, 24*, 11-27.

McNaughton, K.G., and T.A. Black. 1973. A study of evapotranspiration from a Douglas fir forest using the energy balance appraoch. *Water Resourc. Res*., *9*(6), 1579-1590.

McNaughton, K. G., & Jarvis, P. G. (1983). *Predicting effects of vegetation changes on transpiration and evaporation* (Vol. 7). New York: Academic Press.

Meyers, T., & Hollinger, S. (2004). An assessment of storage terms in the surface energy balance of maize and soybean. *Agricultural and Forest Meteorology, 125*(1-2), 105-115.

Monin, A. S., & Obukhov, A. M. (1954). Osnovnye zakonomernosti turbulentnogo peremesivanija v prizemnom sloe atmosfery. *Trudy geofiz. inst. AN SSSR, 24*, 163-187.

Monteith, J. (1965). *Evaporation and environment. The state and movement of water in lliving organsisms.* XIXth Symposiam, Society for Experimentala Biology, Swansea. Cambridge University, Cambridge, England.

Monteith, J. L., & Unsworth, M. H. (Eds.) (1990). *Principles of environmental physics, 2nd edn*. NewYork: Chapman & Hall.

Montero, J. (1999). Análisis de la distribución de agua en sistemas de riego por aspersión estacionario. Desarrollo del Modelo de Simulación de Riego por Aspersión (SIRIAS). *Colección Tesis Doctorales Nº103. Ediciones Universidad de Castilla La Mancha, España*.

Montero, J., Tarjuelo, J., & Carrión, P. (2003). Sprinkler droplet size distribution measured with an optical spectropluviometer. *Irrigation Science, 22*(2), 47-56.

Moore, C. (1986). Frequency response corrections for eddy correlation systems. *Boundary-Layer Meteorology, 37*(1), 17-35.

Morton, F. (1990). Studies in evaporation and their lessons for the environmental sciences. *Canadian Water Resources Journal, 15*(3), 261-286.

Myers, J. M., Baird, C. D., & Choate, R. E. (1970). *Evaporation losses in sprinkler irrigation* (Publication NO 12). University of Florida Resources Resersch Centre.

NCEA, (2005). *Laundry Grey Water Potential Impact on Toowoomba Soils*, NCEA Publication (NCEA 1001420/2), National Centre for Engineering in Agriculture University of Southern Queensland, Toowoomba, Australia.

Norman, J. M. (1982). Simulation of microclimates. In J L. Hatfield & I. J. Thompson (Eds.), *Bio-meteorology in integrated pest management (155-188).* New York: Academic Press.

Norman, J. M., and Campbell, G.S., . (1983). Application of a plant-environmental model to problems in irrigation. *Advance in Irrigatin, 2*, 155-188.

Oke, T. R. (Eds.) (1987). *Boundary layer climates*. Cambridge: University Press.

Oliphant, A., Grimmond, C., Zutter, H., Schmid, H., Su, H., Scott, S., et al. (2004). Heat storage and energy balance fluxes for a temperate deciduous forest. *Agricultural and Forest Meteorology, 126*(3-4), 185-201.

Ortega, J., Tarjeuelo, J., Montero, J., & Juan, J. D. (2000). Discharge efficiency in sprinkler irrigation: analaysis of the evaporation and drift losses in semi-arid areas. . *CIGR J. Agric. Emg. Sci. Res . March 2000., 2*.

Panofsky, H., Tennekes, H., Lenschow, D., & Wyngaard, J. (1977). The characteristics of turbulent velocity components in the surface layer under convective conditions. *Boundary-Layer Meteorology, 11*(3), 355-361.

Paw U, K. T., Baldocchi, D. D., Meyers, T. P., & Wilson, K. B. (2000). Correction of eddy-covariance measurements incorporating both advective effects and density fluxes. *Boundary-Layer Meteorology, 97*(3), 487-511.

Penman, H. L. (1948). Natural evaporation from open water, bare soil and grass, *Proc. Roy. Soc. London, A193, 120-146.*

Perrier, A., & Tuzet, A. (1991). Land surface processes: Description, theoretical approaches, and physical laws underlying their measurements. In T. J. Schmugge & J. C. Andre (Eds.), *Land Surface Evaporation: Measurement and Parameterization (pp. 145-155).* Berlin: Springer-Verlag.

Playan, E., Garrido, S., Faci, J., & Galan, A. (2004). Characterizing pivot sprinklers using an experimental irrigation machine. *Agricultural Water Management, 70*(3), 177-193.

Playan, E., Salvador, R., Faci, J., Zapata, N., Martínez-Cob, A., & Sánchez, I. (2005). Day and night wind drift and evaporation losses in sprinkler solid-sets and moving laterals. *Agricultural Water Management, 76*(3), 139-159.

Priestley, C., & Taylor, R. (1972). On the assessment of surface heat flux and evaporation using large-scale parameters. *Monthly Weather Review, 100*(2), 81-92.

Pruegar, J., Hatfield, J. L., Aase, J. K., & Pikul Jr, J. L. (1997). Bowen-ratio comparisons with lysimeter evapotranspiration. *Agronomy Journal, 89*(5), 730-735.

Raine, S. R., Wallace, S., & Curran, N. (2008). *IPART-An irrigation performance audit and reporting tool for pressurised application systems*. Paper presented at the conference Share the Water, Share the Benefits, Melbourne, Australia.

Rannik, U., Aubinet, M., Kurbanmuradov, O., Sabelfeld, K., Markkanen, T., & Vesala, T. (2000). Footprint analysis for measurements over a heterogeneous forest. *Boundary-Layer Meteorology, 97*(1), 137-166.

Ranz, W., & Marshall, W. (1952). Evaporation from drops. *Chemical Engineering Progress, 48*(3), 141-146, 173-180.

Reicosky, D. (1985). *Advances in evapotranspiration measured using portable field chambers*. Paper presented at the National conference on advances in evapotranspiration, Hyatt Regency Chicago, USA.

Reynolds, O. (1895). On the dynamical theory of incompressible viscous fluids and the determination of the criterion. *Philosophical Transactions of the Royal Society of London. A, 186*, 123-164.

Rosenberry, D., Sturrock, A., & Winter, T. (1993). Evaluation of the energy budget method of determining evaporation at Williams Lake, Minnesota, using alternative instrumentation and study approaches. *Water Resources Research, 29*(8), 2473-2483.

Rutter, A. (1967). An analysis of evaporation from a stand of Scots pine. *Forest Hydrology, 403*, 417.

Rutter, A. (1975). The hydrological cycle in vegetation. *Vegetation and the Atmosphere, 1*, 111-154.

Saadia, R., L. , Huber, & Lacroix, B. (1996). Modification du microclimat d'un couvert de maïs au moyen de l'irrigation par aspersion en vue de la gestion des stress thermiques des organes reproducteurs. *Agronomie, 16*, 465–477.

Sakuratani, T. (1981). A heat balance method for measuring water flux in the stem of intact plants. *Journal of Agricultural Meteorology, 37*(1), 9-17.

Sammis, T., Mexal, J., & Miller, D. (2004). Evapotranspiration of flood-irrigated pecans* 1. *Agricultural Water Management, 69*(3), 179-190.

Samson, R., & Lemeur, R. (2001). Energy balance storage terms and big-leaf evapotranspiration in a mixed deciduous forest. *Annals of Forest Science, 58*(5), 529-541.

Schmid, H. (1994). Source areas for scalars and scalar fluxes. *Boundary-Layer Meteorology, 67*(3), 293-318.

Schmid, H. (1997). Experimental design for flux measurements: matching scales of observations and fluxes. *Agricultural and Forest Meteorology, 87*(2-3), 179-200.

Schmid, H. (2002). Footprint modeling for vegetation atmosphere exchange studies: a review and perspective. *Agricultural and Forest Meteorology, 113*(1-4), 159-183.

Schmid, H. P., & Lloyd, C. R. (1999). Spatial representativeness and the location bias of flux footprints over inhomogeneous areas. *Agricultural and Forest Meteorology, 93*(3), 195-209.

Schmid, H. P. (2002). Footprint modeling for vegetation atmosphere exchange studies: a review and perspective. *Agricultural and Forest Meteorology, 113*(1-4), 159-183.

Schotanus, P., Nieuwstadt, F., & Bruin, H. (1983). Temperature measurement with a sonic anemometer and its application to heat and moisture fluxes. *Boundary-Layer Meteorology, 26*(1), 81-93.

Schuepp, P., Leclerc, M., MacPherson, J., & Desjardins, R. (1990). Footprint prediction of scalar fluxes from analytical solutions of the diffusion equation. *Boundary-Layer Meteorology, 50*(1), 355-373.

Schulze, E. D., ermák, J., Matyssek, M., Penka, M., Zimmermann, R., Vasicek, F., et al. (1985). Canopy transpiration and water fluxes in the xylem of the trunk of Larix and Picea trees—a comparison of xylem flow, porometer and cuvette measurements. *Oecologia, 66*(4), 475-483.

Seginer, I. (1965). Tangential velocity in sprinkler drops. *Transactions of the ASAE, 8*(1), 90-93.

Seginer, I. (1967). Net losses in sprinkler irrigation. *Agricultural Meteorology, 4*(4), 281-291.

Seginer, I., Kantz, D & Nir, D. (1991). The distortion by wind of the distribution patterns of single sprinklers. *Agric. Wat. Manag, 19*, 341-359.

Shi, T., Guan, D., Wang, A., Wu, J., Jin, C., & Han, S. (2008). Comparison of three models to estimate evapotranspiration for a temperate mixed forest. *Hydrological processes, 22*(17), 3431-3443.

Shuttleworth, W., Gash, J., Lloyd, C., Moore, C., Roberts, J., Marques Filho, A., et al. (1984). Eddy correlation measurements of energy partition for Amazonian forest. *Quarterly Journal of the Royal Meteorological Society, 110*(466), 1143-1162.

Singh, B., & Szeicz, G. (1979). The effect of intercepted rainfall on the water balance of a hardwood forest. *Water Resources Research, 15*(1), 131-138.

Singh, V., & Xu, C. (1997). Evaluation and generalization of 13 mass-transfer equations for determining free water evaporation. *Hydrological processes, 11*(3), 311-323.

Singh, V. P. (Eds.) (1989). Hydrologic systems: watershed modeling (Vol. 2). Prentice Hall.

Smajstrla, A. G., & Zazueta, F. S. (2003). *Evaporation Loss during Sprinkler Irrigation*. Agricultural and Biological Engineering Department, Institute of Food and Agricultural Sciences, University of Florida, USA.

Smajstrla, A. G., & Hanson, R. (1980). Evaporation effects on sprinkler irrigation efficiencies. *Proc. Soil & Crop Sci. Soc., 39*, 28-33.

Smith, P. (n.d.) *How to evaluate the performance of center pivot and lateral move systems*. Cotton Catchment Communities (CRC).

Smith, R. J., Baillie, C.P., & Gordon, G 2002, 'Performance of travelling gun irrigation machines', Proc Australian Society of Sugar Cane Technologists, 24, 235-240.

Solomon, K. H., Kincaid, D. C., & Bezdek, J. C. (1985). Drop size distributions for irrigation spray nozzles. *Transactions of the Asae, 28*(6), 1966-1974.

Steinberg, S., Van Bavel, C., & McFarland, M. J. (1989). A gauge to measure mass flow rate of sap in stems and trunks of woody plants. *Journal of the American Society for Horticultural Science, 114*(3), 466-472.

Steinberg, S., Van Bavel, C., & McFarland, M. (1990). Improved sap flow gauge for woody and herbaceous plants. *Agron. J, 82*, 851-854.

Steiner, J., Kanemasu, E., & Clark, R. (1983). Spray losses and partitioning of water under a center pivot sprinkler system. *Trans. ASAE, 26*(4), 1128-1134.

Sternberg, Y. M. (1967). Analysis of sprinkler irrigation losses. *Journal of the Irrigation and Drainage Division, 93*, 111-124.

Stewart, D. W., & Lemon, E. R. (1969). *The energy budget at the earth's surface: a simulation of net photosynthesis of field corn. Rep. ARS-SWC-407 US Dep.* Agric., Res. Rep. 878 Cornell Univ. Coll. Agric., Res. Dev. Tech. Rep. ECO M 2-68 1-6 US Army.

Stewart, J. (1977). Evaporation from the wet canopy of a pine forest. *Water Resources Research, 13*(6), 915-921.

Sumner, D. (2002). *Evapotranspiration from a cypress and pine forest subjected to natural fires in Volusia County* (Report No 01-4245). Florida: U.S. Geological Survey.

Sun, X. M., Zhu, Z. L., Wen, X. F., Yuan, G. F., & Yu, G. R. (2006). The impact of averaging period on eddy fluxes observed at ChinaFLUX sites. *Agricultural and Forest Meteorology, 137*(3-4), 188-193.

Swinbank, W. (1951). The Measurement of Vertical Transfer of Heat and Water Vapor by Eddies in the Lower Atmosphere. *Journal of Atmospheric Sciences, 8*, 135-145.

Tanaka, K., Tamagawa, I., Ishikawa, H., Ma, Y., & Hu, Z. (2003). Surface energy budget and closure of the eastern Tibetan Plateau during the GAME-Tibet IOP 1998. *Journal of Hydrology, 283*(1-4), 169-183.

Tanner, B. D. (1987). *Use requirements for Bowen ratio and eddy correlation determination of evapotranspiration*. Paper presented at the Specialty Conference of the Irrigation and Drainage Division, Lincoln, USA

Tarjuelo, J. M., Ortega, J. F., Montero, J., & de Juan, J. A. (2000). Modelling evaporation and drift losses in irrigation with medium size impact sprinklers under semi-arid conditions. *Agricultural Water Management, 43*(3), 263-284.

Teklehaimanot, Z., & Jarvis, P. (1991). Direct measurement of evaporation of intercepted water from forest canopies. *Journal of Applied Ecology*, 603-618.

Temesgen, B., Simon Eching, M., Davidoff, B., & Frame, K. (2005). Comparison of some reference evapotranspiration equations for California. *Journal of irrigation and drainage engineering, 131*(1), 73-84.

Testi, L., Villalobos, F., & Orgaz, F. (2004). Evapotranspiration of a young irrigated olive orchard in southern Spain. *Agricultural and Forest Meteorology, 121*(1-2), 1-18.

Thom, A. (1975). Momentum, mass and heat exchange of plant communities. In J., L. Monteith (Eds.), *Vegetation and the Atmosphere (pp. 57-109).* London: Academic Press.

Thompson, A., (1986). *Simulation of sprinkler water droplet evaporation above a plant canopy* (Doctoral dissertation), The University of Nebraska, Lincoln.

Thompson, A., Gilley, J., & Norman, J. (1993a). A sprinkler water droplet evaporation and plant canopy model: I. Model development. *Transactions of the Asae, 36*(3), 735-741.

Thompson, A., Gilley, J., & Norman, J. (1993b). A sprinkler water droplet evaporation and plant canopy model: II. Model application. *Transactions of the ASAE, 36*(3), 743-750.

Thompson, A. L., J.R. Gilley, & Norman, J. M. (1988b). Modeling water losses during sprinkler irrigation. *ASAE Paper No. 88-2130. ASAE, St. Joseph, MI.*

Thompson, A. L., Martin, D. L., Norman, J. M., Tolk, J. A., Howell, T. A., Gilley, J. R., et al. (1997). Testing of a water loss distribution model for moving sprinkler systems. *Transactions of the Asae, 40*(1), 81-88.

Thornthwaite, C. W., & Holzman, B. (1939). The determination of evaporation from land and water surfaces. *Monthly Weather Review, 67*, 4.

Tillman, J. (1972). The Indirect Determination of Stability, Heat and Momentum Fluxes in the Atmospheric Boundary Layer from Simple Scalar Variables During Dry Unstable Conditions. *Journal of Applied Meteorology, 11*, 783-792.

Todd, R. W., Evett, S. R., & Howell, T. A. (2000). The Bowen ratio-energy balance method for estimating latent heat flux of irrigated alfalfa evaluated in a semi-arid, advective environment. *Agricultural and Forest Meteorology, 103*(4), 335-348.

Tolk, J. A. (1992). *Corn aerodynamic and canopy surface resistances and their role in sprinkler irrigation efficiency,* (Doctoral dissertation), Texas Tech University, USA.

Tolk, J. A., Evett, S. R., & Howell, T. A. (2006). Advection Influences on Evapotranspiration of Alfalfa in a Semiarid Climate. *Agron. J.*, *98*, 1646–1654.

Tolk, J. A., Howell, T. A., Steiner, J. L., Krieg, D. R., & Schneider, A. D. (1995). Role of Transpiration Suppression by Evaporation of Intercepted Water in Improving Irrigation Efficiency. *Irrigation Science, 16*(2), 89-95.

Tomo'omi Kumagai, S. A., Kyoichi Otsuki and Yasuhiro Utsumi. (2009). Impact of stem water storage on diurnal estimates of whole-tree transpiration and canopy conductance from sap flow measurements in Japanese cedar and Japanese cypress trees. *Hydrological Processes, 23*, 2335–2344.

Trimmer, W. L. (1987). Sprinkler evaporation loss equation. *Journal of irrigation and drainage engineering, 113*(4), 616-620.

Twine, T. E., Kustas, W., Norman, J., Cook, D., Houser, P., Meyers, T., et al. (2000). Correcting eddy-covariance flux underestimates over a grassland. *Agricultural and Forest Meteorology, 103*(3), 279-300.

Uddin, J., Smith, R., Nigel, H., & Joseph, F. (2011). *Eddy covariance measurements of the total evaporation during sprinkler irrigation-Preliminary results*. Paper presented at the conference Society for Engineering in Agriculture (SEAg), Gold Coast, Australia.

U.S. Geological Survey, 2011, Water science glossary of terms: U.S. Geological Survey, access date June 1, 2011.

Van der Tol, C., Gash, J., Grant, S., McNeil, D., & Robinson, M. (2003). Average wet canopy evaporation for a Sitka spruce forest derived using the eddy correlation-energy balance technique. *Journal of Hydrology, 276*(1-4), 12-19.

Van Dijk, A., Kohsiek, W., & DeBruin, H. A. R. (2003). Oxygen sensitivity of krypton and Lyman-alpha hygrometers Lyman-alpha hygrometers . *Journal of Atmospheric and Oceanic Technology, 20*(143-151).

Verma, S. B., Baldocchi, D. D., Anderson, D. E., Matt, D. R., & Clement, R. J. (1986). Eddy fluxes of CO2, water vapor, and sensible heat over a deciduous forest. *Boundary-Layer Meteorology, 36*(1), 71-91.

Villalobos, F. (1997). Correction of eddy covariance water vapor flux using additional measurements of temperature. *Agricultural and Forest Meteorology, 88*(1-4), 77-83.

Villalobos, F., Testi, L., & Moreno-Perez, M. (2009). Evaporation and canopy conductance of citrus orchards. *Agricultural Water Management, 96*(4), 565-573.

Waggoner, P., Begg, J., & Turner, N. (1969). Evaporation of dew. *Agricultural Meteorology, 6*(3), 227-230.

Walter, I. A., et al. . (2000). *"ASCE's standardized reference evapotranspiration equation.* Proc. 4th National Irrigation Symp., ASAE, St., Joseph, Mich.

Wang, J., Miller, D. R., Sammis, T. W., Gutschick, V. P., Simmons, L. J., & Andales, A. A. (2007). Energy balance measurements and a simple model for estimating pecan water use efficiency. *Agricultural Water Management, 91*(1-3), 92-101.

Wang, Q., Kang, Y., Liu, H., & Liu, S. (2006). Method for Measurement of Canopy Interception under Sprinkler Irrigation. *Journal of irrigation and drainage engineering, 132*, 185.

Wanqin, Y., Kaiyun, W., Kellomäki, S., & Ling, X. (2004). Wet canopy evaporation rate of three stands in Western Sichuan, China. *Journal of Mountain Science, 1*(2), 166-174.

Webb, E., Pearman, G., & Leuning, R. (1980). Correction of flux measurements for density effects due to heat and water vapour transfer. *Quarterly Journal of the Royal Meteorological Society, 106*(447), 85-100.

Wichura, B., & Foken, T. (1995). Anwendung integraler Turbulenzcharakteristiken zur Bestimmung von Energie-und Stoffflüssen in der Bodenschicht der Atmosphäre. *Deutscher Wetterdienst, Geschäftsbereich Forschung und Entwicklung, Arbeitsergebnisse, Nr.29, 54S.*

Wilczak, J. M., Oncley, S. P., & Stage, S. A. (2001). Sonic anemometer tilt correction algorithms. *Boundary-Layer Meteorology, 99*(1), 127-150.

Williams, D., Cable, W., Hultine, K., Hoedjes, J., Yepez, E., Simonneaux, V., et al. (2004). Evapotranspiration components determined by stable isotope, sap flow and eddy covariance techniques. *Agricultural and Forest Meteorology, 125*(3-4), 241-258.

Williamson, R., & Threadgill, E. (1974). A simulation for the dynamics of evaporation spray droplets. *Transactions of the ASAE, 17*(2), 254-261.

Wilson, K. B., Hanson, P. J., & Baldocchi, D. D. (2000). Factors controlling evaporation and energy partitioning beneath a deciduous forest over an annual cycle. *Agricultural and Forest Meteorology, 102*(2-3), 83-103.

Wilson, K. B., Hanson, P. J., Mulholland, P. J., Baldocchi, D. D., & Wullschleger, S. D. (2001). A comparison of methods for determining forest evapotranspiration and its components: sap-flow, soil water budget, eddy covariance and catchment water balance. *Agricultural and Forest Meteorology, 106*(2), 153-168.

Wilson, K., Goldstein, A., Falge, E., Aubinet, M., Baldocchi, D., Berbigier, P., et al. (2002). Energy balance closure at FLUXNET sites. *Agricultural and Forest Meteorology, 113*(1-4), 223-243.

Wyngaard, J. (1988). Flow-distortion effects on scalar flux measurements in the surface layer: implications for sensor design. *Boundary-Layer Meteorology, 42*(1), 19-26.

Wyngaard, J., Cote, O., & Izumi, Y. (1971). Local free convection, similarity, and the budgets of shear stress and heat flux. *Journal of Atmospheric Sciences, 28*, 1171-1182.

Xiaomin, S., Zhilin, Z., Xinzai, T., Hongbo, S., & Renhua, Z. (2001). *The impact of local advection on the accuracy of surface fluxes based on remote sensing, IEEE, 4*, 23223-2325.

Yang, X., Chen, F., Gong, F., & Song, D. (2000). Physiological and ecological characteristics of winter wheat under sprinkler irrigation condition. *Trans. Chin. Soc. Agric. Eng, 16*(3), 35–37.

Yazar, A. (1980). *Determination of evaporation and drift losses from sprinkler irrigation systems under various operating and climatic conditions* (Doctoral disseration), The University of Nebraska, Lincoln.

Yazar, A. (1984). Evaporation and drift losses from sprinkler irrigation systems under various operating conditions. *Agricultural Water Management, 8*(4), 439-449.

Yonts, C. D., Kranz, W. L., & Martin, D. L. (2007). *Water Loss from Above-Canopy and In-Canopy Sprinklers*. Lincoln: Institute of Agrculture and natural resources, University of Nebraska.

Yu, G. R., Wen, X. F., Sun, X. M., Tanner, B. D., Lee, X., & Chen, J. Y. (2006). Overview of ChinaFLUX and evaluation of its eddy covariance measurement. *Agricultural and Forest Meteorology, 137*(3-4), 125-137.

Appendix A: Eddy covariance footprint analysis

A.1 Introduction

An assessment of the representativeness of eddy covarience (ECV) measurements in any application is important for the reliability and the quality of ECV measurements made. Therefore, ECV usage in differing conditions and ecosystems has created an increasing interest in (and need for) ECV footprint analysis.

In a heterogeneous landscape the ecosystems contributing to the flux may change with wind direction, atmospheric stability, measuring height and surface roughness (Schmid 1997, Rannik et al. 2000). Since the footprint of a turbulent flux measurement defines the ‘‘field of view’’ of the measuring system, its estimation is essential for data interpretation (Schmid 2002). The representativeness is often demonstrated by analyzing the sensor footprint for source area (Gash 1986, Baldocchi 1997, Schmid 2002). Therefore, the footprint analysis of the ECV measurements on some selected days was undertaken and is presented in this appendix.

A.2 Theory of footprint analysis

Gash (1986) proposed the use of an approximate solution given by Calder (1952) for the atmosphere at neutral stability, which gives the concentration ρ at point (x,z) at height z resulting from an infinite crosswind line source located at an upwind

distance *x* and has been demonstrated to be valid over a wide range of heights, zero plane displacement and roughness length:

$$\rho(x,z) = \frac{Q_L}{ku_* x} e^{-Uz/ku_* x} \tag{A.1}$$

where Q_L is the source strength per unit length,

k is the Von Karman constant (0.41),

u_* is the friction velocity (m s^{-1}),

z is the height above the zero plane displacement (m), and

U is the average wind speed between the surface and the measurement height *z* (m s^{-1}),

Schuepp et al. (1990) provided an approximate solution of equation A.1 for the relative contribution to the vertical flux at height *z*, stemming from an infinite crosswind source of strength $Q(x)$ and unit width at an upwind distance *x* expressed by equation:

$$f(x) = \frac{1}{Q_o}\frac{dQ}{dx} = -\frac{U(z-d)}{u_* kx^2} \exp\left(\frac{-U(z-d)}{ku_* x}\right) \tag{A.2}$$

where $f(x)$ is the relative contribution of the land surface area to the major flux,

x is the distance upwind from the point of measurement (m),

Q_0 is the area flux density, and

d is the zero plane displacement.

The relative flux-density designation of $(1/Q_0)(dQ/dx)$ underlines the fact that integration of the right hand side of equation A.2, or summation of (dQ/dx) from *x* = 0 to infinity, is unity, i.e., the total relative flux density at the observation point. Thus the cumulative normalized contribution to the surface flux from upwind locations *CNF(x)* is given by:

$$CNF(x) = \int_0^x f(x) = \int_0^x \frac{U(z-d)}{u_* k x^2} \exp\left(\frac{-U(z-d)}{k u_* x}\right) dx$$

(A.3)

Integration of equation A.3 gives the equation:

$$CNF(x) = \exp\left(\frac{-U(z-d)}{k u_* x}\right) \qquad \text{Gao et al. 2005)} \qquad \text{(A.4)}$$

Assuming a logarithmic profile for horizontal wind speed $u(z)$ with height z, U is then given by Schuepp et al. (1990) as:

$$U = \frac{\int_{d+z_0}^{z} u(z)dz}{\int_{d+z_0}^{z} dz} = \frac{u_* \left[\frac{\ln(z-d)}{z_0} + \frac{z_0}{(z-d)}\right]}{k\left(\frac{1-z_0}{z-d}\right)} \qquad \text{(A.5)}$$

where z_0 is the roughness length (m).

According to Allen et al. (1998), for a wide range of crops the zero plane displacement height (d), and roughness length governing momentum transfer (z_0) can be estimated by:

$$d = 0.66h \qquad \text{(A.6)}$$

$$z_o = 0.1h \qquad \text{(A.7)}$$

where h is the height of the crop.

A.3 Methodology

The representation of the ECV measurements at the centre of the 50 m circle was evaluated by footprint analysis confirming the layout of the small scale experimental

plot of cotton crop (section 3.5). The day time (9.00AM-4.00PM) data on different days (DOY 78, DOY 105 & DOY 120) of year 2010 at different wind speed (low to high) under the preliminary measurements were used to evaluate the footprint. Using the climatic data of those days, footprint analysis of the ECV measurements was performed considering an arbitrary crop height of 1.0 m at 2.0 m measurement height. Equations (A.1 - A.7) were programmed in MATLAB to obtain the numerical values of relative flux footprint, *f(x)* and cumulative normalized footprint, *CNF(x)*. Using these numerical values the footprint of ECV measurement under the irrigated area (50 m circle) was established.

After getting the experimental data under real crop condition, the reliability of measurements were then again verified using the real climatic data on some selected relatively clear (less cloud coverage) days for different stages of crop (DOY 50 at 50% crop canopy conditions, DOY 84 at 75% crop canopy condition and DOY 105 at full canopy condition) as representative of other days.

A.4 Results and discussion

A.4.1 With assumed crop data

According to the footprint analysis, the effective fetch influencing the measurements at the ECV station was found about 70 m towards the upwind distance ranging from low (3 m/s) to high (6 m/s) wind speed (Figure A.1). It was observed from the analysis that data measured at 2.0 m heights were mainly affected by fluxes coming from an upwind area at a distance of about 6 m (Figure A.1, 'Relative footprint') on the selected days using the arbitrary crop height of 1.0 m.

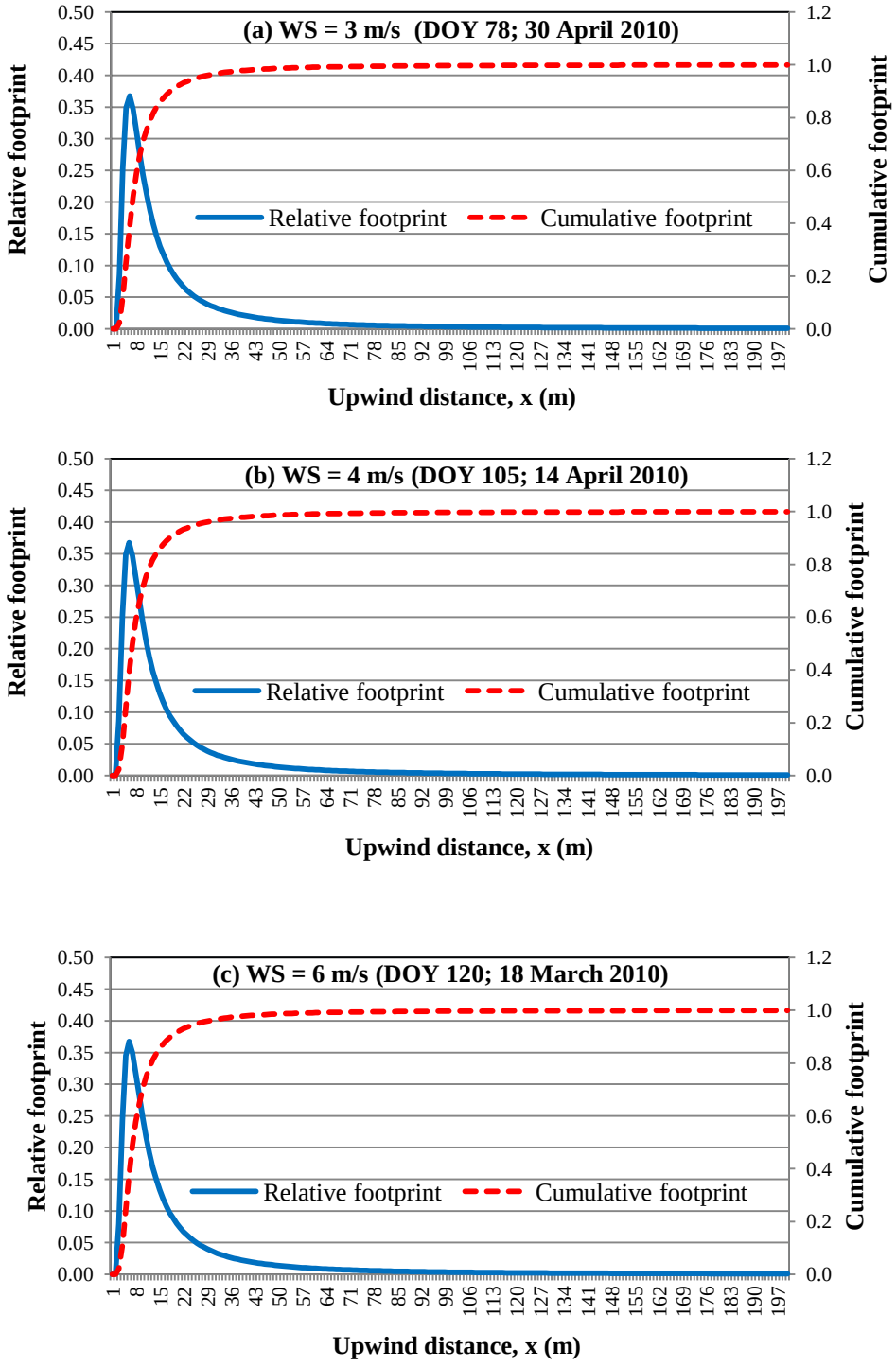

Figure A.1: Footprints of ECV daytime measurements with different wind speed at measurment height 2 m

The Figure A.1 'Cumulative footprint' results show that the major peak flux contribution is well with the 25 m radius. The results indicate that at measurements height 2 m, about 90% flux will come from within the 25 m radius of 50 m crop circle. Furthermore, 100% of each turbulent flux measurement includes contributions from distances extending to roughly 70 m upwind of the ECV station (Figure A.1 'Cumulative footprint').

It follows that for the range of average wind speed from 3 m/s to 6 m/s roughly 10% of the flux measured at 2 m height would come from outside the 50 m diameter crop circle. Therefore, it is expected that measurements of fluxes placing ECV station at the centre of the cropped area in a small scale (50 m circle) will represent the 90% of fluxes, however it may vary according to the crop and weather condition of particular day.

A.4.2 With measured crop data

The footprint analysis in real crop condition at different stages of crop on different days also shows that most of the fluxes coming from the upwind area of about 8-15 m at measurement height of 2.0 and 2.5 m (Figure A.2a-c) depending on the weather and crop canopy conditions.

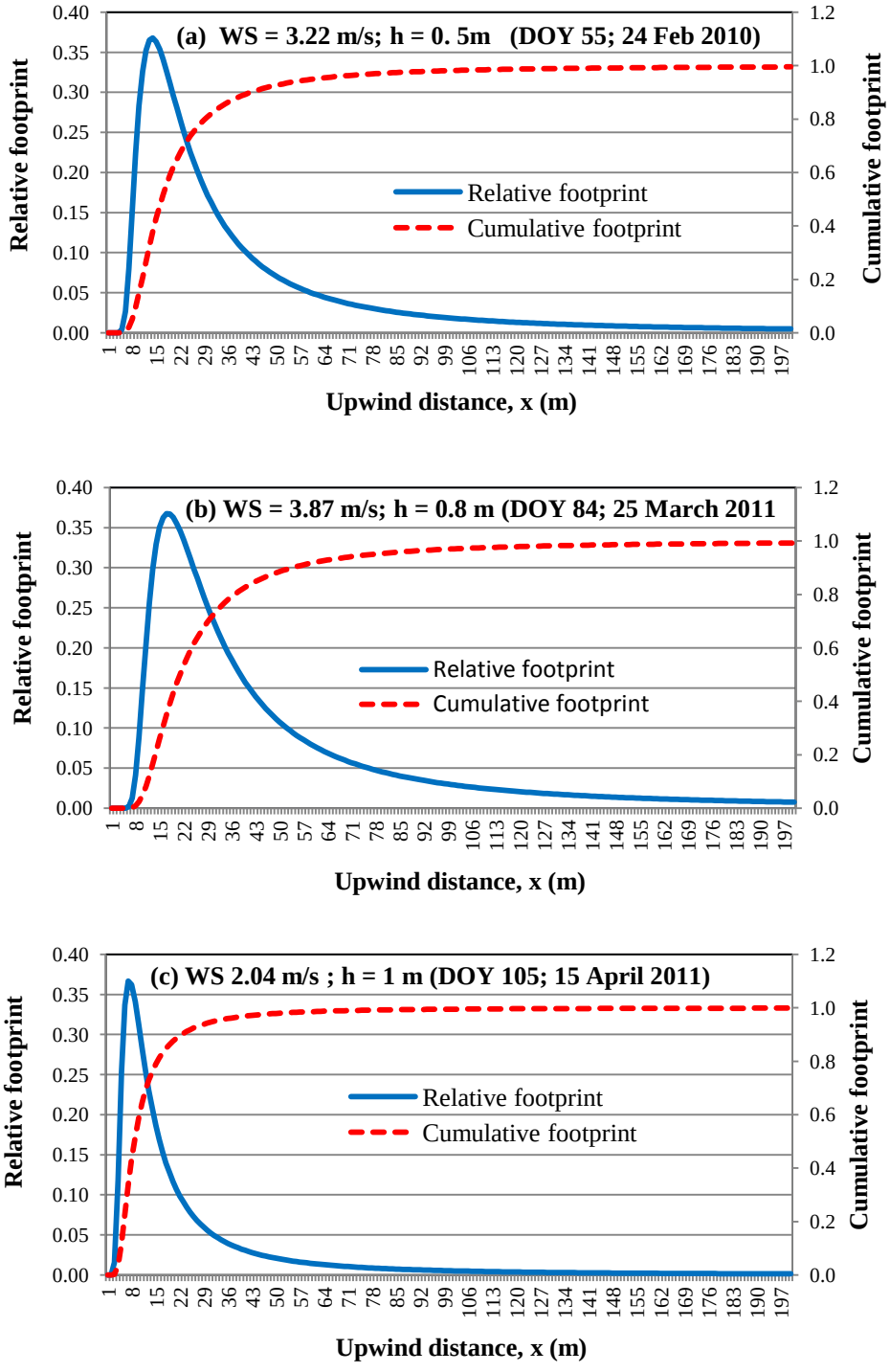

Figure A.2: Representative footprints of ECV measurements for different stages of crop on different days at different heights and wind speeds

Cumulative fluxes also varied with the measurement height as well as crop canopy height. At the initial stage of crop with lower (2 m) measurement height, about 75% fluxes came from the cropped area with moderate wind speed (WS = 3.22 m/s) and canopy height (h = 0.5m) (Figure A.2a). The percentage of cumulative fluxes came from the cropped area varied with wind speed at the same measurement height (2.5 m). On DOY 84, the percentage of flux came from within the radius 25 m was 70% slightly less than other day (DOY 105) might be due to relatively high wind speed (WS = 3.87 m/s) and lower canopy height (h = 0.8 m) (Figure A.2b). However, about 90% of flux came from the radius 25 m at same measurement height due might be to the fact of low (2.05 m/s) wind speed and higher canopy height (h = 1 m) (Figure A.2c). Due to this reason, there was an imbalance of energy fluxes (Appendix B) observed in flux measurements which is recognized in eddy covariance measurements.

A.5 Conclusions

Footprint analysis shows that the ECV station reasonably represented the flux measurement at different stages of crop at different height with some degree of underestimation of fluxes. Although the maximum flux came from the distance about 8-15 m of upwind of ECV station which was well within the cropped area, the cumulative flux represented on an average about 80% of flux of the cropped area. The results suggest that ECV measurements need some adjustment with appropriate method for accurate and quality data.

Appendix B: Data processing and quality assessment

B.1 Introduction

Data processing and assessment of quality of data are important in micrometeorological measurement especially in eddy covariance method. Review of literature (Chapter 2) revealed that ECV method has a tendency to underestimate the latent and sensible heat flux for several reasons (outlined in Chapter 2, section 2.5.2) and hence the measured data should be adjusted using appropriate methods.

In addition, quality assessment of the measured data is important for the reliability and interpretation purposes, so that valid conclusions can be drawn. Comparison of relative magnitude of evapotranspiration changes during irrigation in comparison with pre irrigation periods is another issue to estimate the additional evaporation occurs during irrigation. All the issues are demonstrated using selected data as example in this appendix.

B.2 Data quality assessment methodology

Data quality assessment was conducted on the basis of energy balance closure and the atmospheric stability analysis described in section 3.8 of Chapter 3. Underestimated values of sensible and latent heat fluxes from the ECV measurements were adjusted to achieve energy balance closure by maintaining the Bowen Ratio (BR) following the well-recommended Bowen Ratio method (section

3.9, Chapter 3). To permit comparison, the experimental data of ET were then normalized using the nondimensionalisation technique set out in the Chapter 3, section 3.11.

B. 3 Results and discussion

B.3.1 Data quality assessment

The λE data quality from this system has been verified by studying the energy balance closure of 5 mins averaged flux data, which provides an idea about the underestimation of the ECV measurements. To demonstrate the process, the daytime (8:00 AM – 17:00 PM) data of a relatively clear (minimum cloud coverage) 'irrigated' (DOY 60) and 'nonirrigated' day (DOY 57) was selected as example. The nonirrigated day was selected to observe the effect of irrigation on energy balance closure.

The results are shown in Figures B.1 and B.2 from which it was found that the slope of the regression lines indicated mean energy closure ratio of 0.52 and 0.54 for irrigated day and nonirrigated day, respectively. The slope of the regression lines also indicated that there was an about 48% and 46% imbalance in energy balance on irrigated and nonirrigated day respectively due mostly to the underestimation of sensible and latent heat flux. However, there was no significant difference of energy balance closure observed in irrigated and nonirrigated day. It means that the ECV system underestimated the flux data regardless of irrigation and nonirrigation conditions.

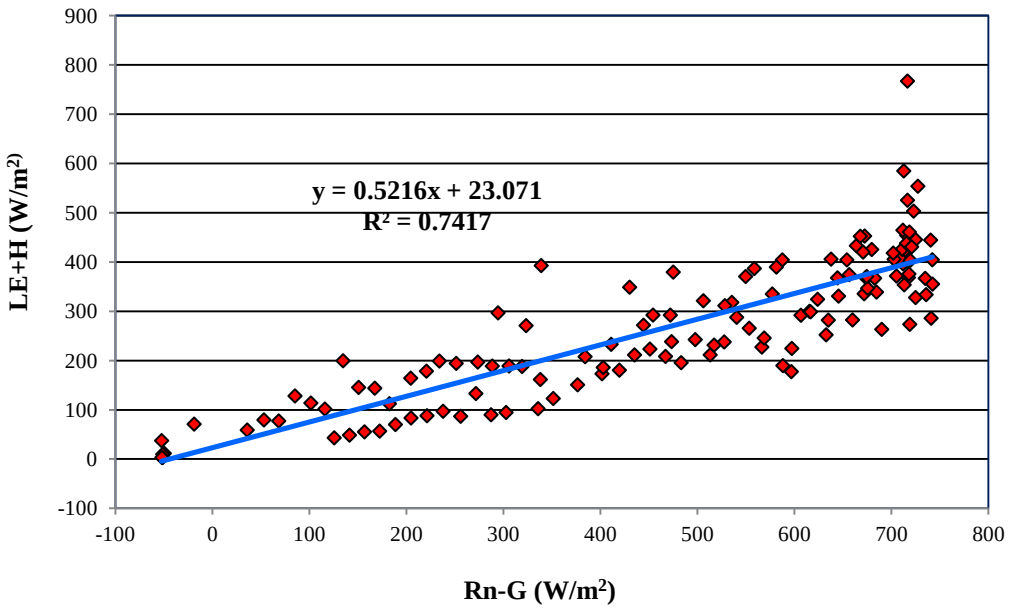

Figure B.1: Energy balance closure on an irrigated day (DOY 60, 1 Mar 2011)

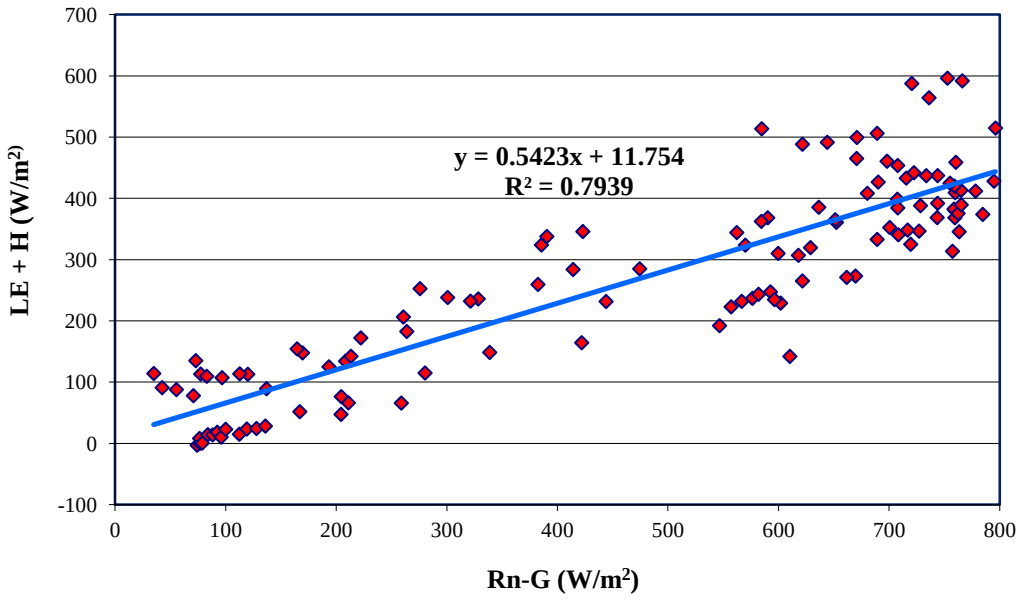

Figure B.2: Energy balance closure on a nonirrigated day (DOY 57, 26 February 2011)

Twine et al. (2000), Wilson et al. (2002) and Foken (2008) reported that the lack of closure of the surface energy budget is a common feature of EC measurements due to

some limitations of the measurements. The known causes of the underestimation are the lack of coincidence of the source areas for the various flux components, sensor timing measurement error (i.e. the correlated variables not being measured simultaneously) due to sensor separation, insufficient fetch, and non-stationarity of measured time series over the averaging time Mahrt (1998), distortion of flow by sonic anemometer (Wyngaard 1998), water vapour fluctuations (Shuttleworth et al. 1998). Foken (2008) reported that the residual of the energy balance closure over agricultural crop is 20-30%. Chavez et al. (2005), in a study involving a network of EC system on rainfed corn and soybean fields, found that the ECV systems EB closure in a average ranged from 57 – 109% being the under estimation of H and λE. Most recently, Chavez et al. (2009) estimated the EB closure over the cotton crop as 35-37% considering the daytime fluxes. However, in our case the lack of closure was somewhat higher, perhaps due to the small experimental area. Hence, as previously noted, the data were adjusted using the Bowen Ratio method.

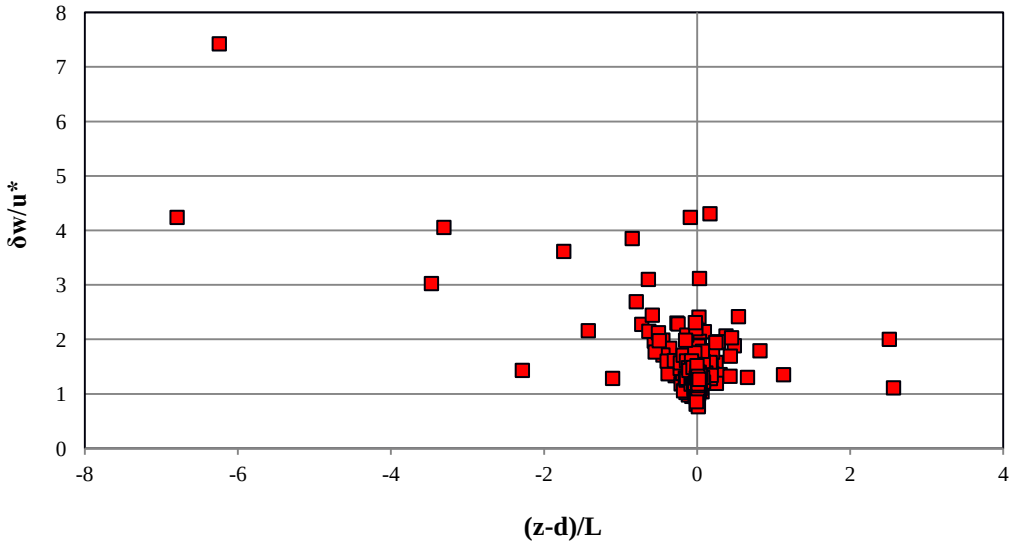

Figure B.3: Measured $\sigma U_z / U_*$ for all the days as a function of $(z-d)/L$ during the period 28 February – 1 March 2011

From the atmospheric stability analysis (Figure B.3) it was found that the most of the data (nondimensional standard deviation of vertical speed as a function of $(z - d)/L$) lie in the stability range $-0.5 \leq (z - d)/L \geq +0$ which indicates that an unstable atmospheric condition prevailed during the measurements.

B.3.2 Evaluation of evapotranspiration (ET) measurements

The comparison of adjusted and unadjusted EC based data on a nonirrigated day (DOY 57) is presented in Figure B.4 as the representative of other day's measurements. The figure shows that before adjustment, ECV system underestimated the evapotranspiration in comparison with reference evapotranspiration (ET_{ref}) which is supported by imbalance of energy balance closure presented in the previous section (Section B.2). Similar underestimation was reported by Chevez et al. (2009), Ding et al. (2010), Dugas et al. (1991), Villalobos (1997) in comparison with a lysimeter. The reasons for this underestimation might be due to the reasons stated in the previous section.

Statistical analysis demonstrated that the EC-based ET without adjustment underestimated the ET by 48.5% compare to ET_{ref}. From the energy balance closure analysis, similar (46%) underestimation was found. Chevaz et al. (2009) found the average approximate underestimation of ET measurements using ECV technique as 30% comparing with lysimeter over the cotton crop. After adjustment the EC-based ET improved significantly on the agreement between adjusted actual ET (ET_{ecadj}) and ET_{ref}. The mean bias error (MBE) reduced from -43.31% to -3.55%, while the RMSE decreased from 48.50% to 7.85% (Table B.1).

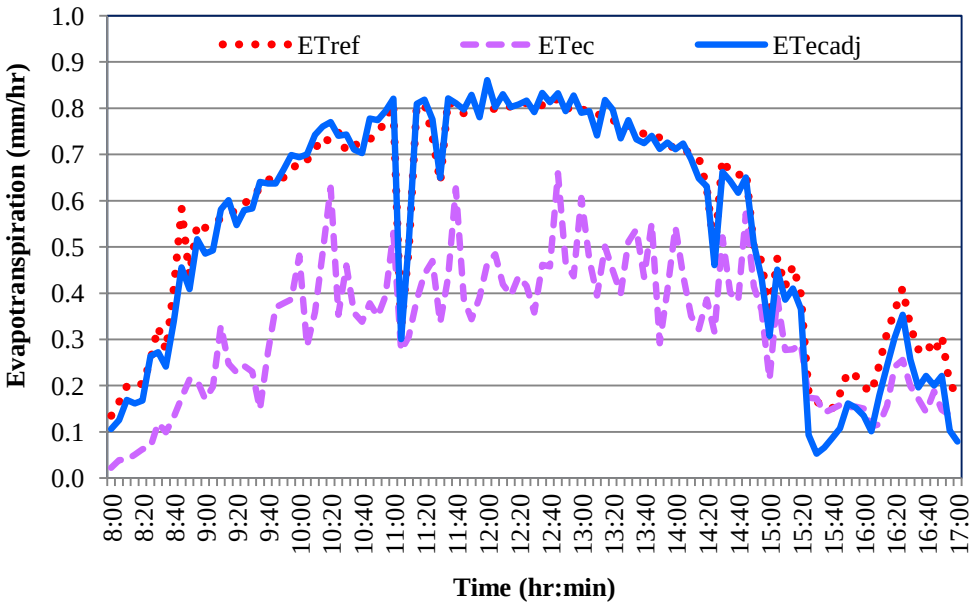

Figure B.4 : Comparison of measured evapotranspiration before adjustment (ET_{ec}) and after adjustment (ET_{ecadj}) with reference ET

Table B.1: Comparison of 5 min averaged EC-based ET and FAO Penman-Monteith based ET

		MBE (mm/hr)	MBE (%)	RMSE (mm/hr)	RMSE (%)	Slope	Intercept (mm/day)	R^2
EC-based ET	Before adjustment	-0.25	43.31	-0.28	48.50	0.58	-0.0006	0.73
	After adjustment	-0.02	3.55	-0.04	7.85	1.13	-0.0940	0.99

The regression analysis shows that before the adjustment the slope and coefficient of determination were 0.57 and 0.73 respectively. After adjustment the correlation line became much closer to the 1:1 line (slope of 1.13 and coefficient of determination 0.99) comparing with FAO Penman-Monteith method (Figure B.5).

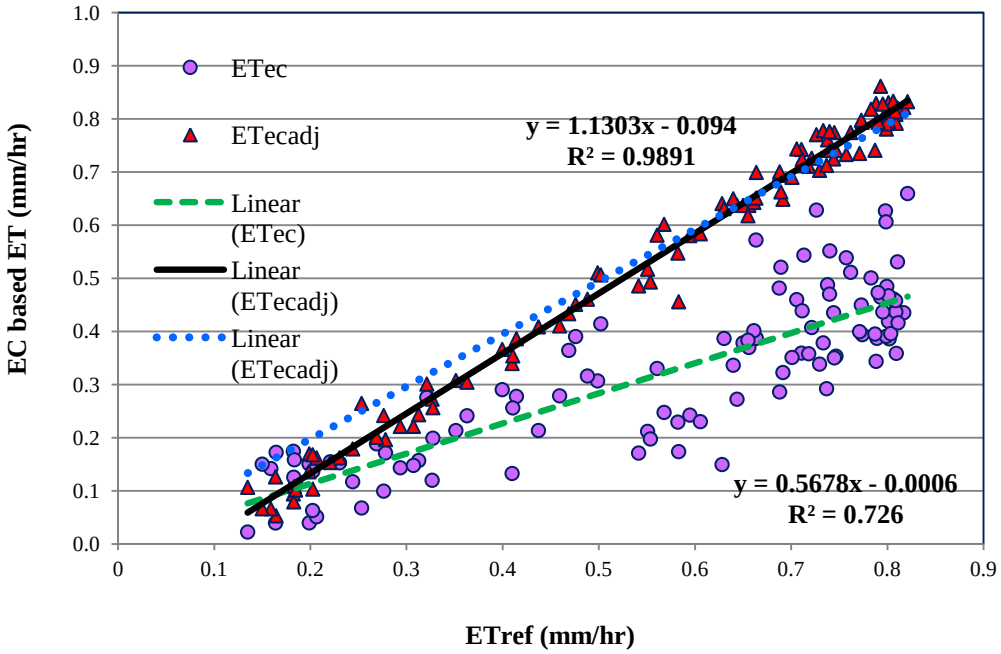

Figure B.5: Comparison of EC-based ET and reference ET before and after adjustment

B.3.3 Effect of nondimensionalisation of ET

From the analysis of the data it was found that, evepotranspiration measured by the ECV system in most of the day had lots of fluctuation over the time due to the fluctuation of radiation (Figure B.6). The effect of fluctuations were still remained after averaging all the irrigation trials in a single day (Figure B.7) which was a real difficulty to compare the data at different conditions like irrigation and non irrigation period.

The example of nondimensionalisation of the data on 19 February 2011 (DOY 50) is presented in Figure B.8. From the figure it is seen that after nondimensionalisation, the curve became smoother indicating clear picture of the rate of change of evapotranspiration at different period than before nondimensionalisation (Figure B.8) although the data were same.

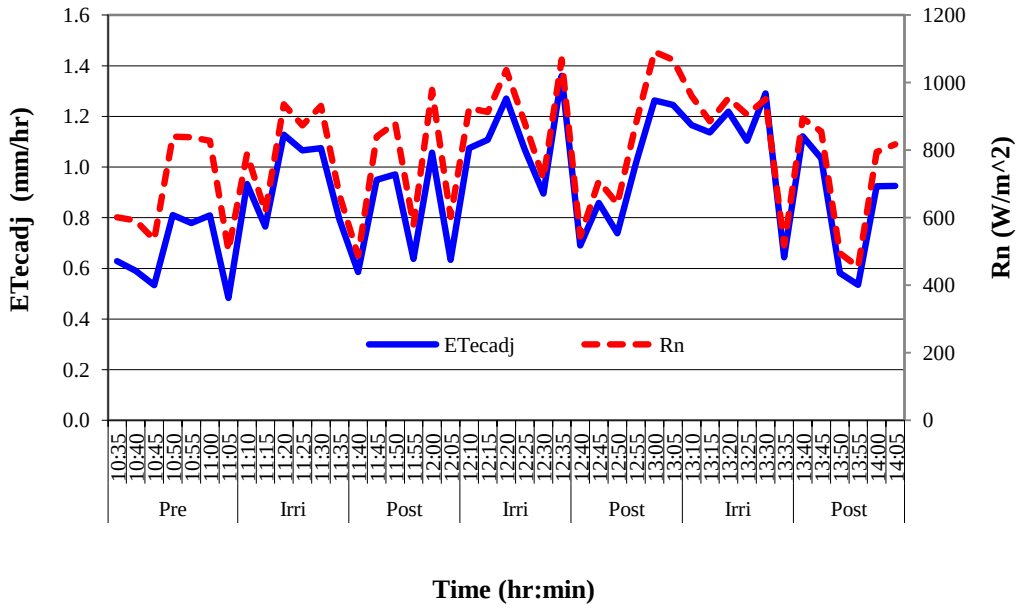

Figure B.6 : Measured net radiation R_n and evapotranspiration using ECV technique ET_{ecadj} on a cloudy day (DOY 50, 19 February 2011)

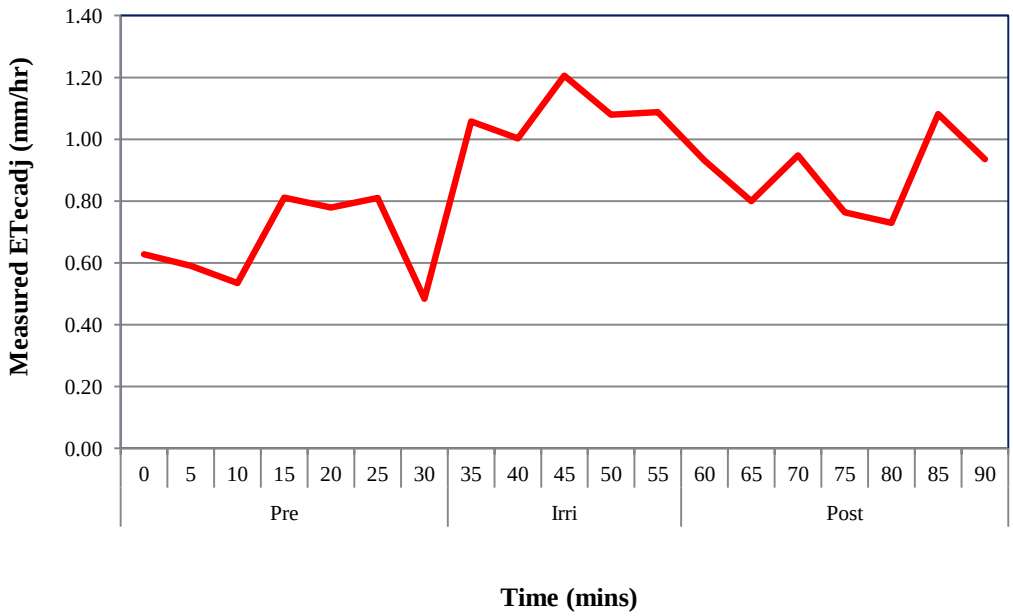

Figure B.7: Average value of evapotranspiration (ET_{ecadj}) for 3 irrigation trials on the same day (DOY 50, 19 February 2011)

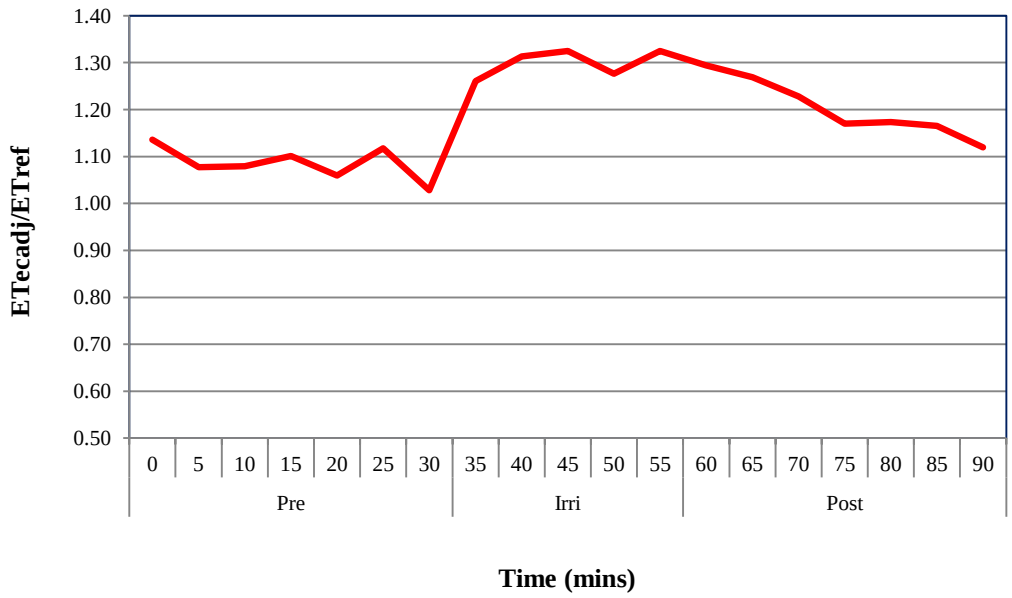

Figure B.8: Nondimensionalised ET at different period on 19 February 2011 (DOY 50)

B.4 Conclusions

Atmospheric stability analysis indicated the unstable atmospheric condition prevailed during the selected period which is the one of the criteria of eddy covariance measurements. About 50% energy imbalance represented the underestimation of latent and sensible heat flux in ECV-based measurements. However, adjustment of fluxes using the same Bowen Ratio significantly improved the values improving the coefficient of determination from 0.73 to 0.99. After adjustment the RMSE also reduced from 0.28 mm/hr (48.5%) to 0.04 mm/hr (7.85%). It means that ECV-based measurement error can significantly be reduced by adjusting the values using Bowen Ratio method.

Nondimensional analysis shows that this technique allows representation and comparison of the trends in the rate of change of ET in different phases of irrigation by normalising out the variation caused by differences in net radiation R_n due to the

change in solar zenith angle and variations in cloud cover, and hence the evaporative demand. This technique also assists in averaging out random fluctuations resulting from sampling error.

Appendix C: Evaluation of sap flow sensors

C.1 Introduction

Partitioning of evapotranspiration (ET) into transpiration, soil evaporation and canopy evaporation is not common practice in sprinkler irrigation due to limitations of the measurement techniques. Limited information is available about the components of ET especially transpiration during irrigation. But this information is important to design an efficient sprinkler irrigation system and precise irrigation scheduling. The accuracy of partitioning depends largely on the ability to independently and accurately measure transpiration (T) of the plants (Ham et al. 1990). Among the available methods, heat balance sap flow measurements have been used for several years to determine the transpiration of canopies due to several advantages. However, before going to field the capability of sap flow sensors to measure the rate of flow during irrigation and subsequent periods should be evaluated. This appendix provides the evaluation of the capability of the sap flow gauges (sensors) to measure the sap flow and hence transpiration during wetting (sprinkler irrigation) and drying before undertaking field experiments.

C.2 Materials and methods

C.2.1 Theory of heat balance method

The method is based on the application of a heat balance to a section of stem (section 2.10.2). The stem is heated electrically and the heat balance is solved for the amount

of heat taken up by the moving sap stream which is then used to calculate the mass flow of sap in the stem.

The xylem sap flow rate (*F*) was calculated from the following (Baker & van Bavel 1987) through the equations 2.30-2.35 in chapter 2;

$$F = \frac{P_{in} - K_{st} A(dt_u + dt_d) - (K_{sh} dt_r)}{C_{p\,x} dT} \quad \text{(C.1)}$$

where P_{in} is the input power (W),

K_{st} is the conductivity of the stem (W m^{-1} K^{-1}),

A is the cross-sectional area of the heated section of the stem (m^2),

dt_u is the temperature difference of two thermocouples above the heater (^{O}C),

dt_d is the temperature difference of two thermocouples below the heater (^{O}C),

K_{sh} is the effective thermal conductance of the sheath of materials surrounding the heater (W m^{-1} K^{-1}),

dt_r is the temperature difference of two thermocouple in radially (^{O}C),

C_p is the specific heat of water (4.186 J g^{-1} ^{o}C), and

$dT = (dt_u + dt_d)/2 * 0.04$ is the temperature difference between upper and lower junctions.

C.2.2 Sap flow and transpiration measurements

The accuracy of the digital dynagage sap flow sensor (SGA10, Dynamax Inc. TX, USA) was tested in a glasshouse of the University of Southern Queensland, Toowoomba, Australia. Pot plants, Tulipwood (*Harpullia pendula*) with trunk diameters ranging from approximately 10 to 13 mm were used as test plants. During the tests, the plants were kept well watered at all times. The gauges were tested in

several ways under normal sap flow conditions. The gauge sensors were protected from corrosion by an electrical insulating compound placed between the gauge interior and the plant stem, and the exterior of the gauge was covered with additional foam insulation, plastic wrap, and aluminium foil for thermal insulation. The gauges were checked weekly to remove moisture build-up and to assess damage to plant stems and/or gauges. The evaluation of the sensors was conducted through valid comparisons of sap flow and the rate of transpiration measured using mini lysimeters. Load cell based mini lysimeters (22 kg capacity) were used to estimate the transpiration rate of plants, measuring the weight loss of the pot plants over time. The plants were placed on the pre calibrated mini lysimeters (Figure C.2) with the soil surface of the pot covered with polythene to prevent soil evaporation. Pot mass was continuously monitored by the load cells whose output was monitored by the data logger (CR3000, Campbell Scientific, Inc, Logan, UT, USA). The signals from the load cells were sampled every second and averaged over 5 minute time intervals. The sap flow was recorded using a Smart data logger (ITC International, Australia) sampled at 1 min (minimum as specification) and averaging over 5 mins time intervals. The 5 mins averaged values were again averaged at 15, 30 and 60 minute time intervals to compare with the transpiration rate at different time interval. As the sensors contained digital interface, the value of applied power (P_{in}) of 100 mW was considered constant and the value of stem conductivity of 0.42 $Wm^{-1}K^{-1}$ (Sakuratani 1981, Baker & van Bavel 1987) was used for woody plant. Micro-meteorological data (RH and air temperature) were measured by temperature and relative humidity probe (model HMP 45C, Campbell Scientific, Inc, Logan, UT, USA) using the same data logger to observe the effects of them on sap flow and transpiration. The canopy temperature of the plants was measured by infrared thermometer (4000L, ITC International Ltd, Australia). To study the effect of wetting of plant on sap flow and transpiration, the plants were wetted (spray irrigation) at different intervals using a small spray bottle.

Figure C.1: Pot plants with installed sap flow gauge placed on mini lysimeter

C.2.3 Calibration of the lysimeter

Before using the mini lysimeter for measuring the weight loss of the potted plants to calculate the transpiration rate, each lysimeter requires calibration in order to convert the voltage signal (mV V^{-1}) data into actual load or weight. The load cell was calibrated using a set of loads including zero within the range of 0 to 10.5 kg. During calibration of the lysimeters, the weight of the desired load was first measured with a pre-calculated electronic platform balance of 32 kg capacity. For a given load, the load cell signal (mV V^{-1}) was measured by data logger (CR 3000, Campbell Scientific Ltd., USA) at 1 min intervals and then averaged the over 5 mins and plotted against the load (g). From the obtained data, the regression of load (g) against signal (mV V^{-1}) for each load cell was drawn with a coefficient of determination, slope and intercept parameters of the regression equations. These parameters were used in the data logger program to estimate the pot weights (g).

C.3 Results and discussion

C.3.1 Diurnal pattern of sap flow and transpiration

The diurnal pattern of sap flow and transpiration on the basis of hourly measurements is presented in Figure C.2. From the Figure it is seen that the sap flow and transpiration followed the same trend over the period with a time lag of transpiration and sap flow. Steinberg et al. (1989) indicated that in woody plants, sap flow and transpiration may differ appreciably due to the water stored in the stem and branches of trees. A possible cause for such an effect mentioned by (Tomo'omi Kumagai 2009) is that, it might be the thermal mass of the sensor itself. A change in heat transfer from the sensor and the surrounding area to the xylem stream will take some time before it affects the inner part of the sensor where the temperature sensor is located. Such a time lag between transpiration and sap flow is often attributed to the capacitance, that is, the water buffering capacity, of the plant (Fichtner & Schulze 1990, Schulze et al. 1985).

However, from the Figure C.2, it is seen that, transpiration is leading the sap flow, but according to the dynamics of sap flow and transpiration, sap flow should lag behind the transpiration. The reason behind this phenomenon could not be identified reasonable. However, one reason might be the use of two different data loggers for the separate measurements of sap flow and transpiration. Another reason might be the local time adjustment error in data loggers.

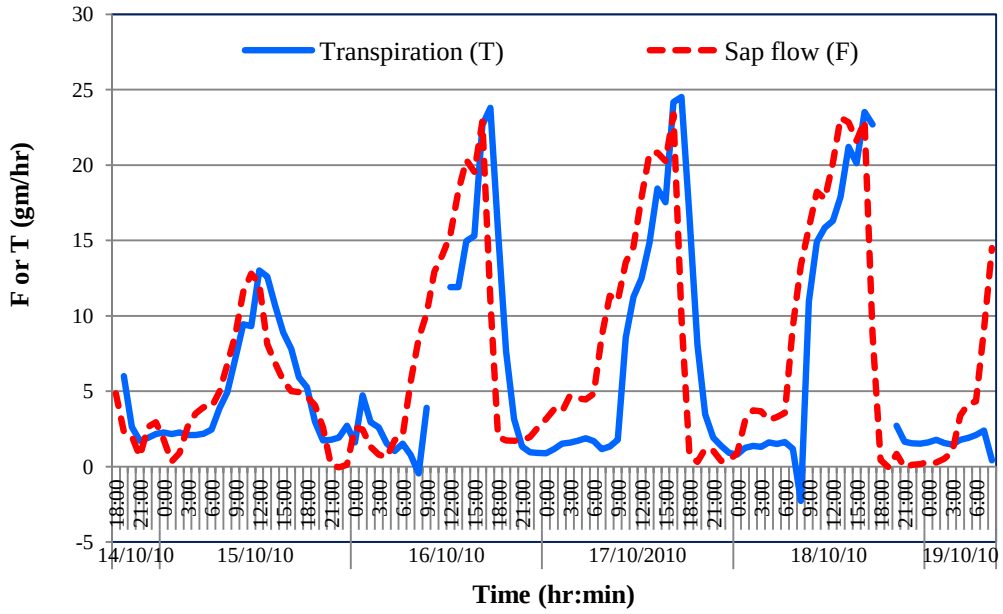

Figure C.2: Diurnal pattern of (hourly values) of sap flow (*F*) and transpiration (*T*)

The commonest pattern of diurnal variation in sap flow and transpiration is a symmetrical curve about midday, with a rapid increase after sunrise and rapid decrease in the late afternoon which mainly depends on meteorological condition of surrounding area (Figure C.2). During the period 15-18 October 2010 (DOY 258-261), transpiration was higher than sap flow followed until mid night and sap flow exceeded the transpiration at the morning until reached at its peak value at the afternoon. The possible reason might be the, the plant extracts more water from the soil to store the water in the stem at its maximum level resulting higher value of transpiration Tomo'omi Kumagai (2009). On the other hand the sap flow exceeded the transpiration at the morning due to the use of stored water decrease at its maximum level by the plants (Tomo'omi Kumagai 2009). They reported that the stem water storage increased at its maximum value at the afternoon and decrease in the morning at its maximum level. They also mentioned that after mid night plant use stored water, can increased the sap flow continued until afternoon (Tomo'omi

Kumagai 2009). Similar trend was observed by Dugas (1990) in comparative measurements of stem flow and transpiration in cotton at the glass house.

Considering day night time, the average value of sap flow and transpiration was found 6.37 gm/hr and 5.72 gm/hr respectively. The root mean square error (RMSE) between two values was estimated 2.73 gm/hr which was 18.29% in terms of normalized root mean square error (NRMSE). From the average value of sap flow and transpiration, it was calculated that the sap flow was overestimated by bout 12%. Several authors (e.g. Dugas, 1990, Ham et. al. 1990 etc.) have also obtained overestimation of sap flow measurements ranged from 10-15% using this type of sensor at different conditions.

C.3.2 Effect of wetting on sap flow and transpiration

The effect of sprinkler irrigation (canopy wetting) on the sap flow was studied in different ways. In the first trial the plant canopy was periodically wetted instantaneously followed by a drying period of one hour. The effect of irrigation on the sap flow is shown in Figure C.3. Figure shows that after wetting the plant through spray irrigation the sap flow decreased smoothly and reached at its minimum value about 20 mins later almost in all cases of irrigation. After that it started to increase and recovered at around 35 mins.

For continous wetting for 30 mins, the sap flow followed the same trend as in the previous trial, but the effect of irrigation on sap flow was longer, remaining at the lowest value for about 30 mins. After that the sap flow started to rise and recovered after about 35 mins (Figure C.4). The sap flow at different heights in the stem followed the same pattern as in Figure C.5, however the amplitude of the variation was greatest at the lower position.

This difference in sap flow at different heights on the plant stem was confirmed by reversing the position of the two gauges on the stem on two consecutive days. Figure C.6 represnts that the upper sensor measured higher sap flow (sensor a on 3 October and sensor u on 5 October 2010) than the lower sensor (sensor u on 3 October and sensor a on 5 October 2010) due to the storage and buffering capacity of the stem. Tomo'omi Kumagai, (2009) found a similar trend for tree plants.

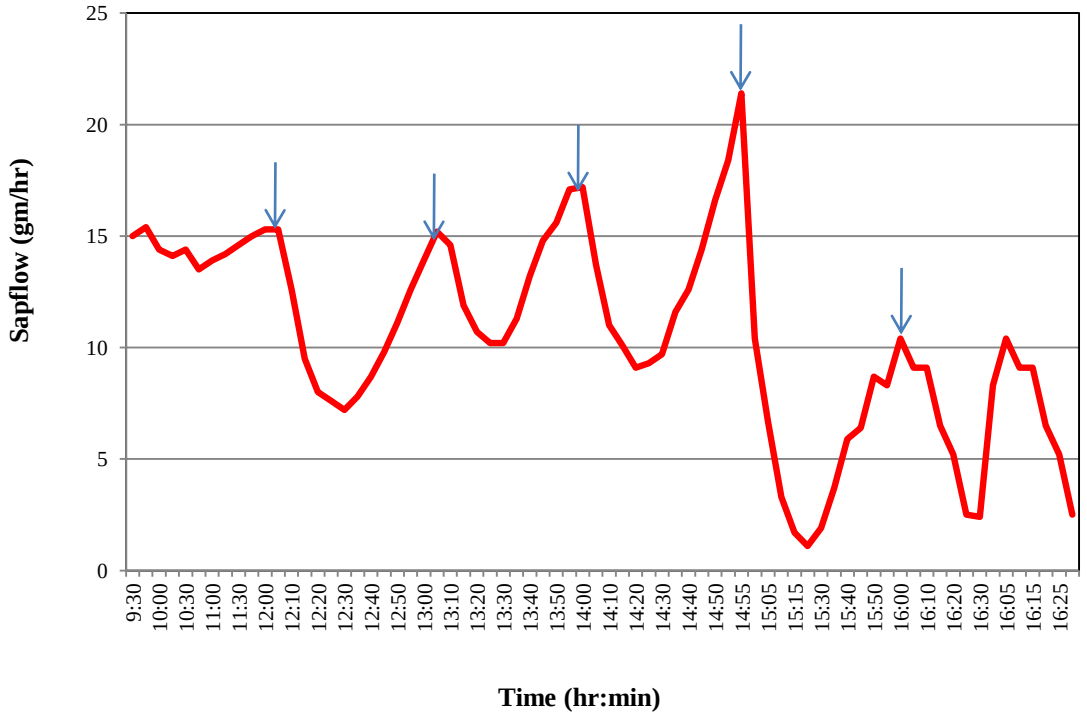

Figure C.3: Effect of irrigation on sap flow on 15 September 2010 (DOY 258)
indictaes the wetting time of the plant)

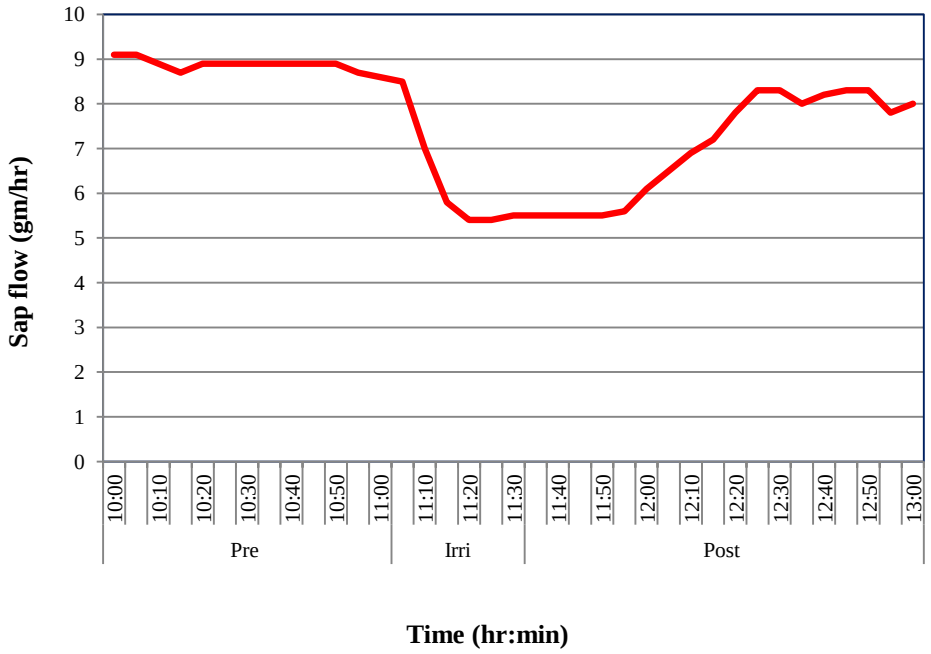

Figure C.4: Effect of irrigation on sap flow on 17 September 2010 (DOY 260) for 30 mins irrigation

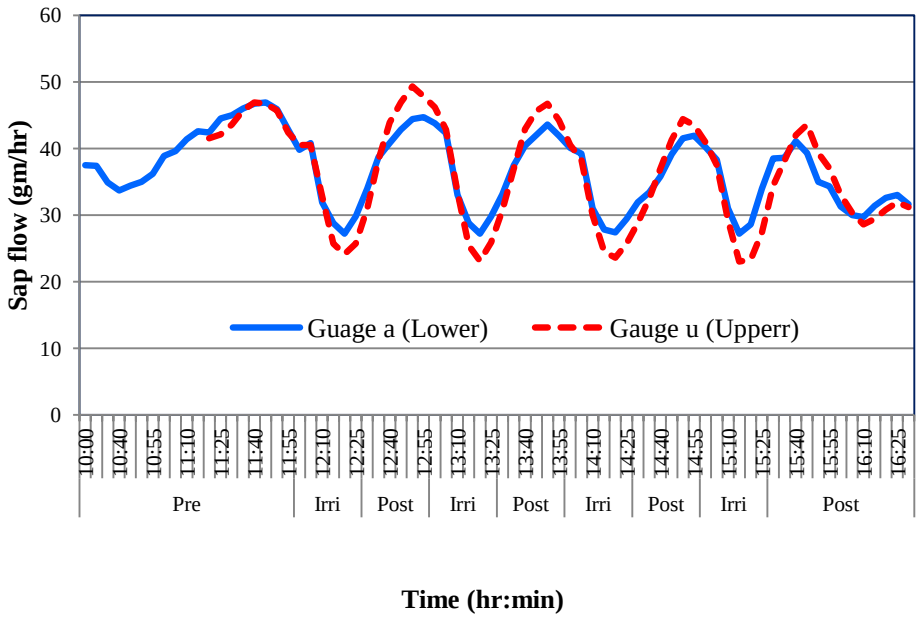

Figure C.5: The response of sap flow due to irrigation at different heights of plant on 27 September 2010 (DOY 270)

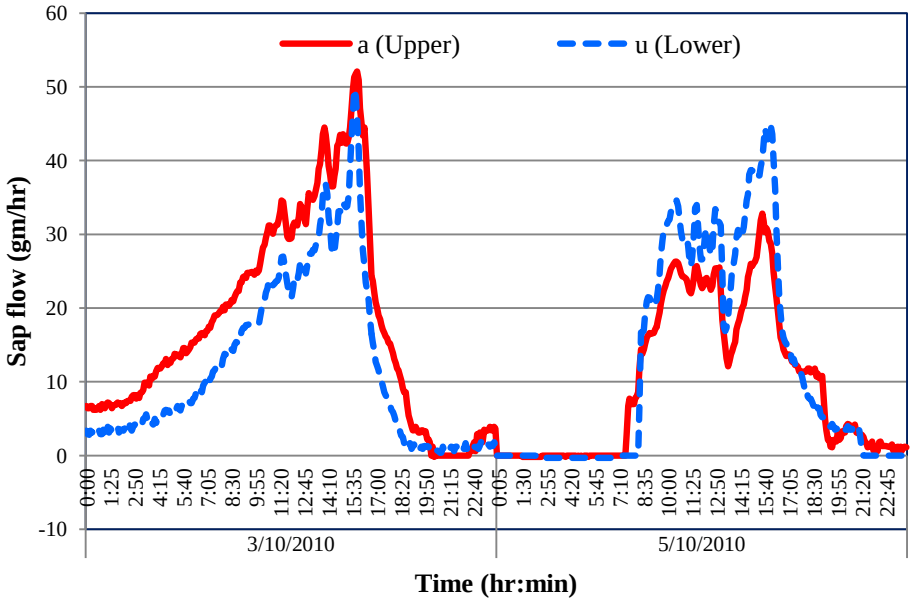

Figure C.6: Sap flow at two heights in the same plant

The use of the mini-lysimeters provided a different perspective on the water loss following wetting (Figure C.7). The rate of water loss immediately following the canopy wetting (spray irrigation) was higher than the sap flow due to the evaporation of the canopy intercepted water but declined rapidly to the steady transpiration rate as the canopy dried. After complete drying of the canopy the sap flow and transpiration again matched each other (Figure C.7). During the post wetting (canopy drying) period the water loss followed the exponential relationship (Figure C.8).

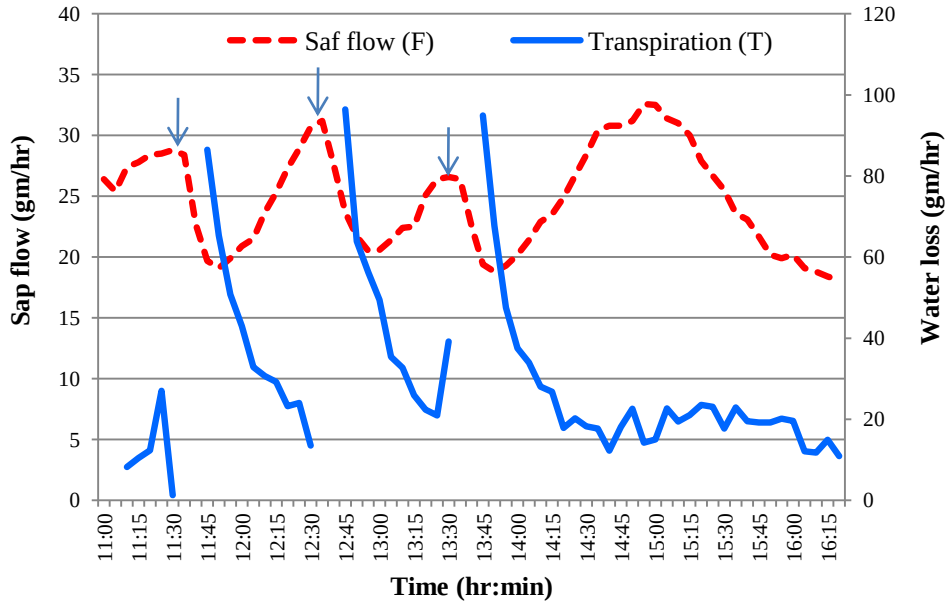

Figure C.7: The rate of sap flow and water loss following wetting of the plant (▼ indictaes the wetting time of the plant)

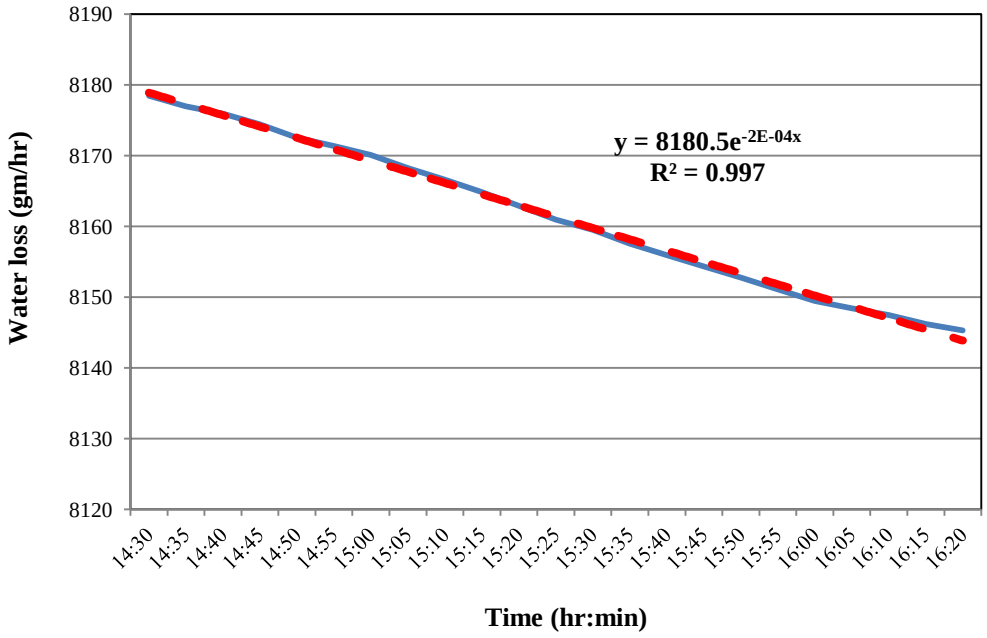

Figure C.8: Water loss during post wetting period

C.3.3 Effect of climatic variables on sap flow and transpiration

The meteorological variables (air temperature, canopy temperature, relative humidity (RH) and vapour pressure deficit (VPD), transpiration and sap flow are plotted in Figure C.9 over a period of five days. Figure illustrates that the, sap flow and transpiration are directly proportional to the air temperature, canopy temperature and VPD and inversely proportional to the RH.

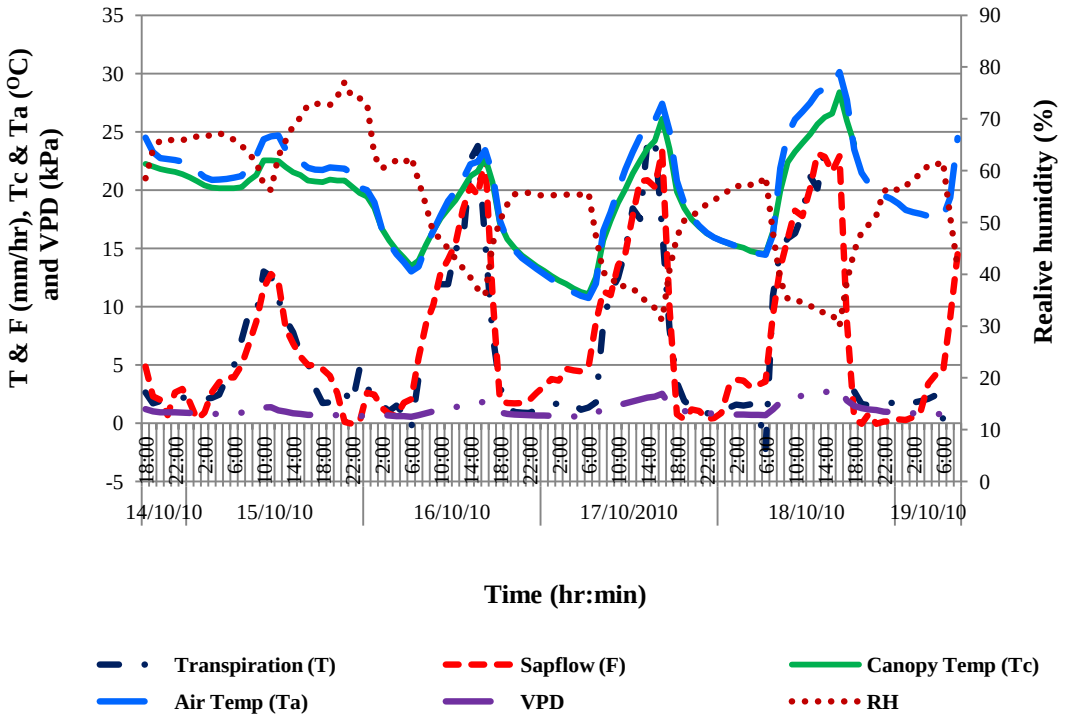

Figure C.9: Effect of climatic variables on sap flow and transpiration

C.4 Conclusions

The study showed that the sap flow sensor was able to measure the transpiration rate of plants quite reasonably in a non-wetting condition. However, it was found that the

sap flow overestimated the transpiration rate by approximately 12%. A lag between sap flow and transpiration was observed due to the storage and buffering capacity of the stem. The flow rate at higher height was found higher due to the same reason. During the wetting period the gauges measured the sap flow quite reasonably in response to the wetting and drying period. However, the transpiration rate was high due to the extra evaporation of the canopy intercepted water. During the drying period the loss of water followed the exponential relationship. The sap flow gauges were also responded quite well to the meteorological conditions of the outside environment. The study concluded that during wetting period the sap flow sensor is able to measure the sap flow which will be required to interpret the transpiration of the plants during sprinkler irrigation in field condition.

Appendix D: Regression analysis to model pre-, during- and post-irrigation phases

D.1 Introduction

The regression analysis technique is a popular data analysis and synthesis method widely used in agronomic and irrigation studies; most notably (in relation to the present research) in the development of empirical equations for predicting various evaporation and evapotranspiration characteristics using more routinely measured climatic variables as inputs (e.g. Kovor & Nandagiri 2007). However, no literature has been found reporting the use this technique in sprinkler irrigation. Hence, the regression model obtained from the ECV measurements in this appendix could be an important tool to predict the additional evaporation in sprinkler irrigation on the basis of local climatic data. This appendix sets out the development of best fitted regression equations for different phases of irrigation, namely pre-, during- and post-irrigation.

D.2 Materials and methods

The regression equations for different phases were obtained using the regression analysis. The equations were fitted to the nondimensional values of ET ($=ET_{ecadj}/ET_{ref}$) at different period of irrigation. The best regression equation was investigated by multiple combinations of different equations. Best fitted equations were then obtained following the linear and nonlinear curve fitting method using Excel's solver to minimize the sum of the squared error.

The reduced value of χ^2, root mean square error (RMSE) and modelling efficiency (EF) were used as the primary criteria to select the best equation to account for variation in each curve. Reduced χ^2 is the mean square of the deviations between the experimental and calculated values for the models (Equation D.1) and was used to determine the goodness of the fit. The lower the values of the reduced χ^2, the better the goodness of the fit. The RMSE gives the deviation between the predicted and experimental values and it is required to reach zero. The model efficiency (EF) also gives the ability of the model and its highest value is 1. These statistical values were calculated following the equations given by Ertekin and Yaldiz (2004):

$$\chi^2 = \frac{\sum_{i=1}^{N}\left((\mathrm{R}_{et})_{\exp,i} - (\mathrm{R}_{et})_{pred,i}\right)^2}{N-n} \tag{D.1}$$

$$RMSE = \sqrt{\frac{\sum_{i=1}^{N}\left((\mathrm{R}_{et})_{\exp,i} - (\mathrm{R}_{et})_{pred,i}\right)^2}{N}} \tag{D.2}$$

$$EF = \frac{\sum_{i=1}^{N}\left((R_{et})_{\exp,i} - (R_{et})_{\exp,mean}\right)^2 - \sum_{i=1}^{N}\left((R_{et})_{pred,i} - (R_{et})_{\exp,mean}\right)^2}{\sum_{i=1}^{N}\left((R_{et})_{\exp,i} - (R_{et})_{\exp,mean}\right)^2} \tag{D.3}$$

where $(R_{et})_{\exp,i}$ is the *i*-th experimental ET ratio,

$(R_{et})_{pred,i}$ is the *i*-th predicted ET ratio,

N is the number of observations,

n is the number of constants in drying model and

$(R_{et})_{\exp,mean}$ is the mean value of experimental ET ratio.

D.3 Results and discussion

Considering a three hours irrigation period, an idealized picture for three periods was established using the average nondimnsionalised values of ET for several day trials. Five distinct phases can be distinguished from the Figure D.1:

(i) a period of more or less constant value of nondimensional number;

(ii) a period of rapid increment of ET just after starting irrigation;

(iii) approximately stable ET during irrigation;

(iv) a period of declining rate of ET at post irrigation (drying) period followed by

(v) approximately constant rate of ET (in terms of nondimensionalised values).

Figure D.1: Schematic representation of the different phases of irrigation in terms of nondimensionalised values

(i) **The period of almost constant value of nondimensional number**: This phase represents the period before starting the irrigation where the actual and reference ET were almost similar. Hence, the nondimensionalised ET was almost constant throughout this period. Most of the statistical criteria (RMSE, χ^2 and EF) indicate that the linear relationship is the best fitted relationship for pre-irrigation period although the coefficient of determination (R^2) slightly less than the logarithmic and exponential relationship (Table D.1).

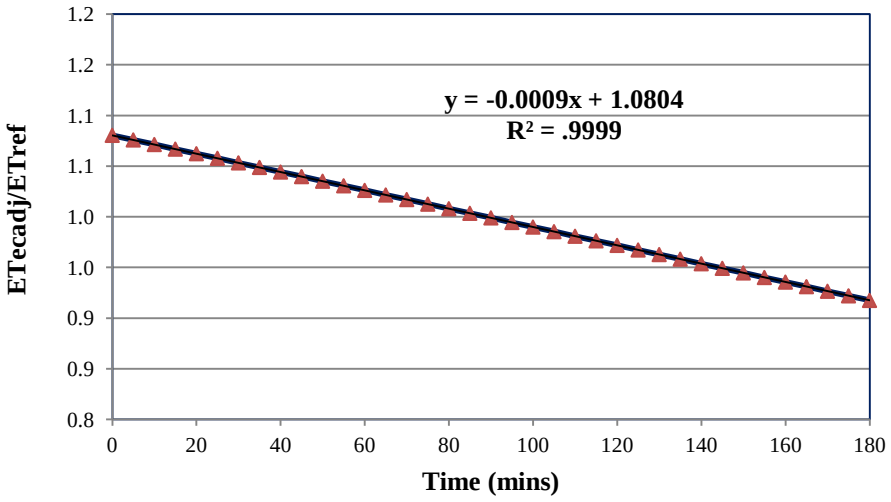

Figure D.2: Regression analysis for pre-irrigation period

(ii) **Period of rapid increment of ET just after starting irrigation:** This phase represents a short period when the rate of nondimensionalised ET quickly jumped from relatively constant value at 1.0 to significantly higher value just after starting the irrigation. Due to the limited number of point, it was not possible to fit a suitable equation for this short period. In this case, the first data points after starting irrigation were considered followed the same relationship as pre-irrigation period.

(iii) **Approximately stable (nondimensionalised) ET during irrigation:** In this phase the value of nondimensionalised ET reached at significantly higher value within the time about 10 mins after starting irrigation and maintained an almost steady level until complete the irrigation. Best fitting regression analysis (Table D.1) shows that it followed the linear relationship with time (Figure D.3).

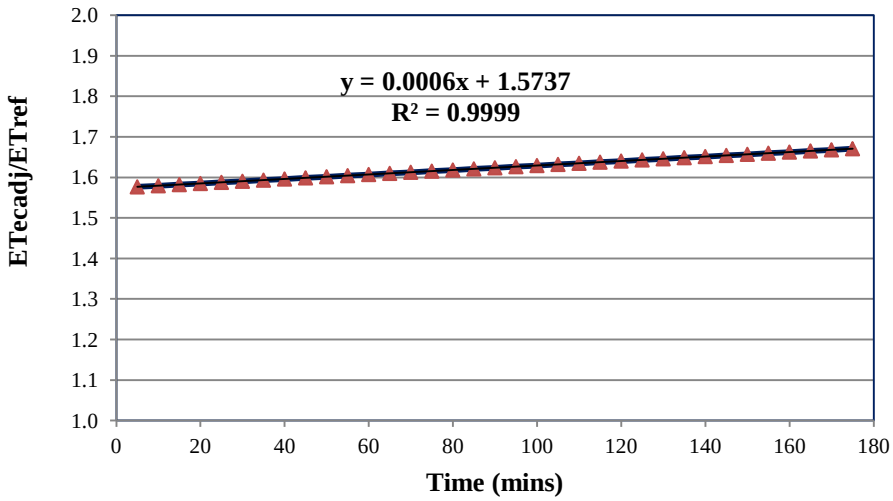

Figure D.3: Regression analysis for irrigation period

(iv) **Period of declining rate of ET at post irrigation (drying) period:** In this phase, the rate of nondimensionalised ET decreased slowly over the time until complete drying of the canopy. The approximated drying time was estimated 60 mins after ceasing the irrigation. According to the statistical criterion, it was found that exponential and power relationships are very close and describe the rate of evaporation quite confidently. Although in terms, RMSE and χ^2 values, power relationship equation is best suited, however in terms of the model efficiency (*EF*), the exponential curve was

found best fitted. A similar trend was found in glass house experiments conducted under this project ((Figure C.8, Appendix C).

Therefore, it can be concluded that during the drying period the best fitted data followed exponential relationship (Figure D.4).

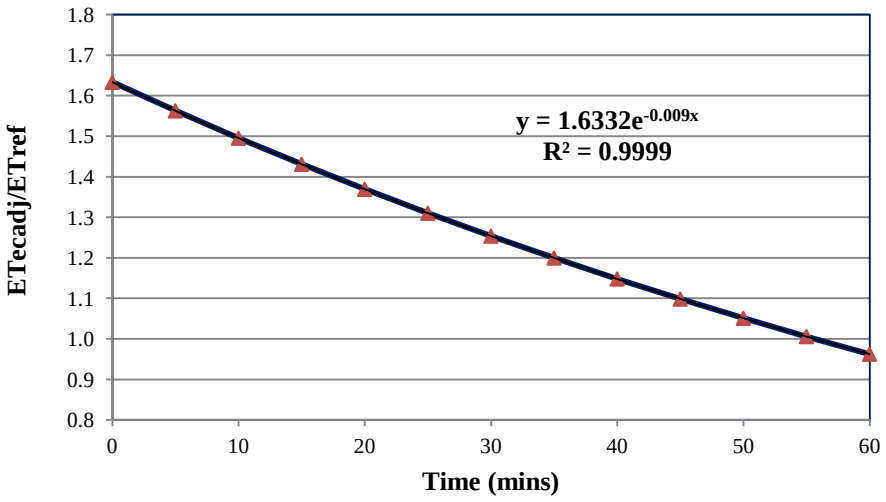

Figure D.4: Regression analysis for first phase of post irrigation period

(v) **More or less constant rate of** ET **in terms of nondimensional value:** This phase actually represent the dry canopy condition of the post irrigation periods. Statistical analysis shows that linear relationship was the best fitted curve at this phase (Table D.1).

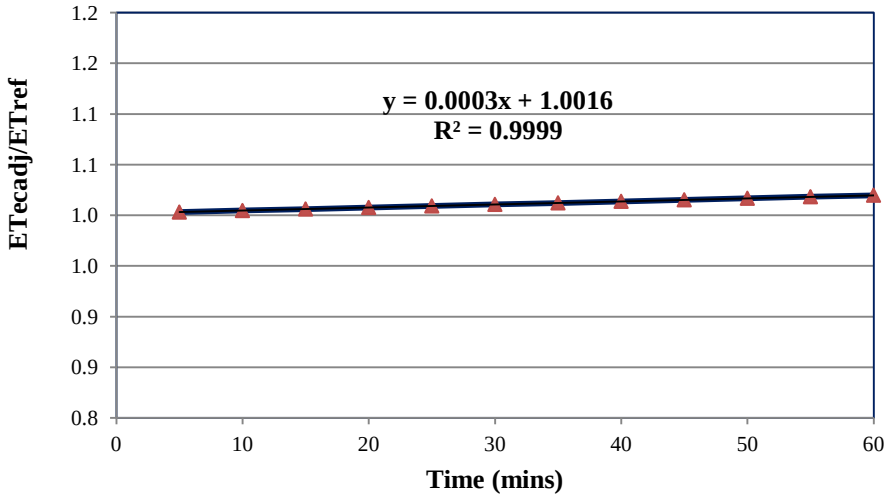

Figure D.5: Regression analysis for second phase of post irrigation period

Table D.1: The regression equations and statistical analysis for nondimensionalised ET **at different irrigation phases**

Period	Form of equation	RMSE	χ^2	EF
Pre irrigation	Linear	0.0131	0.0002	0.1684
	Exponential	0.0189	0.0004	1.8104
	Power	0.0149	0.0002	1.9830
	Quadratic	0.0151	0.0002	1.2362
	Logarithmic	0.0153	0.0002	2.0603
During irrigation	Linear	0.0112	0.0001	0.3973
	Exponential	0.0451	0.0021	19.8717
	Power	0.0149	0.0002	1.2689
	Quadratic	0.0109	0.0001	0.3477
	Logarithmic	0.0139	0.0002	0.9770
1st phase of post irrigation	Linear	0.0753	0.0062	0.9938
	Exponential	0.0758	0.0063	0.8503
	Power	0.0436	0.0021	5.0391
	Quadratic	0.1208	0.0160	0.7572
	Logarithmic	0.0444	0.0022	5.1053
2nd phase of post Irrigation	Linear	0.0106	0.0001	0.9902
	Exponential	0.0133	0.0002	0.5363
	Power	0.0108	0.0001	0.8109
	Quadratic	0.0114	0.0001	0.6642
	Logarithmic	0.0108	0.0001	0.8066

Similarly the regression analysis was performed for sap flow and the results are presented in Table D.2.

Table D.2: The regression equations and statistical analysis for nondimensionalised *F* at different phases

Period	Form of equation	RMSE	χ^2	EF
Pre irrigation	Linear	0.0134	0.0002	0.8937
	Exponential	0.0134	0.0002	0.8949
	Power	0.0147	0.0002	0.4535
	Quadratic	0.0128	0.0002	0.9451
	Logarithmic	0.0365	0.0014	-7.5965
During irrigation	Linear	0.3135	0.1072	-12.1694
	Exponential	0.0165	0.0003	0.2650
	Power	0.0430	0.0020	-0.8067
	Quadratic	0.0225	0.0006	-0.3437
	Logarithmic	0.0145	0.0002	-0.0137
1st phase of post irrigation	Linear	0.0650	0.0048	0.0245
	Exponential	0.2573	0.0756	-0.7233
	Power	0.1104	0.0139	-0.0355
	Quadratic	0.0551	0.0035	0.0005
	Logarithmic	0.6862	0.5381	-0.3712
2nd phase of post Irrigation	Linear	0.2739	0.1000	-19.4459
	Exponential	0.0106	0.0002	-0.0150
	Power	0.0176	0.0004	0.0326
	Quadratic	0.0320	0.0014	0.3711
	Logarithmic	0.0159	0.0003	0.0772

D.4 Conclusions

On the basis of statistical criteria and curves fitted, the best-suited equation for different phases of ET and sap flow (*F*) are as listed in Table D.3, D.4 and D.5.

Table D.3: Best fitted regression equations of nondimensionalised evapotranspiration for different period of irrigation at nonadvective condition (where R_{et} is the nondimensional ET and *t* is the time)

Period	Best fitted equation
Pre-irrigation	$R_{et} = -0.0009t + 1.0804$
During irrigation	$R_{et} = 0.0006t + 1.5737$
Post-irrigation (0-60 mins)	$R_{et} = 1.6332\exp(-0.009t)$
Postirrigation (60-120 mins)	$R_{et} = 0.0003t + 1.0013$

Table D.4: Best fitted regression equations of nondimensionalised evapotranspiration for different period of irrigation at advective condition (where R_{et} is the nondimensional ET and *t* is the time)

Period	Best fitted equation
Pre-irrigation	$R_{et} = -0.0002t + 1.0387$
During irrigation	$R_{et} = 0.0024t + 1.8318$
Post-irrigation (0-60 mins)	$R_{et} = 2.0412\exp(-0.013t)$
Postirrigation (60-120 mins)	$R_{et} = 0.0018t + 0.9718$

Table D.5: Regression equations of nondimensionalised sapflow sap flow **for different period of irrigation (where R_f is the nondimensional F and t is the time)**

Phase	Best fitted equation
Pre irrigation	$R_f = 0.00004t + 1.0572$
First stage of irrigation	$R_f = -0.387 \ln t + 1.5572$
Second stage of irrigation	$R_f = -0.0001t + 0.1042$
First stage of Post irrigation	$R_f = 0.0053t^{1.56}$
Second stage of Post irrigation	$R_f = -0.209 \ln t + 1.5809$

Appendix E: Nondimensionalised ET curves on different days over grass

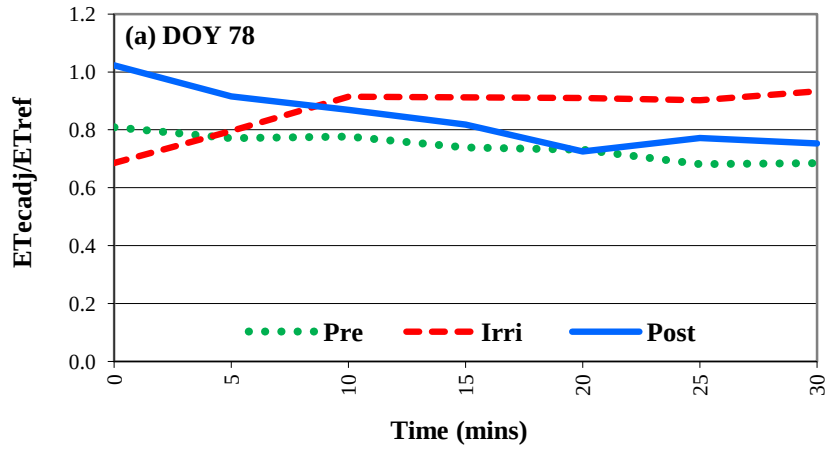

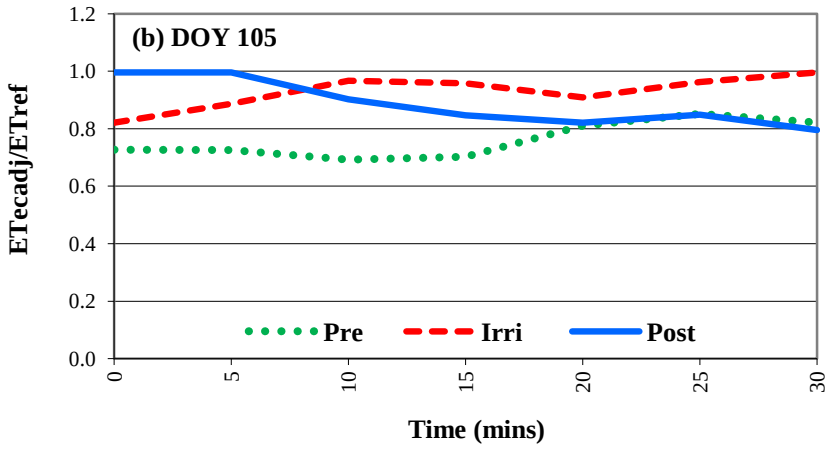

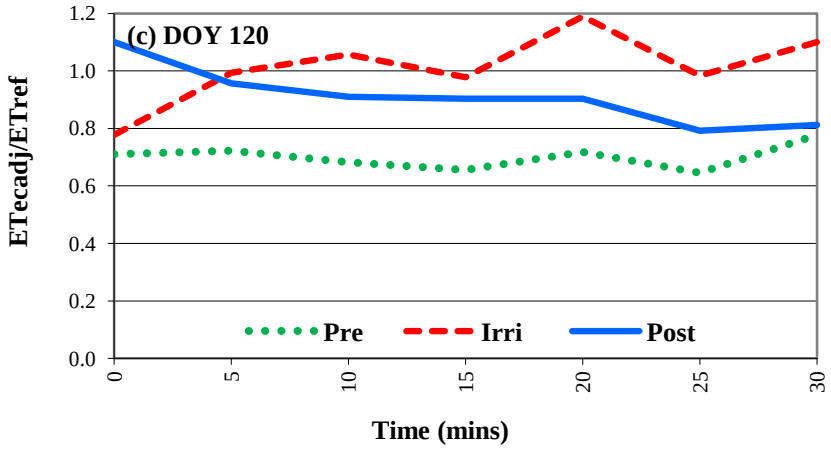

Appendix F: Average of reference evapotranspiration ET_{ref} at pre, during and post irrigation period during 19 February – 7 May 2011

DOY	Date	Combination of irrigation (hr)			Average ET_{ecadj} (mm/hr)		
		Pre	Irri	Post	Pre	Irri	Post
50	19/2/11	1/2	1/2	1/2	0.62	0.81	0.80
51	20/2/11	1/2	1/2	1/2	0.81	0.90	0.85
55	24/2/11	1/2	1/2	1/2	0.71	0.65	0.63
56	25/2/11	1/2	1/2	1/2	0.49	0.65	0.65
59	28/2/11	1/2	1/2	1/2	0.66	0.75	0.81
60	01/3/11	1/2	1/2	1/2	0.67	0.80	0.81
75	16/3/11	1	1/2	1	0.38	0.59	0.52
81	22/3/11	1	1/2	1	0.45	0.44	0.45
82	23/3/11	1	1/2	1	0.84	0.56	0.68
84	25/3/11	1	1/2	1	0.57	0.60	0.64
86	26/3/11	1	1/2	1	0.54	0.64	0.59
90	31/3/11	1	1/2	1	0.61	0.49	0.40
91	1/4/11	1	1/2	1	0.39	0.39	0.31
92	2/4/11	1	1/2	1	0.43	0.59	0.58
93	3/4/11	1	1/2	1	0.41	0.46	0.46
94	4/4/11	1	1/2	1	0.36	0.56	0.53
96	6/4/11	1	1/2	1	0.50	0.58	0.56
97	7/3/11	2	2	2	0.52	0.55	0.48
98	8/3/11	1	1	1	0.35	0.42	0.28
99	9/3/11	3	3	3	0.36	0.43	0.32
102	12/3/11	3	3	3	0.52	0.57	0.42
103	13/3/11	3	3	3	0.42	0.57	0.42
104	14/3/11	3	3	3	0.40	0.57	0.24
105	15//3/11	3	3	3	0.41	0.58	0.33
107	17/3/11	3	3	3	0.37	0.43	0.23
112	22/4/11	3	3	3	0.36	0.26	0.15
113	23/4/11	3	3	3	0.31	0.51	0.25
114	24/4/11	3	3	3	0.39	0.50	0.37
115	25/4/11	3	3	3	0.67	0.49	0.29
116	26/4/11	3	3	3	0.26	0.40	0.16
119	29/4/11	3	3	3	0.33	0.44	0.09
120	30/4/11	3	3	3	0.35	0.48	0.17
121	1/5/11	3	3	3	0.35	0.46	0.27
125	5/5/11	3	3	3	0.34	0.44	0.20
126	6/5/11	3	3	3	0.31	0.41	0.18
127	7/5/11	3	3	3	0.33	0.51	0.40

Appendix G: Average of actual ET (ET_{ecadj}) at pre, during and post irrigation period during 19 February –7 May 2011

DOY	Date	Combination of irrigation (hr)			Average ET_{ecadj} (mm/hr)		
		Pre	Irri	Post	Pre	Irri	Post
50	19/2/11	1/2	1/2	1/2	0.67	1.05	0.96
51	20/2/11	1/2	1/2	1/2	0.87	1.16	1.01
55	24/2/11	1/2	1/2	1/2	0.65	0.81	0.69
56	25/2/11	1/2	1/2	1/2	0.56	0.87	0.77
59	28/2/11	1/2	1/2	1/2	0.65	0.92	0.89
60	01/3/11	1/2	1/2	1/2	0.70	1.22	1.07
75	16/3/11	1	1/2	1	0.40	0.86	0.64
81	22/3/11	1	1/2	1	0.45	0.91	0.79
84	25/3/11	1	1/2	1	0.59	1.19	0.95
85	26/3/11	1	1/2	1	0.55	0.88	0.69
90	31/3/11	1	1/2	1	0.61	0.74	0.53
91	1/4/11	1	1/2	1	0.39	0.55	0.44
92	2/4/11	1	1/2	1	0.47	0.96	0.72
93	3/4/11	1	1/2	1	0.41	0.73	0.60
94	4/4/11	1	1/2	1	0.34	0.88	0.64
96	6/4/11	1	1/2	1	0.33	0.64	0.58
97	7/4/11	2	2	2	0.48	0.85	0.57
98	8/4/11	1	1	1	0.31	0.61	0.36
99	9/4/11	3	3	3	0.29	0.71	0.34
102	12/4/11	3	3	3	0.55	1.40	0.48
103	13/4/11				0.49	0.90	0.16
104	14/4/11	3	3	3	0.40	1.18	0.46
105	15//4/11	3	3	3	0.39	1.00	0.34
107	17/4/11	3	3	3	0.39	0.64	0.48
112	22/4/11	3	3	3	0.38	0.42	0.24
113	23/4/11	3	3	3	0.33	0.65	0.37
114	24/4/11	3	3	3	0.38	0.70	0.42
115	25/4/11	3	3	3	0.26	0.74	0.34
116	26/4/11	3	3	3	0.24	0.59	0.23
119	29/4/11	3	3	3	0.31	0.78	0.27
120	30/4/11	3	3	3	0.33	0.78	0.27
121	1/5/11	3	3	3	0.33	0.82	0.34
125	5/5/11	3	3	3	0.28	0.59	0.13
126	6/5/11	3	3	3	0.28	0.59	0.13
127	7/5/11	3	3	3	0.3	0.82	0.42

Appendix H: Average of ET_{ecadj}/ET_{ref} at pre, during and post irrigation period during 19 February – 7 May 2011

DOY	Date	Combination of irrigation (hr)			Average ET_{ecadj}/ET_{ref}			Increment of ET_{ecadj}/ET_{ref} during irrigation with respect to pre irrigation period	Additional evaporation
		Pre	Irri	Post	Pre	Irri	Post	mm/hr	%
50	19/2/11	1/2	1/2	1/2	1.08	1.30	1.20	0.22	20
51	20/2/11	1/2	1/2	1/2	1.07	1.29	1.20	0.22	21
55	24/2/11	1/2	1/2	1/2	0.92	1.25	1.07	0.33	36
56	25/2/11	1/2	1/2	1/2	0.94	1.35	1.17	0.41	44
59	28/2/11	1/2	1/2	1/2	1.00	1.73	1.50	0.73	73
60	01/3/11	1/2	1/2	1/2	1.05	1.53	1.32	0.48	46
75	16/3/11	1	1/2	1	0.96	1.35	1.18	0.39	41
81	22/3/11	1	1/2	1	1.00	1.57	1.28	0.57	57
82	23/3/11	1	1/2	1	1.10	1.36	1.22	0.26	24
84	25/3/11	1	1/2	1	1.03	1.79	1.50	0.76	74
86	26/3/11	1	1/2	1	1.03	1.32	1.17	0.29	28
90	31/3/11	1	1/2	1	1.03	1.60	1.28	0.57	55
91	1/4/11	1	1/2	1	1.00	1.43	1.27	0.43	43
92	2/4/11	1	1/2	1	1.08	1.58	1.28	0.50	46
93	3/4/11	1	1/2	1	1.00	1.59	1.29	0.59	59
94	4/4/11	1	1/2	1	0.96	1.57	1.21	0.61	64
96	6/4/11	1	1/2	1	0.84	1.43	1.17	0.59	70
97	7/4/11	2	2	2	0.91	1.54	1.06	0.63	69
98	8/4/11	1	1	1	0.86	1.58	1.14	0.72	84
99	9/4/11	3	3	3	0.79	1.76	0.98	0.97	123
102	12/4/11	3	3	3	1.04	2.04	1.09	1.00	96
103	13/4/11	3	3	3	0.91	1.57	1.14	0.66	73
104	14/4/11	3	3	3	1.02	2.08	1.28	1.06	104
105	15//4/11	3	3	3	0.96	1.71	1.12	0.75	78
107	17/4/11	3	3	3	1.07	1.57	1.12	0.50	47
112	22/4/11	3	3	3	1.06	1.73	1.21	0.67	63
113	23/4/11	3	3	3	1.06	1.31	1.11	0.25	24
114	24/4/11	3	3	3	0.98	1.42	1.13	0.44	45
115	25/4/11	3	3	3	0.82	1.52	1.12	0.70	85
116	26/4/11	3	3	3	0.93	1.50	1.22	0.57	61
119	29/4/11	3	3	3	1.00	1.84	2.04	0.84	84
120	30/4/11	3	3	3	1.00	1.52	1.10	0.52	52
121	1/5/11	3	3	3	1.00	1.96	1.14	0.96	96
125	5/5/11	3	3	3	0.85	1.44	1.25	0.59	69
126	6/5/11	3	3	3	0.95	1.42	1.21	0.47	49
127	7/5/11	3	3	3	0.93	1.62	1.22	0.69	74

Appendix I: Average of actual sap flow (*F*) at pre, during and post irrigation period during 25 March – 17 April 2011

Date	Combination of irrigation (hr)			Average sap flow (*F*) (mm/hr)		
	Pre	Irri	Post	Pre	Irri	Post
25/03/2011	1	1/2	1	0.39	0.33	0.48
31/03/2011	1	1/2	1	0.77	0.46	0.41
01/04/2011	1	1/2	1	0.40	0.17	0.34
02/04/2011	1	1/2	1	0.53	0.38	0.46
03/04/2011	1	1/2	1	0.46	0.37	0.38
04/04/2011	1	1/2	1	0.42	0.38	0.46
06/04/2011	1	1/2	1	0.41	0.37	0.25
07/04/2011	2	2	2	0.59	0.11	0.34
09/04/2011	3	3	3	0.35	0.01	0.31
12/04/2011	3	3	3	0.56	0.12	0.42
13/04/2011	3	3	3	0.50	0.07	0.40
15//04/2011	3	3	3	0.64	0.23	0.35
17/04/2011	3	3	3	0.56	0.23	0.35
22/04/2011	3	3	3	0.64	0.06	0.25
23/04/2011	3	3	3	0.33	0.09	0.13
24/04/2011	3	3	3	0.48	0.09	0.30
25/04/2011	3	3	3	0.37	0.08	0.27
26/04/2011	3	3	3	0.29	0.06	0.30
29/04/2011	3	3	3	0.25	0.04	0.04
30/04/2011	3	3	3	0.28	0.04	0.11
1/05/2011	3	3	3	0.27	0.06	0.30
5/05/2011	3	3	3	0.26	0.04	0.15
6/05/2011	3	3	3	0.29	0.05	0.15
7/05/2011	3	3	3	0.37	0.05	0.19

Appendix J: Average of F/ET_{ref} at pre, during and post irrigation period during 25 March – 7 May 2011 (Data were average considering pre for 1 hr irrigation, 3 hrs and 1 hr post irrigation period)

Date	Combination of irrigation (hr)			Average F/ET_{ref}			Reduction of F/ET_{ref} during irrigation	
	Pre	Irri	Post	Pre	Irri	Post	R_f	%
25/03/2011	1	1/2	1	0.77	0.37	0.81`	0.40	52
01/04/2011	1	1/2	1	1.05	0.42	1.00	0.63	60
02/04/2011	1	1/2	1	1.25	0.62	0.82	0.63	50
03/04/2011	1	1/2	1	1.13	0.69	0.89	0.44	39
04/04/2011	1	1/2	1	1.23	0.64	0.89	0.59	48
06/04/2011	1	1/2	1	1.07	0.86	0.63	0.21	20
07/04/2011	2	2	2	0.96	0.18	0.75	0.78	81
09/04/2011	1	3	1	0.86	0.03	0.54	0.83	97
12/04/2011	1	3	1	1.06	0.21	0.90	0.85	80
13/04/2011	1	3	1	0.93	0.13	0.84	0.80	86
15//04/2011	1	3	1	1.24	0.41	0.89	0.83	67
17/04/2011	1	3	1	1.14	0.59	0.94	0.55	48
22/04/2011	1	3	1	1.14	0.10	0.94	1.04	91
23/04/2011	1	3	1	0.98	0.17	1.21	0.81	83
24/04/2011	1	3	1	1.09	0.17	0.64	0.92	84
25/04/2011	1	3	1	1.01	0.13	0.80	0.88	87
26/04/2011	1	3	1	1.25	0.13	0.80	1.12	90
29/04/2011	1	3	1	0.74	0.09	0.52	0.65	88
30/04/2011	1	3	1	0.80	0.10	0.36	0.70	88
1/05/2011	1	3	1	0.69	0.12	0.70	0.57	83
5/05/2011	1	3	1	0.81	0.09	0.43	0.72	89
6/05/2011	1	3	1	1.05	0.12	0.49	0.93	89
7/05/2011	1	3	1	0.97	0.09	0.51	0.88	91

Appendix K: Meteorological data recorded during the experiment: average air temperature (T_a), relative humidity (RH), wind speed (WS), vapour pressure deficit (VPD), adjusted latent heat flux (λE_{adj}), adjusted sensible heat flux (H_{adj}), actual net radiation (R_{nact}), soil heat flux, canopy temperature (T_c), Bowen ratio (BR) and advection index (AI)

Date		*Ta*	RH	WS	VPD	λE_{adj}	H_{adj}	*Rn*	*G*	*Tc*	BR	AI
		(°C)	(%)	m/s	kPa	W/m^2	W/m^2	W/m^2	W/m^2	(°C)		
19/02/11	Pre	23.4	78.3	4.2	0.6	455	214	689	21		0.47	0.68
	Irri	24.7	69.4	3.1	1.0	693	101	830	36		0.15	0.87
	Post	25.1	66.4	2.7	1.1	583	116	739	41		0.20	0.84
20/02/11	Pre	27.7	64.1	2.1	1.3	589	152	786	46		0.26	0.80
	Irri	29.6	53.4	1.3	2.0	793	1	857	63		0.00	1.01
	Post	29.7	51.0	1.2	2.1	666	42	775	67		0.05	0.97
24/02/11	Pre	21.3	60.4	2.3	1.0	443	274	774	57		0.62	0.62
	Irri	22.3	55.5	3.2	1.2	599	91	742	52		0.14	0.88
	Post	22.6	54.7	3.3	1.2	499	147	694	48		0.29	0.78
25/02/11	Pre	20.4	68.8	3.8	0.7	379	273	673	21		0.72	0.58
	Irri	22.5	59.0	2.6	1.1	606	128	791	57		0.22	0.84
	Post	23.0	57.3	2.6	1.2	526	153	735	56		0.29	0.78
26/02/11	pre	22.2	59.5	1.1	1.1	450	189	664	25		0.42	0.70
	irr	24.1	53.4	2.3	1.4	443	161	658	55		0.34	0.75
	post	24.3	52.4	2.4	1.4	437	155	646	54		0.31	0.77
28/02/11	Pre	25.5	58.2	1.0	1.4	464	151	634	35		0.35	0.75
	Irri	27.9	50.6	0.9	1.9	599	25	686	62		0.02	1.00

	Post	27.9	50.6	0.9	1.9	606	28	696	62		0.02	0.99
1/03/11	Pre	25.5	60.2	2.2	1.3	479	140	643	24		0.29	0.77
	Irri	28.3	49.4	1.7	2.0	829	-48	848	67		-0.04	1.06
	Post	28.9	45.5	1.5	2.2	727	31	829	71		0.05	0.96
16/03/11	Pre	21.0	78.6	2.6	0.5	260	149	414	5	23.8	0.57	0.64
	Irri	23.6	63.4	2.0	1.1	534	40	603	29	23.6	0.06	**0.96**
	Post	23.8	61.7	1.9	1.1	377	56	460	27	24.2	0.07	1.00
22/03/11	Pre	23.3	83.0	1.9	0.5	308	143	464	13	25.8	0.47	0.68
	Irri	26.5	63.9	3.0	1.3	640	-59	616	35	24.3	-0.07	**1.11**
	Post	26.8	59.9	3.2	1.4	555	12	600	33	26.0	0.02	1.00
23/03/11	Pre	24.0	61.0	2.6	1.2	439	98	570	33	24.6	0.21	0.83
	Irri	24.5	57.8	3.3	1.3	329	57	408	22	22.8	-0.54	**0.91**
	Post	24.1	55.1	3.2	1.3	341	5	362	16	23.2	-0.10	1.45
25/03/11	Pre	19.8	56.8	2.9	1.0	335	141	472	-5		0.41	0.70
	Irri	22.2	52.4	3.8	1.3	869	-209	683	24		-0.17	1.32
	Post	22.5	49.5	3.7	1.4	563	45	635	26		0.11	**0.94**
26/03/11	Pre	21.8	59.2	3.0	1.1	504	114	656	37		0.24	0.83
	Irri	21.8	58.4	2.8	1.1	689	55	788	44		0.10	0.93
	Post	22.3	55.4	2.9	1.2	461	102	601	37		0.19	0.85
31/03/11	Pre	21.8	69.0	2.3	0.8	429	186	654	39		0.42	0.70
	Irri	22.0	64.9	2.7	0.9	515	44	598	39		0.05	0.99
	Post	22.3	62.2	2.9	1.0	366	50	448	32		0.09	0.94
1/04/11	Pre	19.3	78.1	4.7	0.5	265	181	447	1		0.68	0.60
	Irri	20.0	74.8	3.6	0.6	374	78	472	20		0.16	0.88
	Post	19.1	80.7	3.9	0.4	296	66	386	24		0.36	0.89
2/04/11	Pre	19.4	73.8	2.8	0.6	317	150	470	3		0.47	0.68

	Irri	21.5	64.0	1.8	0.9	622	67	720	31		0.13	0.90
	Post	22.1	59.3	1.6	1.1	454	92	581	35		0.39	0.88
3/04/11	Pre	19.7	71.9	4.0	0.6	348	111	475	16		0.27	0.99
	Irri	19.9	70.1	4.0	0.7	425	60	506	21		0.13	0.91
	Post	20.0	70.6	3.9	0.7	337	100	458	20		0.15	1.19
4/04/11	Pre	18.2	73.3	4.0	0.6	233	159	392	-1		0.68	0.60
	Irri	19.8	59.4	3.9	0.9	596	48	667	23		0.09	0.94
	Post	20.3	56.4	3.9	1.0	433	103	560	24		0.23	0.83
6/04/11	Pre	17.0	74.9	5.1	0.5	222	249	468	-3		1.12	0.47
	Irri	17.9	72.8	4.4	0.6	442	102	564	20		-0.82	0.95
	Post	18.0	72.6	3.8	0.6	357	144	522	21		0.45	0.76
7/04/10	Pre	18.7	68.0	4.8	0.7	343	273	642	26	22.4	0.79	0.56
	Irri	18.7	67.6	4.2	0.7	570	125	726	32	19.8	0.22	0.83
	Post	19.7	62.0	3.6	0.9	307	110	436	19	22.4	0.39	0.73
8/04/11	Pre	18.2	69.5	4.3	0.6	239	165	420	16	19.9	0.63	0.62
	Irri	18.6	65.4	4.1	0.7	441	40	499	18	18.8	0.07	0.96
	Post	18.2	68.6	3.3	0.7	227	10	252	15	18.1	-0.02	1.10
9/04/11	Pre	17.8	72.4	4.5	0.6	194	201	397	3	21.0	1.07	0.49
	Irri	19.3	63.3	3.3	0.8	486	39	558	33	19.6	0.05	0.98
	Post	20.2	60.9	3.2	0.9	228	59	300	14	22.2	0.24	0.84
12/04/11	Pre	16.2	63.9	2.3	0.7	221	132	353	1	19.3	0.61	0.63
	Irri	19.6	54.1	2.7	1.1	831	-148	707	24	18.1	-0.13	1.22
	Post	20.5	38.5	2.2	1.5	270	15	294	9	21.5	0.02	1.07
13/04/11	Pre	19.9	44.4	1.0	1.3	262	146	411	4	22.5	0.55	0.65
	Irri	22.0	45.6	1.7	1.4	289	373	702	39	18.5	-0.09	1.13
	Post	22.8	34.6	1.6	1.8	269	0	287	18	23.0	-0.04	1.10

14/04/11	Pre	20.1	67.7	1.4	0.8	277	125	413	10	22.5	0.46	0.69
	Irri	23.1	43.3	2.6	1.6	814	-213	631	30	18.7	-0.26	1.37
	Post	22.1	36.9	1.8	1.7	199	-30	180	11	21.1	-0.24	1.45
15/04/11	Pre	19.8	69.5	1.7	0.7	268	133	410	9	22.5	0.50	0.67
	Irri	21.4	48.0	1.8	1.3	678	-15	701	39	21.6	-0.01	1.02
	Post	22.0	41.6	2.6	1.5	237	16	271	18	22.4	-0.07	1.21
17/04/11	Pre	17.9	77.2	2.9	0.5	265	158	428	5	19.9	0.55	0.65
	Irir	19.0	73.5	3.5	0.6	436	61	528	31	19.4	0.12	0.90
	Post	18.7	75.0	3.3	0.5	173	39	225	13	19.2	0.12	0.92
22/04/11	Pre	21.3	76.0	0.9	0.6	263	95	365	7	23.3	0.36	0.75
	Irri	22.4	61.0	1.4	1.1	294	-38	278	23	20.9	-0.16	1.21
	Post	22.7	58.5	1.1	1.2	117	3	135	15	21.5	-0.16	1.33
23/04/11	Pre	19.8	80.0	1.5	0.5	224	106	334	4	21.6	0.45	0.71
	Irri	21.4	67.5	2.0	0.8	448	54	532	30	21.6	0.09	0.93
	Post	21.4	66.6	2.7	0.9	148	25	188	15	21.4	-0.04	1.20
24/04/11	pre	18.4	76.6	3.6	0.5	214	117	327	-4	19.9	0.52	0.66
	Irri	19.9	69.7	3.3	0.7	436	83	539	20	20.4	0.24	0.84
	Post	20.9	59.5	2.5	1.0	207	26	246	13	21.0	0.02	1.06
25/04/11	pre	17.0	81.9	3.8	0.4	168	133	296	-5	18.5	0.76	0.57
	irr	17.8	73.6	3.4	0.6	381	61	455	14	18.8	0.18	0.87
	post	18.7	66.0	3.1	0.7	159	25	194	10	18.8	0.00	1.07
26/04/11	pre	16.7	79.6	3.3	0.4	166	128	291	-4	18.4	0.73	0.59
	irri	18.9	66.7	3.0	0.7	424	7	448	17	18.6	0.00	1.02
	post	17.9	77.3	2.4	0.5	152	10	172	11	17.9	0.08	1.67
29/04/11	pre	16.3	72.2	3.3	0.5	212	150	362	0	18.5	0.68	0.61
	irri	18.8	80.0	2.9	0.4	535	11	569	23	18.4	0.01	1.00

	post	17.2	83.3	1.5	0.3	131	-15	128	12	16.8	-0.17	1.88
30/04/11	Pre	16.7	73.9	2.0	0.5	202	106	303	-5	18.7	0.49	0.68
	irri	18.9	77.1	2.8	0.5	442	92	558	24	19.7	0.28	0.82
	post	19.1	75.0	2.1	0.6	124	13	152	15	18.9	-0.15	1.51
1/05/11	pre	17.1	79.5	1.4	0.4	200	104	298	-6	19.0	0.50	0.67
	irri	19.9	71.9	2.0	0.6	440	110	571	21	19.5	0.10	0.64
	post	21.0	58.9	2.2	1.0	236	-9	241	14	20.4	-0.18	0.95
5/05/11	pre	15.1	64.0	1.6	0.6	190	165	352	-3	17.8	0.83	0.55
	irr	17.9	58.1	1.4	0.9	439	25	489	25	18.1	0.06	0.97
	post	18.4	52.1	1.4	1.0	152	9	174	13	18.2	-0.18	1.44
6/05/11	pre	14.7	66.8	2.1	0.6	192	155	345	-2	17.4	0.75	0.59
	irr	17.7	59.0	1.0	0.8	404	33	461	25	17.8	0.06	0.96
	post	18.1	54.2	1.0	1.0	81	64	159	14	17.6	-0.23	2.32
7/05/11	pre	15.9	59.8	1.3	0.7	202	143	341	-4	18.3	0.68	0.60
	irr	18.7	47.8	1.7	1.1	565	-58	532	25	16.9	-0.10	1.12
	post	19.3	33.1	1.3	1.5	27	146	186	12	17.7	-0.20	3.67

Appendix L: Nondimensionalised ET curves for individual trials

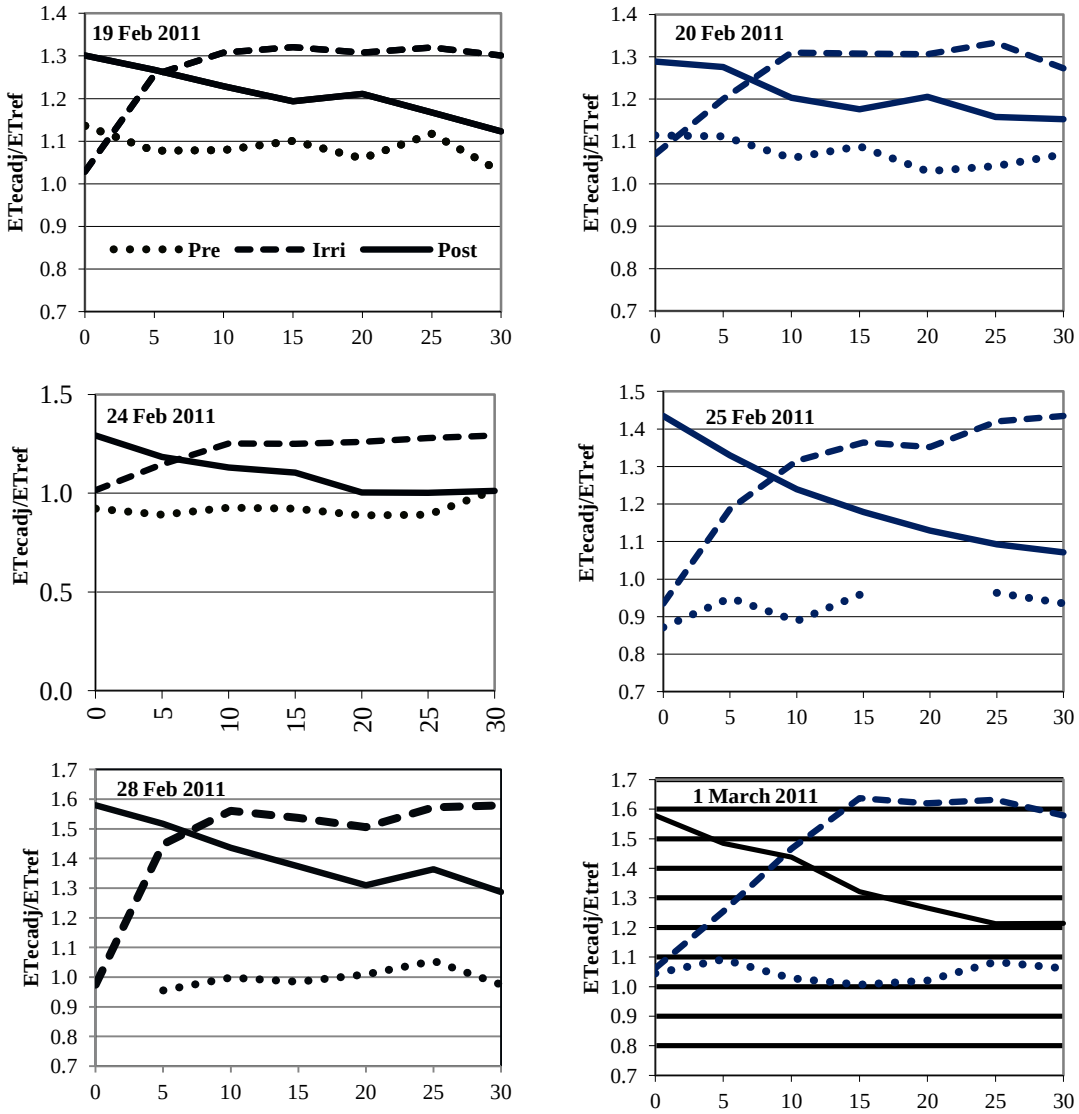

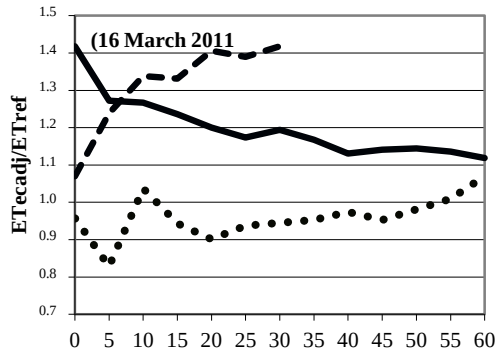
(16 March 2011
ETecadj/ETref

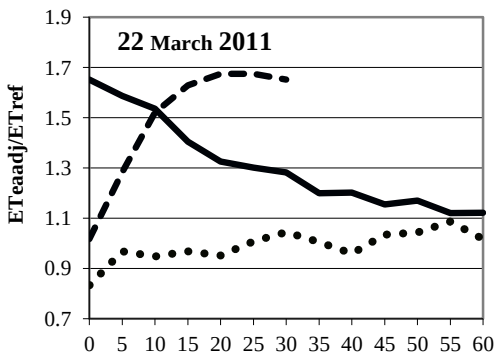
22 March 2011
ETeaadj/ETref

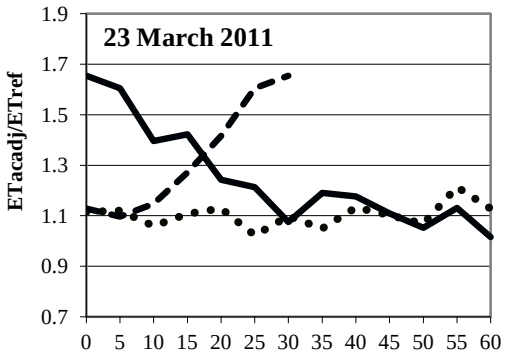
23 March 2011
ETacadj/ETref

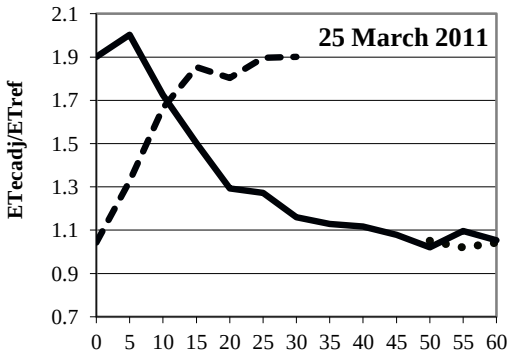
25 March 2011
ETecadj/ETref

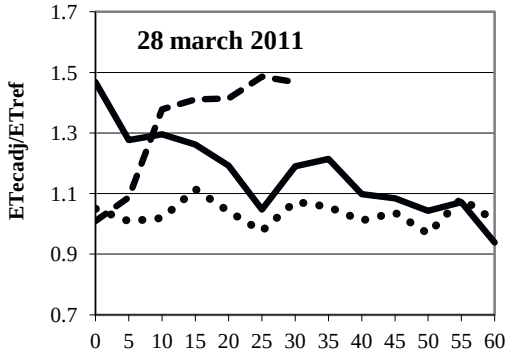
28 march 2011
ETecadj/ETref

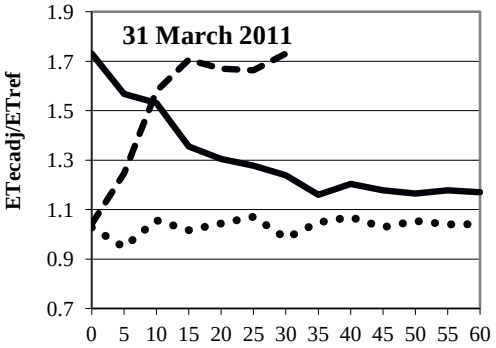
31 March 2011
ETecadj/ETref

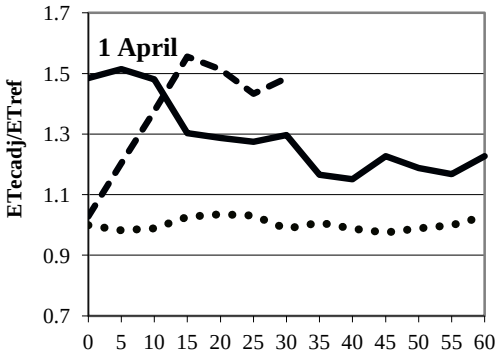
1 April
ETecadj/ETref

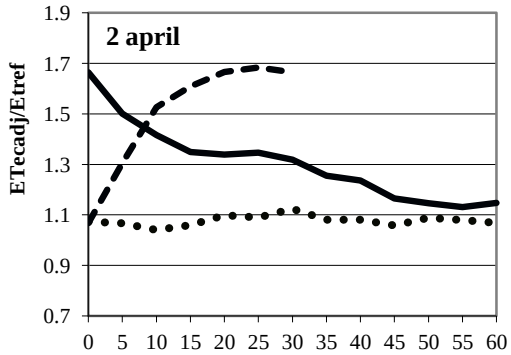
2 april
ETecadj/Etref

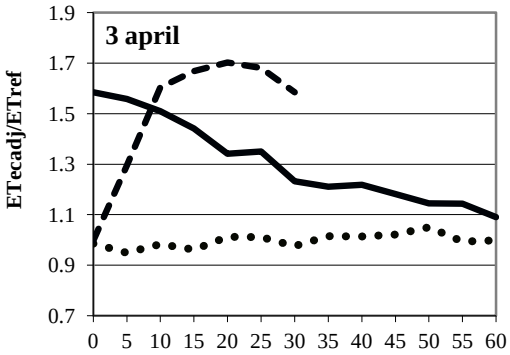
3 april
ETecadj/ETref

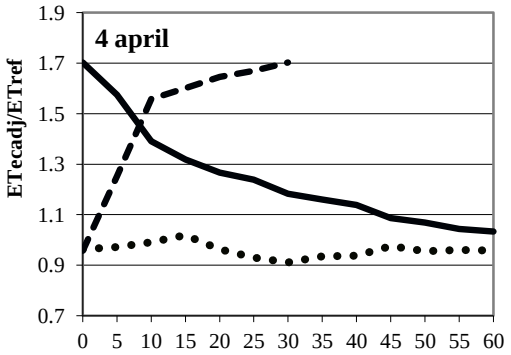
4 april
ETecadj/ETref

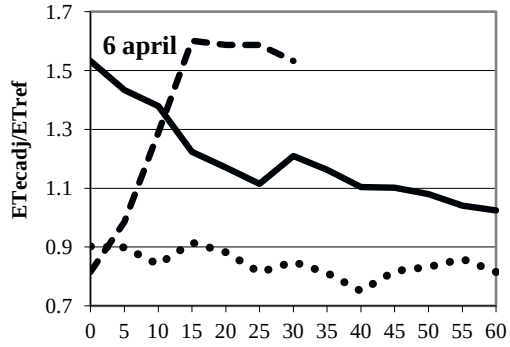
6 april
ETecadj/ETref

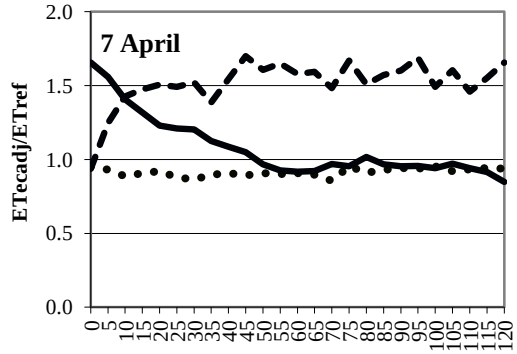
7 April
ETecadj/ETref

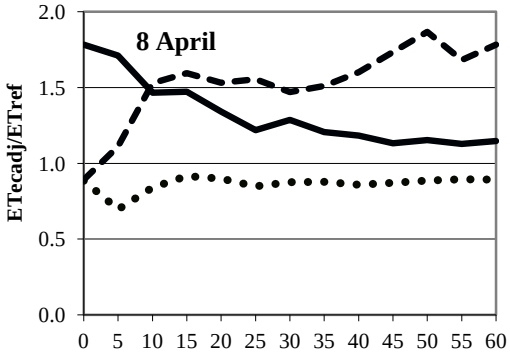
8 April
ETecadj/ETref

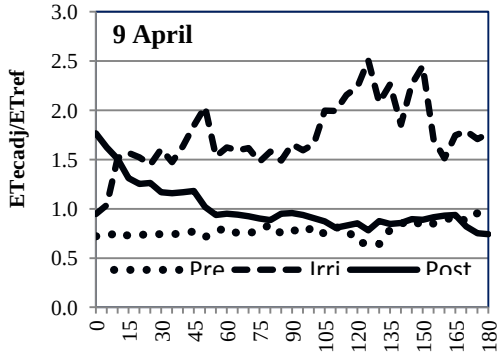
9 April
ETecadj/ETref
Pre
Irri
Post

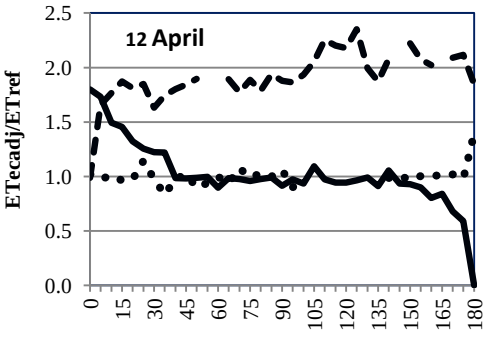
12 April
ETecadj/ETref

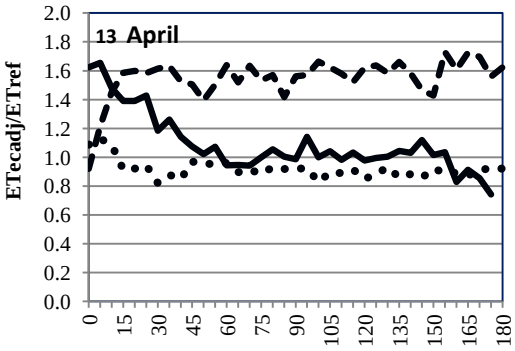
13 April
ETecadj/ETref

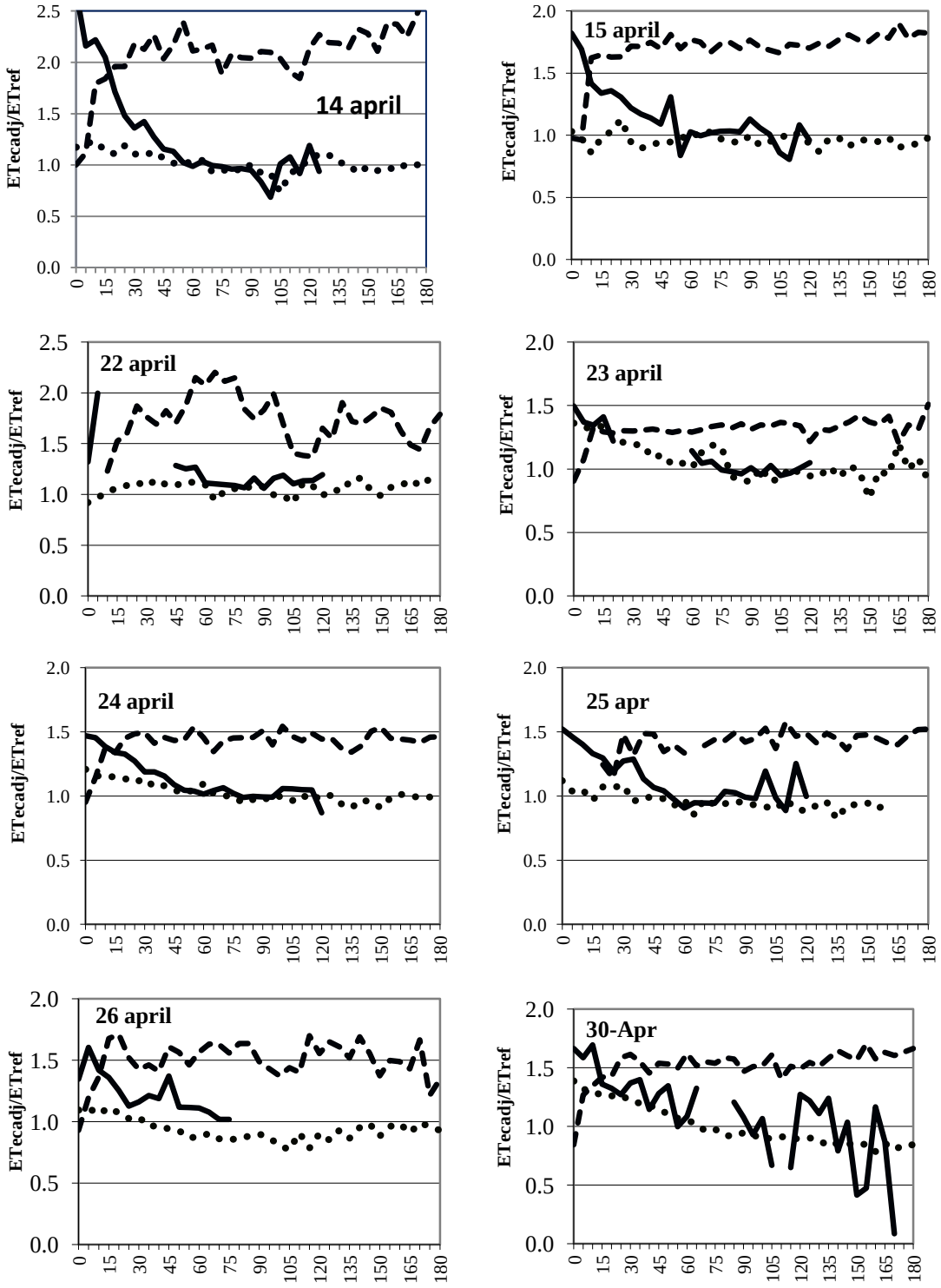
14 april
15 april
22 april
23 april
24 april
25 apr
26 april
30-Apr
ETecadj/ETref

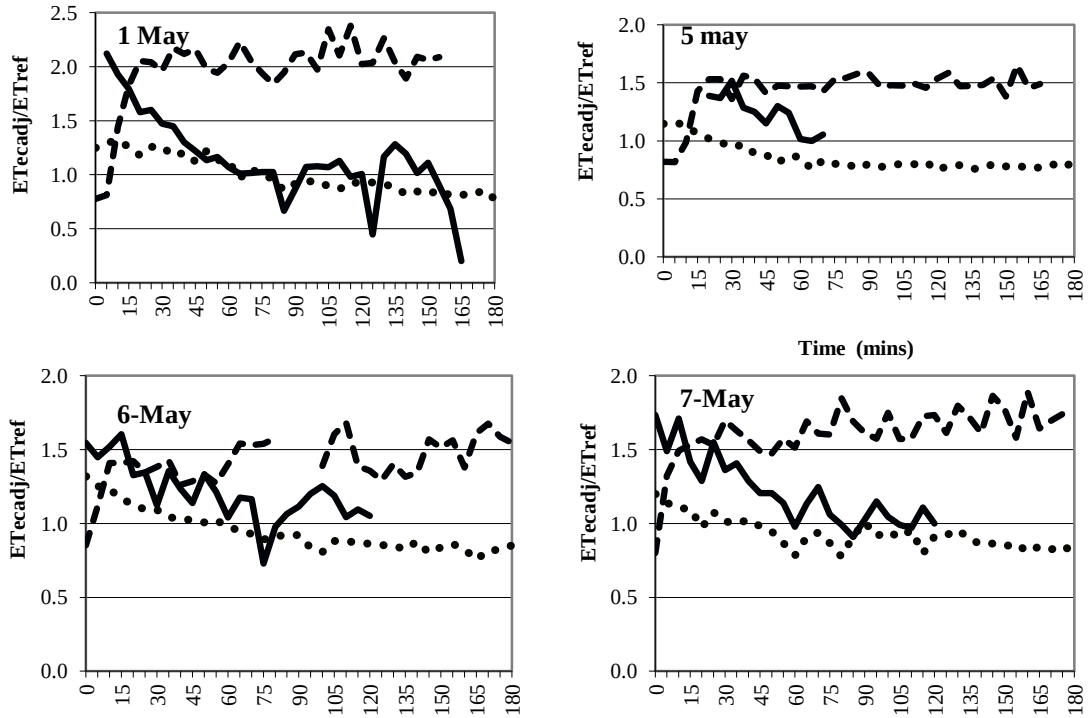
1 May
5 may
6-May
7-May
ETecadj/ETref
Time (mins)

Appendix M: Day time (8 AM-17 PM) average daily climatic data of different locations of cotton growing areas for January 2009

Date	Emerald				Saint George				Bourke				Hillston				Trangie			
	T_a	RH	WS	P	T_a	RH	WS	P	T_a	RH	WS	P	T_a	RH	WS	P	T_a	RH	WS	P
	^{O}C	%	m/s	kPa	^{O}C	%	m/s	kPa	^{O}C	%	m/s	kPa	^{O}C	%	m/s	kPa	^{O}C	%	m/s	kPa
1/01/09	28.0	69	15	1007	28.0	69	15	1007	28.0	69	15	1007	28.0	69	15	1007	28.0	69	15	1007
2/01/09	23.2	91	15	1008	29.7	43	11	1008	35.0	25	14	1010	20.2	25	21	1016	25.6	18	21	1012
3/01/09	27.1	70	17	1010	30.1	46	17	1012	37.3	18	17	1006	25.7	21	11	1015	29.0	38	14	1013
4/01/09	25.9	70	18	1011	28.8	41	17	1013	31.7	21	17	1008	31.8	19	16	1011	30.8	38	19	1012
5/01/09	28.7	57	15	1009	30.7	30	15	1011	32.9	34	14	1007	33.5	8	15	1011	34.1	26	19	1011
6/01/09	29.7	50	14	1009	32.7	32	17	1009	35.8	21	18	1010	37.0	6	18	1008	36.4	21	16	1009
7/01/09	30.5	54	15	1007	32.4	33	15	1008	33.1	13	22	1011	37.5	11	24	1004	32.7	28	20	1008
8/01/09	29.3	61	16	1006	32.8	39	12	1007	34.4	28	19	1010	24.3	23	26	1014	30.9	23	24	1009
9/01/09	29.0	65	15	1007	31.3	100	19	1007	25.9	66	21	1012	26.7	29	16	1013	27.7	37	19	1012
10/01/09	28.1	59	21	1007	29.5	99	21	1007	35.1	39	12	1006	28.1	32	20	1008	25.3	44	25	1009
11/01/09	27.4	60	14	1008	29.8	99	20	1007	37.0	29	14	1010	30.2	32	13	1007	29.1	46	18	1007
12/01/09	25.5	59	16	1011	31.8	100	14	1010	35.1	26	20	1011	32.0	17	16	1012	32.1	32	9	1011
13/01/09	25.3	68	25	1011	31.7	48	18	1012	34.4	26	23	1012	35.7	21	17	1011	32.7	33	16	1013
14/01/09	28.0	54	26	1011	30.8	28	19	1013	28.0	54	26	1011	39.8	15	27	1008	34.0	28	19	1012
15/01/09	**29.1**	**48**	**17**	**1012**	**32.0**	**32**	**16**	**1012**	**29.1**	**48**	**17**	**1012**	**31.1**	**19**	**27**	**1011**	**36.4**	**20**	**23**	**1009**
16/01/09	28.6	62	8	1012	36.1	22	14	1009	28.6	62	8	1012	24.6	29	28	1015	30.7	14	28	1012
17/01/09	33.1	45	9	1009	33.5	10	24	1010	33.1	45	9	1009	26.0	19	16	1017	27.3	26	13	1014
18/01/09	30.1	57	19	1013	30.7	41	17	1013	30.1	57	19	1013	29.0	20	13	1017	27.7	32	13	1016
19/01/09	29.0	55	21	1014	27.2	52	22	1014	29.0	55	21	1014	34.7	16	16	1011	29.8	42	19	1013
20/01/09	28.5	50	19	1013	31.2	37	18	1012	28.5	50	19	1013	34.8	29	24	1007	33.5	33	22	1010
21/01/09	31.0	52	16	1011	31.4	41	17	1011	31.0	52	16	1011	34.8	24	25	1007	31.0	42	24	1011
22/01/09	31.6	58	16	1008	23.6	94	9	1011	31.6	58	16	1008	30.9	48	35	1002	25.2	70	24	1008
23/01/09	28.7	80	15	1009	30.3	63	14	1008	28.7	80	15	1009	31.5	43	23	1005	30.8	55	15	1008
24/01/09	28.4	83	7	1009	33.6	50	13	1007	28.4	83	7	1009	27.9	30	26	1009	35.6	28	25	1006
25/01/09	29.7	73	10	1010	33.5	52	13	1009	29.7	73	10	1010	29.8	25	17	1014	32.6	31	14	1012
26/01/09	29.5	71	16	1011	32.5	49	16	1012	29.5	71	16	1011	34.7	21	14	1014	34.3	34	11	1013
27/01/09	28.6	65	16	1012	30.4	44	17	1014	28.6	65	16	1012	36.2	23	17	1013	33.1	35	13	1015
28/01/09	28.8	56	24	1010	30.5	40	19	1013	28.8	56	24	1010	37.8	19	17	1012	33.9	29	15	1013
29/01/09	28.8	53	26	1010	30.7	37	20	1013	28.8	53	26	1010	38.7	16	15	1011	33.6	30	15	1013
30/01/09	28.2	56	27	1010	30.5	38	20	1013	28.2	56	27	1010	39.2	16	13	1010	33.5	32	17	1013
31/01/09	28.8	58	23	1010	30.8	35	22	1013	28.8	58	23	1010	39.2	16	16	1011	33.4	32	17	1014

Appendix N: MATLAB Code for footprint analysis

```
ustar=0.24;        % Friction velocity
k=0.4;             %Von Karman constant
z=2;               % Measurement height
h =1;          % Crop height
d=2/3*h;        % Zero plane displacement
z0=1/10*h;         % Roughness length
U =ustar*((log(z-d)/z0)+ z0/(z-d))/(k*(1-z0)/(z-d));
X=1:200;
f(X)=U*(z-d)./(ustar*k*X.^2.* exp(-U*(z-d)./ustar*k*X.^2));
Y=U*(z-d)./(ustar*k*X.^2);
f(X)=Y.* exp(-Y)
Fx18=f(X)';
CNF=exp(-Y);
CNF18=CNF';
```